Underwater noise from pile-driving and its impact on Hector's dolphins in Lyttelton Harbour, New Zealand.

Eva Leunissen

A thesis submitted for the degree of

Master of Science in Marine Sciences at

the University of Otago, Dunedin

November 2017

Abstract

Noise levels were measured in Lyttelton Harbour in order to study pile-driving noise produced during wharf reconstruction. Sound recordings were made throughout the harbour, using several moored and mobile recording systems. In addition, an autonomous system recorded sound over a one-month period. Ambient noise in Lyttelton was heavily influenced by anthropogenic sources such as large and small vessel traffic, particularly in the low frequency range, as well as natural sources such as wind, rain and snapping shrimp in the mid-to-high frequency range. Measured noise levels were highly variable in time and space, with an overall RMS broadband level of 118 dB re 1 μPa near the channel. Recordings made over a month-long period showed higher levels during the day across a broad frequency range. Compared to other places heavily influenced by anthropogenic activities, noise levels in Lyttelton harbour were similar, although some very busy ports show much higher levels.

Repairs to the port of Lyttelton involved 15 months of pile-driving. At a range of 100 m, 1/3 octave-band levels were raised by up to 45 dB across a wide frequency range due to pile-driving noise, exceeding background levels over an area of up to 16.3 square km. The maximum source Sound Exposure Level was estimated to be 194 dB re 1 $\mu Pa^2 s$ @ 1 m (average 182 dB). Most of the energy was within the 100-1000 Hz frequency range, but with significant energy well above 100 kHz at close range. An empirically based propagation model was fitted to estimate the loss in dB with range, and to allow visualisation of how the noise spread throughout the harbour. The bathymetry of the harbour and the breakwater significantly influenced propagation of pile-driving noise. Levels measured in this study tended to be lower than in other studies of pile-driving noise, due mainly to smaller pile drivers and softer substrate in Lyttelton.

The impact of this noise on Hector's dolphins was investigated using passive acoustic monitoring devices (T-PODs). T-PODs were moored in the inner, mid and outer harbour for three months. Statistical analysis of dolphin positive minutes per day and per hour, and how these detection rates were influenced by pile-driving noise as well as environmental variables, was carried out using Generalised Additive Models. Hector's dolphins showed a clear avoidance reaction to pile-driving noise. A decrease in the rate of detections was evident on days with piling. The detection rates recovered to pre-piling levels after 50-83 hours. A simultaneous increase in detections at the mid-harbour T-POD suggests that the animals disturbed by the noise were displaced toward the mid harbour. Based on hearing studies of harbour porpoise, pile-driving noise levels in Lyttelton could cause temporary hearing damage to Hector's dolphins. The shallowness and form of the harbour restricted noise propagation and therefore reduced the potential zone of impact on hearing. Hector's dolphin show avoidance reactions at slightly lower levels than estimated for harbour porpoise, indicating Hector's dolphin may be more sensitive to the disturbance of pile-driving.

Acknowledgements

To my wonderful supervisors Steve Dawson and Will Rayment, thank you for your invaluable advice, your patience and kindness and for always having time for me. Steve, I will never forget the many long drives to Lyttelton and listening to pile-driving noise with you. You have taught me so much, about Hector's dolphins and acoustics but also about so many other things. I am grateful to have been able to hear your stories, you are a wise teacher. You were great at keeping me on track and helping me focus especially when I was going off on all kinds of tangents. Will, thank you for your amazing help with the statistical modelling. Thank you for your patience through all my questions about GAMs and making sure I didn't over-complicate things. Your support and encouragement has been awesome and I am very grateful. I am extremely lucky to have had the opportunity to work with you both, and to be able to see some of the amazing creatures you study.

I have been incredibly fortunate to have the generous support of the New Zealand Whale and Dolphin trust. They provided all the recording equipment, the research vessels *Grampus* and *Cetos*, the towing vehicles, and the wonderful accommodation at French farm in Banks Peninsula. This project was not possible without their immense support.

Thank you to the R & E Seelye Trust for generously providing my Master's scholarship. Also, to the Graduate Research Committee for providing additional funding.

To the Lyttelton Port Company, thank you for providing pile-driving records and weather data, and for your helpful communication with us about the pile-driving schedules. Also for arranging the site visit to view the piling operation up close, your help was very important and much appreciated.

Many thanks to Elisabeth Slooten for all your help with fieldwork and all your great advice.

To all the people in the Marine Mammal Lab, thank you for letting me be a part of the family, it has been great getting to know you and learning from you all. Special thanks to Marta for all your help during fieldwork, teaching me how to use PAMGuard and for helping me make sense of stats! And also for just being an extremely lovely person. Also to Tom, thank you for all your amazing help with the T-PODs and your boating skills. I'm very lucky to have had all the incredible help from you both. Rob, thanks for all your help with ArcGIS, for providing distraction when (and sometimes when not) required, and of course your friendship, moral support and comic relief. Also Tamlyn, David, Jesu, Lindsay and Madda, thanks for all the great chats and potlucks. You are all amazing humans.

And to my family. My parents, Jan and Marloes, you have been so understanding and supportive. Thanks for always looking out for me and feeding me even if I could only pay a short visit. It's been wonderful being in the same town while doing this thesis and I have loved being able to see you often. My brother, Rick, I've missed you lots but it's been great to catch up when we can, thanks for always being supportive and enthusiastic. Alex, my partner, thank you for your love and encouragement, and being so accepting of my busy-ness all this time. Thank you for your music, hearing you play always makes me happy, and your unique and refreshing perspective on life. My friends, Sam thank you for your kindness, support and deep understanding of all things Master's. Your advice has been incredibly helpful, and the catch ups were always wonderful. Crystal, thanks for being a super inspiring human and giving me the hurry up when I needed it!

Finally my utmost gratitude to Katie. Thank you for keeping me sane, by always being extremely excited to see me no matter how long I sometimes left you at home, and by bringing me toys after sitting at the desk for too long. Thanks for ALWAYS encouraging me to go out for a walk (did someone say "walk"??) and for keeping me company during late nights and weekends at the office, my sweet and loyal friend.

Table of Contents

List of Tables

List of Figures

Chapter 1

Chapter 2

Chapter 3

Chapter 4

Appendix

Glossary

dB (decibel): unit for measuring sound levels

DPM (Detection Positive Minutes): the number of minutes per hour or per day during which Hector's dolphin clicks were detected

PSD (Power Spectral Density): the sound pressure level per Hertz, measured in dB re 1 $\mu Pa^2 Hz^{-1}$

RMS level ('Root Mean Square' level): A metric used to give an average level over a period of continuous noise, where the average is taken in the pressure domain, not the dB domain.

SEL (Sound Exposure Level): a decibel measure of the energy in pulsed sound

SPL_{0p} (zero-to-peak Sound Pressure Level): the decibel level of the instantaneous sound pressure between zero and the absolute maximum pressure

SPL_{pp} (peak-to-peak Sound Pressure Level): the decibel level of the instantaneous sound pressure between the maximum and minimum sound pressures

TOL (Third-Octaveband Level): the sound pressure level (in dB) for frequency bands specified according to third-octaves

TTS (Temporary threshold shift): An increase in detection threshold for hearing which indicates temporary hearing damage.

CTD (Conductivity-Temperature-Depth): An instrument used to measure salinity and temperature with depth in the water column.

Chapter 1

General introduction

Pile-driving noise is among the loudest underwater anthropogenic sounds (Richardson 1995) and has been established as a serious threat to some marine mammal species (Thompson et al., 2013). The most frequently studied species in this context is harbour porpoise (*Phocoena phocoena*). Numerous studies using passive acoustic monitoring devices indicate that harbour porpoise show strong avoidance responses and dramatically alter their distribution during pile-driving operations (e.g., Tougaard et al., 2009; Brandt et al., 2011; Dähne et al., 2013). Since this species is broadly similar to Hector's dolphin (*Cephalorhynchus hectori*) in size and ecology, and has almost identical echolocation signals (Dawson and Thorpe 1990; Au 1993; Kyhn et al., 2009), observations of responses by harbour porpoise are clearly relevant. At close range, the sound levels of some pile-driving operations exceed safe levels; causing damage to hearing in some species, including harbour porpoise.

Hector's dolphin is categorised as Endangered by the IUCN (Reeves et al., 2013). Hector's dolphins in Lyttelton harbour were also exposed to pile-driving noise during the Port Lyttelton rebuild and development. The primary aims of this study are to characterise the Lyttelton harbour soundscape and pile-driving noise, and to determine the impact of this noise on the distribution of dolphins around the harbour.

1.1 Hector's Dolphins

Hector's dolphin is endemic to New Zealand. Its genus has three other species in the inshore waters of South Africa, Namibia (C. heavisidii), Chile (C. eutropia), Argentina and the Falkland islands (C. commersonii). They are among the smallest dolphins in the world (Dawson 2009).

Hector's dolphins are found in shallow coastal waters and have not been seen in water deeper than 90 m (Dawson 2009). There are four genetically distinct regional populations off the east, west and south coasts of the South Island and a very small population off the west coast of the North Island that is considered a separate subspecies (*Cephalorhynchus hectori maui*). South Island Hector's dolphins reach a maximum of 145 cm long and weigh up to 50 kg, with females 5-10% bigger than males (Dawson 2009). The maximum known age for Hector's dolphins is around 24 years (Slooten, unpub. data). Females bear their first calf by six to nine years of age and males reach sexual maturity at five to nine years of age. Mature females calve every two to four years with a gestation period of 10-11 months (Slooten, 1991).

The principle threats are from by-catch in gill nets and trawling (Dawson 1991a; Slooten et al., 2000) which have led to an estimated population decline to 27% of the 1970 population (Slooten & Dawson 2009). A marine mammal sanctuary at Banks Peninsula established in 1988, and further gillnet closures made under the Fisheries Act in 2008, have led to lower by-catch. However, nationwide the population is still predicted to decline under current management (Slooten 2013).

Hector's dolphin use high frequency click trains for echolocation and communication. These clicks are about 140 ms in duration and most are centred at a frequency of 125 kHz. All clicks have maximum energy above 82 kHz, mostly in the 115-135 kHz range (Dawson and Thorpe 1990). Some sounds consist of rapidly repeating high-frequency clicks. The repetition rate of these sounds can be audible to humans, heard as a tonal cry or squeal (Dawson 1991b). A distinct type of click appears to be used while feeding and more complex clicks are recorded during social behaviour, with a higher proportion of complex clicks used in larger groups (Dawson 1991b). Hector's dolphin signals are low-level compared to those recorded from other cetaceans, with an estimated peak-to-peak source level of 161 - 187 dB re 1 μPa @ 1 m (Kyhn et al., 2009). For harbour porpoise this is 178 – 205 dB re 1 μPa @ 1 m (Villadsgaard et al., 2007).

There are no data on the hearing sensitivity of Hector's dolphin. However, many studies have investigated the hearing sensitivity of harbour porpoise, a species that is anatomically similar and produces almost identical narrowband clicks as Hector's dolphins (Villadsgaard et al., 2007). The echolocation frequency range for the harbour porpoise is 125-136 kHz (Teilmann et al., 2002) for captive animals and 129-145 kHz for wild animals (Villadsgaard et al., 2007); closely comparable to the 115-135 kHz range of the Hector's dolphin (Dawson and Thorpe 1990). It is reasonable to assume that their hearing sensitivities are similar. Despite their clicks being narrowband, harbour porpoise has one of the widest auditory bandwidths of any animal (Miller and Wahlberg 2013). Hearing sensitivity at 2 kHz is only 25 dB less than the very high sensitivity at 120-140 kHz (Kastelein et al., 2010). Interestingly, while the echolocation frequency range of bottlenose dolphins is lower, harbour porpoise hearing is significantly more sensitive to lower frequencies (Au et al., 1999). The hearing system is directional (Kastelein et al., 2005), and filters sound into critical bandwidths. These bands are approximately described by third-octave bands (Johnson 1968; Merchant et al., 2015), an approach developed to mimic the filters inherent in human hearing. It appears that the auditory system of dolphins is more sensitive to brief broadband pulses (such as pile-driving) than to the pure-tone signals often used in studies of hearing (Au et al., 2002).

Hector's dolphins are highly valued for various reasons. The species is one of only two marine mammals endemic to New Zealand (the other is NZ sea lion, *Phocarctos hookeri*). Mammals can function as keystone species in some marine communities. Serious depletion in their numbers can cause major changes in the ecosystem of which they are part (Estes et al., 1998; Harwood 2001). Hector's dolphins may play an important role as top-predators in the coastal ecosystem. Furthermore they are a taonga (of special cultural significance and importance) species to tangata whenua (MPI 2007) and are the focus of lucrative marine mammal tourism at Banks Peninsula, the Catlins, Kaikoura and the west coast of the South Island.

1.2 Pile-driving noise characteristics

Impact pile-driving produces an impulsive, repetitive sound that is among the loudest underwater sounds, particularly when steel piles are driven. Pile-driving is usually carried out using a hammer or drop weight, sometimes augmented with a gas explosion that occurs as the hammer strikes the pile. Many studies have investigated the properties of the sound produced by pile-driving in the construction of offshore windfarms (see table 1.1). The two most common metrics used in measuring pile-driving noise are peak-to-peak sound pressure level (SPL_{pp}) and sound exposure level (SEL) measured at a given range. SPL_{pp} is the decibel measure of the difference between the maximum positive and maximum negative instantaneous peak pressure. SEL is a measure of the energy over the duration of the strike. The duration of the strike is typically defined as the time window which contains 90% of the total energy (of the entire duration of the strike) and, hence, labelled T_{90} (Southall et al., 2007, see Ch. 2 for equations), see figure 1.1 for more detail on these metrics. Cumulative SEL quantifies the energy in multiple successive exposures, which occurs in repetitive pile-driving, and is calculated as the decibel measure of the sum of pressure-squared of all pulses (Southall et al., 2007). A combination of these two metrics is useful: while high peak pressure is known to cause temporary hearing loss (e.g., belugas in Finneran et al., 2002), repeated exposure to lower pressures can lead to similar effects (Kastelein et al., 2015). Source level is commonly used for point sources of sound, but is inappropriate for pile-driving because of the complex sound pathways involved as the pile penetrates both the seabed and the water surface (De Jong et al., 2011).

Table 1.1 Summary of pile-driving noise measurements in various situations. Pile type refers to the pile's material and shape, location indicates whether the piling was coastal or offshore, 'NS' indicates that measurement was 'Not Specified'. Measurements which are 'M-weighted' have been calculated using a frequency filter based on a marine mammal audiogram (Southall et al., 2007)

Pile Type (diameter)/ location	**Energy (kJ)**	**SPL_{pp} (dB re 1 µPa), [range (m)]**	**SEL (dB re 1 µPa^{2}s) [range (m)]**	**Recording frequency range (kHz)**	**Dominant frequency (Hz)**	**Reference**
NS (4.74 m)/ offshore	1600	180 [1500]	153 [1500],	0.02-22	200 - 300	Lepper 2009
Steel shell (3.9 m)/ offshore	900	196 [720]	176 [720], 107 (M-weighted)	0.015 - 20	80 - 200	Brandt et al., 2011
NS (2 m)/ offshore	800	211 [57]	178 [57]	? - 200	200 - 600	Robinson et al., 2007
Steel shell (4 m) / offshore	800	200 (RMS) [100]	180 [100]	0.003 - 100	50 - 1000	De Jong & Ainslie 2008
Steel shell (2 m) / coastal	800	187 [200]	154 [200]	0.01 - 32	125 - 250	Yang et al., 2015
Steel shell (4-5 m)/ offshore	526-965	196 [520]	NS	.05 - 44.1	100 - 200	Norro et al., 2010
Steel shell (2.4 m)/ NS	500	212 [25]	188 [25]	.03 - 50+	150 – 200	Rodkin & Reyff 2008
Steel Shell (4 m) / offshore	360-450	191 [230]	NS	? - 100+	160	Tougaard et al., 2009
Steel shell (4 m)/ offshore	334	203 [500]	NS	0.1 - 100+	200	Nedwell et al., 2007
Steel shell (0.91 m)/ coastal	223	206 [62]	178 [62]	0.1 – 2	350 – 450	Blackwell 2005
Steel shell (1.8 m)/ offshore	200-400	205 [100]	166 (M-weighted) [100]	0.001 – 170	100 - 2000	Bailey et al., 2010
NS (-)/ NS	90	170 (RMS) [250]	NS	Up to 25	400 - 800	Würsig et al., 2000

(coastal) Steel shell (0.711 m)/ Impact	59	~200 [~40]	~165 [~150]	Up to 24	300 - 400	Duncan et al., 2010
Steel shell (-) / Impact (coastal)	NS	NS	158 [54]	0.01 - 24	NS	Paiva et al., 2015
Steel shell (0.3 m)/ Impact	NS	190 [10]	NS	NS	NS	Rodkin & Reyff 2008
Concrete (0.6 m)/ Impact	NS	183 [10]	160 [10]	NS	NS	Rodkin & Reyff 2008
Timber (0.3 m)/ Drop	NS	177 [10]	157 [10]	NS	NS	Rodkin & Reyff 2008
Steel shell (0.3 m)/ Drop	NS	177 [10]	152 [10]	NS	NS	Rodkin & Reyff 2008

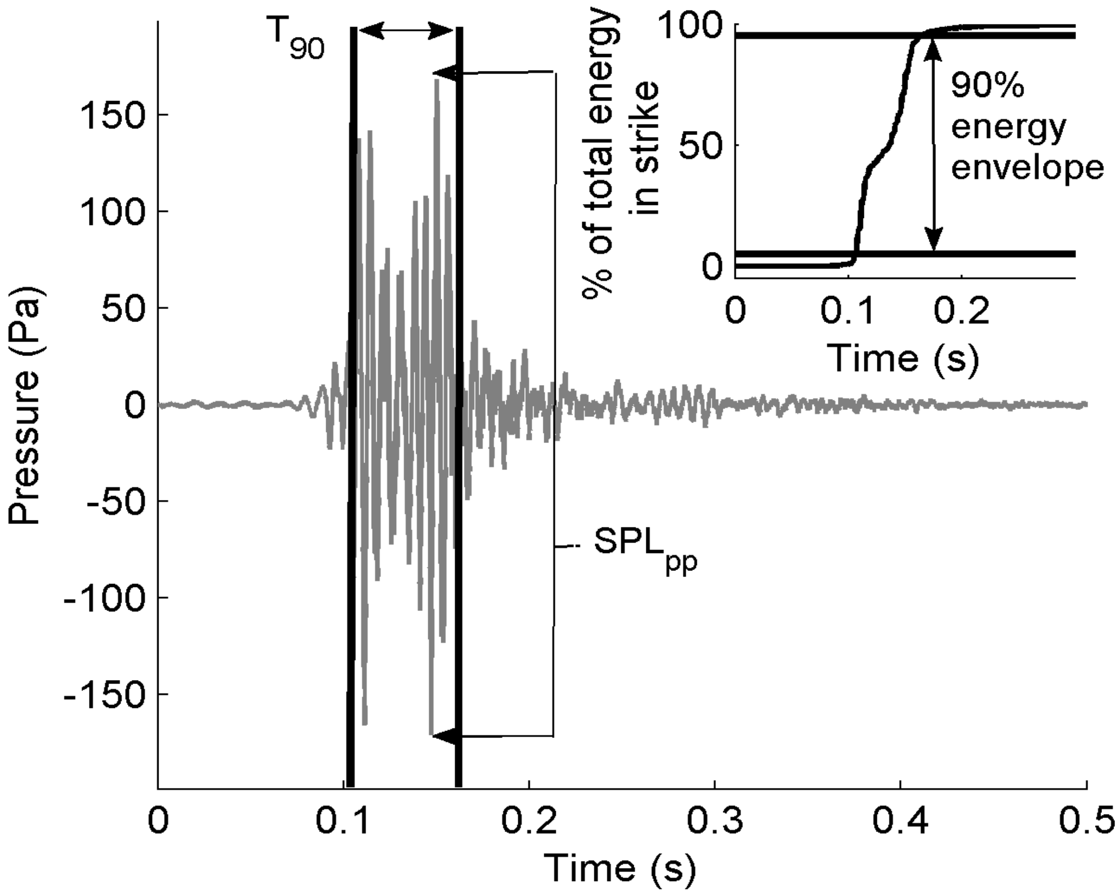

Figure 1.1 Pressure waveform of a single pile strike, bold vertical lines indicate start and end of T_{90}, the duration of the strike defined in terms of its 90% energy envelope. Inset: Cumulative sum of pressure squared of single pile strike with bold horizontal lines at 5 and 95 %

The spectrum of a typical pile strike is dominated by low frequencies with most of the energy below 2 kHz but with significant energy into the high frequencies well above 10 kHz, especially at close range (see Fig. 1.2). Sound propagation involves two kinds of losses, spreading losses and absorption. The latter is dramatically frequency dependent (100 kHz = -36 $dBkm^{-1}$, 1 kHz = -0.04 $dBkm^{-1}$; Malme 1995). Hence, high frequencies are rapidly absorbed, while low frequencies can be detected above ambient noise at very large ranges. However, shallow water imposes a lower limit on the frequencies it can support based on depth (Forrest et al., 1993; Jensen et al., 2011).

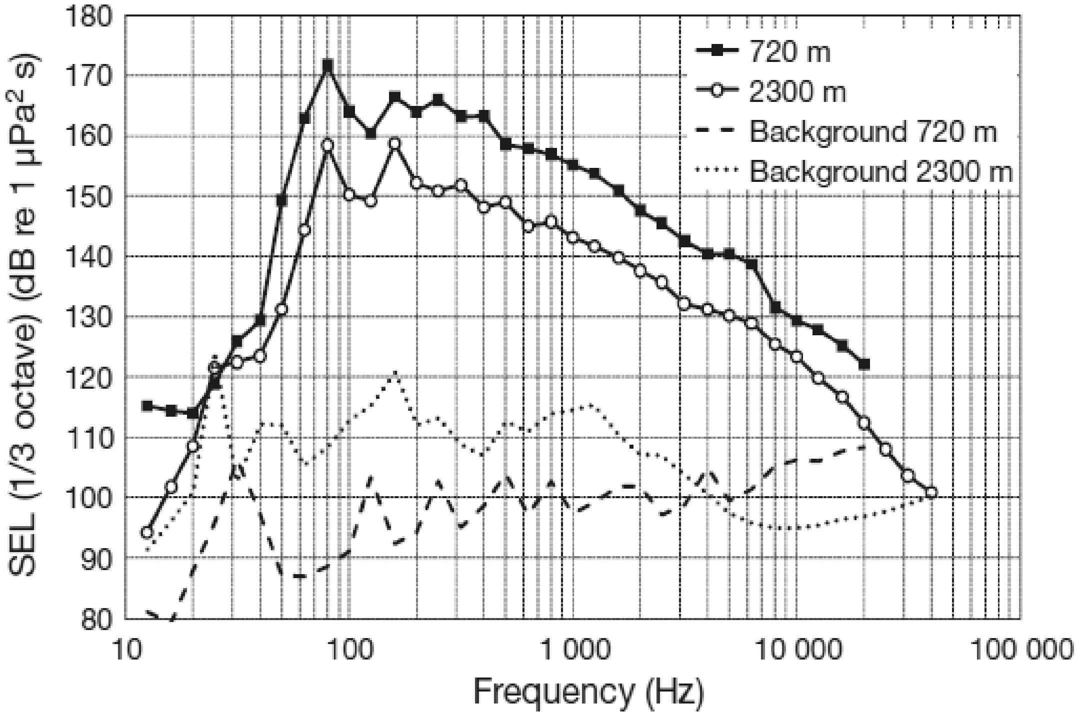

Figure 1.2 Example of 1/3 octave band levels of impact piling at 2 recording distances, including background noise (from Brandt et al., 2011).

A combination of modelling and experimental observation shows that the majority of the sound transferred to the water is due to the radial expansion of the pile immediately after hammer impact (Reinhall & Dahl 2011; Tsouvalas & Metrikine 2014). This expansion travels down the pile at ~5015 ms^{-1} (about 3.3 times the speed of sound in water) and produces a conical wave of sound termed a ‘Mach wave’, both in the water and the sediment (Reinhall & Dahl 2011). At the bottom of the pile this pressure wave is reflected and travels back up the pile, producing another conical Mach wave. A third Mach wave, responsible for pressures of significant amplitude, is produced upon reflection of the top of the pile. The amplitude of each wave diminishes due to losses from structural damping in the pile, radiation damping, sediment attenuation along the pile, and reflection losses at the sediment end of the pile (Reinhall & Dahl 2011). This gives the typical pile-strike pressure waveform shape shown in figure 1.3

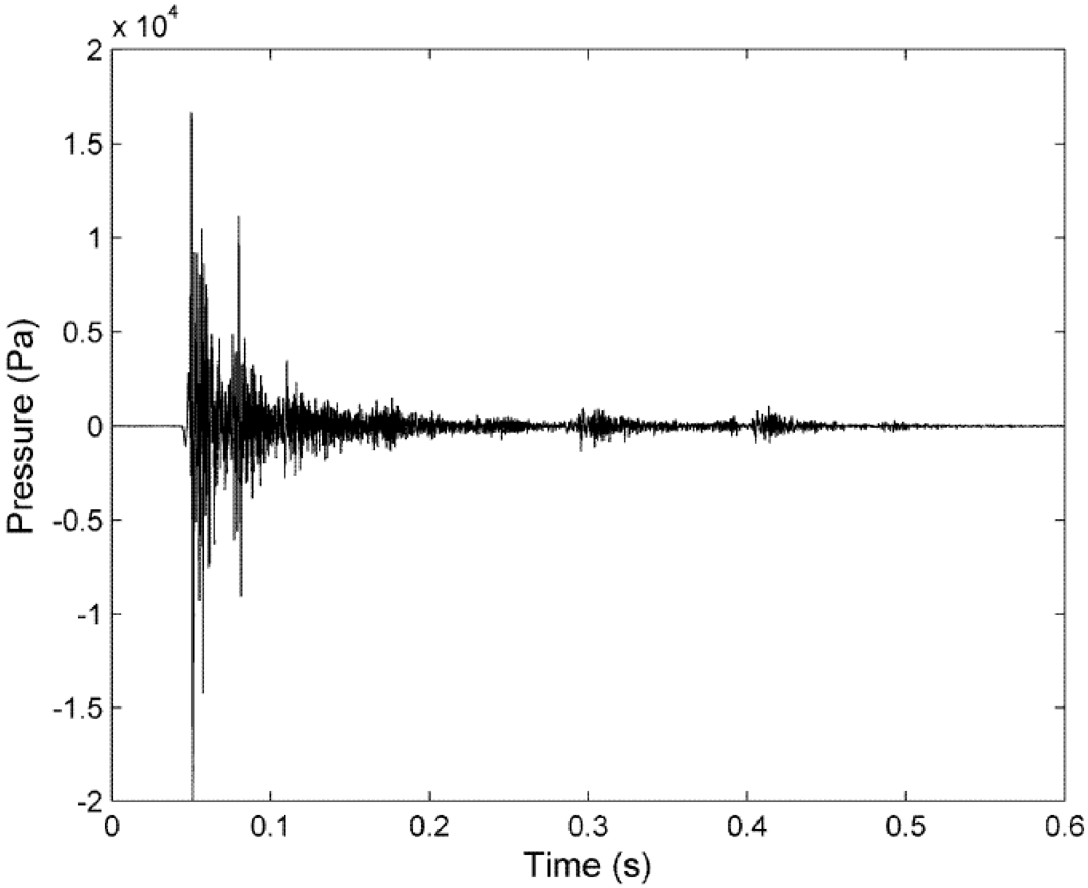

Figure 1.3 Pressure waveform of one pile strike measured during windfarm construction, showing diminishing amplitude with time (from Robinson et al., 2007).

1.3 Effect of pile-driving noise on dolphins

Anthropogenic noise can have a range of effects on marine mammals. Richardson et al., (1995) identified four zones of influence: The zone of *audibility*, in which the animal might hear the noise; the zone of *responsiveness*, within which the animal reacts behaviourally or physiologically; the zone of *masking*, in which the noise interferes with other sounds such as those used in communication, echolocation, prey, predator or other natural sounds from the environment; and the zone of *injury*, where the noise results in damage to the auditory (or other) system.

Zone of injury

The outer extent of the zone of injury for a certain species is determined by the onset of temporary threshold shift (TTS) in hearing. Due to the difficulties involved, no measurements have ever been made on TTS in wild animals. Instead, TTS is estimated from controlled studies with captive animals being exposed to a variety of sounds. After exposure to the sound of interest the animal's hearing is tested, using a trained behavioural response, at different frequencies to quantify the corresponding TTS. One study reported that a 60 minute playback of a repeated sequence of piling induced a TTS in a harbour porpoise at 4 and 8 kHz but not at higher frequencies (Kastelein et al., 2015). The latter was not appropriately tested, however, because the original recording of the pile-driving was made with a sampling frequency of 62 kHz therefore contained no frequencies above 31 kHz. This is an important problem because harbour porpoise hearing reaches maximum sensitivity around 125 kHz (Kastelein et al., 2010) – frequencies that are certainly present in pile-driving strikes recorded at close range. The same study also observed erratic swimming patterns in response to the piling playback. Cumulative SEL is an important metric of noise exposure for marine mammals: while a single strike may not cause TTS, repeated strikes may well do so (Kastelein et al., 2014). The same study also showed that inter-pulse-interval significantly influences the amount of TTS induced. Other types of sound tested included tonal sweeps (Kastelein et al., 2014) and octave band noise (Kastelein et al., 2012).

TTS studies have also been performed on bottlenose dolphins. Schlundt et al., (2000) exposed two dolphins to intense one-second tones at increasing frequency and tested their hearing (using a trained behavioural response) at those frequencies before and after the exposure. TTS was induced at some of these frequencies with significant differences between the two dolphins. Behavioural change, including aggression directed at the testing equipment, was observed at noise levels between 178-193 dB re 1 μPa. Similarly Finneran et al., (2005) observed TTS in two bottlenose dolphins after exposure to 4 kHz tones with an SEL of 195 dB re 1 $\mu Pa^2 s$ and suggests this level to be a reasonable threshold of onset of TTS in dolphins and white whales. Mooney et al., (2009) used octave band noise (between 4 and 11 kHz) of longer duration than the previously mentioned studies (<2-30 mins) and tested the dolphin's hearing by measuring the auditory evoked potentials using an electro-encephalogram (EEG). This demonstrated that shorter signals require higher sound levels to induce TTS than signals of longer duration, however, the results are inconsistent with an equal-energy model to predict TTS, which is indicative of the complexity of predicting TTS in odontocetes. They also found the rate at which the threshold of hearing is restored to be around -1.8 dB per doubling of time following the exposure. Finneran et al., (2002) exposed a bottlenose dolphin to an airgun pulse in the presence of masking noise but no TTS was observed. However, a beluga (*Delphinapterus leucas*) exposed to a lower level pulse from the same airgun did show TTS. Problems with using a trained animal for TTS studies include that it is likely to behave differently, may be habituated, may have less sensitive hearing (see Lucke et al., 2008) and that it cannot display the full range of behavioural responses (e.g. it cannot leave the area). Using playback of noise in captive conditions is unlikely to represent the propagation of noise in natural conditions. These could lead to unsafe estimates of the level at which TTS occurs in wild animals.

For ethical reasons there are no measured data on the criteria for permanent threshold shift (PTS), the level at which permanent hearing damage occurs. For marine mammals, this level has only ever been inferred from the level at which TTS occurs. PTS in terrestrial mammals occurs when the hearing threshold has shifted by 40 dB and it is assumed to be similar for marine mammals (Southall et al., 2007).

Zone of masking

The zone of masking due to pile-driving noise was investigated for bottlenose dolphins (David 2006), who found that communication whistles may be masked up to 40 km from the piling source and echolocation clicks up to 6 km. No studies have specifically investigated the zone of masking for harbour porpoise. It was initially thought that piling noise was unlikely to mask sounds of importance for this species, due to lack of significant energy at the frequencies used by harbour porpoise, i.e. >100 kHz (Tougaard et al., 2005; Madsen et al., 2006). More recent studies, however, have observed significant energy above 100 kHz (Tougaard et al., 2009), hence the noise spectrum overlaps that of harbour porpoise sounds. Additionally, the noise could mask sound cues from predators, prey or conspecifics, which may reduce the animal’s fitness or its chance of finding a mate. These impacts are difficult to measure but may lead to important population impacts, particularly for vulnerable populations like the Hector’s dolphin.

Zone of responsiveness

Several studies have observed wild animals in uncontrolled settings and used passive acoustic monitoring devices (T-PODs or CPODs) to detect changes in animal distribution (Brandt et al., 2011; Tougaard et al., 2009; Carstensen et al., 2006). Using several of these at increasing distances from the piling, the devices can be used to detect changes in the rate of echolocation detections prior to, during and after piling. These studies have reported a marked decrease in porpoise clicks in a radius of at least 20 km from the source (Tougaard et al., 2009; Brandt et al., 2011). At 2.6 km from the source this response lasted up to 72 hours (Brandt et al., 2011). Since the latter is longer than the breaks between piling activity in that particular study, the effect may have lasted for the entire five month construction period. Dähne et al., (2013) combined this method with simultaneous aerial surveys to show that the animals do actually leave the area and not just reduce their vocalisation rate. The instantaneous decrease in clicks following the onset of piling noise, however, implies that vocalisation rate is also affected (Brandt et al., 2011).

Using noise exposure criteria, Bailey et al., (2010) calculated that the range of behavioural disturbance for bottlenose dolphins due to pile-driving noise could extend to 50 km. Detections of Indo-Pacific bottlenose dolphins in a harbour channel, recorded from high definition video recordings, decreased significantly during pile-driving activity in wharf construction (Paiva et al., 2015). This study could not determine whether decreased detections were due to lower dolphin abundance (or other reasons such as masking of communication signals) leading to reduced surface socialising, or a change in foraging behaviour due to reduced prey abundance and/or reduced ability to detect prey (Paiva et al., 2015).

The studies reviewed above show that pile-driving noise can elicit strong reactions. Fully controlled experiments are very difficult to achieve with wild dolphins, so it is impossible to conclude that these reactions were purely due to noise; other factors may include prey movement or unknown environmental changes.

Kastelein et al., (2013a) used a trained harbour porpoise exposed to the sound of a single pile strike at increasing SPL to determine a threshold at which the animal would change its behaviour in response to the noise. Based on changes in respiration rates and aerial activity, this was at an SPL of 142 dB re 1 µPa.

Zone of audibility

By definition, the zone of audibility can only be inferred from a species' audiogram combined with noise measurement data gained at various ranges. As mentioned before, the audiogram of Hector's dolphin will likely be similar to that of harbour porpoise (described in Kastelein et al., 2010). A study using a trained harbour porpoise in a quiet pool found the animal detected the sound of a played back pile strike 50% of the time at an SEL of 72 dB re 1 μPa^2s. The threshold decreased by about 5 dB for multiple sounds in succession (Kastelein et al., 2013a). It is important to note that there are several limitations to this study that reduce the applicability to real life situations. The original recordings were sampled at 88.2 kHz, therefore they are unable to represent the part of the strike's spectrum above 44.1 kHz. While 90% of the strike's energy was contained in the 63 Hz to 400 Hz 1/3-octave bands, piling noise often contains significant energy well above 100 kHz. This is of particular importance given that harbour porpoise's range of best hearing is between 100 and 140 kHz (Kastelein et al., 2002 & 2010), therefore, this threshold is likely an underestimate of the true level for these quiet pool conditions. The shallowness of the pool environment also introduces a lower cut-off frequency. The part of the noise spectrum below this frequency will not propagate in the pool. The bottom of the 2 m deep pool was covered with sand, therefore we could expect a cut-off frequency at ~350 Hz (see Fig. A.1 in appendix). Given that this is well within the range of peak energy in most pile-driving noise spectra, this could lead to a significant reduction in overall noise levels in the pool. Additionally, the ambient noise levels in the ocean are likely to be much higher than the below sea state-zero levels measured in the pool (in the absence of the playback sound and the dolphin), particularly when considering the high levels of ambient noise typical of harbour environments.

Seismic airgun pulses

Airgun pulses, used in seismic surveys, are another example of impulsive sounds that could cause harm to marine mammals. Studies have observed: avoidance reactions near seismic surveys in common dolphins (Goold 1996) and spotted dolphins (Weir 2008); increased stress in a captive beluga and bottlenose dolphin after exposure to the sound of seismic gun pulses (Romano et al., 2004); and TTS at 4 kHz in a trained harbour porpoise when exposed to an airgun pulse with an SEL of 164 dB re 1 μPa^2s (Lucke et al., 2009). The latter study predicted that the animal's hearing sensitivity could be affected up to 55 hours after the exposure. Akinesia, likely leading to death, was observed in a spotted dolphin 600 m from an active seismic airgun array (Gray & Van Waerebeek 2011).

Bubble curtains

The effect of an air-bubble curtain to attenuate piling noise and thereby decrease the extent of impact on marine mammals has been investigated. Lucke et al., (2011) observed a strong avoidance reaction (including speed swimming and porpoising) in captive harbour porpoise exposed to pile-driving noise at a range of 100-175 m. After installing a bubble curtain around the animals' enclosure the avoidance behaviour was no longer observed during pile-driving. The bubble curtain reduced the SEL by 13 dB (±2.5 dB) at the location of the curtain. It must be noted, however, that the placement of the bubble curtain will influence the relative decrease in noise level - close up to the piles part of the sound energy will go under the curtain, via the sediment (Scholte waves; Tsouvalas & Metrikine 2014), while further away (i.e., at the range of the enclosure) most of this energy will have transmitted into the water, and hence a bubble curtain would be more effective here. Observations of wild Indo-Pacific hump-backed dolphins during pile-driving activity, with a bubble curtain in place, did not indicate strong avoidance reactions to the piling noise, however, the animals' swimming speed was more than double that in the periods without piling (Würsig et al., 2000). The curtain, located around the noise source with a radius of 25 m, caused a reduction in broadband pulse levels of 3-5 dB at the location of the curtain.

Long term effects

No studies have investigated the long-term population effects of exposure to pile-driving noise. However, a framework for predicting the population effects of a disturbance has been proposed as an interim solution to the lack of long term data (King et al., 2015). Short-term avoidance reactions may not necessarily lead to long-term effects and a lack of observable reaction does not imply lack of impact on the animal (Southall et al., 2007). Temporary displacement out of a particular area does not necessarily constitute a population level effect. However, in the case of Hector's dolphins, displacement further from the harbour may increase the risk of by-catch if this extends beyond the marine mammal sanctuary (Forney et al, 2017).

The extent of risk to marine mammals depends on several factors including the characteristics of the pile-driving sound, the environmental characteristics of the area, and the species' acoustic sensitivity, behavioural responses and habitat use characteristics (Richardson et al., 1995).

Noise Exposure Criteria

It is clear that noise can have various negative effects on marine mammals, therefore, it is important to establish safe limits for anthropogenic noise in the ocean. It is challenging to define a ‘safe’ limit as it is difficult to know to what extent a reaction to noise – whether behavioural or physiological – represents a significant problem for animals in the wild. Southall et al., (2007) suggested initial exposure criteria in relation to injury. Due to the lack of experimental results, however, they could not provide general limits for safe exposure regarding behavioural response.

These criteria have recently been reviewed by Tougaard et al., (2015), who also report that harbour porpoise hearing is more sensitive than previously believed. It is suggested that TTS due to exposure to a pure tone can be estimated to occur at an SEL about 100 dB above the hearing threshold. For example, given that the hearing threshold at 100 kHz is about 50 dB re 1 µPa (Kastelein et al., 2010), it is reasonable to assume TTS may be induced at an SEL of 150 dB re 1 $\mu Pa^2 s$, for a 100 kHz pure tone. It was shown that sound pressure levels (SPL) 40-50 dB above the hearing threshold of harbour porpoise induced behavioural reactions, and suggested that this level could be used to define the extent of the zone of responsiveness for a particular source, given that SPL is known at various ranges. Finally, this study highlights that it is important to consider frequency weighting when assessing the impact of noise on a species and not simply rely on the SEL alone.

1.4 The Banks Peninsula Hector's dolphin population

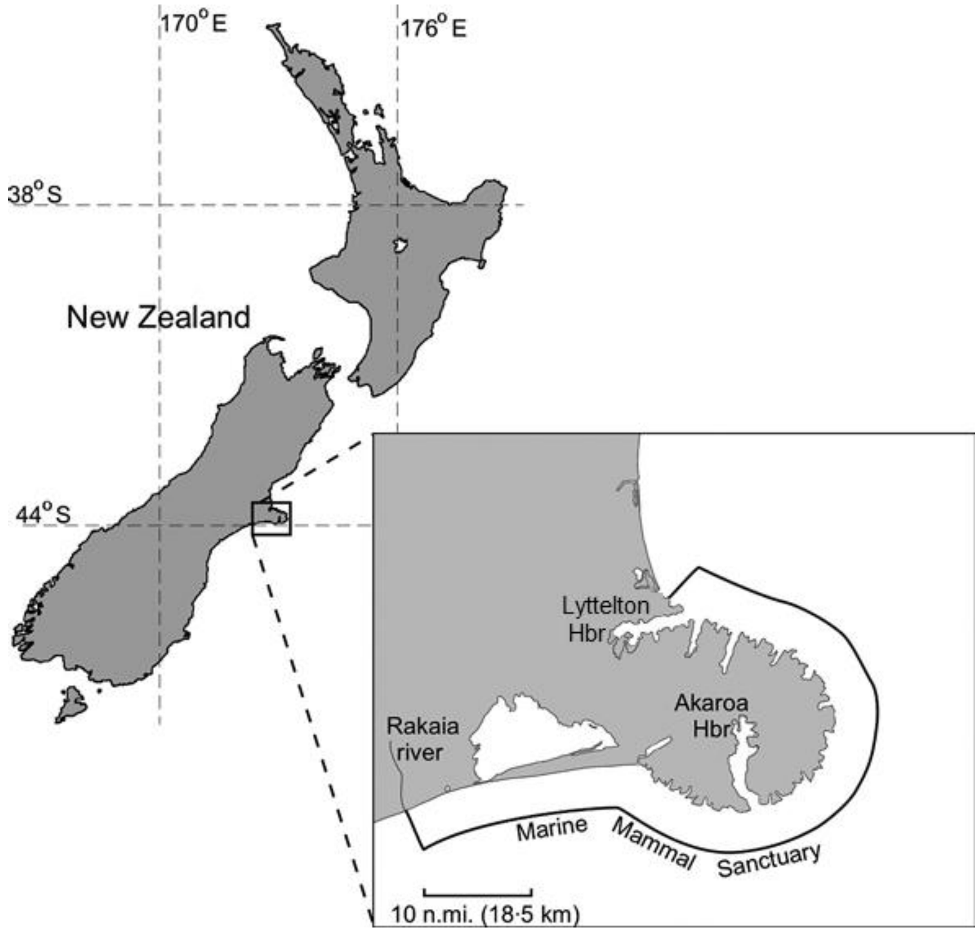

Figure 1.4. The Banks Peninsula Marine Mammal Sanctuary (as established in 1988) on the east coast of the South Island of New Zealand (adapted from Gormley et al., 2012)

Banks Peninsula, on the east coast of the South Island of New Zealand, contains many sheltered bays including Akaroa and Lyttelton Harbour. Banks Peninsula hosts a local population of about 1100 Hector's dolphins (CV = 28 %; Gormley et al., 2005), the largest on the east coast of the South Island. Hector's dolphins at Banks Peninsula have a long history of significant by-catch, mostly in gillnets set by commercial fishers, but also in trawls, and in gillnets set by amateur fishers (Dawson, 1991a). In the mid-1980s, an average of 57 dolphins were caught in gillnets around Banks Peninsula per year (Dawson 1991a). A series of conservation initiatives, starting with the creation of the Banks Peninsula Marine Mammal Sanctuary (BPMMS) in 1988, has resulted in most of the south island east coast being protected from gillnetting out to four n.mi. (7.4 km). Analyses of survival rates of Hector's dolphin at Banks Peninsula show significant improvement after the creation of the BPMMS, and the population now appears to be nearly stable (Gormley et al., 2012). Trawling, except for flatfish, is banned out to two n.mi. offshore. However, Hector's dolphins range to at least 20 n.mi. offshore (Rayment et al., 2010). By-catch still occurs beyond the boundaries of fisheries restrictions, hence additional threats such as habitat modification and shipping are likely to affect an already vulnerable population. The 2008 amendment to the marine mammal sanctuary includes somewhat minimal restrictions on seismic survey activity. Seismic surveys are permitted if non-explosive sources are used, a soft start procedure is followed, and that qualified observers are present in order to detect presence of cetaceans within 1000 m. Acoustic activation must cease if a mother-calf pair is observed within 1000 m and any cetacean is observed within 500 m (DOC 2008). The effectiveness of these restrictions is unstudied.

1.5 Hector's Dolphins in Lyttelton Harbour

Boat surveys of Banks Peninsula for photo-identification research have been conducted for the past 30 years by the Marine Mammal Research Group (MMRG) of the University of Otago. This study includes Lyttelton Harbour and the outer coastline area. The data provide some insight into the dolphins' use of the harbour prior to the recent development activities. The research for which these data were gathered was not designed to quantify fine scale patterns of habitat use, and the survey route did not cover the entire area of Lyttelton Harbour. Nevertheless, dolphins, including calves, have been sighted in the middle of the harbour and near the wharves (MMRG unpub. data). The data from 1991 to 2014 resulted in 302 dolphin sightings in Lyttelton Harbour and show that Hector's dolphin use of this harbour is routine.

The majority of the sightings are around the outer coastline (Fig. 1.5). However, many have been made in the inner harbour - as far as Quail Island (Fig. 1.5). Note that there are also sightings within the (shaded) port development area. These dolphins are likely to be disproportionately affected by pile-driving noise due to being closer to the port. Groups with calves show a similar distribution around Lyttelton harbour.

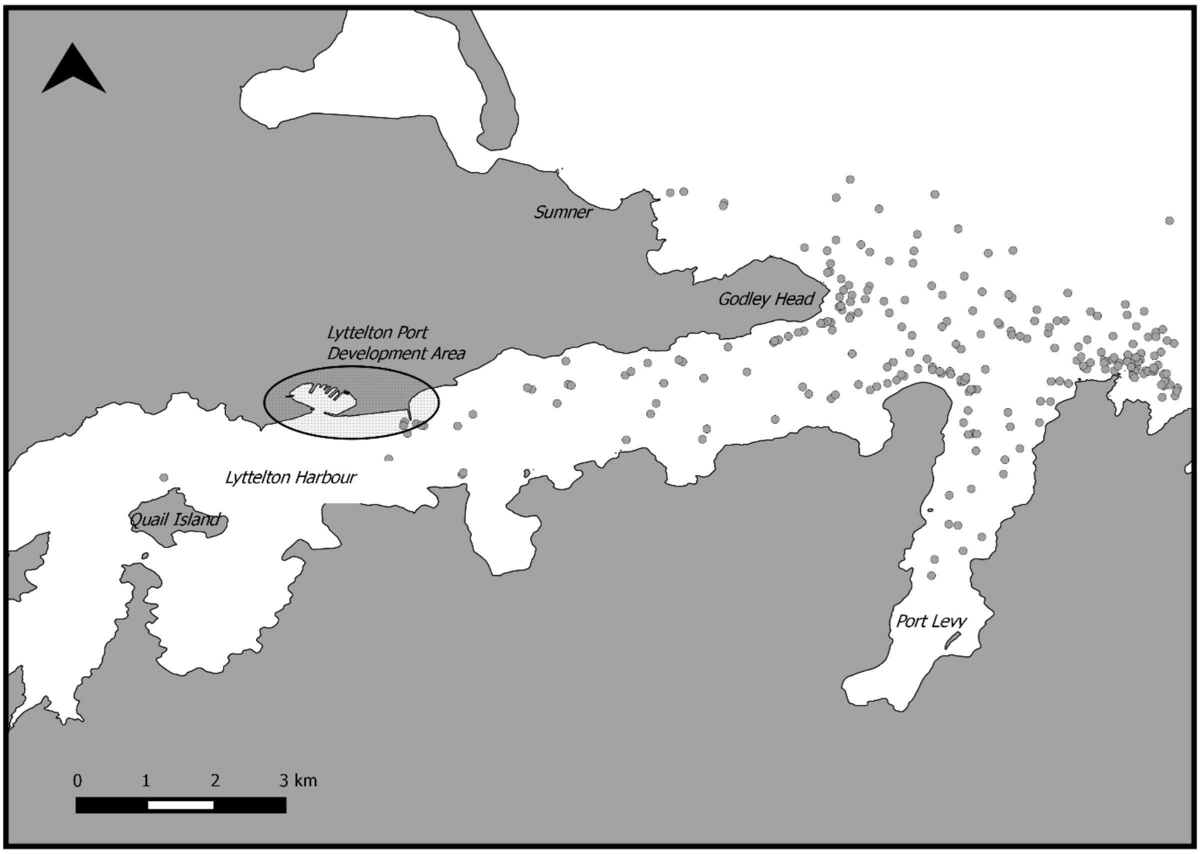

Figure 1.5 Total Hector's dolphin sightings in and around Lyttelton Harbour from 1991 to 2014. The shaded area indicates Port Lyttelton, where development activities are taking place (from Brough et al., 2014).

During the summer Hector's dolphins are found closer to shore, in shallower water (Brough et al., 2014). Habitat use by Hector's dolphins of Lyttelton Harbour is broadly similar to that of Akaroa Harbour (Dawson et al., 2013) and the rest of Banks Peninsula (Rayment et al., 2010).

Port reconstruction and redevelopment

The Christchurch earthquakes in September 2010 and February 2011 resulted in significant damage to the Port of Christchurch (Port Lyttelton), including to 75 % of its wharves (LPC 2014). The Cashin Quay wharf, used for container cargo, cruise ships and vehicle unloading, suffered from land movement, particularly Cashin Quay 2 (CQ2) where the wharf deck and supporting piles fractured. Starting in December 2013, the concrete deck and piles were removed, followed by the regrading of the shore and replacement of its boulder edge. New piles were driven into the seabed by first using a vibrating hammer to position the pile, then repeatedly dropping a large weight onto the pile using a pile driver. The piles were 710 or 610 mm in diameter, with closed ends, approximately 80 m long and driven an average of 66 m into the seabed. A “soft start” is standard practice (i.e., required by the pile-driver manufacturers). This starts with a 100-200 mm drop (the first “bar” on the control unit) for 2 mins, then 25 % power for one min., then power as required. Drop height increases as the pile meets further resistance. Piling ceases when maximum power hammer blows move the pile 2.5 mm or less (Doyle Smith, HEB project engineer, pers. comm. 21 January 2015). The wharf was expected to be fully operational by the end of 2015 (LPC 2014). While CQ1, 3 and 4 were also damaged they could be used with operational restrictions. Repairs or rebuild involved similar works to that of CQ2. Other structures that need repairs include the breakwater, which sank into the soft sediment, the dry dock and a number of wharves in the inner harbour (LPC 2014).

In addition to repairs, the Lyttelton Port Company planned to redevelop the port to manage a forecasted 400% increase in container cargo in the next 30 years (LPC 2014). Together, the repairs and redevelopment involve pile-driving to repair and extend wharves, dredging to facilitate access by larger ships, and reclamation to provide space during the recovery for support of vehicle imports and container terminal activities. Ultimately 30 ha will be reclaimed for the port’s future container terminal.

The Hector’s dolphin’s Threat Management Plan lists construction, coastal development and pollution as threats to the species (MPI 2007). Marine mammals are sensitive to changes in their habitat and so are potentially vulnerable to the effects of coastal development (Harwood 2001; see Jefferson et al., 2009; for a review on potential impacts on small cetaceans). Hector’s dolphins are top predators, and hence are susceptible to changes in abundance and distribution of lower trophic levels and changing prey availability (Tynan & DeMaster, 1997). Additionally they are likely to be exposed to bio-accumulation of pollutants (Tanabe et al., 1983) which are usually associated with spoil used in reclamation (and can be re-suspended in the water column after dredging (Goossens & Zwolsman 1996)). Hence the Lyttelton Port development has the potential to affect Hector’s dolphins directly and indirectly, in several ways. Understanding the direct threat of pile-driving takes us a step closer to establishing the extent of the impact of development activities on an already endangered marine mammal.

1.6 Thesis objectives

Based on the results from previous studies on the effects of pile-driving on harbour porpoise and other marine mammals it is crucial to investigate the effect on Hector's dolphins. The current study is the first to examine Hector’s dolphin responses to pile-driving noise, in relation to port construction activities. This will be investigated in two parts: Chapter 2 and 3 quantify the ambient and pile-driving noise in Lyttelton harbour, then, via analysis of the passive acoustic monitoring data I investigate whether and how Hector’s dolphin distribution changes in response to the pile-driving noise (Ch. 4).

The principal objectives in this study are to:

i. Investigate and characterise the soundscape and the pile-driving noise in Lyttelton Harbour.
Data will be gathered from underwater sound recordings made at various locations around the harbour using a recording platform on board the research vessel (RV). Additionally, two self-contained recording platforms moored at different ranges from the piling will provide a reference for the RV recordings. Spatial analysis of recordings will be used to map the sound environment of Lyttelton Harbour. I intend to produce a map of equal-loudness contours, with spectral information, for the pile-driving and ambient noise. This will show how significant features of the harbour, such as Sticking Point, or Kamautaurua Reef affect the propagation of pile-driving sounds. CTD casts will be conducted to determine the salinity and temperature at varying depth, from which sound speed can be calculated, and to observe any stratification in the water column. Additionally we will moor a long-term recorder on a duty cycle to document natural and anthropogenic noise in the harbour over a one-month period.

ii Determine the impact of this noise on the distribution of dolphins around the harbour.
T-PODs can be set to reliably detect only Hector’s dolphins. We will moor three T-PODs in Lyttelton; one each in the outer, mid, and inner harbour. Via analysis of the T-POD dolphin detections and the pile-driving records, we hope to quantify if/how dolphin presence is affected by pile-driving noise. Based on noise exposure criteria for a similar species (harbour porpoise) we will determine approximate spatial zones of expected behavioural influence and temporary hearing damage.

1.7 Thesis structure

Each chapter in this thesis is written as an independent manuscript, resulting in some content overlap between chapters, particularly in the methodology. Chapter 2 describes the ambient noise recorded in Lyttelton Harbour, Chapter 3 characterises the pile-driving sound, while Chapter 4 describes the effect of pile-driving on the dolphins. A general discussion is presented in Chapter 5, where I discuss the potential implications of pile-driving noise on the Hector's dolphin population, provide recommendations for future pile-driving work in Hector's dolphin habitat, outline some study limitations and provide research recommendations for the study of noise impacts on Hector's dolphins.

Chapter 2

Ambient Noise in Lyttelton Harbour

2.1 INTRODUCTION

Ambient sound is an important habitat quality for marine species (Richardson et al., 1995). Anthropogenic contribution to underwater ambient noise is becoming an increasing concern as recent research reveals more about its many potential impacts on marine life, particularly on cetaceans (e.g., Weilgart 2007; Hatch et al., 2012). Our oceans have become much noisier in recent decades (McDonald et al., 2008); in the low frequency range (20-80 Hz) this is almost certainly due to the increase in commercial shipping (Andrew et al., 2002). Harbours are therefore amongst the noisiest underwater environments (e.g., Hatch et al., 2012; Salgado et al., 2012; Bittencourt et al., 2014). Other studies that measured ambient noise include those in recreational areas (Samuel et al., 2005; Rako et al., 2013), offshore windfarms (Bailey et al., 2011), and other industrialised areas (Wursig & Greene et al., 2002; Blackwell et al., 2005)

Ambient noise in Lyttelton Harbour was defined as any underwater sound that would usually be present, excluding the noise of port construction/repair activities. Ambient noise includes noise from boats and usual port activities such as unloading containers, cars and coal, but not noise from excavation or vibro-hammering (a machine that vibrates piles into place before impact pile-driving). The aim was to characterise the ambient noise in Lyttelton Harbour in order to provide a baseline against which to compare the pile-driving noise. Since port repairs had started prior to this project, for recordings of ambient noise I used recordings made during pauses in piling and other construction work. These pauses ranged in duration from tens of seconds within piling sequences to several consecutive days on which piling did not occur. Lyttelton Harbour is part of the Banks Peninsula Marine Mammal Sanctuary. Understanding underwater ambient noise is important for conservation of the marine environment, particularly in a marine protected area.

2.2 METHODS

Field techniques and data collection

Sound recordings were made using four autonomous recorders (three DSG Ocean recorders and a SoundTrap HF) and two boat-based recorders (Table 2.1).

Table 2.1 Recording systems used in measuring underwater noise levels in Lyttelton

Recorder (label in Fig. 2.1)	Hydrophone (amplifier)	Sampling rate	Duty cycle	Function
SoundTrap HF (SoundTrap)	standard	288 kHz/16bit	Continuous when deployed	Static close range monitoring (c.370 m from piling)
DSG ocean (DSG)	HTI-96 min	80 kHz/16bit	Continuous when deployed	Static Medium range monitoring (c. 750 m from piling)
DSG ocean (Duty cycle DSG)	HTI-96 min	80 kHz/16bit	Duty cycle: 5 continuous minutes every hour	Static long-range monitoring (c.1.9 km)
DSG ocean (Diamond hbr. DSG)	HTI-96 min	2.5 kHz/16bit	Continuous throughout study from 7:00am to 19:00pm	Static duty cycle monitoring (c. 1.6 km from piling)
Roland R-44	Reson 4032	192 kHz/16bit	Continuous when deployed	Distant recordings from anchored or drifting boat
PC-based HF recorder NI USB-6351 A-D board (PAMGuard software)	Reson 4013 (Reson VP2000)	500 kHz/16bit	Continuous when deployed	Close-range recordings from anchored or drifting boat

Boat-based sound recordings were made at widely varying ranges from the wharf, between 15 December 2014 and 10 February 2015. Recordings were conducted on calm days (up to Beaufort Sea state 3) to reduce noise due to water movement and wave slap.

A long term recorder (DSG Ocean) was deployed in Diamond Harbour ('Diamond hbr DSG' in Fig. 2.1), 1.7 km from the wharf, from 22/12/14 almost continuously (excluding days required to service the recorder) until 25/3/15. The purpose of these recordings was to provide an acoustic record of pile-driving times, to supplement the pile-driving records provided by HEB construction. Sound quality was less important than battery life and data storage space, hence the low sampling rate of 2.5 kHz.

Ambient noise was recorded over 26 days using a moored DSG recorder set up on a duty cycle ('Duty cycle DSG' in Fig. 2.1), recording for five minutes every hour with a sampling rate of 80 kHz, from 27/2/15 to 25/3/15. The recorder was moored to a permanent fixture (channel marker) in the harbour.

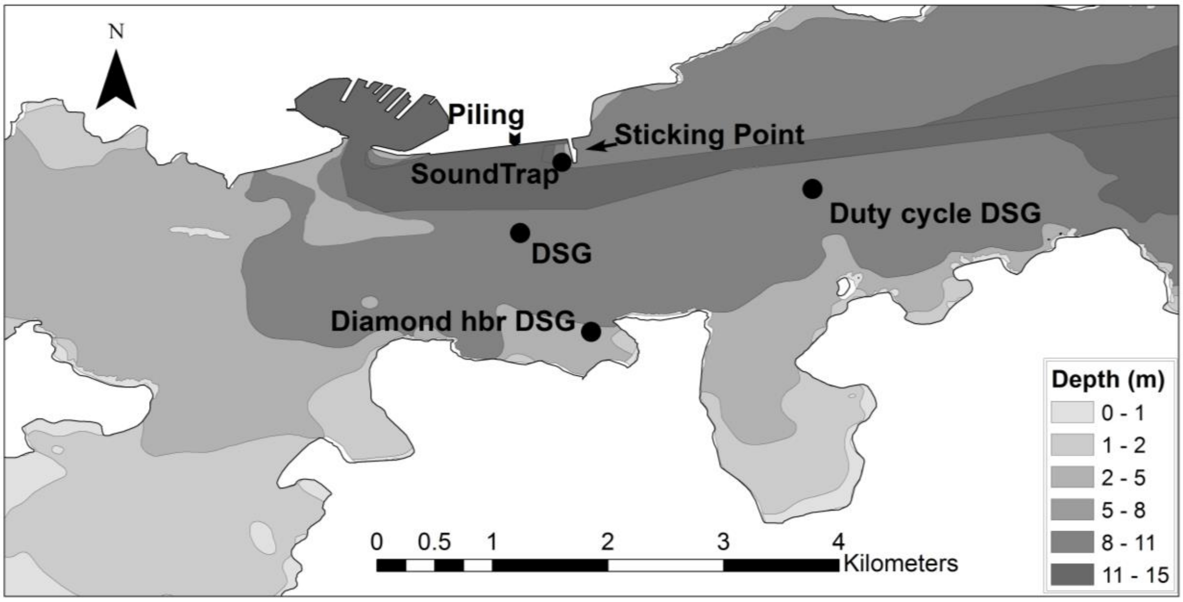

Figure 2.1 Location of moored recorders in Lyttelton Harbour

Each day of boat-based recording started with mooring the systems that recorded continuously for the day. Generally this started around 7:30 am to make the most of favourable weather conditions in the morning. A wideband recorder (Ocean Instruments SoundTrap HF, sampling at 288 kHz) was moored approximately 2 m off the bottom, in an average water depth of 6.5 m (± 1.5 m, varying with tide), approximately 370 m from the piling activity ('SoundTrap' in Fig. 2.1). Wharf areas immediately to the east and west of the piling location were operational, restricting potential locations for this recorder. Hence the SoundTrap was placed very close to the breakwater (Sticking Point), to reduce risk of being damaged by docking vessels while minimising the range to the noise source. It was moored with a buoy at the surface, anchored by chain and danforth anchor. A second recorder (DSG-Ocean Long term recorder, sampling at 80 kHz), moored in the same way as the SoundTrap, was placed outside the harbour channel, in about 8 m of water, directly in front of the piling about 750 m away (‘DSG’ in Fig. 2.1).

Simultaneously, we made recordings throughout the harbour from an anchored or drifting research vessel. For recordings beyond 400 m from the wharf, we used a sensitive, low-noise hydrophone specifically designed for measuring ambient noise (Reson 4032), recorded on a Roland R-44 digital recorder. GPS coordinates of each recording location were noted. Ranges to piling activity, and to any passing vessels, were measured using a laser range finder (Leica Rangemaster 1000-R).

Boat-based recordings were made with the echo-sounder and engine off to minimize unwanted noise. All recording systems were routinely calibrated via a pistonphone (G.R.A.S. 42AA pistonphone, with appropriate couplers) with appropriate atmospheric corrections.

Immediately following any boat-based recording a CTD (Seabird SB-19) cast was made. Temperature and salinity data were used to calculate sound speed profiles, and to quantify any stratification in the water column. These measurements were also taken at locations of the moored recorders (see appendix section 4 for CTD profiles).

Sound Analyses

Anthropogenic contributions to ambient noise (such as boat and generator noise) were generated by continuous processes, as opposed to impulsive sources like pile-driving. This means the metrics used to describe this continuous noise are defined differently to those for the impulsive piling noises. It is not very informative to give the peak-to-peak level of a period of ambient noise (which by definition gives only the range between maximum and minimum instantaneous pressure) as this only describes a very limited feature set, particularly if the noise contains spikes (Southall et al., 2007). Therefore, the most useful metrics are the broadband Sound Pressure Level (SPL_{bb}) over time and the RMS SPL as an average over time (Merchant et al., 2012; Robinson et al., 2014; Merchant et al., 2015).

SPL_{bb} gives the continuous SPL at a given time (Merchant et al., 2015)

$$SPL_{bb} = 10\log_{10}\left(\frac{1}{p_{ref}^2}\sum_{f_l}^{f_u}\frac{P(f)}{B}\right)$$

where p_{ref} is the underwater reference pressure 1 μPa, f_u and f_l are the upper and lower frequency limits considered, *P(f)* is the power spectrum level at frequency *f*, and *B* is the noise power bandwidth of the window function (*B* is 1.5 for the Hanning window used in all sound analyses, see Merchant et al., 2015 for more detail). Essentially the broadband SPL, at a given time, is the SPL summed over the entire frequency range considered, of the noise at that time.

The RMS level is useful to quantify an average level over a period of continuous noise. It is calculated by taking the average of the level over time before converting to dB (i.e., before applying the log function) (Merchant et al., 2015)

$$SPL_{rms} = 10log_{10}\left(\frac{1}{N}\sum\frac{p^2}{p_{ref}^2}\right)$$

where *N* is the number of samples in the averaging period, given by the sampling frequency (in Hertz) multiplied by the averaging period (in seconds).

Absolute sound levels were obtained with the use of the pistonphone calibration tones on each recording. Calibration was carried out using the *PAMGuide* toolbox (from Merchant et al., 2015) in Matlab (Matlab 2014b, The Mathworks Inc.). The uncalibrated level a of the pistonphone tone at 250 Hz was determined using a power spectrum in *PAMGuide* (1s Hanning window, 50% overlap). This was then compared to the known level b produced by the pistonphone (re 1 μPa: taking into account the effect of the couplers for each hydrophone) to produce a system sensitivity *S*:

$$S = b - a$$

S was then used as a correction factor for the corresponding recording.

Third Octaveband levels (TOLs), power spectral densities (PSDs) and broadband levels were calculated using the *PAMGuide* toolbox (see Merchant et al., 2015 appendix S1 for equations). The difference between TOL and PSD levels is that TOLs are summed within a frequency band, i.e. the 1/3 octave bands, while PSDs give levels per 1-Hertz band. Hence the TOLs are higher than the PSD levels for the same frequency and increase with frequency due to the increasing size of 1/3 octave band (with frequency). PSD levels are useful for comparing to measurements in other studies of noise, while TOLs may be more biologically relevant - by filtering sound into critical bandwidths it mimics how dolphin hearing systems are thought to work (Johnson 1968, Merchant et al., 2015).

2.3 RESULTS

Long term monitoring

Variation in harbour noise over a one month period was measured using the broadband level (Fig. 2.2), with corresponding power spectral density (PSD) (Fig. 2.3). A circadian pattern is apparent, particularly in the PSD plot, with higher levels observed during the day than at night. The majority of the energy is between 100 Hz and 20 kHz, with the lower frequencies most likely due to large vessel traffic, while the medium frequencies are likely due to sea surface agitation (such as breaking waves, wind, spray and bubble collapse) as well as small vessel traffic (Hildebrand 2009). These records included some piling noise (arrows in Fig. 2.2). At this mid-harbour site there is no clear distinction between broadband levels on days with piling to those on days without. This is so for several reasons. Firstly, the piling was happening 1.9 km away from the recording location. Secondly, periods with piling made up a relatively small portion of the noise record for a 24 hour period. Finally, while the peak-to-peak levels of the pile-driving noise are high, the duration is very short, particularly relative to the amount of background noise in a given sequence of strikes. The RMS level of the duty cycle period was 117.9 dB re 1 μPa, with a median of 106.7 dB re 1 μPa.

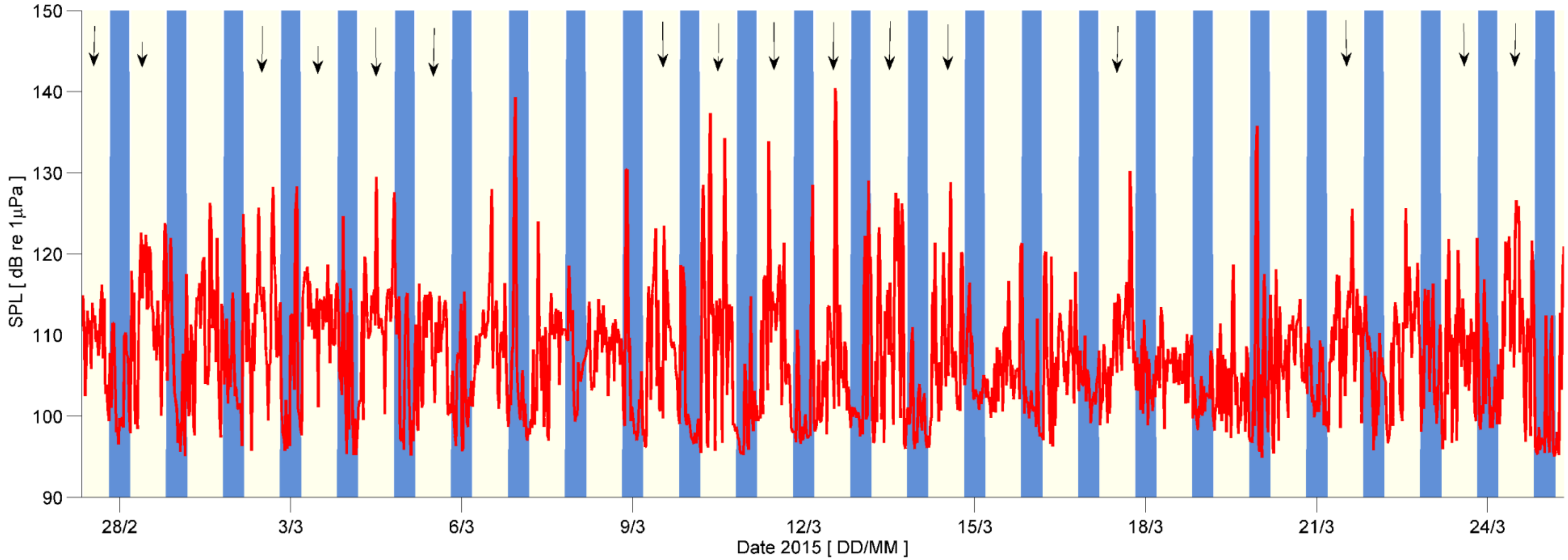

Figure 2.2 Variation in broadband level, from DSG recorder setup on a duty cycle recording 5mins every hour from 27/2/15 to 25/3/15, with frequency range 30 Hz-40 kHz, range to piling is 1.9 km, with shielding from Sticking Point. Each 5 min section has been time averaged to one data point using the Welch method. The light yellow background represents daylight hours from 6:00 am to 9:00 pm, while the dark blue background represents darkness hours. Date labels correspond to 00:00 am at the start of the corresponding day. Arrows indicate days which contained piling.

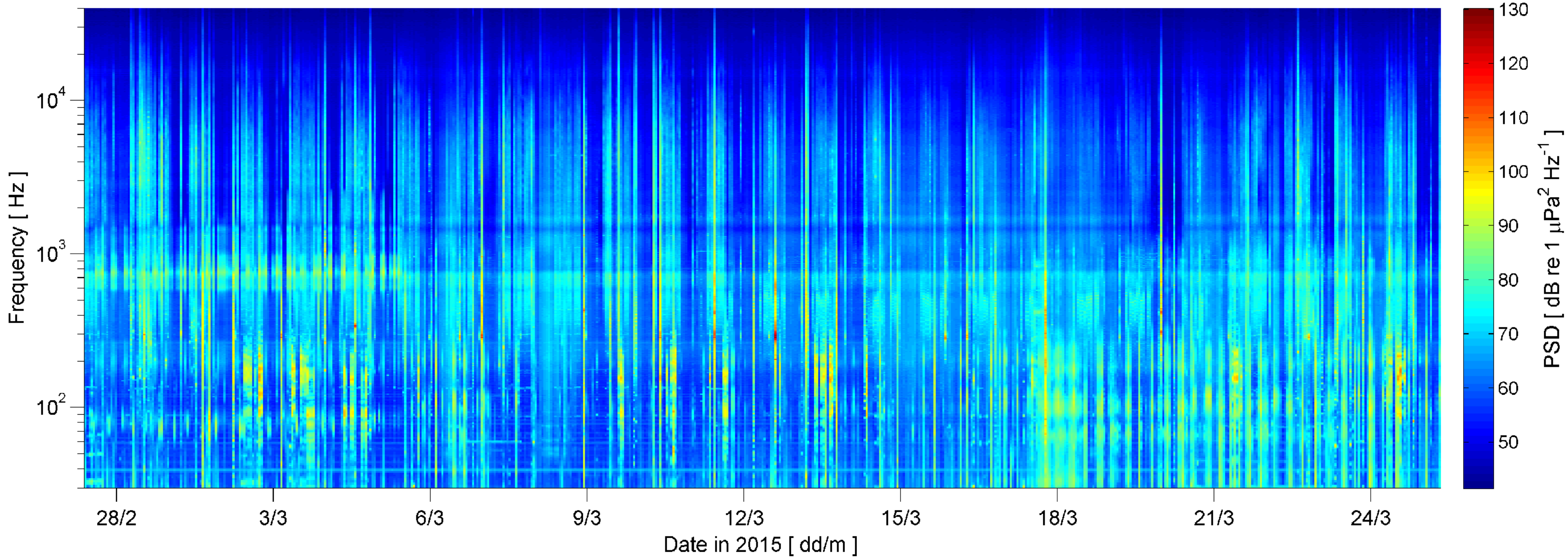

Figure 2.3 Variation in PSD, from DSG recorder setup on a duty cycle recording 5 mins every hour from 27/2/15 to 25/3/15, with frequency range 30 Hz-40 kHz, at a range of 1.9 km from the piling, with shielding from Sticking Point. Each 5 min section has been time averaged to one data point using the Welch method. Date labels correspond to 00:00 am at the start of the corresponding day.

Ambient noise levels had a peak frequency at around 300 Hz and reached a maximum PSD level of 126 dB re 1 μPa^2 Hz^{-1} (Fig. 2.4). Usually, however, ambient levels were around 60 dB re 1 μPa^2 Hz^{-1}. There appear to be two broad peaks in the spectrum, centred around 300 Hz and 4 kHz respectively, with the former about 10 dB higher (RMS) than the latter. Most energy is contained within the range from 100 Hz to 10 kHz, with a dip around 1.5 kHz.

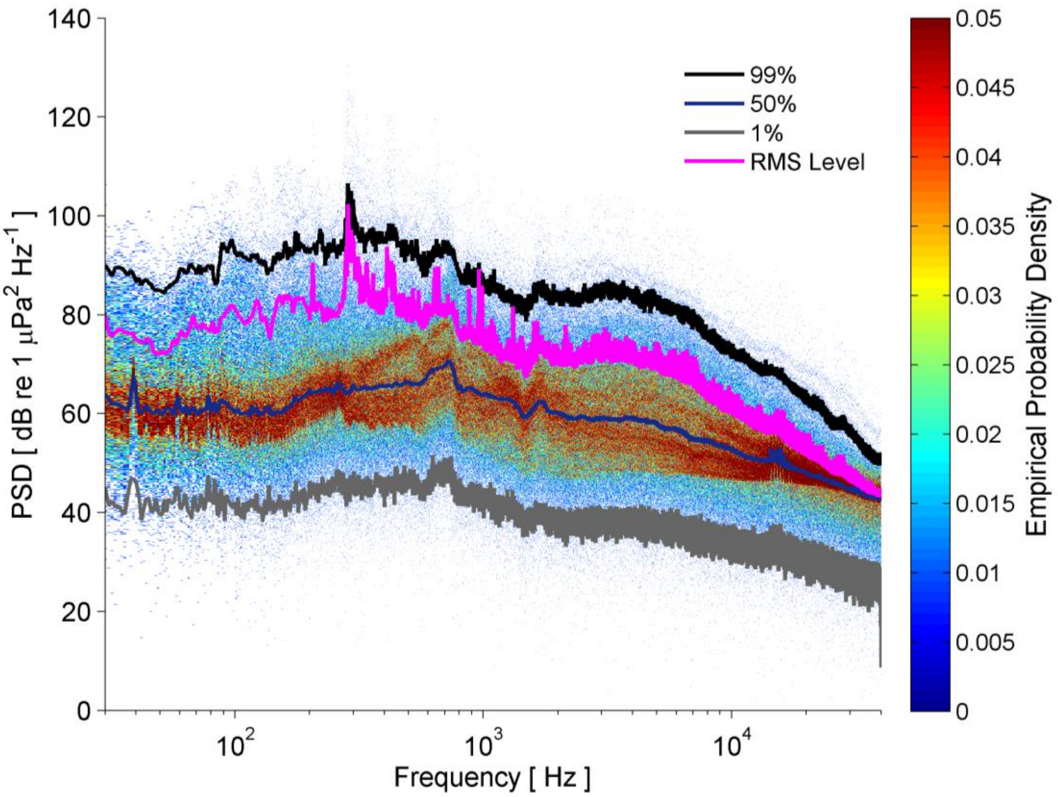

Figure 2.4 Power spectral density levels averaged over period from 27/2/15 to 25/3/15, sampling 5 minutes every hour, excluding samples that contain pile-driving or vibro-hammer noise. Frequency range 30 Hz to 40 kHz

Short-term measurements of ambient noise

Having a DSG recorder sampling on a duty cycle enabled the collection of ambient noise data over an extended period (26 days) from the mid-harbour site. Shorter recordings made with other moored recorders (during breaks in piling activity) allow measurement of ambient noise in two more locations (‘SoundTrap’ and ‘DSG’ on map in Fig. 2.1). The large variation in SPL (Fig. 2.5) reflects the nature of the area; being a harbour, the sounds observed can range from quiet sea state zero background noise to the noise of large commercial vessels. Mean levels across this period were 118.4 dB re 1 μPa for the SoundTrap and 119.4 dB re 1 μPa for the DSG.

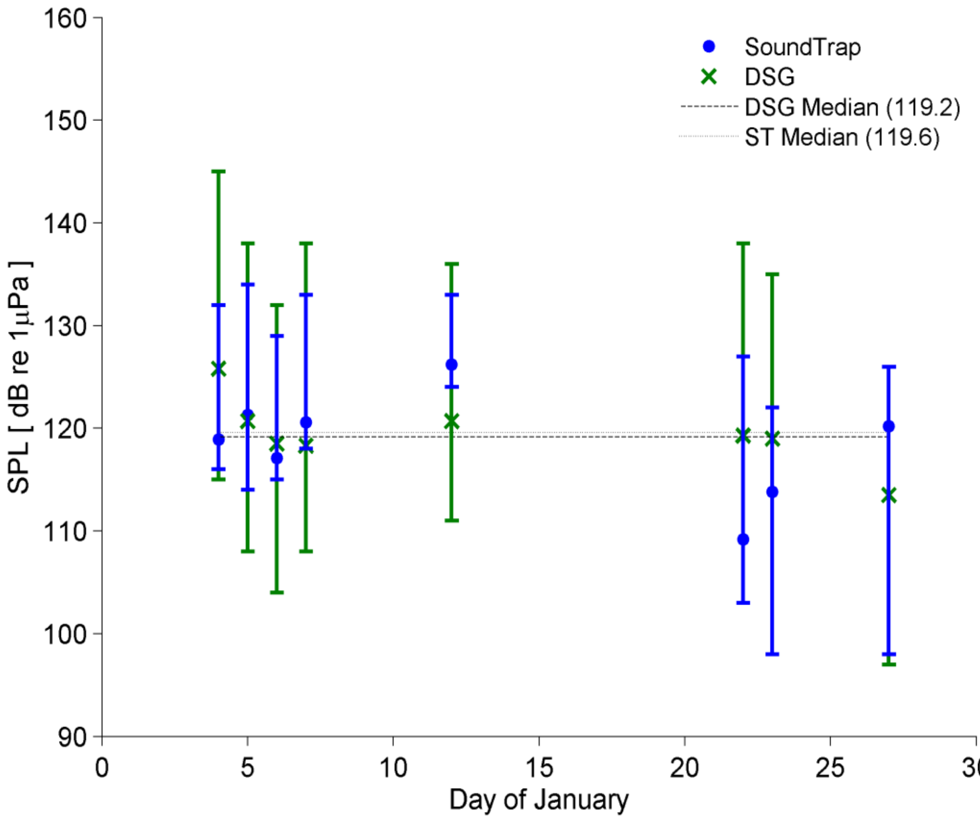

Figure 2.5 RMS level of 30 mins of ambient noise during periods without piling noise. The levels for 4/1/15 and 12/1/15 were taken from 12:14pm and 13:42pm respectively, the rest were all taken at 10:00am. The blue dots are levels recorded by the SoundTrap, approx. 370 m from the piling, frequency range 30 Hz-144 kHz, the green dots are levels recorded by the DSG at a range of approx. 750 m (30 Hz-40 kHz). Error bars show the range of SPLs recorded in the 30 min sample.

RMS third octave levels (TOLs) were calculated for each day for both the SoundTrap (Fig. 2.6) and the DSG (Fig. 2.7). Self-noise (grey line at 'day' 30) was recorded with the recorder enclosed in a metal case to shield the 50 Hz hum of building wiring, placed in a quiet room, and programmed to record for 10 minutes in the middle of the night.

Close to the wharf (SoundTrap, see Fig. 2.1 for location) the peak energy is around 1 kHz though some days the noise contained significant energy below 100 Hz (Fig. 2.6). At the channel (location 'DSG' in Fig. 2.1) it appears there are two dominant frequency ranges around 300 Hz and 5 kHz (Fig. 2.7). The higher frequencies above 10 kHz do not contain a significant amount of energy, and levels decrease with increasing frequency at both locations. Above 60 kHz self-noise of the SoundTrap exceeds ambient noise.

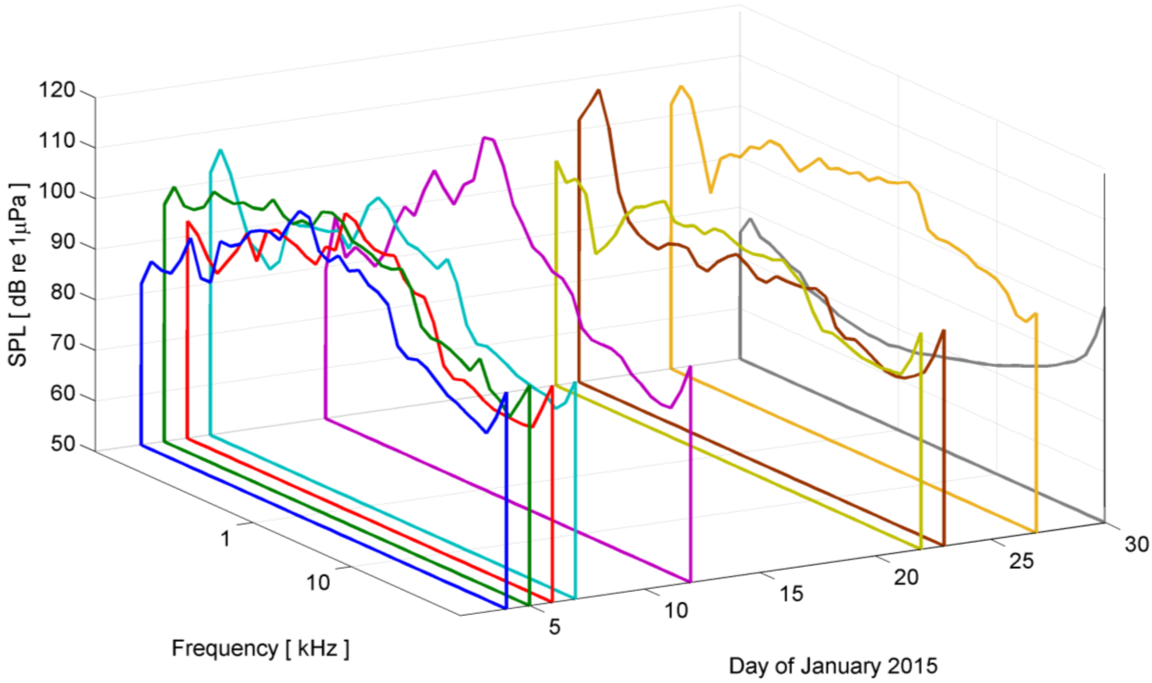

Figure 2.6 Variation in TOLs (RMS) from 4/1/15 to 27/1/15, at the SoundTrap location (370 m from wharf), frequency range 30 Hz-144 kHz. The levels (calculated from 30 min sections) for 4/1/15 and 12/1/15 were taken from 12:14pm and 13:42pm respectively, the rest were all taken at 10:00am. The grey line indicates self-noise of the SoundTrap.

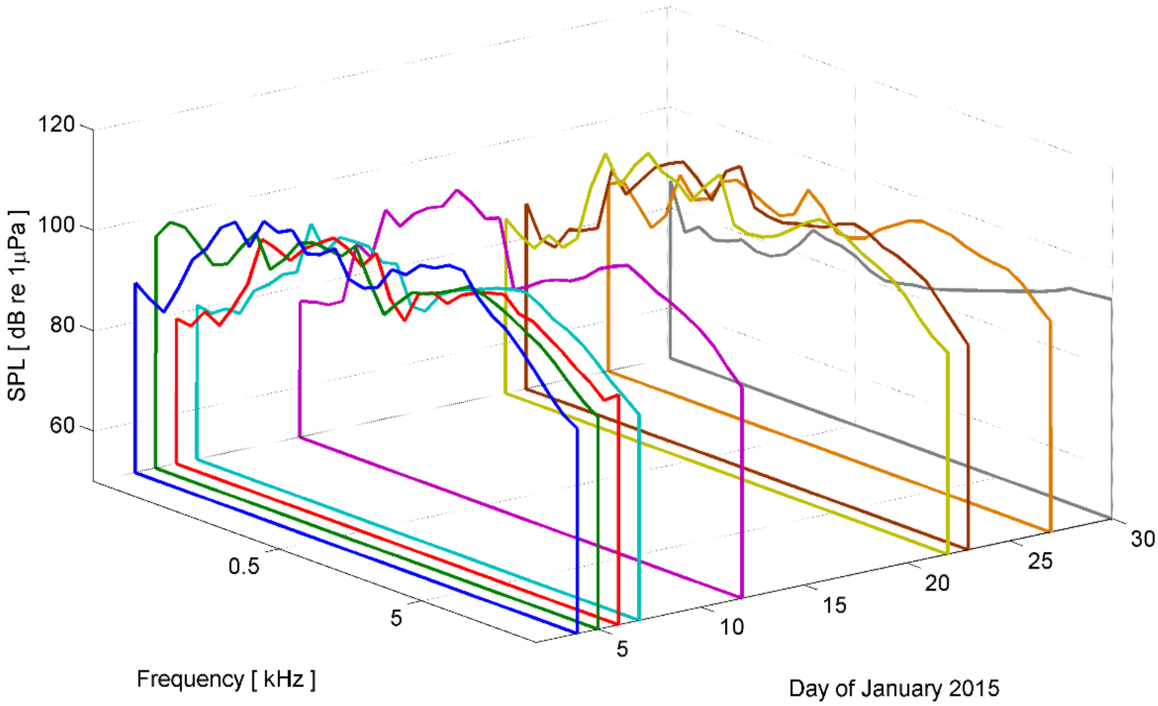

Figure 2.7 Variation in TOLs (RMS) from 4/1/15 to 27/1/15 at the DSG location (750 m from the wharf), frequency range 30 Hz-40 kHz. The levels (calculated from 30 min sections) for 4/1/15 and 12/1/15 were taken from 12:14pm and 13:42pm respectively, the rest were all taken at 10:00am. The grey line indicates self-noise of the DSG.

Average spectra for ambient noise at three sites show highest SPLs at the SoundTrap and Channel DSG locations (Fig. 2.8).

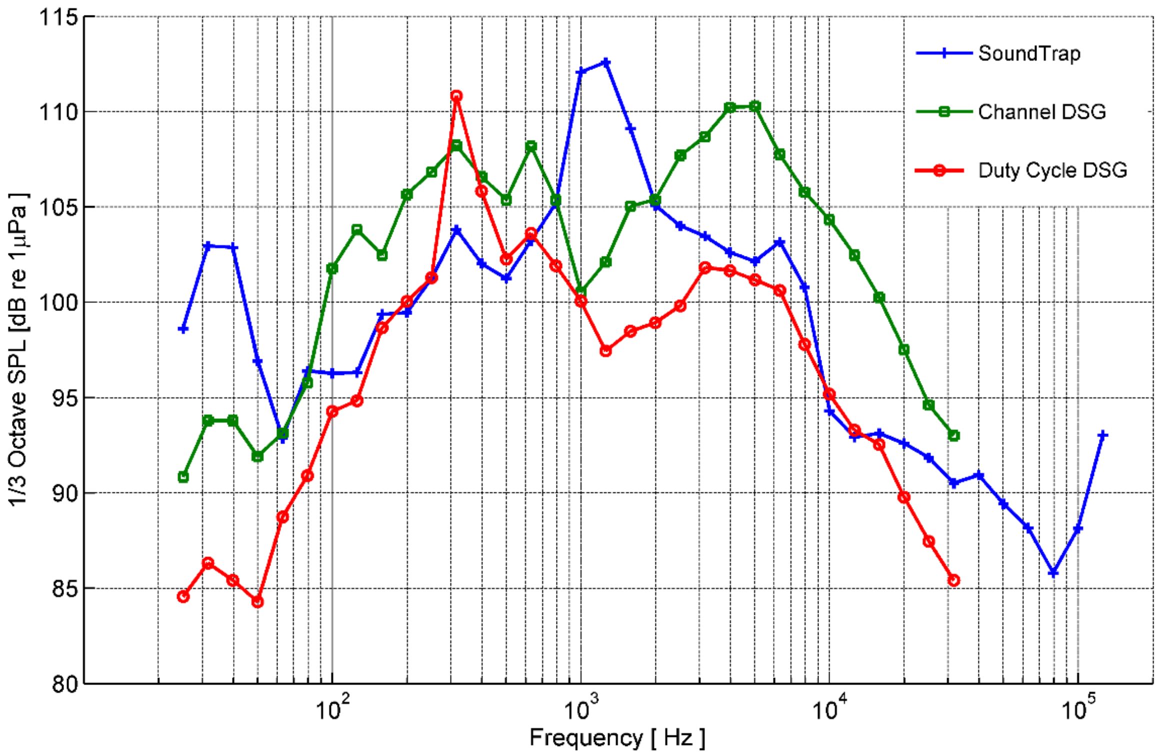

Figure 2.8 Average TOLs at 3 ranges from wharf: 370 m (SoundTrap, blue crosses), averaged (in the pressure domain) over the recording period 4/1/15-27/1/15, frequency range 30 Hz-144 kHz; 750 m (channel DSG, green dots), frequency range (30 Hz-40 kHz) and 2 km (duty-cycle DSG, red squares) averaged over duty cycle recording from 27/2/15 to 25/3/15, frequency range 30 Hz-40 kHz.

The outermost site, where the duty-cycle DSG was deployed, was quietest, apart from a peak around 300 Hz. The SoundTrap and channel DSG levels are averaged over recordings made between 4/1/15 to 27/1/15, while the duty cycle DSG was in place from 27/2/15 to 25/3/15. Hence, the differences in averages may be due to differences in shipping and other port noise between these periods. Except for the peak around 300 Hz, the duty cycle DSG and channel DSG show a similar spectrum shape, with the duty cycle DSG having slightly lower levels.

An example of the variation in broadband ambient noise over the course of a few hours can be seen in figure 2.9. This noise was recorded on 5 January 2015 from 8:18am to 12:36pm, a day on which no piling occurred in the morning. The recording was time-averaged every five seconds using the Welch method in *PAMGuide* (Merchant et al., 2015) to produce the broadband SPL level. The median SPL level of the recording was 117.3 dB re 1 µPa at close range from the wharf and 114.1 dB re 1 µPa at medium range (Fig. 2.9).

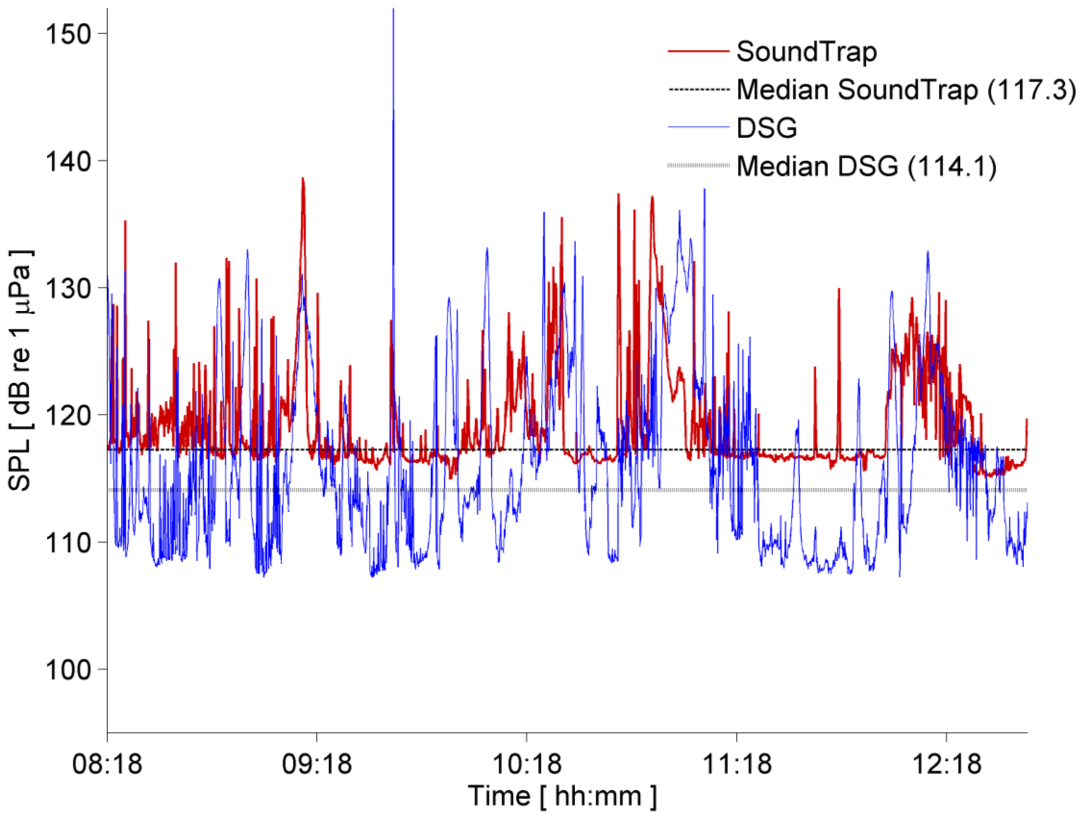

Figure 2.9 Short-term variation of ambient noise in Lyttelton Harbour (on the morning of 5/1/15). The red line indicates the broadband level measured by the SoundTrap (30 Hz-144 kHz) at a range of 370 m from the wharf, blue is the broadband level measured by the DSG (30 Hz-40 kHz) at a range of 750 m. Levels calculated from a recording time-averaged every 5 seconds. The grey line is the median SPL across the 4 hours for the DSG, the dotted line for the SoundTrap (mean SPLs were 123.4 and 122.1 dB re 1 µPa respectively).

The power spectral densities (PSDs) of the two recordings (SoundTrap in Fig. 2.10, DSG in Fig. 2.11) show that most of the ambient noise is below 2 kHz with broadband noise events (passing vessels) containing energy above 10 kHz. The higher overall dB level of the broadband noise at the SoundTrap location (Fig. 2.9) is reflected in the higher dB level across the lower frequencies (mainly below 2 kHz) in the corresponding PSD (Fig. 2.10). This is likely due to an increase in general port noise such as generator and engine noise as well as other construction noise at close range to the port.

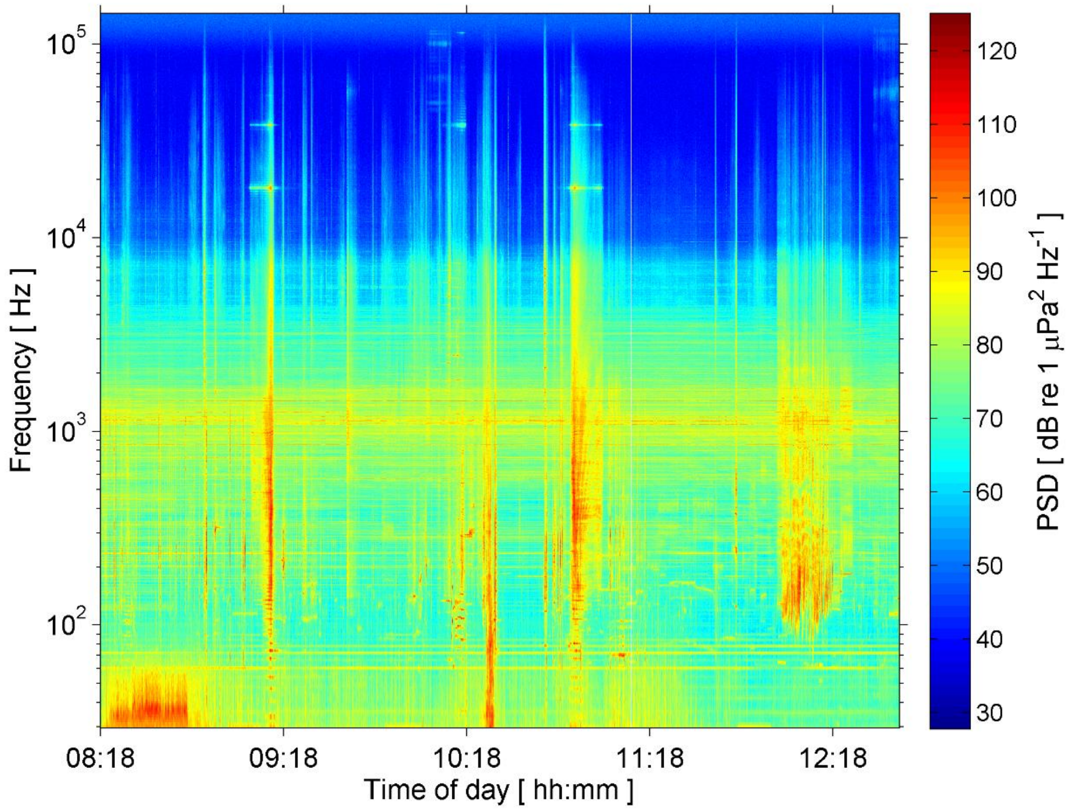

Figure 2.10 Power spectral density of ambient noise on the morning of 5/1/15, at a range of 370 m from the wharf, with a 5 s averaging time, frequency range of 30 Hz-144 kHz

There appears to be a low frequency (below 100 Hz) noise for several minutes at the start of the close-range recording that is not apparent in the DSG recording. This again may be due to the shallow water low frequency cut-off proposed by Jensen et al. (2011), see appendix section 1 for more detail.

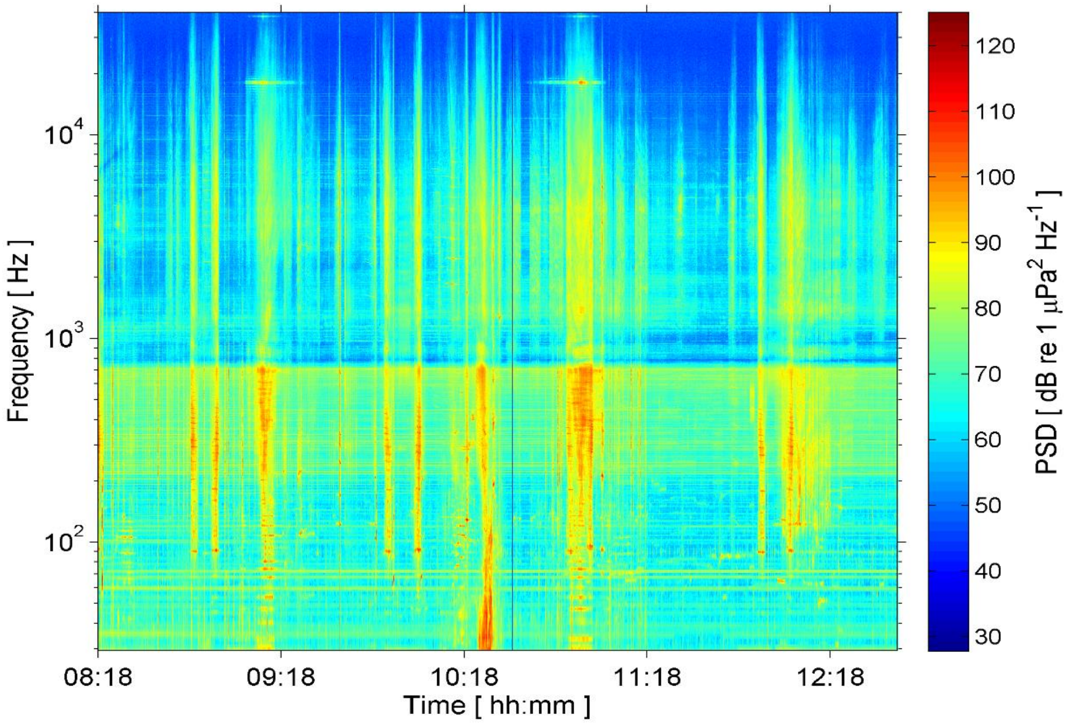

Figure 2.11. Power spectral density of ambient noise on the morning of 5/1/15, at a range of 750 m from the wharf, with a 5s averaging time, frequency range of 30 Hz-40 kHz

Analyses of ambient noise were restricted to periods without piling. We also recorded ambient noise on 23 January from 8:34 am to 11:44 am. This was the only day we were able to make recordings with no ships docked in the harbour. However, piling did occur, restricting the amount of ambient noise data available. To avoid this contamination I sampled 10 s every 20 mins to represent the ambient noise in the recording (Fig. 2.12).

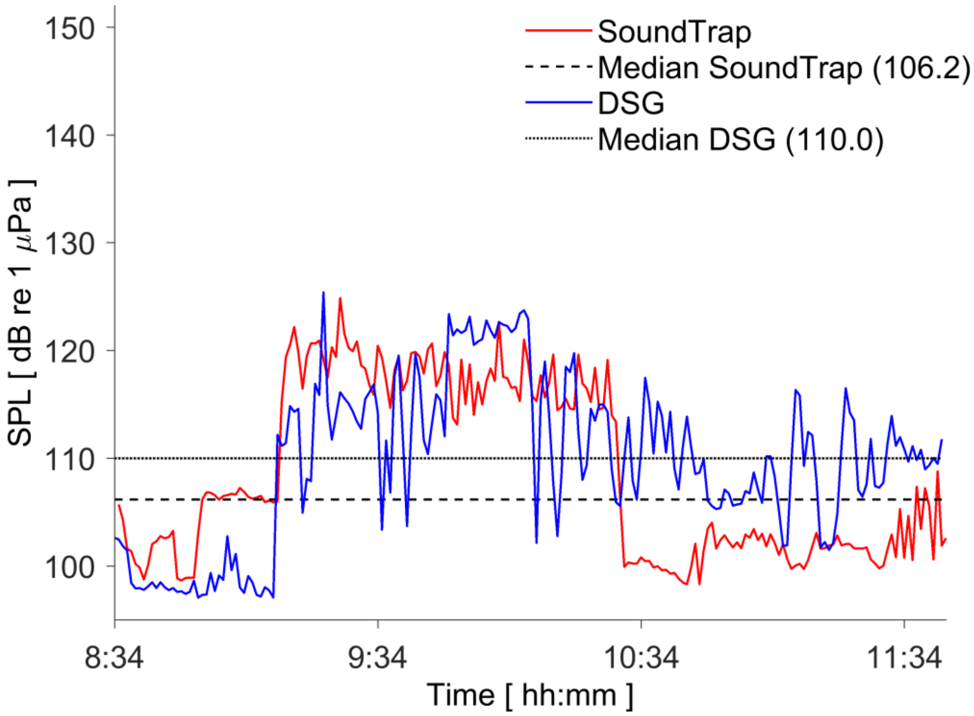

Figure 2.12 Variation of ambient noise in Lyttelton harbour on the morning of 23/1/15. The red line indicates the broadband level measured by the SoundTrap (30 Hz-144 kHz) at a range of 370 m from the wharf, blue is the broadband level measured by the DSG (30 Hz-40 kHz) at a range of 750 m. Levels are calculated from a recording sampled for 10 seconds every 20 minutes. The grey line is the average level across the 4 hours for the DSG, the dotted line for the SoundTrap (mean SPLs were 115.1 and 114.8 dB re 1 µPa respectively).

The median SPL levels at both locations were significantly lower than the levels for the morning of 5/1/15. This is most likely due to the lack of ships docked at the wharf this day. Even when docked, ships usually have generators and other machinery running (C. Coleman, Lyttelton Pilot, 2017, pers. comm.), and there is noise associated with loading and unloading. The higher median level recorded on the DSG is probably due to its closer proximity to vessel movements. Additionally, water movement was likely higher in the channel than at the wharf next to the breakwater, contributing to the higher overall noise level at the DSG. Flow noise is likely to be responsible for the band of noise centred on 700 Hz (Fig 2.13). The power spectral densities for this period are shown in figures 2.13 and 2.14. As for the PSDs of 5/1/15 (Figs 2.10, 2.11), the majority of the energy is below 2 kHz. A low frequency component can be seen in the SoundTrap recording from about 9:14 to 10:30am while not apparent in the DSG recording, similar to the PSDs for 5/1/15.

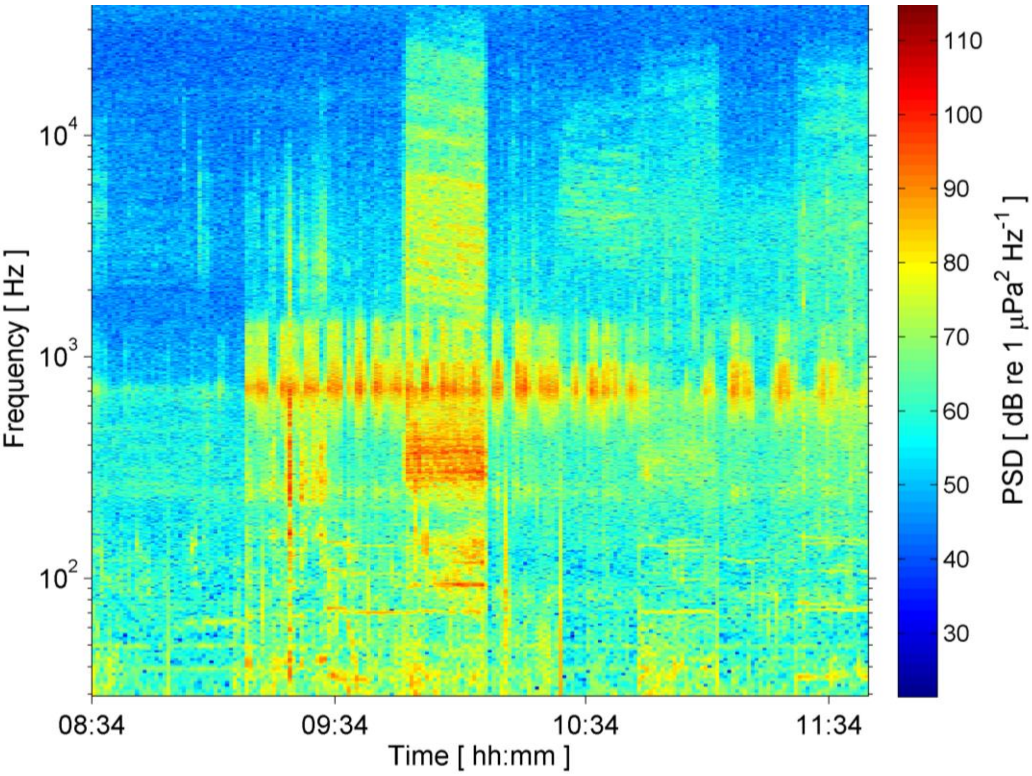

Figure 2.13 Power spectral density of ambient noise on the morning of 23/1/15, recorded on the DSG at a range of 750 m from the wharf, sampled at 10 s every 20 mins, frequency range of 30 Hz-40 kHz

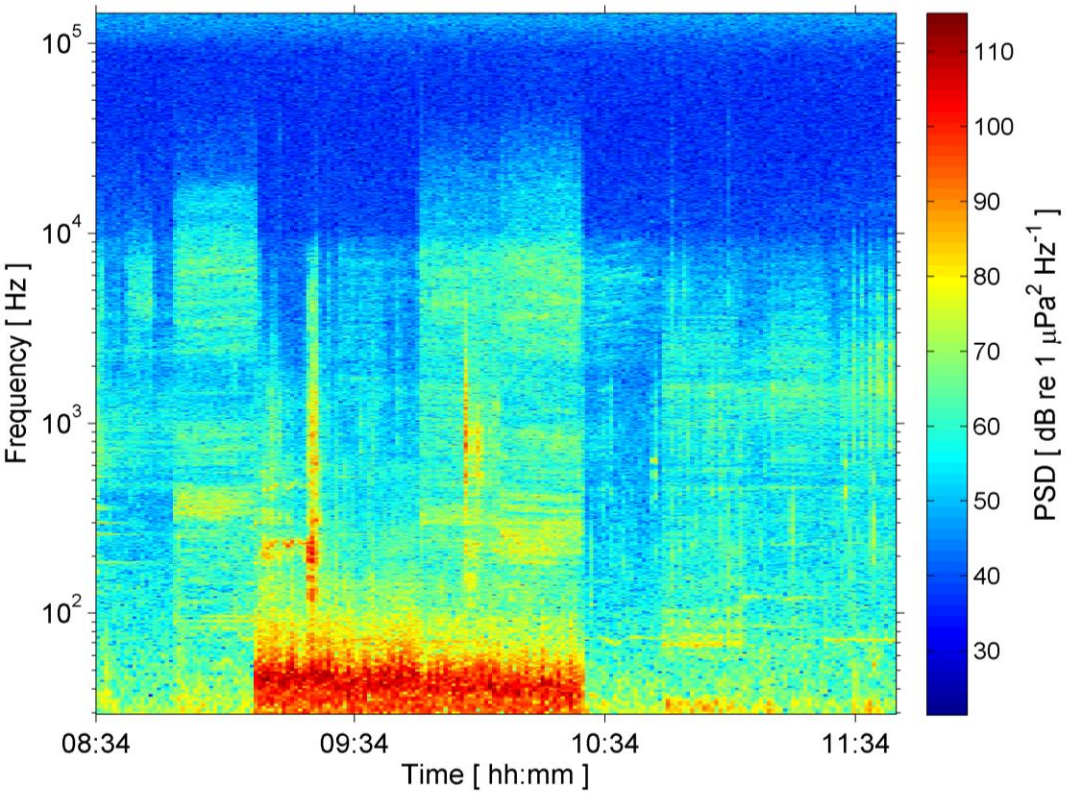

Figure 2.14 Power spectral density of ambient noise on the morning of 5/1/15, recorded on the SoundTrap at a range of 370 m from the wharf, sampled at 10 s every 20 mins, frequency range of 30 Hz-144 kHz.

2.4 DISCUSSION

The main objectives of this thesis were to characterise piling noise and its propagation within Lyttelton Harbour (Ch. 3), and to quantify how dolphin distribution was influenced by piling activity (Ch. 4). These objectives cannot be realised without understanding ambient noise conditions in Lyttelton Harbour.

Ambient noise as defined in this study included anthropogenic noise, apart from the additional noise from the construction work. Recordings of specific vessels regularly seen in Lyttelton harbour are presented in the appendix, section 2.

The classic study of ambient noise, Wenz (1962), gives general levels of common ambient noise sources, summarising data provided by Knudsen (1948) and others. They report the equivalent of a power spectral density level of 63 dB re 1 µPa at 500 Hz (Beaufort scale 3) as being typical of shallow water. Over a month of recording in the mid-harbour in March 2015, average PSD levels (RMS, at 500 Hz) were measured to be over 20 dB higher (see Fig. 2.4). Some of this difference may be due to those recordings being made in higher Beaufort Sea states, but the major difference probably arises from Lyttelton being a busy industrialised port. Bailey et al., (2011) recorded much lower ambient noise levels in deeper water near an offshore windfarm in Scotland. On the other hand, much higher background noise levels (by up to 20 dB higher than the current study) were recorded in Blackwell (2005) in the coastal waters of Port MacKenzie, Alaska. These high levels were due to the recording location being near an industrial area and some recordings were made in the presence of strong currents.

The TOLs at the channel marker (recorded by the duty cycle DSG) and in the channel (recorded by the reference DSG) show a similar spectrum shape apart from a peak at 300 Hz, and overall slightly lower levels, in the duty cycle DSG record (Fig. 2.8). The latter may be explained by the duty cycle data containing recordings across the entire 24-hour day, including the often quieter night-time hours (as seen in Fig. 2.3). The peak at 300 Hz may be due to recordings made in high wind speeds, rain and high sea states, contributing to elevated ambient noise levels compared to the boat based recordings, which were necessarily made on reasonably calm days. It is possible this peak is partly due to shipping noise as this recording, being next to the shipping channel, would have recorded many passing vessels (see Fig A.3). However, the frequency content of small boat sounds generally has most energy in the 1000 – 5000 Hz range, while for cargo ships this is in the 40 - 100 Hz range (Hildebrand et al., 2009). Additionally, the peak may be due to a long term continuous sound (as opposed to the transient passing of a vessel) such as generator noise from the port. A straight horizontal line can be seen in the long term PSD levels of the duty cycle DSG record (Fig. 2.3), and more clearly in Fig. A.3, though this recording was made at the DSG reference position (see ‘DSG’ in Fig. 2.1). These horizontal lines in PSD levels are also seen in the recordings by the SoundTrap and the DSG. At the SoundTrap, this ‘band’ contains energy between 200 and 1100 Hz (Fig. 2.10) with the highest energy between 1000 - 1100 Hz, corresponding to the peak in TOLS at this location (Fig. 2.8). The corresponding DSG recording shows a similar band, although the frequency range is 200 – 700 Hz. If this long term continuous sound originates from the wharf, the reduction is frequency bandwidth at the DSG is likely due to the increased absorption of higher frequencies in propagation. The horizontal band is less apparent in the duty cycle PSD, although horizontal lines appear at 300 Hz and 700 Hz. It is likely that shielding of the breakwater at Sticking Point influenced the frequency content at the location of the duty cycle DSG. This band is less obvious in the PSD levels recorded on a later day (Fig. 2.14), during a time when no ships were docked at the wharf, suggesting that this band of sound could be produced by docked ships and the port servicing them. A similar band is observed in some spectrograms recorded in Fremantle Harbour, Australia (Salgado Kent et al. 2012).

The SoundTrap recorded higher levels at lower frequencies (below 60 Hz) (Fig. 2.8, see also Fig. 2.10 compared to Fig 2.11, and Fig 2.14 compared to Fig. 2.13)). This could be due to water depth. The SoundTrap was moored in deeper water which is more supportive of propagation of low frequencies than shallow water (see Fig. A.1 in appendix).

Several papers report values for either TOL or PSD levels that are similar to our measurements from Lyttelton (e.g., Erbe 2009; Munger et al., 2011; Menze et al., 2013). Likewise, Nedwell et al., (2003) and Lucke (2011) show similar mean spectral levels (PSD and PSD integrated over 1/3 octave-band levels). However, the levels in the current study are relatively higher between 1 and 10 kHz, which may be due to snapping shrimp (Everest et al., 1948). The peak around 1 kHz could be due to the noises of sea urchins (common in New Zealand), amplified by the shape of their skeletons (Radford et al. 2008).

A circadian pattern was observed in the long term PSD levels at the channel marker, with higher levels during the day in a wide frequency range from 60 Hz to 10 kHz (Fig. 2.3). This is likely due to the increased anthropogenic activity (such as shipping, port activity, recreational boat use, and construction work) during the day. However, underwater sound levels in the harbour could vary significantly on a short time scale (e.g., Fig. 2.9), due to transient events such as boats passing by. The RMS broadband levels measured at the SoundTrap and DSG locations could vary by 40 dB within a day (Figs 2.2 and 2.5), while PSD levels at the duty cycle DSG could vary by about 60 dB within one day, at the same frequency (e.g., at 12/3/15 in Fig. 2.3).

Salgado Kent et al., (2012) also recorded ambient noise in a harbour environment (Fremantle Harbour, Australia) obtaining similar SPLs, typically between 110 and 140 dB re 1 μPa, however, their mean hourly levels during the day are around 10 dB higher than the overall RMS level (117.9 dB) recorded in the present study. This could be explained by the fact that Fremantle harbour experiences much higher vessel traffic than Lyttelton (MarineTraffic 2016). Also this could explain the bigger difference between 'day' and 'night' SPLs seen for Fremantle Harbour.

Hector's dolphins in Lyttelton harbour are, thus, regularly exposed to broadband sounds with varying levels both in time and space. Most sounds, however, do not contain significant energy in the frequency range in which Hector's dolphin hearing is expected to be most sensitive (100 – 150 kHz), except noise from transient event such as passing vessels (see Fig. 2.10). Despite the low level of this noise in the sensitive hearing range, it has been shown that exposure to low levels of high frequency vessel noise can lead to strong behavioural responses in harbour porpoise (Dyndo et al., 2015).

Ambient noise levels measured in busy coastal areas were compared to the average level in Lyttelton Harbour (Table 2.2). The order of entries is based on the relative loudness compared to Lyttelton. This order is a very approximate estimate as it is difficult to compare different methods of noise measurement. A more accurate comparison would need to control for range to noise sources, time of day of recordings and recorder depth, which is not possible using the information reported. Therefore, only the metric and frequency range used in each study were accounted for in the comparison (Table 2.2). The table is intended to provide some indication of how average ambient noise level in Lyttelton compares to other locations with a high amount of anthropogenic noise. The overall value for Lyttelton was determined as the mean broadband level across the duty cycle period (as shown in Fig. 2.2), 118 dB re 1 μPa. Most studies did not compute an overall sound level to represent the noise level of the area, as this level would vary considerably over time, as it does in Lyttelton. Also, areas in which recordings took place varied significantly in the types of sound sources that were present. The recorders in Massachusetts Bay, Hong Kong, Guanabara Bay and the Port of Santos would have recorded large vessels travelling to and from the port, while those in Cres-Lošinj and

Peconic Bay would have recorded mostly small vessel traffic. Looking at Lyttelton's rank (Table 2.2) shows that its average ambient noise level is about mid-range, compared to other busy places. Most other harbour studies record higher levels of ambient noise, although their measurements were further from shore with greater likelihood of recording large vessels travelling at higher speed. However, the average Lyttelton level was only 2.5 dB lower than in the shipping lanes in Massachusetts Bay which contains a major seaport, the Port of Boston. Propeller cavitation is often the main contributor to ship noise (Ross 2013) and this noise increases with speed (Arveson & Vendittis 2000). The greatest occurrence of cavitation noise in Lyttelton will likely be near the wharf during berthing of large vessels (Chris Coleman, Lyttelton Pilot, 2017, pers. comm.). Small vessel traffic in Lyttelton will also contribute a significant amount of noise. Compared to other sites with mainly small vessel traffic (Samuel 2005, Erbe 2009) Lyttelton tends to be louder except for Rako et al., (2013).

Table 2.2. Underwater ambient noise levels in places around the world with high anthropogenic activity. The 'Equivalent level for Lyttelton' was adjusted based on the metric and frequency range used in the other studies. Relative order was based on the difference between the measured level (column 2) and the equivalent Lyttelton level (column 5), if the measured level was a range, the midpoint was used as the overall measured level for computing this difference.

Location, country	Distance from recorder to shore	Sound level (dB re 1µPa)	Frequency range (Hz)	Equivalent level for Lyttelton (dB re 1µPa)	Reference
Guanabara bay, Brazil (harbour)	< 10 km	85 – 120	187	83	Bittencourt et al., 2014
Cres-Lošinj, Croatia (tourist area)	< 10 km	125 – 131	63 – 2000	118	Rako et al., 2013
Fuel receiving facility, Hong Kong	100-1000 m	112 – 147	10 – 20000	118	Würsig & Greene 2002
Fremantle Harbour, Australia	< 100 m	110 – 140	10 – 4500	118	Salgado et al., 2012
Port Mackenzie, USA	< 2 km	115 – 133	10 – 10000	118	Blackwell et al., 2005
Port of Santos, Brazil	Close to harbour entrance, range not given	100 – 143	10 – 8000	118	Padovese 2015
Massachusetts Bay, USA (harbour)	40+ km (in shipping lanes)	119.5	10 – 1000	117	Hatch et al., 2008
Lyttelton, NZ (harbour)	1.9 km (distance to wharf)	118 (mean broadband level)	30 – 40000	118	Present study
Moreton Bay Australia (ferry and fishing boats)	< 2 km	87 (mean TOL at 50th percentile)[a]	100 – 1000	87	Erbe 2009
St Lawrence Seaway, Canada	<1 km	117	100 – 23000	118	McQuinn et al., 2011
Edge of St Lawrence estuary, Canada	<5 km	114	100 – 23000	118	McQuinn et al., 2011
Saguenay River, Canada	<1 km	112	100 – 23000	118	McQuinn et al., 2011
Peconic Bay estuary, USA (recreation)	120 m	83 – 113	200 – 700	117	Samuel et al., 2005

[a]*Calculated retrospectively using TOL graph in Erbe 2009, not stated as a measured level.*

It was difficult to achieve quiet recording conditions. Potential recording days were heavily limited by weather and sea state conditions and by the pile-driving schedule. This affected our ambient noise measurements, which would have benefitted from a larger sample size. However, this study presents the first quantitative data on ambient noise in Lyttelton Harbour, and provides baseline levels to compare the pile-driving noise to, and to measure change in ambient noise over time. A more detailed study of ambient noise in Lyttelton would be a useful focus of future work.

General Conclusions

Ambient noise in Lyttelton Harbour was highly variable in time and space. PSD levels over a month-long period showed higher levels during the day across a broad frequency range. Ambient noise levels during this time varied by up to 40 dB within one day. Overall, RMS levels near the wharf tended to be similar to the levels near the channel. However, the spectra showed different peak frequencies: around 1 kHz near the wharf instead of 300 Hz and 4 kHz near the channel. Ambient noise was influenced by various anthropogenic sources such as large and small vessel traffic and generators, particularly in the low frequency range, as well as potential natural sources such as wind, rain and snapping shrimp which are more important contributors to the mid-to-high frequency range. Underwater noise levels in Lyttelton Harbour are comparable to those found in other ports, although very busy ports show much higher levels.

Chapter 3

Pile-driving Noise in Lyttelton harbour

3.1 INTRODUCTION

The loud underwater noise produced by pile-driving has been established as a serious threat to some marine mammal species (Thompson et al., 2013). This noise has been extensively studied in relation to windfarm construction (Nedwell et al., 2003 and 2007; De Jong & Ainslie 2008; Tougaard et al., 2009; Bailey et al., 2010; Norro et al., 2010; Brandt et al., 2011) but less so in terms of wharf construction (Würsig et al., 2000; Blackwell 2005; Paiva et al., 2015)

Impact pile-driving radiates noise into the water and sediment surrounding the pile. The majority of the underwater noise arises from radial expansion of the pile as it is struck by the hammer, radiating directly into the water column (Reinhall & Dahl 2011; Tsouvalas & Metrikine 2014). Energy is also transferred into the seabed, and can radiate back into the water, or travel as surface waves (Sholte waves) along the water-seabed interface. For these reasons pile-driving noise does not behave strictly as a "point" source. Generally the sounds are loud, impulsive and broadband. Studies of harbour porpoise show strong avoidance reactions in wild animals (Tougaard et al., 2009; Brandt et al., 2011; Dähne et al., 2013) and temporary hearing damage in captive animals (Kastelein et al., 2015) when exposed to pile-driving noise. Additionally, a study on bottlenose dolphins has shown the potential for masking of communication whistles for up to 40 km from the pile-driving activity (David 2006).

Limits on noise level exposure have been proposed for pile-driving noise in order to minimise impact on cetaceans (Madsen et al., 2006; Southall et al., 2007, Tougaard et al., 2015). Anthropogenic underwater noise is regulated in some countries (e.g., Germany, the United States and Australia; Erbe 2013). In New Zealand the only restrictions are provided under the (voluntary) 2008 Code of Conduct for Minimising Acoustic Disturbance to Marine Mammals from Seismic Survey Operations (DOC 2008). In order to ensure the noise does not exceed recommended exposure limits, and to be able to compare to similar scenarios, it is important to model the propagation of sound throughout the surroundings.

Propagation of sound in water is generally described by two very simple models which predict spreading loss (in dB) with range. In shallow water, where sound propagates cylindrically (because it is bounded by the bottom and the surface), spreading loss is frequently estimated as 10logR, where R is range in metres. In deep water, where sound can propagate in all directions, spreading loss is described as spherical, represented by 20logR (Urick 1983). In practice, sound propagation is much more complex, especially in shallow water (e.g., Pine et al., 2014). The manner in which sound travels is strongly influenced by its frequency, the roughness of the surface, the depth, the nature of the bottom, and any layering in the water column (Urick 1983). Many sound propagation models and modelling software packages exist. However, due to the complexity of sound propagation from this noise source, modelled sound levels can vary significantly from measured levels, particularly due to the influence of bottom layer properties (Lippert & Estorff 2014) as well as bottom and surface reflections in shallow water transmission (Marsh & Schulkin 1962). Currently, there is no available software that can adequately model this complex process in realistic coastal settings (Duncan et al., 2010; Reinhall and Dahl et al., 2011) although many simpler modelling techniques exist (see section 3.4). That pile-driving noise is not strictly a point source, and therefore its source level cannot easily be defined, adds another layer of difficulty (de Jong et al., 2010; Zampolli et al., 2013). For these reasons I have followed a strongly empirical approach in modelling the sound propagation.

Construction noise is a common source of sound pollution in industrialised marine environments. The 2010 and 2011 Christchurch earthquakes extensively damaged the city's port in Lyttelton Harbour. Port development work, in anticipation of a growing increase in container cargo, has been combined with repair work, under the Canterbury Earthquake Recovery Act (2011). This allows relaxation of environmental protection measures for the repair work. A large part of the construction work in repairing and expanding the main wharf involved pile-driving.

In this chapter I aim to quantify the pile-driving sounds, and their propagation within the harbour. I measured both the ambient and pile-driving noise at various locations around the harbour, using several recording platforms. From these empirical measurements of sound level, and hence propagation loss, I modelled sound propagation within the harbour, producing a map of equal loss contours. The propagation map is later used to estimate the ranges at which temporary hearing damage (TTS) in Hector's dolphins may occur based on TTS studies on harbour porpoise. It is not clear which metric best predicts TTS onset but it has been shown to be a combination of pressure level and duration of the sound signal (Mooney et al., 2009; Kastelein et al., 2014). For this reason, estimates of the ranges at which

TTS may occur in Hector's dolphins are based on the durations the dolphins are likely to spend near the wharf (see Appendix section 7).

3.2 METHODS

Field techniques

Figure 3.1. Construction works at Cashin Quay 2, Lyttelton. The BSP hammer in the centre and a pile being positioned on the left.

The pile-driving was done using three different impact hammers (see table 3.1). In each of these hydraulic power is used to lift a steel hammer which is then dropped via gravity on the top of the pile. The steel piles were hollow and closed-ended, with a diameter of 0.61 m or 0.71 m. Each pile is approximately 80 m long and driven an average of 66 m into the seabed (HEB construction, pers. comm. 2015). The contractor's records of pile-driving activity, which specified pile location, pile-driver, and the sequence of lift heights used, were made available by HEB construction and Port Lyttelton.

Table 3.1 Pile drivers used in Lyttelton harbour

Model	Gross weight (t)	Hammer weight (t)	Drop (m)	Max energy (kJ)
BSP 1146	35	14	1.5	206
Bruce SGH 1015	28	10	1.5	147
Junttan HHK18A	18	9	1.2	106

Underwater sound recordings were made as described in section 2.3.1, using a combination of moored and boat based recorders. The boat-based recorders were used to make recordings at various locations in the harbour, of all three pile drivers (Fig. 3.2).

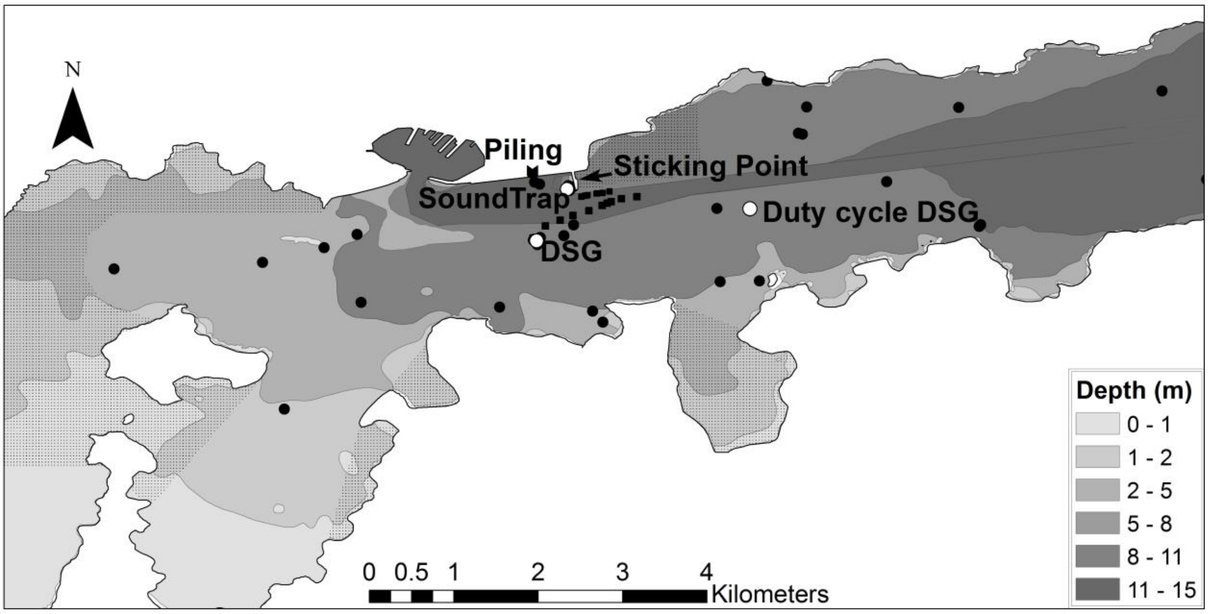

Figure 3.2 Location of moored recorders (white dots) and boat based recordings (black dots) in Lyttelton Harbour.

Boat-based recordings were made while anchored or drifting with the tide or wind. Drifting reduced noise due to wave slap on the boat and enabled measurement of changes in pile-driving noise over a small spatial scale. Drift recordings were conducted in two locations: past Sticking Point, as this feature provides a distinct shadowing effect to the east; and directly in front of the piling (starting around 100 m from the piling site to around 600 m) to measure attenuation at short ranges. Distances from the pile-driving were measured using the laser range finder and were later compared to GPS locations recorded every 30 s on board the drifting vessel.

To measure a broad spectrum of piling noise at close range (about 75-130 m) a very wideband recorder (Laptop PC running PAMGuard software, sampling at 500 kHz, with the Reson TC4013 hydrophone, and VP2000 hydrophone amplifier) was used. This hydrophone has a wider frequency response (20 Hz - 170 kHz +/-3 dB) than the Reson 4032 (10 Hz – 90 kHz +/- 3 dB), and is better suited to recording very high signal levels. This hydrophone's cable was fitted with plastic fairing to reduce the noise induced by cable strumming.

Measurements of pile-driving noise were made in the *far* sound field to avoid any anomalies that might be observed in the *near* field (Urick 1983). While the 'near-field' is not defined for sources like piles that span the water depth in shallow water, typically a distance larger than the maximum of the largest source dimension and the water depth would be outside the near field (de Jong et al., 2011). In Lyttelton this is at around 80 m, the longest dimension of the pile. Thus any recording beyond that range should be in the far field.

Sound analyses

Standards and protocols for studies of underwater noise have only recently become available (De Jong et al., 2011; Müller & Zerbs 2011; Robinson et al., 2014). For this reason previous studies of pile-driving noise do not all use the same measurement standard (see table 1.1).

To analyse the noise from a particular pile driver, hammer setting and location, a section which contained 10 strikes (as recommended by de Jong et al., 2011) was selected from the raw recording. Selections were made to avoid flow noise, wave slap on the recording vessel and construction noise other than piling.

Recordings were calibrated as described in section 2.3.2

A Matlab script, *'strikelocator.m'* was written to process the recordings of piling sequences more efficiently. First the script applies the correction factor S and filters the signal using a 30 Hz digital high-pass filter. This removes a large part of parasitic noise due to water flow past the hydrophone and wave slap noise from the vessel, similarly as in Blackwell et al., (2005) and David (2006) for example. This noise has most of its energy in the low frequency range while the piling noise recorded had very little energy below 30 Hz. Noise filtering is particularly important for the distant recordings (see Fig. 3.3). It should be noted that the signal-to-noise ratio was much higher for recordings at closer range than shown in the figure: this is a worst case scenario used to illustrate the effect of the filter.

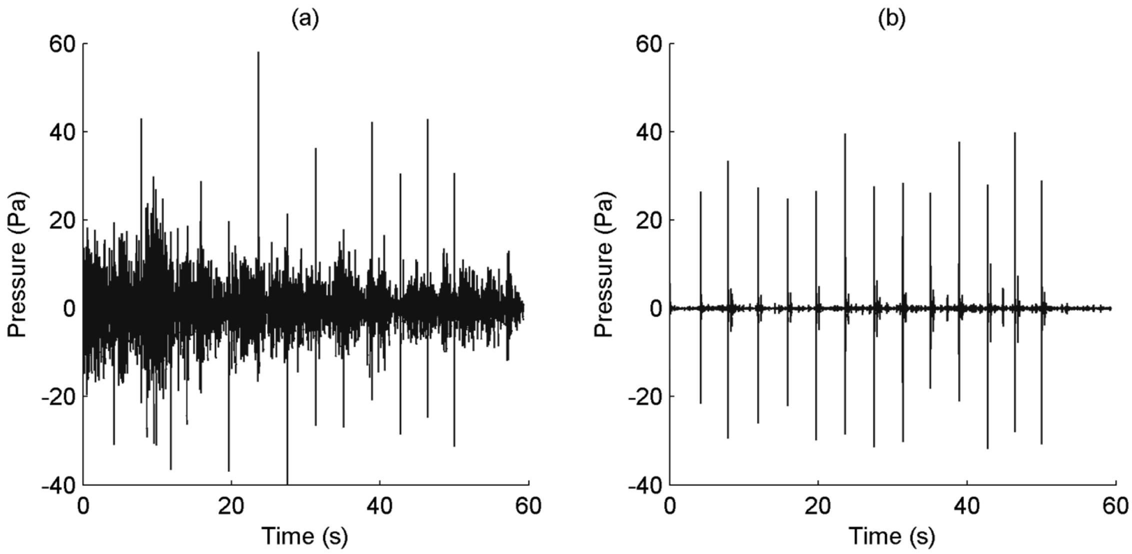

Figure 3.3 Comparison of a raw signal of pile-driving noise (a) and the same signal filtered with a 30 Hz digital high-pass filter (b). The recording was made at a range of 1.6 km from the piling.

The script then plots the filtered signal which allows the user to indicate (using the Matlab function *'ginput'*) the approximate levels of the lowest peak in the pressure waveform due to pile-driving noise and the highest level of background noise. These are used in a peak-finding algorithm (*peakfinder* by Nathaneal Yoder, June 2015) to restrict the peaks found to be above a given absolute threshold and to be above a given signal to noise ratio. In the case of individual strikes having several peaks that satisfy these criteria, strike time is measured as the time at which the maximum peak occurs (see Fig. 3.4). The resulting temporal locations are used to calculate the desired sound metrics for each strike.

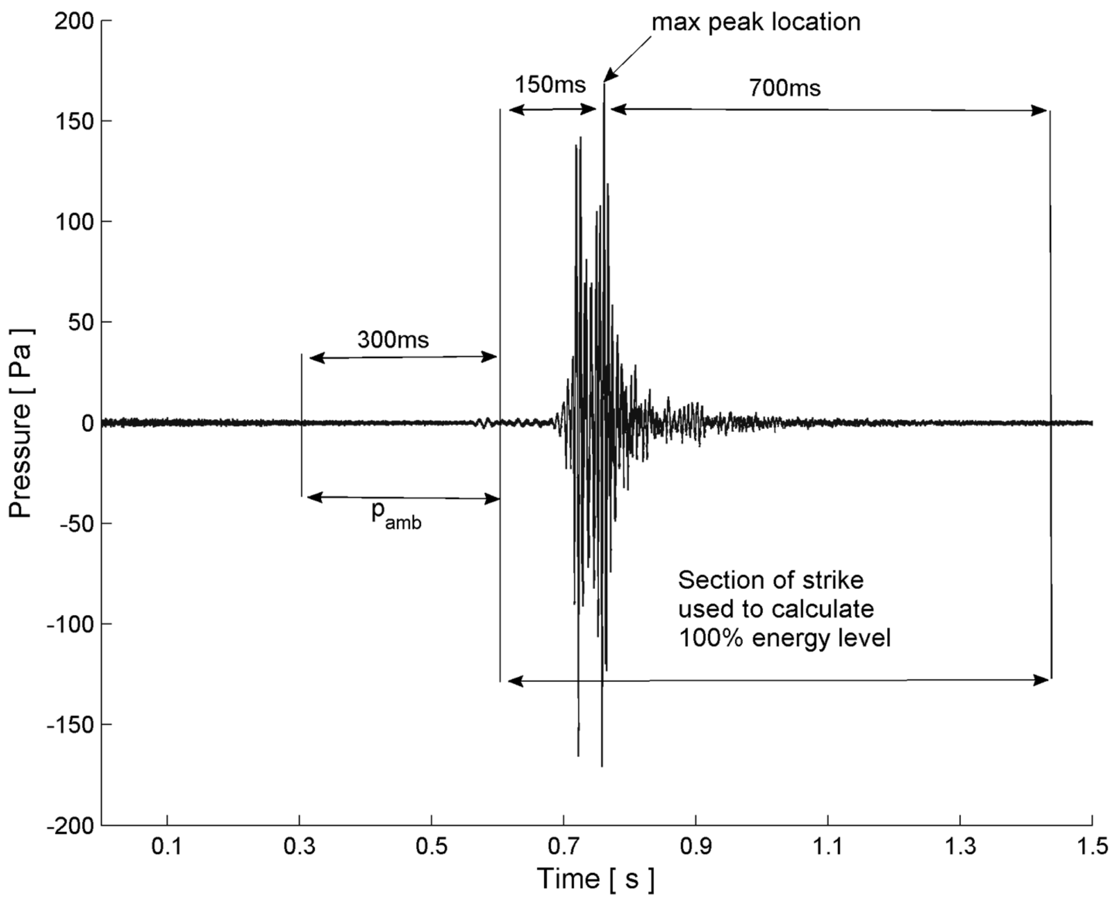

Figure 3.4 Pressure waveform of single pile strike. Once the maximum peak in each strike is located a section starting 150 ms before and ending 700 ms after this location is used for analysis. A 300 ms section immediately prior to this is used to compensate SEL for the contribution of ambient noise.

It has been shown that RMS level, a metric commonly used for measuring ambient noise, is not suitable for measuring noise from transient signals such as a pile strike (Madsen 2005). The most widely used metrics for quantifying pile-driving noise are peak-to-peak Sound Pressure level (SPL_{pp}) and Sound Exposure Level (SEL). SPL_{pp} is the decibel measure of the algebraic difference between the maximum positive and maximum negative instantaneous peak pressure, measured in dB re 1 µPa (peak-to-peak) (Southall et al., 2007):

$$SPL_{pp} = 10log_{10}\left(\frac{(\max(p) + |\min(p)|)^2}{{p_{ref}}^2}\right)$$

Where p is the pressure signal and p_{ref} is the reference pressure which is 1 µPa for underwater sound measurements.

A similar metric, SPL_{0p}, is the decibel measure of the maximum absolute value of the instantaneous pressure:

$$SPL_{0p} = 10log_{10}\left(\frac{\max(p^2)}{{p_{ref}}^2}\right)$$

These are measures of peak pressure. The idea behind Sound Exposure Level (SEL) is to characterise transients in terms of their total energy over a certain period. It is the decibel level of the cumulative sum-of-square pressures over the duration of a sound measured in dB re 1 $\mu Pa^2 s$ (Southall et al., 2007):

$$SEL = 10log_{10}\left(\frac{\int_{t_2}^{t_1} p(t)^2 \ - p_{amb}^2 \ dt}{{p_{ref}}^2}\right)$$

where t_1 and t_2 are the start and end times of the duration of the signal. For transient signals, duration is commonly defined as the '90 % envelope', which contains 90 % of the transient's total energy (Madsen 2005). In this case t_1 would be the time at which the cumulative energy reaches 5 % and t_2 would be the time at which it reaches 95 % as shown by horizontal lines in the bottom plot (Fig. 3.5). These times were calculated within an 850 ms window starting 150 ms before the highest peak. This window fully captured the strike but also contained a small amount of background noise. To exclude the energy contributed by the background noise during the pile strike, the script calculates average background pressure, p_{amb}, from a 300 ms section immediately prior to the strike. This was then subtracted from the total pressure at each sample before integrating) leaving the energy due to the pile strike alone. Finally, the script computes the average and standard deviation of the above metrics across the 10 strikes.

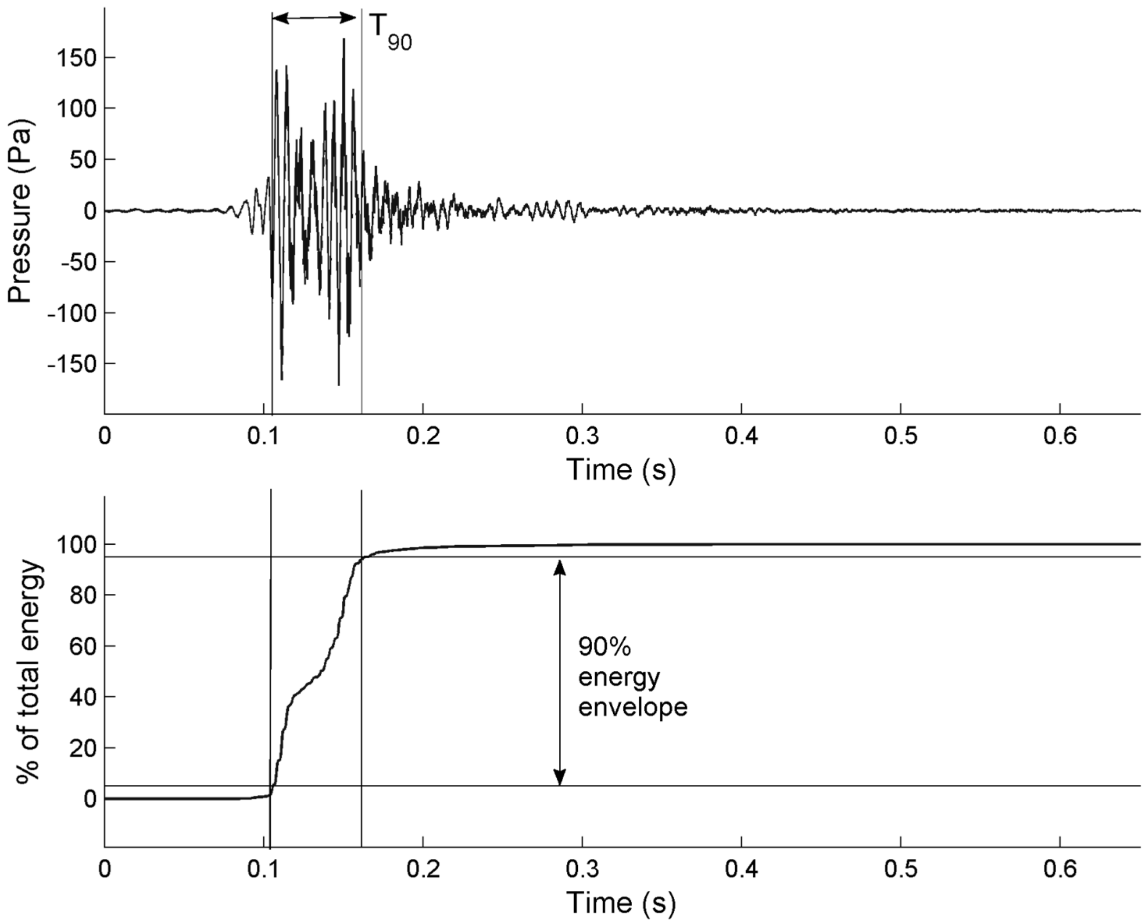

Figure 3.5 TOP. Pressure waveform of a single pile strike showing 5th and 95th percentiles (determined using the cumulative distribution function below) which enclose the section used for calculating SEL. The duration of this section is termed T_{90}. BOTTOM. Cumulative energy of the above strike.

As in section 2.3.2, third-octaveband levels (TOLs) were calculated using the *PAMGuide* toolbox (Merchant et al., 2015). To objectively compare TOLs from different recordings, the inter-pulse-interval of the section to be analysed was manually reduced to 1 second (in the sound editing software *Audacity),* by clipping out small sections of ambient noise between strikes. This ensured the proportion of ambient noise (that is the low noise levels between pile strikes) was relatively constant between recordings of piling sequences of varying inter pulse intervals (IPIs). The adjustment to a one second IPI was chosen to ensure the entire duration of the strike was captured while minimising the amount of ambient noise. This standardisation of IPI led to an increase in TOL of up to 5 dB for some recordings with originally large IPIs.

Propagation modelling

Even though the approach was to measure sound levels empirically in as many places as practical (while also having a recorder moored at 750 m range to capture variation from strike to strike), a propagation model was needed to interpolate between measured points, and to extrapolate beyond them. The best model for this purpose is as simple as possible while being sufficiently adaptable to represent the significant influences on the harbour's soundscape.

Since there are numerous influences on the sound levels measured, only a subset of the data, representing the largest collection of recordings made under similar conditions, was used. Statistical modelling, using general linear modelling (GLM) in R (and the R package *stats*, R Development Core Team, 2016), was used to determine which factors (hammer lift height, pile driver type, pile row on wharf, stage of piling, pile diameter, date and pile ID) were significant influences on measured pile-driving noise levels. From the entire database of recordings, the average SEL of 10 strikes was measured at the DSG reference location (750 m from the wharf, just outside the channel) for each situation we encountered, given the different pile drivers, lift heights, stages in piling, pile diameter, row and day in recording period. Not every combination above was recorded: this was mainly due to some pile drivers only being used for certain rows or a particular pile diameter. A total of 45 records were used and for each record the average SEL, T_{90}, and corresponding pile driver (3 levels), energy (calculated from lift height and hammer weight), stage of pile-driving (3 levels), pile diameter (2 levels), row (6 levels), day in recording period and pile ID were entered. Normality and homogeneity of variances were checked via visual inspections of plots of residuals against fitted values. The results from the statistical model were used to determine the subset of data that ensured these factors were kept constant for the propagation modelling. The subset was further refined to only contain reference recordings in the SEL range of 140 ±3 dB re 1 $\mu Pa^2 s$ (see Fig. 3.6).

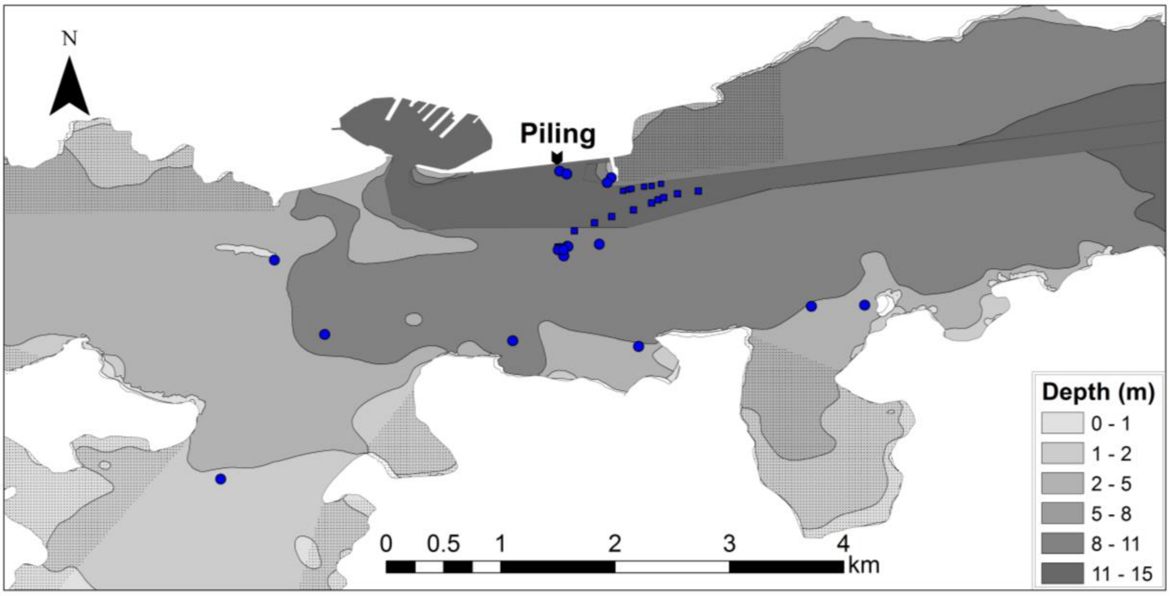

Figure 3.6. Locations of the subset of measurements used in fitting the propagation model. Blue circles indicate stationary measurements, blue squares indicate measurements made during a drift recording.

The fitting parameters of the propagation model were determined using the recorded data at various locations around the harbour, with corresponding reference recordings in the subset. This included measurements from short range drift recordings, however, since in this case each measurement is of a single strike (as opposed to an average of 10 strikes for the stationary recordings) these data were weighted at $1/10^{th}$ of the averaged measurements in the fitting procedure.

It is reasonable to assume that the bottom layer properties and sea surface roughness are constant over the data gathering period. The seabed substrate is unlikely to change in this period and sea surface roughness was limited by the conditions suitable for boat-based sound recording (below Beaufort 3). Norton and Novarini (1996) show that the transmission loss in wind speeds of 5 ms^{-1} (max wind speed allowable for recording) is very similar (± 1 dB) to flat conditions, to at least 4000 m from the noise source.

3.3 RESULTS

The recorded pile-driving noise was characterised using the sound analysis techniques described in section 3.3.2. All metrics, averaged over 10 strikes (recorded from a single pile driven with a constant hammer energy), for a selection of locations, are presented in table 3.2. Note that this table only shows those 39 recordings used in creating the noise map, there were many additional recordings. The Junttan data at the end of the table was included to show measurements from that pile driver (as well as the Bruce and BSP) but they were not used to generate the noise map. The source level of pile strikes varies with pile driver, pile location, substrate, penetration depth and hammer lift. Therefore, the noise-spreading characteristics of the harbour were presented using a noise contour map that shows losses instead of absolute sound pressure levels. It is impossible to construct a noise map only from measurements as it is unrealistic to make recordings at all map locations in time short enough that none of the above variables change (de Jong et al., 2011). Thus, propagation modelling was used to estimate the loss contours between recording locations.

Characterisation

As expected, recordings made at close range (<2 km) show strikes as broadband pulses with high peak-to-peak SPLs and steep rise times. The sound pressure levels and frequency range both decrease with increasing distance from the source.

The maximum level recorded per average of 10 strikes had an SEL of 158 dB re 1 μPa^{2}s and an SPL_{pp} of 183 dB re 1 μPa (370 m from the source). Using the propagation model described in the next section, this would correspond to a peak-to-peak source level of 219 dB re 1 μPa @ 1 m. The duration of the strikes recorded varied between 59 and 624 ms. The longest durations occurred when the hammer was bouncing (see Fig. 3.7), at the end of a piling sequence. The pile driver is stopped when pile movement reaches 2.5 mm/blow or less (D. Smith, HEB project engineer, pers. comm.). At this point the pile has hit solid substrate, and the elasticity of the pile causes the hammer to bounce. This produces the smaller secondary impulse closely following the main strike.

Table 3.2 Sound metrics for pile-driving noise recorded around Lyttelton Harbour (see Fig. 3.19 for recording locations corresponding to the map label in first column). The metrics are averages over 10 consecutive strikes of the same pile, recorded at each location. Each set of rows, separated by an empty row, refers to a set including a reference recording. 'SL' is 'source level' calculated using the estimated Transmission loss at the reference position and 'Loss' refers to the amount of transmission loss at each location relative to the estimated source level (except for the reference recording for which the loss is derived from the propagation model), i.e. the difference between SL (for each set of recordings) and SEL. Drift recordings not shown

Map label	**Pile**	**Range** *m*	**Pile driver**	**Date**	**SEL** *dB re 1 μPa²s*	**SPL_{pp}** *dB re 1 μPa*	**T_{90}** *ms*	**SPL_{0p}** *dB re 1 μPa*	**SL** *dB re 1 μPa²s*	**Loss** *dB re 1 μPa*
1	28E	92	Bruce	23.01.15	158.6	187.9	117	182.4		25.5
2	28E	405	Bruce	23.01.15	142.6	171.5	127	166.3		41.5
3	28E	740	Bruce	23.01.15	140.9	168.6	125	162.9	184.1	43.2
4	30D	702	Bruce	10.02.15	132.3	164.1	411	158.9		49.6
5	30D	770	Bruce	10.02.15	138.2	166.1	344	160.7	181.9	43.7
6	29E	1692	Bruce	12.01.15	121.3	155.2	140	149.7		61.1
7	29E	359	Bruce	12.01.15	143.7	174.9	100	169.7		38.7
8	29E	817	Bruce	12.01.15	137.9	164.3	105	158.7	182.4	44.5
9	28E	1625	Bruce	27.01.15	117.2	154.8	388	149.6		63.7
10	28E	750	Bruce	27.01.15	134.7	166.0	391	161.2		46.3
11	28E	398	Bruce	27.01.15	144.4	174.6	394	169.3	181.0	36.5
12	28E	773	Bruce	23.01.15	134.9	162.4	124	156.9		49.0
13	28E	405	Bruce	23.01.15	142.9	172.4	130	167.4		41.0
14	28E	740	Bruce	23.01.15	140.8	167.5	133	162.1	184.0	43.2
15	29E	1666	Bruce	12.01.15	117.6	144.3	239	138.9		65.0
16	29E	359	Bruce	12.01.15	142.8	171.3	195	165.9		39.8
17	29E	817	Bruce	12.01.15	138.2	164.0	176	158.8	182.7	44.5
18	31F	125	BSP	27.01.15	155.3	183.9	624	178.3		30.7
19	31F	745	BSP	27.01.15	142.7	170.0	563	164.6	186.0	43.3
20	31F	381	BSP	27.01.15	146.1	174.3	619	168.6		39.8

21	30F	1570	BSP	10.02.15	142.3	168.2	107	162.9		58.0
22	30F	758	BSP	10.02.15	141.6	168.1	114	162.3	185.1	43.5
23	38A	1863	BSP	6.01.15	125.7	159.1	75	153.4	184.6	58.9
24	38A	374	BSP	6.01.15	134.5	159.0	219	153.1		50.1
25	30F	3470	BSP	10.02.15	114.7	143.5	120	137.8		71.1
26	30F	758	BSP	10.02.15	142.3	168.7	103	163.0	185.2	43.5
27	33F	2093	BSP	10.02.15	113.0	141.3	152	135.8		71.4
28	33F	758	BSP	10.02.15	140.9	165.4	110	159.8	184.4	43.5
29	30F	1942	BSP	10.02.15	118.8	144.0	149	138.3		68.3
30	30F	758	BSP	10.02.15	143.6	171.2	105	166.2	187.1	43.5
31	30F	2064	BSP	10.02.15	126.0	153.8	148	148.3		59.2
32	30F	758	BSP	10.02.15	141.7	168.5	114	162.8	185.2	43.5
33	38A	2328	BSP	6.01.15	115.1	144.4	155	138.8		71.4
34	38A	374	BSP	6.01.15	134.6	161.0	292	155.2		51.9
35	38A	791	BSP	6.01.15	142.5	168.9	59	163.4	186.5	44.0
36	30F	3738	BSP	10.02.15	97.2	126.8	313	121.2		86.7
37	30F	758	BSP	10.02.15	140.4	167.1	92	161.5	183.9	43.5
38	33F	1973	BSP	10.02.15	110.5	139.0	145	133.6		73.8
39	33F	759	BSP	10.02.15	140.8	165.7	110	160.3	184.3	43.5
	42A	108	Junt	23.01.15	150.3	180.1	140	174.9		
	42A	370	Junt	23.01.15	134.7	159.0	302	153.8		
	41A	750	Junt	22.01.15	135.6	162.5	62	157.3		

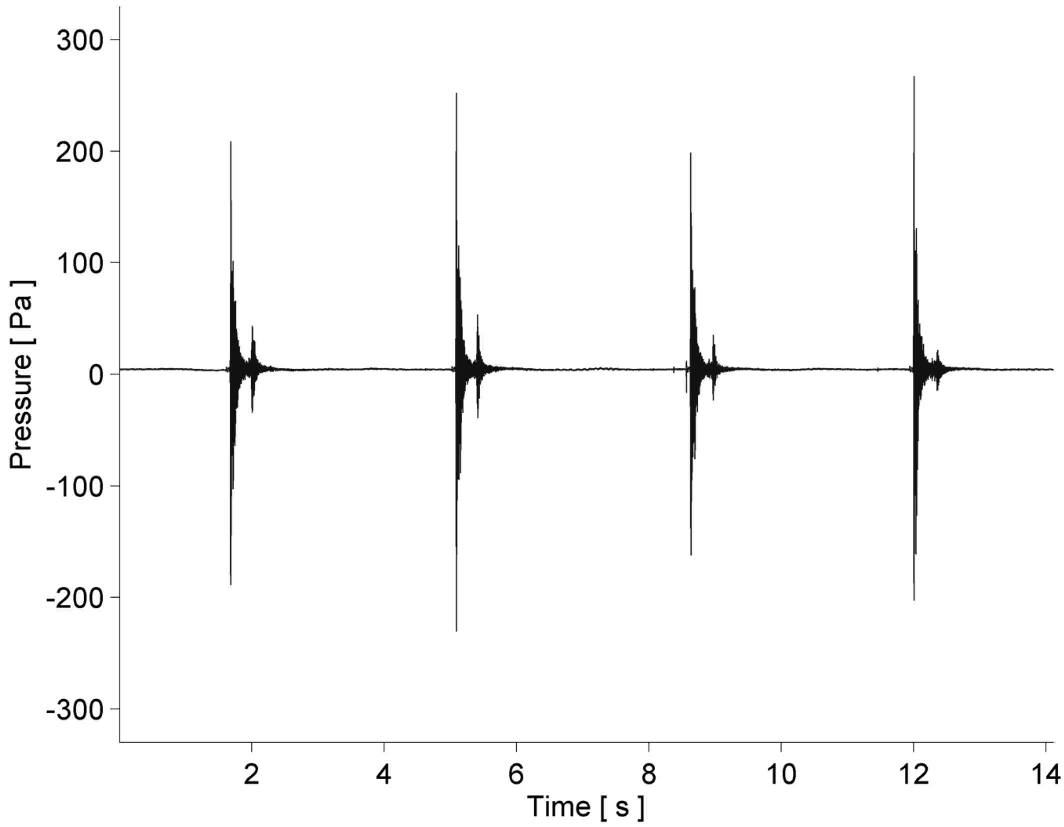

Figure 3.7 Pressure waveform showing 'Bruce' hammer bouncing at the end of the piling sequence. Recordings were made at a range of 370 m from the source, frequency range 30 Hz – 144 kHz.

Factors influencing variation in noise generated by pile-driving

Stage in piling sequence

Each piling sequence begins with a 'soft start' period, in which hammer energy is gradually ramped up by increasing the height the hammer is lifted. A soft start is required by the pile-driver manufacturer. It begins with repeated 100-200 mm drops (first bar on control unit) for two minutes, then 25 % power for one minute, then power as required (D. Smith, pers. comm. 2015). A "soft" start sequence is shown for the 'Bruce' hammer in figure 3.8 (though this record shows the recommendations were not adhered to in this case). The energy of the hammer blow is given by the potential energy the hammer has at the top of its current lift height setting. For example, if the Bruce hammer (10 t weight) is lifted to a height of 0.2 m, the energy with which it hits the pile will be:

$$\text{Energy} = \text{Mass (kg)} \times \text{acceleration due to gravity } (ms^{-2}) \times \text{height (m)}$$

$$= 10000 \times 9.8 \times 0.2$$

$$= 19.6 \text{ kilo Joules.}$$

This is the energy of the lowest setting on the Bruce hammer, as shown by the first set of strikes (Fig. 3.8). Measured at 750 m, the average SEL of these strikes was 136.6 dB re 1 $\mu Pa^2 s$, with a peak-to-peak pressure of 128.8 Pa. The average SEL of the last five strikes shown, with a lift height of 96.1 kJ (full power), was 144.5 dB re 1 $\mu Pa^2 s$, with a mean peak-to-peak pressure of 452.8 Pa (Fig 3.8).

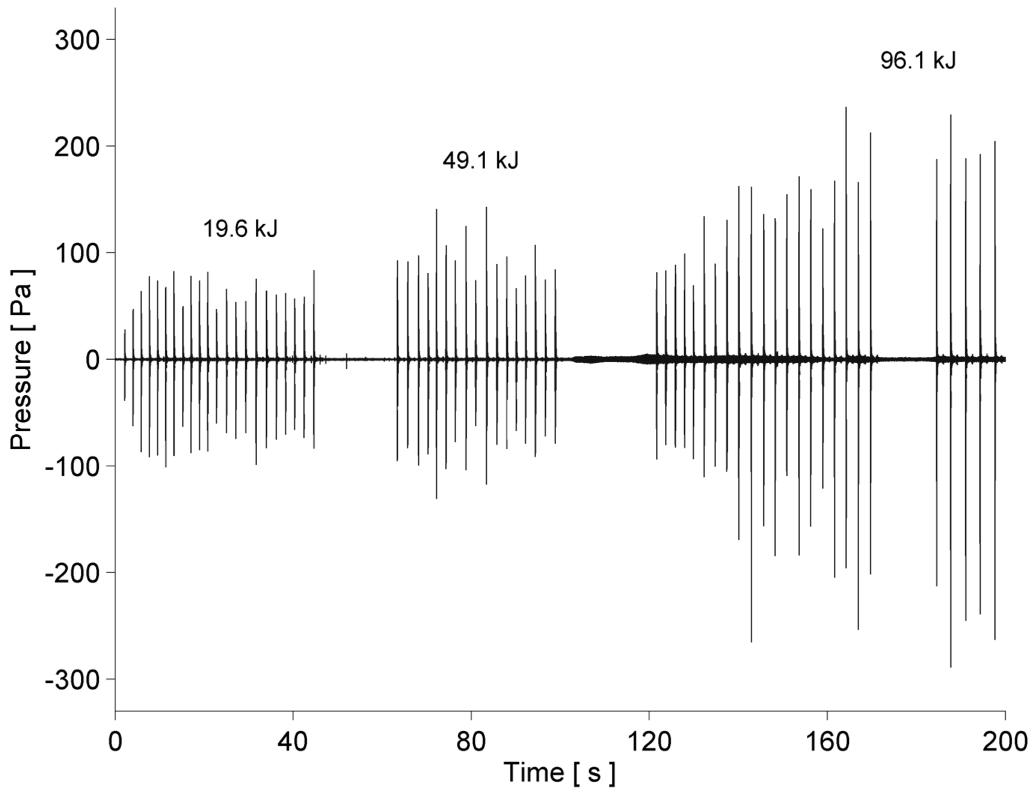

Figure 3.8 Pressure waveform showing 'soft start' piling sequence of the 'Bruce' hammer. Recordings were made at DSG reference position, frequency range 30 Hz – 40 kHz. The annotations refer to the energy levels of the hammer producing the 3 sets of strikes.

TOLs were compared for two lift heights for piles in the same row but at different stages in the piling sequence, both hammered using the 'BSP' (Fig 3.9). In this sequence "Start" is defined as the first 30 m of seabed penetration and 'End' – the remaining distance for the piling sequence (usually at least another 30 m), excluding the strikes for "Setting" the pile – the final 10 strikes in the piling sequence.

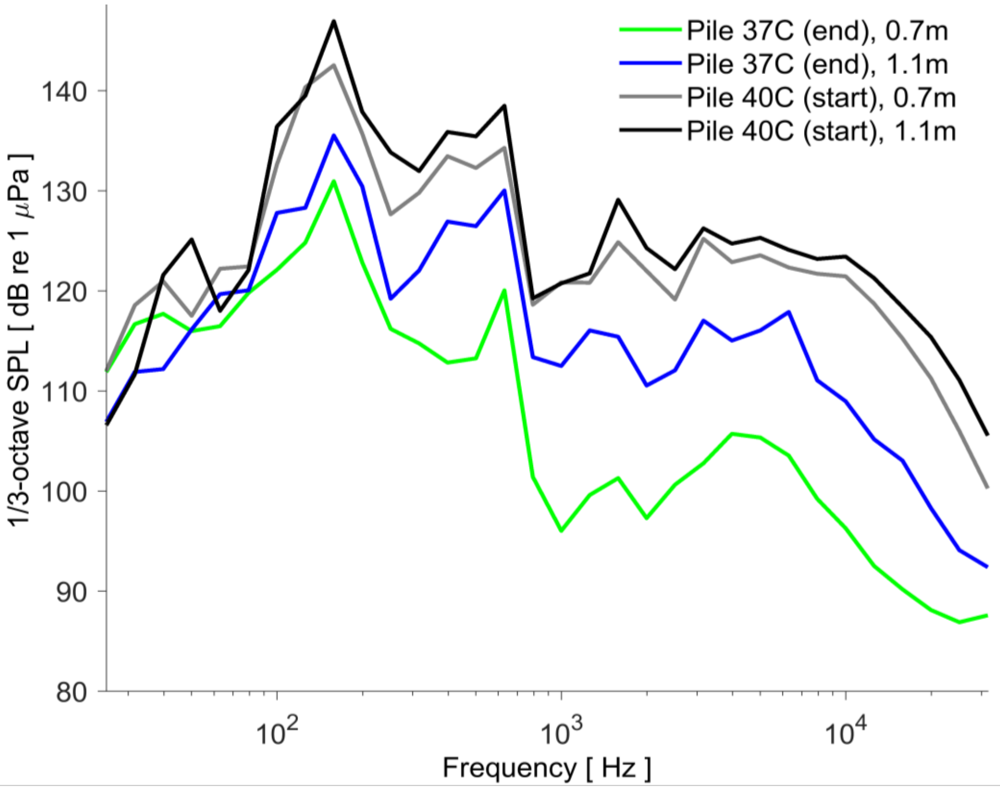

Figure 3.9 Third octave band levels of 'BSP' hammer at two different lift heights for two stages in piling. Pile for start stage (40C) is different to pile for end stage (37C) but are within the same row so conditions are expected to be similar. Recordings were made at DSG reference position, frequency range 30 Hz – 40 kHz.

The start stage produces louder received levels (RLs) than the end stage. This may be due to the fact that during the end stage a greater length of the pile is embedded in the seafloor, increasing the amount of damping which thereby reduces the amount of noise that radiates into the water column. This difference between stages is also seen across our dataset – the *start* stage gives the loudest RL, followed by the *end* stage, with *setting* giving the least loud RL for the same conditions.

Differences among pile drivers

Wideband power spectral densities (recorded at close range using the PAMGuard platform which had the highest sampling rate) show strikes from all three pile driver types: 'Bruce' and 'Junttan' (alternating strikes, Fig. 3.10) and 'BSP' (bouncing, Fig. 3.11). These provide a visual representation of the relative distribution of energy across the broad frequency range of the pulses. All three drivers appear to produce a similar distribution of underwater sound energy across the frequency range: the highest energy is around 200-300 Hz, most energy contained between 50 Hz-10 kHz, but there is some energy to at least 100 kHz, particularly for the Bruce. Note that while the main pulse of the BSP bouncing is much louder as seen in the pressure waveform (Fig. 3.12), the frequency range of the bounce is noticeably wider than that of the main pulse. This was uncommon in our dataset, usually the spectrum of the bounce pulse was less wide than that of the main pulse, which is to be expected as the impact of the bounce strike would have far less energy than that of the main strike. However, this was the only close range, wideband recording of the BSP driver available in our dataset.

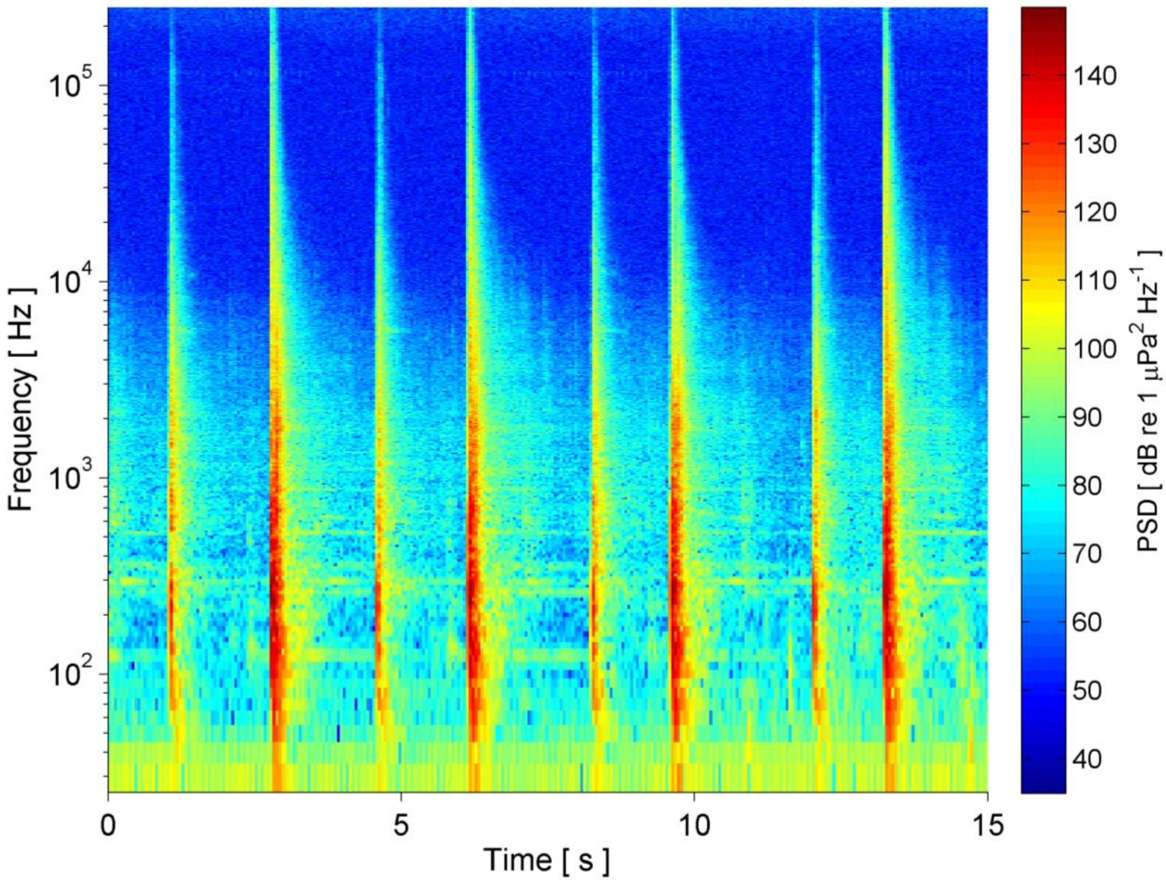

Figure 3.10 Bruce (even numbered strikes, in order of occurrence) on pile 28E, end stage, lift height 1 m, and Junttan (odd numbered strikes) on pile 42B, start stage, lift height 1.2 m, on 23/1/15, frequency range 30 Hz - 250 kHz, range to piling 97 m.

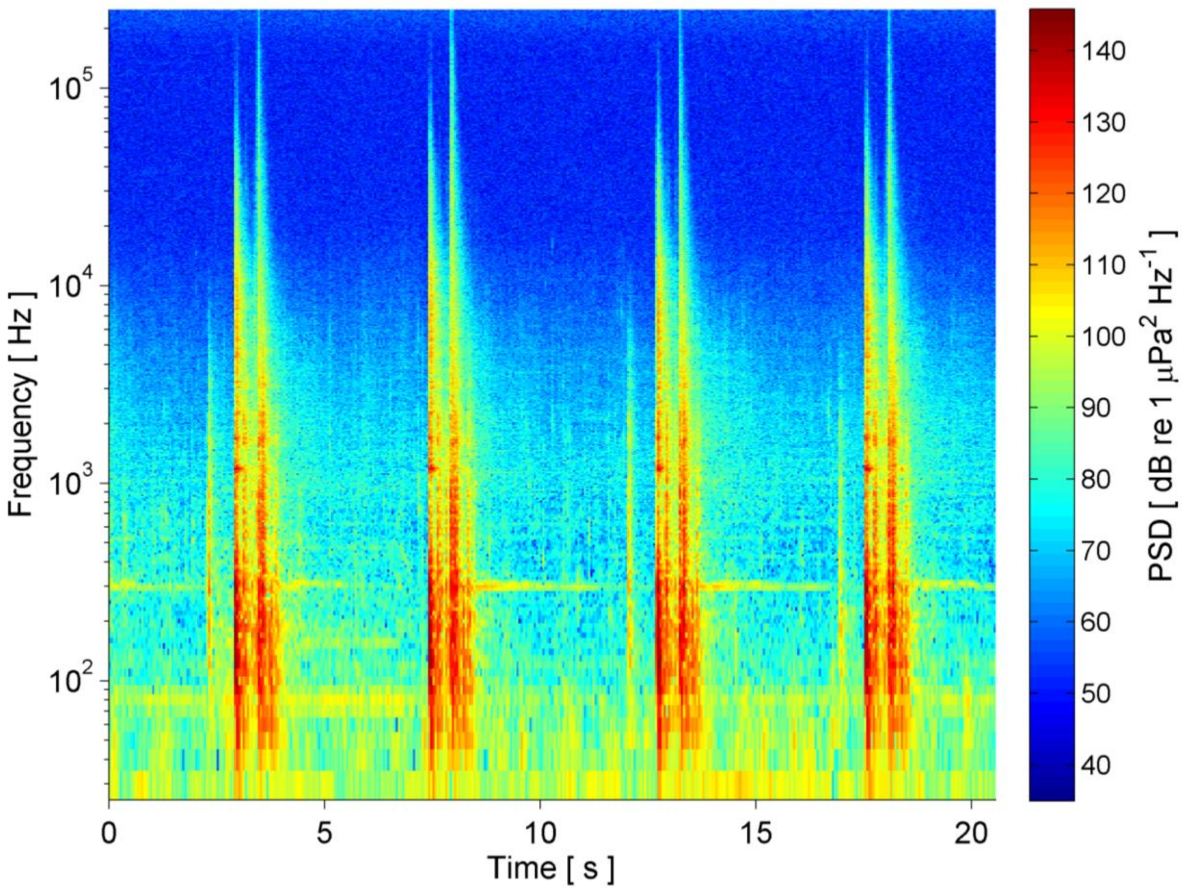

Figure 3.11 Power spectral density of BSP bouncing, on pile 31F, end stage, lift height 1.5 m, on 27/1/15, frequency range 30 Hz - 250 kHz, range to piling 103 m.

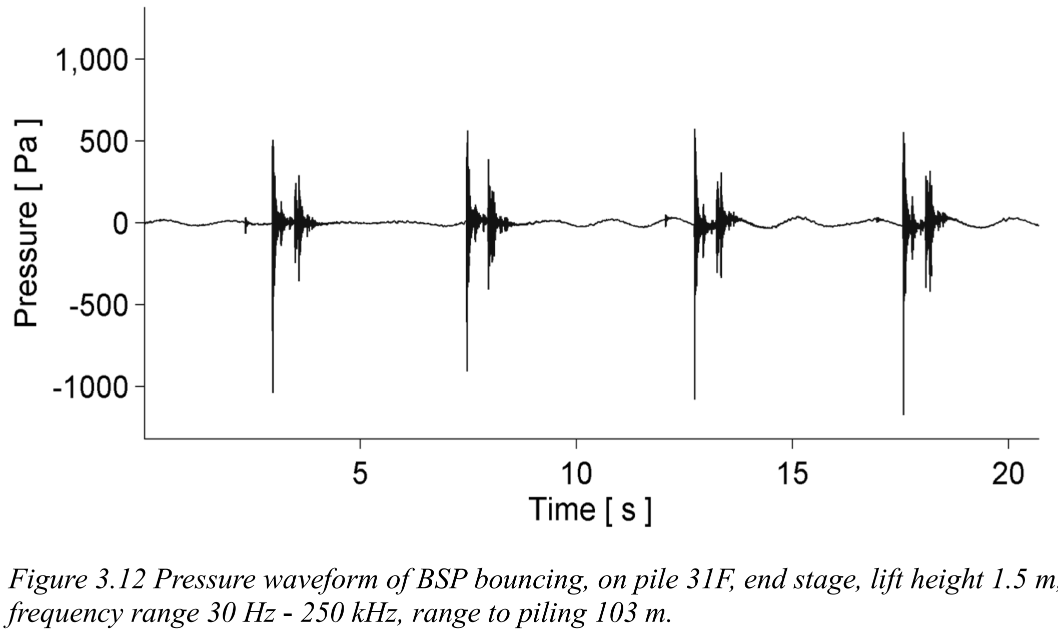

Figure 3.12 Pressure waveform of BSP bouncing, on pile 31F, end stage, lift height 1.5 m, on 27/1/15, frequency range 30 Hz - 250 kHz, range to piling 103 m.

Hammer height

As expected, overall noise levels increase with increasing lift height (Fig. 3.13). Unexpectedly, while the TOLs seem to increase with lift height evenly across the frequency range, this is not observed in the 'setting' case (stage of pile-driving, the very last strikes in the sequence, when the pile moves down less than 2.5 mm with each strike (HEB construction, pers. comm. 2015)). The TOLs are similar in the frequency range below 200 Hz compared to the 1.5 m lift height prior to setting, but much lower levels (5-15 dB less) are recorded for TOLs above 200 Hz.

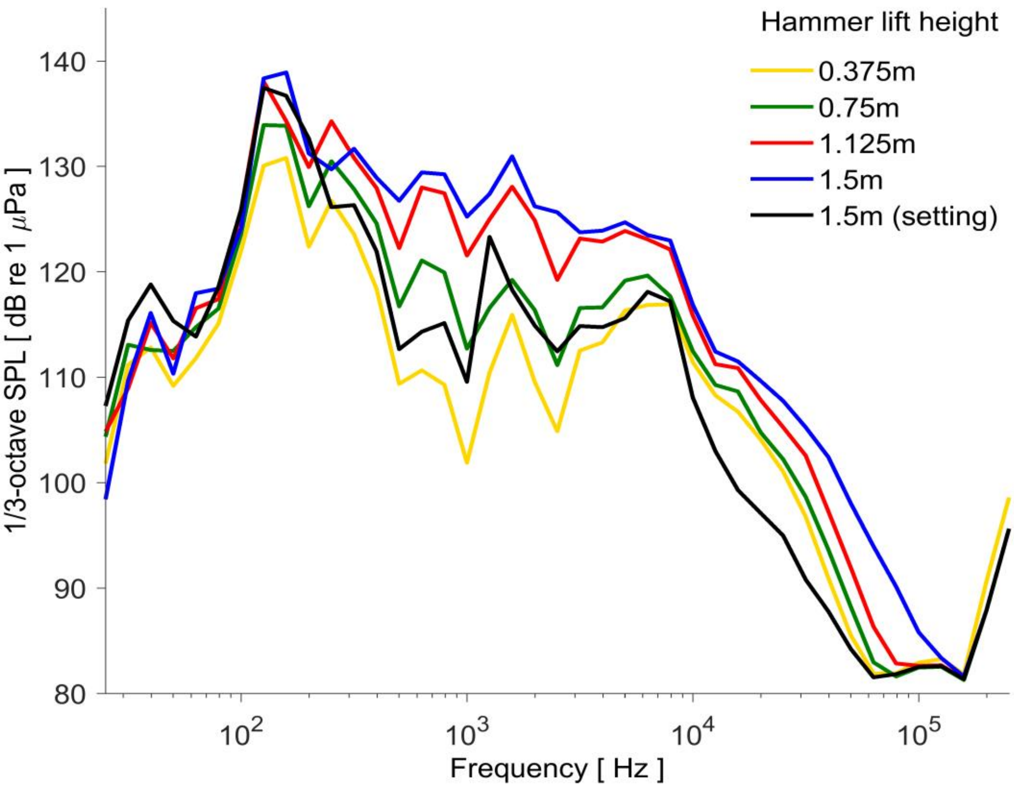

Figure 3.13 Third octave band levels of 'BSP' hammer at increasing lift height as indicated in legend. Recordings were made at DSG reference position (using the SoundTrap) about 750 m from the piling. The frequency range of the recording is 30 Hz – 144 kHz.

Water Depth

The wharf sits above a sloping seabed and is supported by six rows of piles along the wharf – rows A to F, with F being in the deepest water, closest to the dredged channel. There was notable variation in pile-driving noise from pile to pile (Fig. 3.14). The figure suggests that the TOLs were generally higher in row F than row A. This is not unexpected as there is a greater portion of the pile (c.14 m) in contact with water. Hence we would expect higher energy transfer into the water column, and therefore a higher RL for the same hammer settings. Again, as with the 'setting' case above, the difference in TOLs, across all lift heights here, is greatest in the frequency range above 200 Hz.

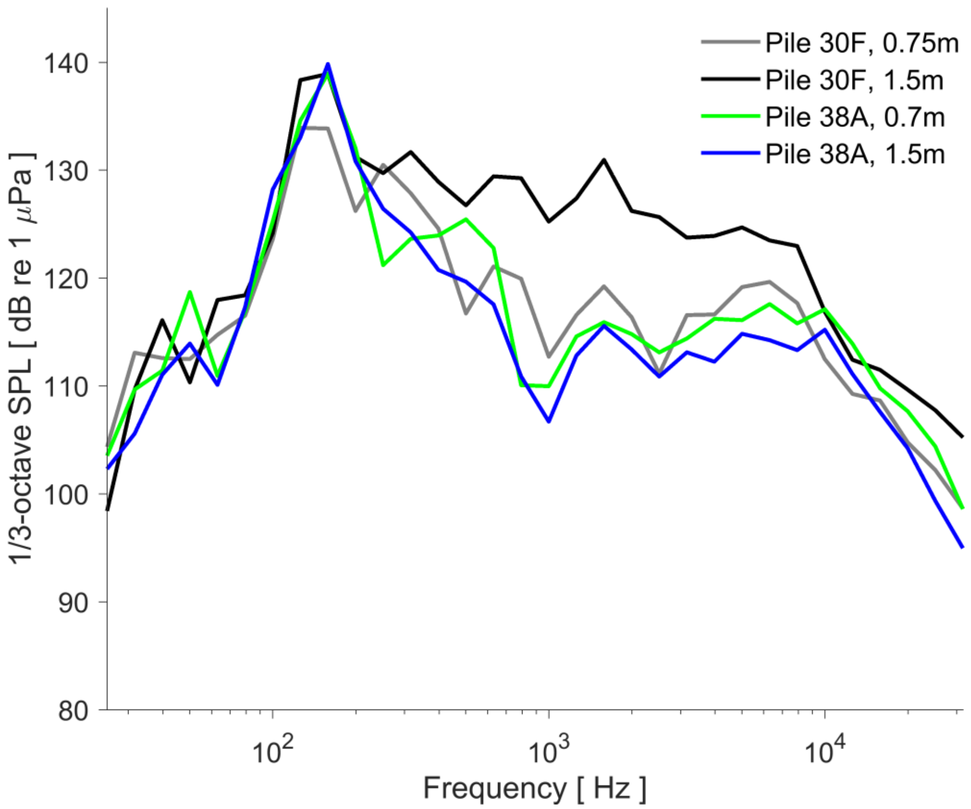

Figure 3.14 Third octave band levels of 'BSP' hammer at two different lift heights for 2 different rows. Row F is the closest to the edge of the wharf, row A (water depth 0-1 m) is 30 m inland from row F (water depth c.14 m). Recordings were made at DSG reference position, frequency range 30 Hz – 40 kHz (using DSG) for pile 38A, and 30 Hz – 144 kHz (using SoundTrap) for pile 30F.

Statistical analysis

Clearly, received levels can be influenced by a number of factors (Figs. 3.9-3.14). This was investigated in more detail using GLMs.

Exploratory data analysis (Fig. 3.15) revealed that:

- the recordings we had of the Junttan pile driver were only during the start stage;
- the set stage was only carried out at the maximum lift height of each hammer;
- the start stage was associated with lower energy than the end stage. This is because more effort is required to move the pile during the end stage as it is deeper in the seabed;
- the received SEL tends to be highest during the start stage.

The boxplots indicate likely interactions between energy, pile driver and stage.

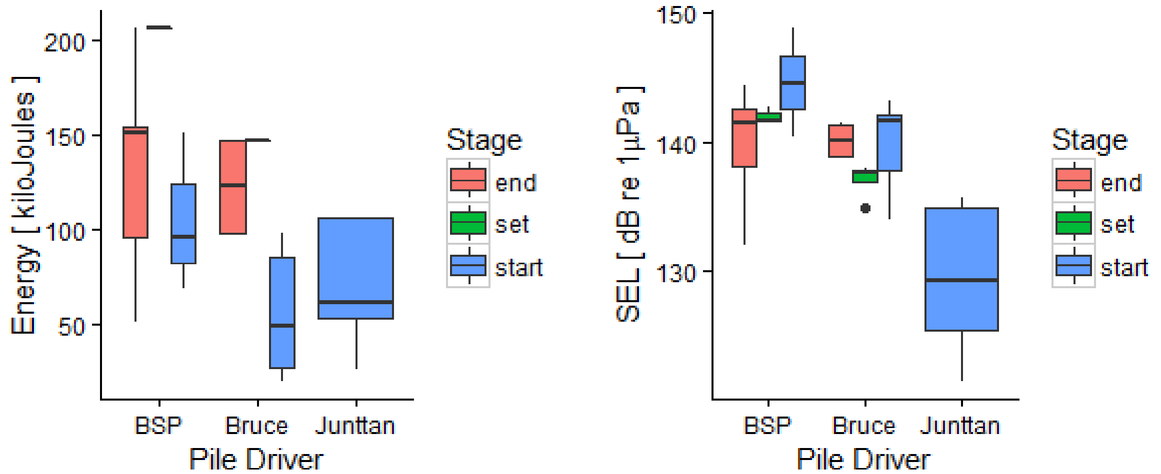

Figure 3.15 Left: boxplot of Energy provided by each pile driver during each stage. Right: boxplot of received SEL for each pile driver at each stage. (Only 'start' stage data available for Junttan pile driver).

The best fitting model was determined by comparing AICc scores and using ANOVA (*stats* package, R Core team 2006) to test the significance of each term. The formula of the final model with the lowest AICc score, containing only significant terms, was:

$$SEL \sim energy * pile\ driver + stage$$

The '*' indicates an interaction between the variables *energy* and *pile driver*. It was concluded from this model that *row, diameter*, *pile ID* and *day* did not significantly influence the received SEL (Table 3.3).

The estimate of each coefficient is relative to the intercept, which represents a ‘baseline’ condition to which all other conditions are compared (Table 3.3). In this case the intercept is the mean SEL for the BSP hammer, at the end stage of piling and at the mean of all energy levels (this is because the energy variable was scaled by subtracting the mean from each level to standardise the continuous predictor). For each kJ of increase in energy there is a 0.055 dB increase in SEL; overall, the SEL for the setting stage was about 2.8 dB lower than for the end stage while for the start stage it was 5 dB higher. SELs for the Bruce hammer for the same conditions were not significantly different from the BSP. The Junttan SELs were about 7 dB lower. The amount SEL increases with energy was not significantly different between the BSP and Bruce hammer, but for the Junttan hammer SEL increased with a slope of 0.116 $dBkJ^{-1}$, about twice as steeply as the BSP hammer.

Table 3.3 Parametric coefficients fitted to pile-driving data using a GLM in R. 'SE' is standard error. The variables highlighted dark blue are highly significant, light blue is significant and white is not significant.

Parametric Coefficients	Estimate	(95% confidence interval)	SE	p-value
Intercept	139.3	(138.2, 140.4)	0.564	$<2*10^{-16}$
Energy (scaled), kJ	0.055	(0.036, 0.075)	0.010	$2.16*10^{-16}$
Stage: setting	-2.812	(-2.425, 1.180)	1.147	0.0191
Stage: start	4.996	(-10.790, -3.288)	1.219	0.0002
Pile driver: Bruce	-0.622	(-5.061, -0.564)	0.920	0.5029
Pile driver: Junttan	-7.039	(2.606, 7.386)	1.914	0.0007
Energy * Bruce	-0.002	(-0.038, 0.033)	0.017	0.8855
Energy * Junttan	0.116	(0.057, 0.174)	0.030	0.0004

Similar analysis of the T_{90} measurements revealed that only the setting stage was significantly different from the other stages. This is not surprising as it is during the setting stage that the hammer bounces, causing a double strike. Hammer type, energy and pile diameter were not significant influences on pulse duration. Additionally T_{90} does not change with recording range in a predictable way (see Fig. 3.16).

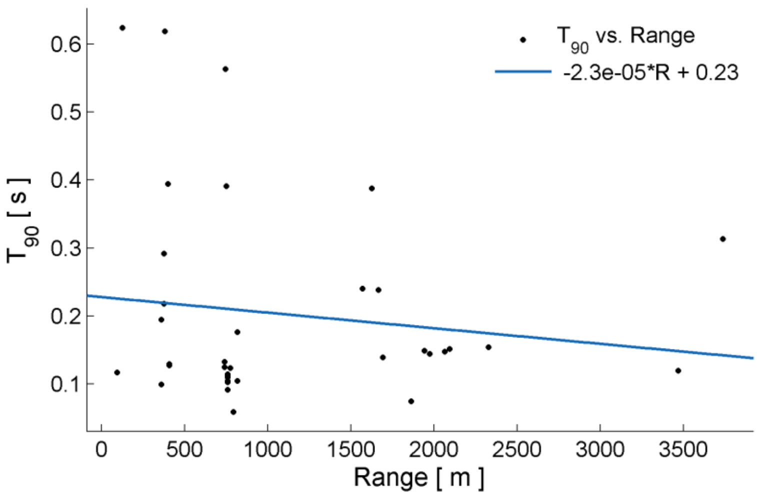

Figure 3.16 Measured pile strike duration (T_{90}) with range, excluding measurements made during setting stage. Blue line is linear fit to the data (R^2 0.018)

Propagation modelling

None of the appropriate models tested (Urick 1983; Nedwell et al., 2005) fitted our measured data adequately (see Fig. 3.17). This is mainly because these models over-simplify the variation induced by the different bathymetry and bottom layer properties within the harbour. Porter & Collins (2005) produced software for Matlab that could integrate these conditions into the modelling (theory from Jensen 1994), however, our current lack of knowledge of bottom layer properties of Lyttelton Harbour prevents application of this model, which is very sensitive to small changes. For the same reason, I could not apply the equations provided by Marsh and Schulkin (1962). Therefore, a simple calculation which is still dependent on the conditions, is needed.

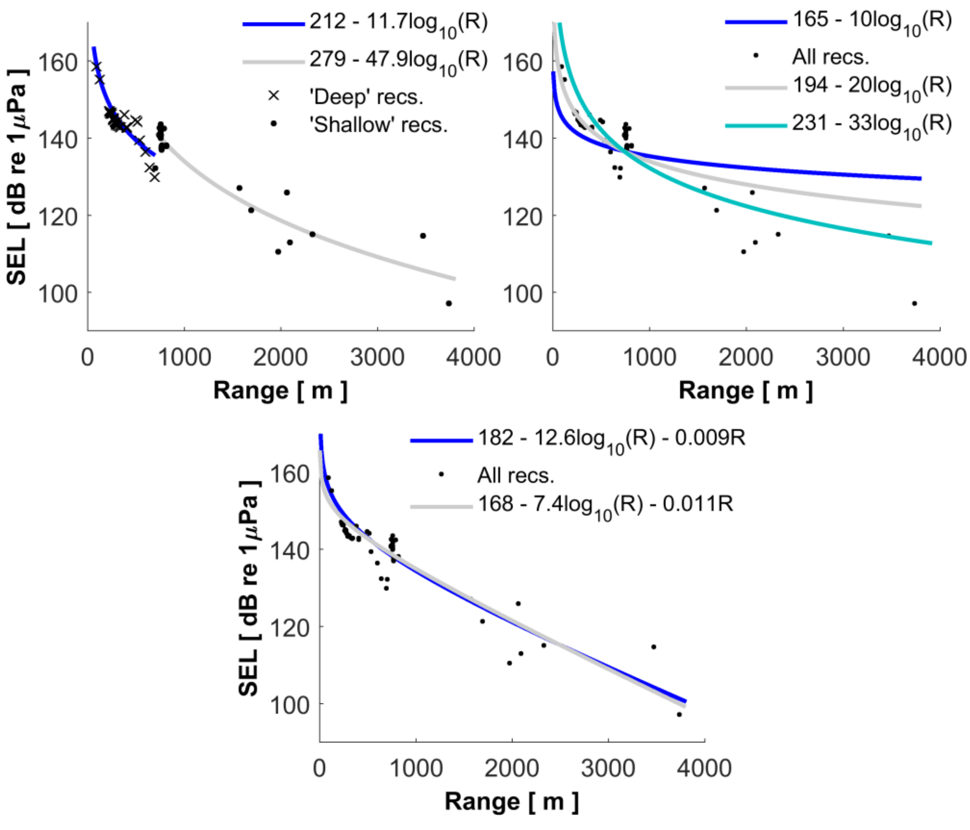

Figure 3.17 Top left: Propagation models fitted to 'deep' and 'shallow' recordings separately, with source level and spreading coefficient as fitting parameters. Top right: Propagation models fitted assuming spherical (grey, adj. R^2 0.65) or cylindrical (blue, adj. R^2 0.40) spreading (Urick 1983) while varying source level as the fitting parameter, the light blue line shows the fitted model varying source level and spreading coefficient (adj. R^2 0.77). Bottom: The grey line represents a propagation model fitted with a predetermined source level (from Nedwell et al., 2005) while varying the spreading and absorption coefficients as fitting parameters (adj. R^2 0.86). The blue line is the propagation model fitted while varying source level and the spreading and absorption coefficients as fitting parameters (adj. R^2 0.86).

The results from the statistical modelling in the previous section were used to select a set of data (for propagation modelling) that ensured the significant factors on received noise level were kept constant. This meant including only recordings made from the Bruce or BSP hammer at the end stage of piling, at lift heights above 1.1 m.

The closest fitting model to the data allows source level (SL), geometric spreading coefficient (*a*) and absorption coefficient (*b*) to vary:

$$RL = SL - a\log_{10}(\mathrm{R}) - b\mathrm{R} \quad (1)$$

where RL is the received level at range R. This model is described in Urick (1983) and was fitted to the measured data in Matlab, producing the fitting parameters shown in Table 3.4 and the graph shown as the blue line in the bottom plot in figure 3.17. Note that while absorption is heavily dependent on frequency, the absorption coefficient, *b*, in the propagation model includes absorption across the entire frequency range of the pile-driving noise, not just a single frequency.

Table 3.4 Fitted parameter values for propagation model calculated using Matlab. SSE was 7952, Adjusted R^2 was 0.86

Parameter	Predicted value (95% confidence bounds)
SL	182 (167, 197)
a	12.6 (6.65, 18.6)
b	0.0095 (0.0071, 0.0118)

It must be noted that these values do not necessarily represent the physical properties they were intended to in Urick (1983). They are the best fitting parameters to describe the combination of all the influences on transmission loss, not only geometric spreading and absorption.

Absorption, due to sound interaction with molecules in the water (such as $MgSO_4$), can lead to significant propagation loss over long distances, particularly for high frequencies (see table 3.5). However, for the range considered here (<4 km) the absorption at the largest range would exceed 1 dB only for frequencies above 4.4 kHz (using average Lyttelton water conditions: Temperature = 17 ^{0}C, depth = 7 m, Salinity = 34 PSU) (Ainslie and McColm 1998). Considering that most of the pile strike's energy is around 200 Hz, the overall contribution to propagation loss due to absorption in the water will be much less than the propagation loss due to spreading.

Table 3.5 Absorption increases with frequency. Values shown are calculated for average Lyttelton Harbour conditions, calculations according to Ainslie & McColm (1998).

Frequency (kHz)	Absorption (dB km^{-1})
0.1	0.001
0.3	0.007
2	0.127
4.4	0.265
10	0.792
40	9.365
100	37.673

While there will be significant absorption of high frequency (>40 kHz) components of the pile-driving noise at larger ranges, these frequencies contribute very little to measured pile-driving sound pressures, as described earlier. However, it is expected that the shallow water depth combined with the soft sediment found on the bottom will contribute significantly to the loss in the low frequencies at large range (>1 km) from the piling (Jensen et al., 2011). This is likely due to the depth dependent lower cut-off frequency, with a value of up to 2000 Hz for shallow parts of the harbour (see Fig. A.1 in the appendix). Since most of the energy in the pile-driving noise is below 2000 Hz we can expect a large portion of the energy to be lost due to this phenomenon. Additionally, the soft bottom layer gives poor reflection of the sound waves as they travel through the harbour leading to increasing loss with range. Hence the -*b*R term allows the model to reflect these losses as an effect that increases with range.

Noise Map

The fitted propagation model was used to generate a grid of 'loss with range' within the harbour area. Grid points were spaced 0.005 degrees in both latitude and longitude. Loss at each point was calculated using the range from each point to the pile-driving location. The purpose of the grid of losses is to estimate values between the recording locations to enable smooth interpolation between all points. This allows a useful visual representation of the propagation loss throughout the harbour, in the form of loss contours (Fig. 3.19). An additional adjustment to the grid was to integrate the results of recordings at locations where pile-driving could not be distinguished above background noise. That is, where there was no detectable change in pressure between ambient and piling noise in the waveform. In these cases it was often still possible to hear the pile-driving in the recording, but due to the high signal to noise ratio, it was not possible to measure the pile-driving strikes.

To determine what level of propagation loss would be required for the piling noise to be indistinguishable from ambient noise I compared average ambient broadband SPL in the inner harbour (as explained below) and average pile-driving source SPL_{0p}. While there is no exact way to compare these rather different noise measures, this approach most accurately represents the decibel difference between the peak levels of pile-driving noise and the average ambient noise. To obtain an overall level for this I first determined an average level for the ambient broadband SPL by taking the median of the RMS levels, recorded at 'smoko' time during the boat based recording days when the pile drivers were not operating. These median levels for the DSG and ST reference locations are 119.6 dB re 1 μPa and 119.2 dB re 1 μPa respectively (see Fig. 2.10 in previous section), with a mean of 119.4 dB re 1 μPa. The overall average of the source SPL_{0p} was derived by converting the modelled source SEL using the linear relationship between the measured data for these metrics (see Fig. 3.18).

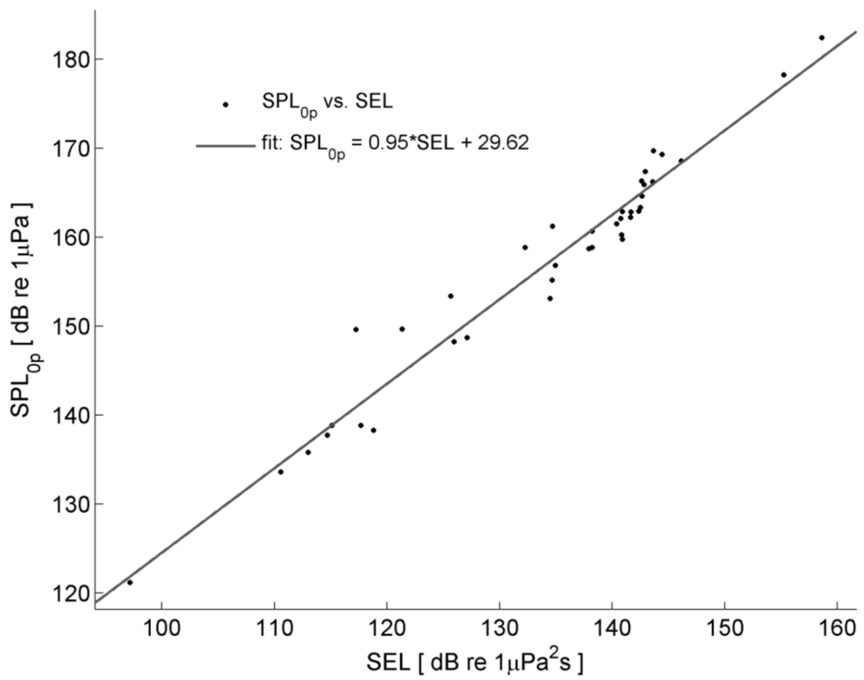

Figure 3.18 Linear relationship between measured SEL and SPL_{0p} data. Fitting done using cftool in Matlab, adjusted R^2 was 0.95

A fitted source SEL of 182 dB therefore corresponds to a source SPL_{0p} of 202.4 dB and this value was used to estimate the overall source SPL_{0p}. This is effectively what the zero-to-peak source level of the Bruce or BSP driver would be, in the end stage of piling, if it behaved as a point source of sound. The difference between this and the overall ambient noise level is 202.4 – 119.4 = 83.0 dB. We investigated the modelled loss at grid points beyond a location where piling noise was measured to be indistinguishable from ambient noise. If the loss was less than 83 dB, indicating an underestimation of loss by the model, we would increase the loss to 83 dB. In this way the contours more accurately represent the unique shadowing effects of the harbour environment on propagation loss.

Interpolation between loss points was calculated in ArcGIS (v10.3) using the local polynomial technique (with settings: polynomial order 2, smoothing factor 0.2 and an exponential kernel). The levels measured from point and drift recordings were weighted 100x and 10x higher respectively than the modelled grid points. The contours were drawn at 6 dB loss intervals. A 6 dB loss indicates a halving of sound pressure, therefore each contour represents half the sound pressure of that at the previous contour.

The non-circular contours (Fig. 3.19) indicate that the soundscape is clearly influenced by factors other than range. The most notable feature is the relatively low transmission loss towards location 31 compared to those shielded from the pile-driving by Sticking Point though at a similar range (such as 15 or 29). Some of the sound energy will be lost as it passes through the breakwater, although, the sound is likely to diffract around this point. The other interesting pattern on the western side is a large spacing in contours between locations 27 and 25. A possible explanation for this relatively low loss with range could be the shallowness of the water in this area, leading to cylindrical rather than spherical spreading. The increased loss with range to the north of location 36 could be explained by the shielding effect of the Kaumataurua Reef behind location 38.

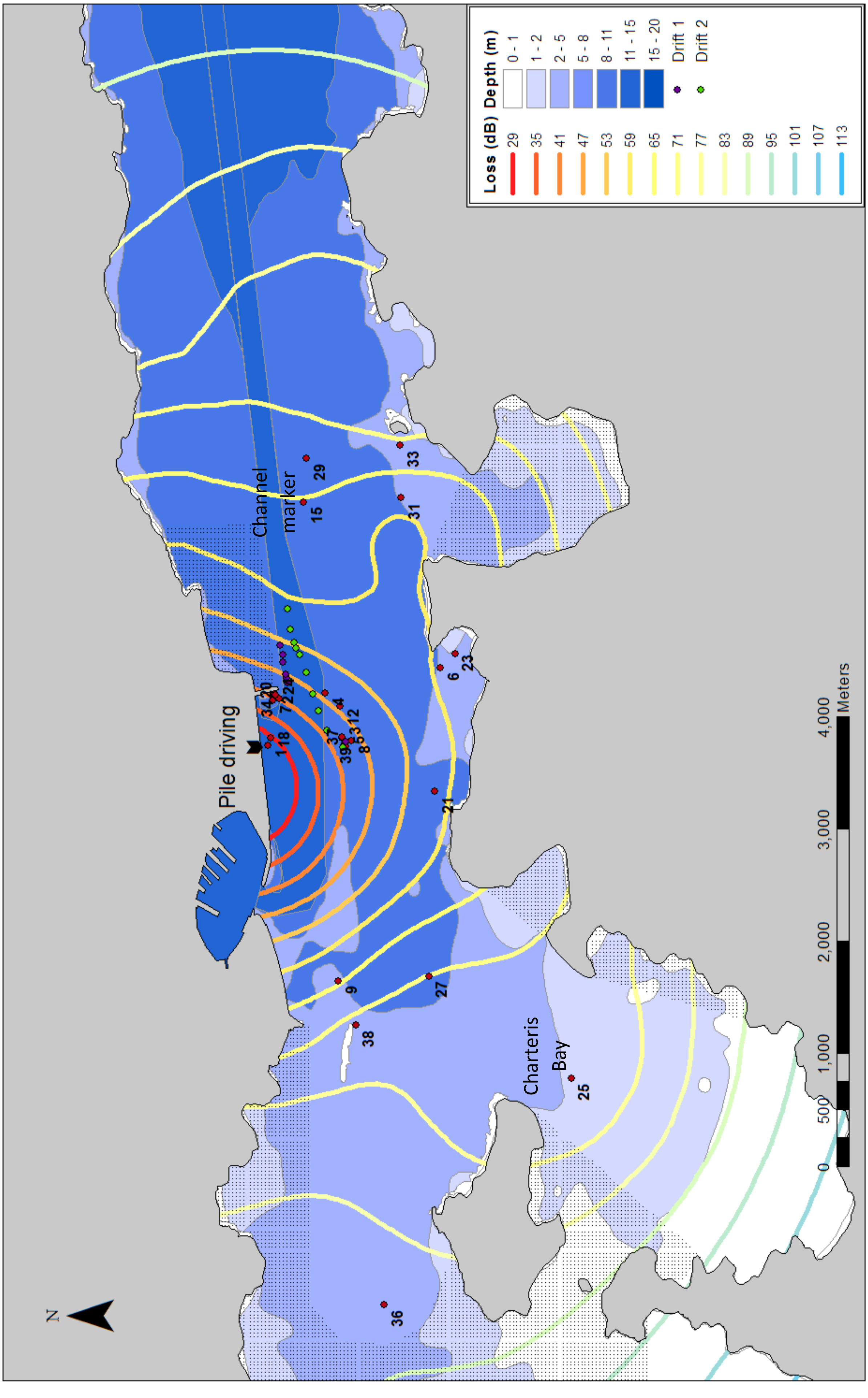
Loss (dB)
29
35
41
47
53
59
65
71
77
83
89
95
101
107
113
Depth (m)
0 - 1
1 - 2
2 - 5
5 - 8
8 - 11
11 - 15
15 - 20
Drift 1
Drift 2
Pile driving
Channel marker
Charteris Bay
N
0
500
1,000
2,000
3,000
4,000
Meters

Figure 3.19 (On previous page) Loss contours in dB (coloured lines) are plotted over the harbour bathymetry (blue fields). Recording locations are indicated as red dots with the number labels corresponding to the labels in table 2.1. Some labels could not be displayed due to the many neighbouring measurements. The two drifts are shown as purple dots for the drift on 10/2/15, and green dots for the drift on 7/1/15. The shaded areas indicate where the loss contours are likely unrealistic based on the fact that shielding will greatly increase the loss at these locations.

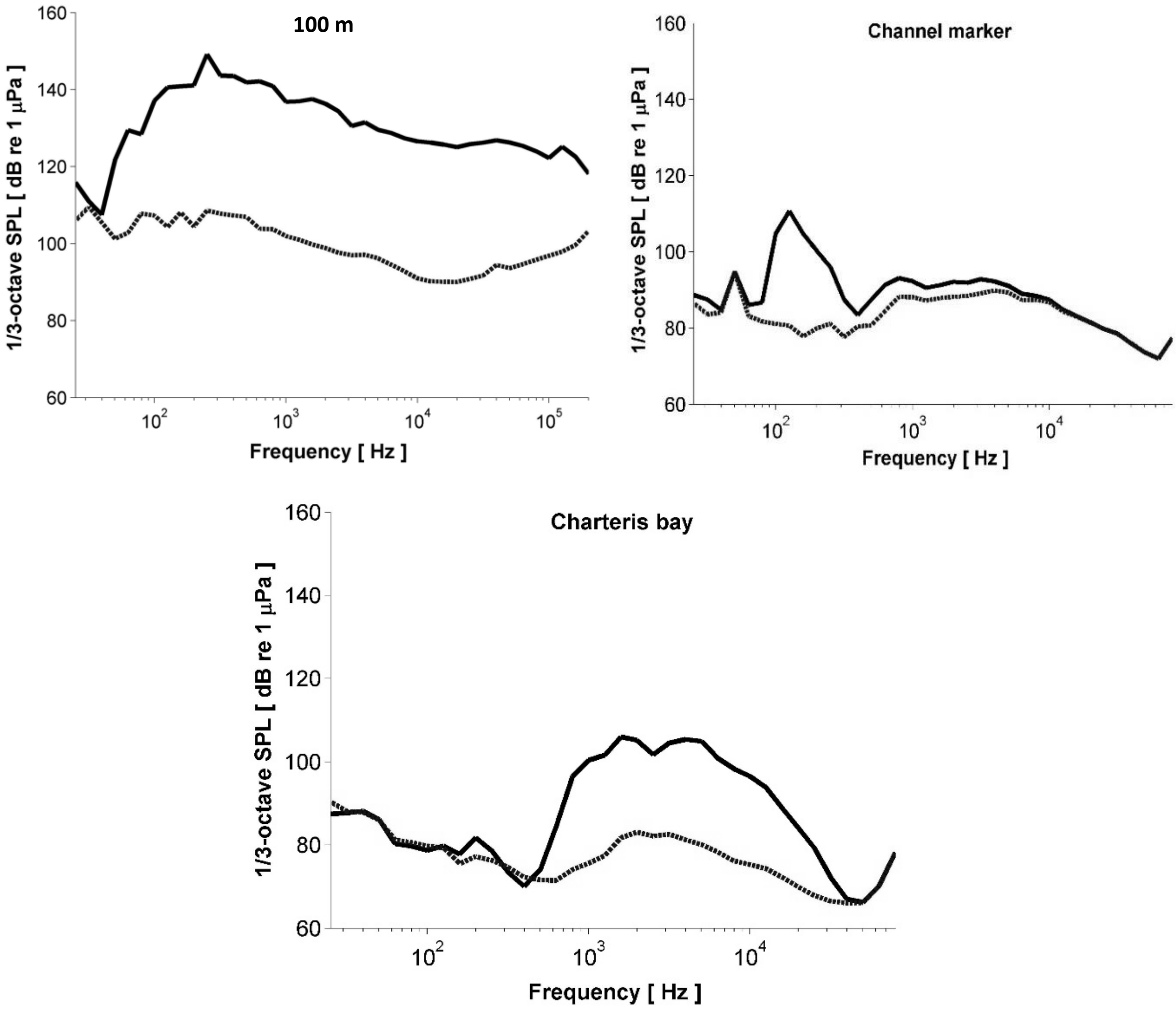

Figure 3.20 Piling noise TOLs (solid black line) and ambient noise TOLs (dashed line) measured at three locations around the harbour. TOP LEFT: 100 m from piling, location 1 on Fig. 3.18, TOP RIGHT: at the channel marker by location 15, BOTTOM: Charteris bay by location 25.

Frequency content changes as we get further away from the piling. At close range, piling noise is very broadband, as shown in Fig 3.20 (top left). Further out, both piling and ambient noise levels decrease. Sticking Point was in the straight line path of the sound from the wharf to the channel marker, which may explain the loss of most of the high frequencies (Fig. 3.20, top right). At another distant recording, made in very shallow water, only the high frequencies persist (Fig. 3.20, bottom).

To further examine how the sound is influenced by the breakwater we conducted a drift recording past Sticking Point to measure the SEL and PSD with time (Figs. 3.21 and 3.22 respectively).

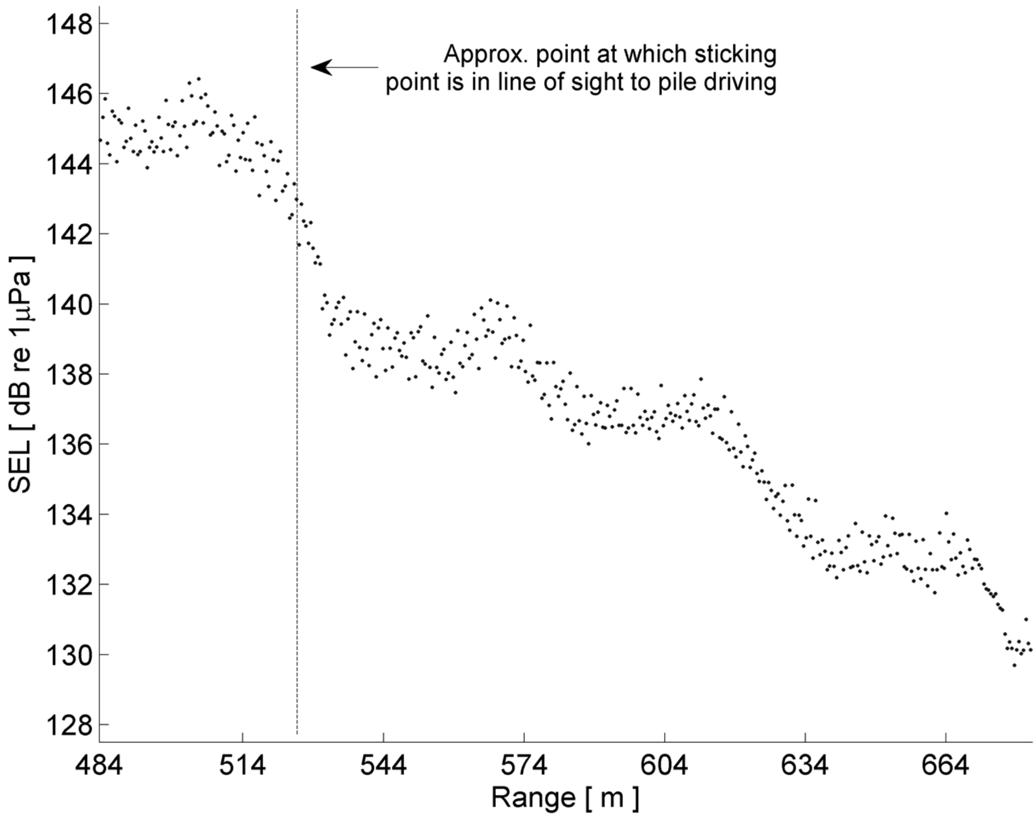

Figure 3.21 SEL of each strike recorded while drifting past sticking point over a period of 11 mins. Approximate range at which breakwater starts shielding pile-driving sound from the boat-based recording system is indicated by the vertical dotted line (526 m). Frequency range 30 Hz – 96 kHz.

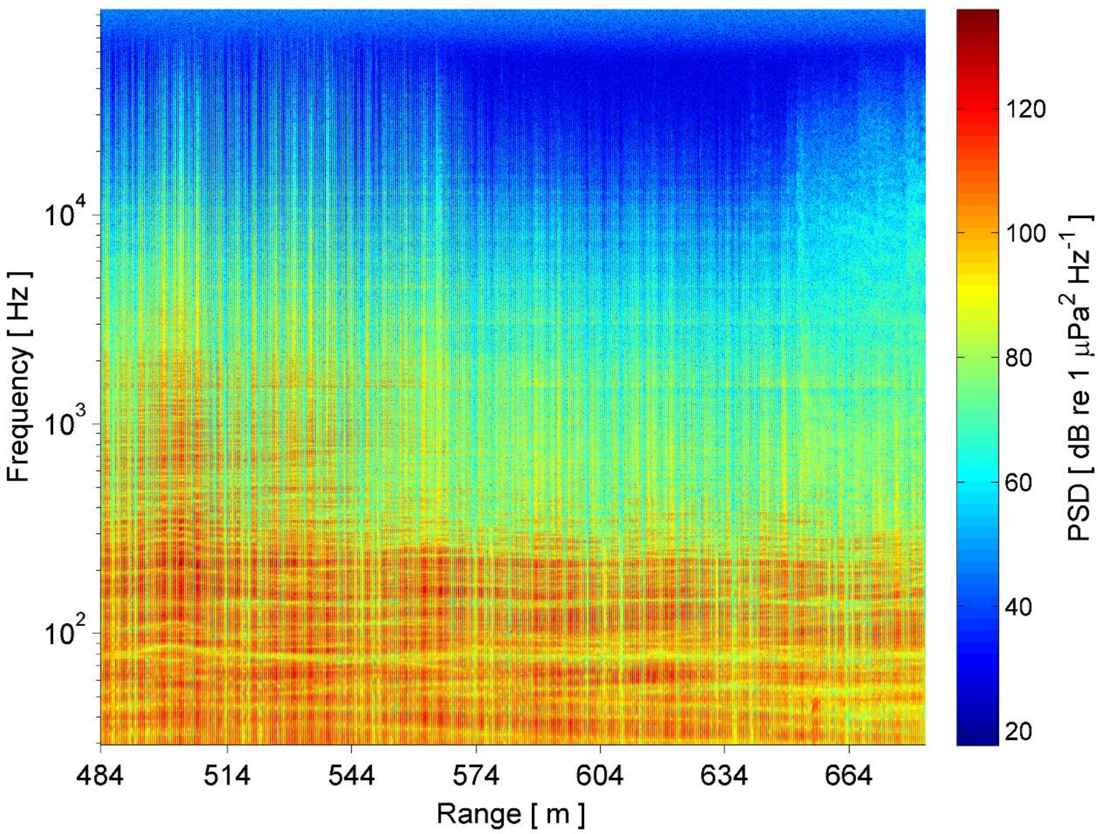

Figure 3.22 Power spectral density of pile strikes recorded while drifting past Sticking Point (approx. passing range around 526 m) over a period of 11 mins. Frequency range 30 Hz - 96 kHz.

The effect of the breakwater in the path of the sound is clearly seen in the sudden decrease in SEL at point of passing Sticking Point (c. 526 m mark, Fig. 3.21), which causes a significant amount of shielding, through absorption or reflection off the large rocks in the breakwater structure. Spectral content (Fig. 3.22) changes more gradually, with an obvious shielding effect seen after 570 m.

3.4 DISCUSSION

For simplicity, I used pile-driving noise levels estimated by the best fitting propagation model to compare pile-driving to ambient noise in Lyttelton and to pile-driving noise measured in other studies. It should be noted, however, that measured noise levels in Lyttelton varied significantly around the model.

Pile-driving activities introduced a large amount of noise pollution even in a “noisy” harbour environment. Peak pressure levels changed by over 1000 Pa (see Fig. 3.12). At close range TOLs were raised by up to 45 dB across a wide frequency range (see Fig. 3.20), exceeding background levels over an area of up to 16.3 square km. However, the noise can be heard over a greater area than this. While passing vessels introduce loud sounds particularly if heard at close range, the peak SPLs of the pile-driving noise greatly exceed boat noise even when range to piling is much larger than range to the vessel (see Fig. A.6 in appendix for more detail).

Duncan et al., (2010) measured pile-driving noise in Port Phillip Bay, Australia, under very similar conditions to the pile-driving in Lyttelton. Pile type (diameter and material), hammer energy and water depth were comparable to those for Lyttelton. The main difference was the substrate. The two locations measured in Duncan’s study were above a silt layer on sand and sand on calcarenite. Both layer types are much harder, with higher densities, than the mud/sand layer in Lyttelton. Comparing SELs at the same range from pile-driving shows that the levels measured in the present study are lower by about 12 dB. While the frequency content of pile-driving is relatively similar for most studies, the sound pressure levels recorded in this study are much lower than those for previous studies. Most studies had either a larger pile diameter (for example Nedwell et al., 2007; Tougaard et al., 2009; and Brandt et al., 2011 – see table 1.1), harder substrates (for example Nedwell et al., 2007; Robinson et al., 2007; Tougaard et al., 2009) or higher hammer energy (for example Lepper 2009; Bailey et al., 2010; Brandt et al., 2011 – see table 1.1). Most studies were in much deeper water. This study has sound recordings from among the shallowest water depths (a few m), which contributes to greater propagation loss for low frequencies.

Similar pressure levels have been measured in only a few studies. For example, Rodkin and Reyff (2008) give SELs recorded at a range of 10 m for timber (0.3 m diameter), concrete (0.6 m diameter) and steel (0.3 m diameter) piles that are 10, 7 and 15 dB lower than our modelled levels at that range, respectively. Information on substrate or hammer energy was not available. These measurements, however, were made at very close range, well within the “near” field, where measurements of absolute sound levels are not reliable. For this same reason, we have no measurements at this range for comparison, only modelled levels.

The most comparable levels were recorded in inner Fremantle Harbour, Australia, where the SEL at 54 m was within 1 dB of our modelled level (Paiva et al., 2015). No information was available on hammer energy or pile diameter but since this harbour also experiences high siltation rates the top layer of substrate is possibly similar to the fluid mud layer in Lyttelton.

This comparison may be compromised, as above, by the Fremantle recording being made too close to the sound source, probably within the near field.

There are surprisingly few studies of the kind of pile-driving activity used for wharf construction in harbours. In contrast there has been considerable research interest in quantifying sounds generated by piling for offshore wind farms. The latter use much larger diameter piles, larger pile drivers, and are usually driven in deeper water. So it is not surprising that such studies produce very different results. For example, Brandt et al., (2011) made recordings at very similar range 720 m) to our cross-channel DSG location (750 m), yet their levels exceed levels in Lyttelton Harbour by 37 dB, a sound energy difference of more than 5000 times. Pile diameter was 3.9 m (compared to 0.611 or 0.711 m), and hammer energy was 900 kJ (compared to a maximum of 206 kJ).

Our range of T_{90} durations (0.059-0.62 s) were similar to the range of measurements made on other pile-driving operations (Bailey et al., (2010): 0.01-0.2 s; Nedwell et al., (2007): ~0.5 s; Tougaard et al., (2009): 0.2 s; Blackwell et al., (2005): 0.06-0.0.26 s; de Jong et al., (2008): 0.01s; Lepper et al., (2009) 0.15-0.5 s). Some studies observe an increase in T_{90} with range (Blackwell et al., 2005; Bailey et al., 2010; Yang et al., 2015). This can be expected as the signal will spread out in time as it propagates through a medium, recombining with time-lagged reflections (Urick et al., 1983), often referred to as “multipath”. This was not observed in the present study (see Fig. 3.16).

Propagation modelling

To our knowledge there is no recommended number of measurements required in order to fit a propagation model. Our study had a larger sample size of recording locations, over a greater range of distances from the piling, than several published studies (for example Blackwell et al., 2005; Tougaard et al., 2009; Duncan et al., 2010). Studies with more measurement points include Nedwell et al., (2007) and Bailey et al., (2010). The most sophisticated attempt at modelling propagation, which incorporates the most influences on propagation loss, is by Duncan et al., (2010). This model considers spreading and absorption loss as well as influences of bathymetry and bottom layer properties. The same modelling techniques were applied to our data, using the AcTUP v2.2L toolbox for Matlab (Collins & Porter 2005). However, the limited knowledge of Lyttelton’s bottom layer properties and the model’s high sensitivity to these inputs restricted the value of the modelling outputs. Our approach was to develop a simple propagation model based on as much data as we could, referenced to measured pressure levels from multiple locations. The empirical data were weighted heavily in producing a contour map of losses (Fig. 3.19). The result is that the spot recordings act to define the pressure levels, while the model interpolates between, and beyond them.

Our geometric spreading coefficient of 12.6 was closer to cylindrical propagation (10) than to spherical propagation (20), most likely due to the shallow water depths in Lyttelton (2-15 m). Studies in deeper water show spreading losses of 20 (Bailey et al., 2010), 17-21 (Nedwell et al., 2007) and 16-29 (Blackwell et al., 2005). The absorption coefficient found in Lyttelton (0.0095 dBm^{-1}) is much higher compared to 0.0004 dBm^{-1} and 0.0003-0.0047 dBm^{-1} found by Bailey et al., (2010) and Nedwell et al., (2007) respectively. This is most likely due to the higher absorptiveness of the bottom layers in Lyttelton compared to gravelly sand (Barne et al, 1996) and sand respectively, but also affected by the shallower water depths in Lyttelton.

Simpler models, excluding the absorption parameter (Blackwell et al., 2005; Tougaard et al., 2009) do not fit our data as well as the three-parameter equation used (Fig 3.17). The three-parameter fit has a higher adjusted R^2 than all the two-parameter fits. The simpler models are also less realistic because the imputed source level and spreading coefficient are unrealistically high - higher than any equivalent values in other studies. The values for our three-parameter equation are much more reasonable. The first two fitted values are within a reasonable range: a geometric spreading coefficient of 12.6 is reasonable, as outlined above. Also, the imputed source level (182 dB re 1 µPa @ 1 m) is between the source level predicted for this pile diameter by Nedwell et al., (2005) and the source level calculated for similar conditions (Duncan et al., 2010), 168 and 205 dB re 1 µPa @ 1 m respectively.

The noise map (Fig 3.19) helps visualise how the noise spreads throughout the harbour. It is especially useful for considering how noise generated by future construction in Lyttelton Harbour is likely to propagate, and potentially affect species sensitive to noise. The contours, however, are broad estimates. Error is introduced during the propagation modelling which generalises influences on sound level, such as bottom layer properties, bathymetry and frequency content of the signal. It is likely that the higher than expected absorption coefficient reflects the additional absorption through the fluid mud layer. Additionally, the use of an average ambient noise level, to determine at which level the piling noise is indistinguishable from ambient noise, does not reflect the varying ambient noise levels at different locations around the harbour. Maps of underwater noise have been produced in previous studies (see for example Cobo et al., 2007; Erbe et al., 2014) but to our knowledge none are based on the combination of modelled and empirical measurements, as in the current study.

General conclusions

Measurements of the ambient and pile-driving noise clearly show that pile-driving introduces a large amount of impulsive broadband noise into the inner harbour environment. Most of the energy is within the 100-1000 Hz frequency range but there is significant energy well above 100 kHz, particularly at close range. Frequency content varied at different recording locations around the harbour. Using a GLM it was found hammer energy, pile driver type and stage of piling were the significant influences on the noise levels measured.

A simple propagation model was applied to estimate the loss (dB) with range (m). While it is complex to model propagation loss in a realistic environment, including all the various influences combined with a complex noise source, the simple model combined with empirical measurements allow visualisation of how the noise spreads throughout the harbour using loss contours on a map.

The pile-driving noise levels measured at all ranges in the present study tended to be lower than many previous studies. This was mainly due to a smaller pile diameter, lower hammer energy and a softer substrate in Lyttelton.

Chapter 4

Impact of pile-driving on Hector's dolphins in Lyttelton Harbour

4.1 INTRODUCTION

With the increase in anthropogenic noise in the ocean (e.g. McDonald et al 2006) there is a growing interest in researching the impact of noise on marine mammals. Since marine mammals rely on sound for foraging and sociality it is important to know how the added noise may affect them. Underwater anthropogenic noise has been shown to have a negative impact on marine mammals in many ways, through sources including airgun pulses used in seismic surveys (e.g. Romano et al., 2004; Lucke et al., 2009; Gray & van Waerebeek 2011), shipping (Aguilar Soto et al., 2006; Castellote et al., 2012; Rolland et al., 2012) and sonars (e.g. Fernández et al., 2005; Filadelfio et al., 2009; Tyack et al., 2011). Pile-driving, another source of underwater noise pollution, is of particular concern since the noise is loud, impulsive and broadband in frequency (Madsen et. al., 2006).

Studies of harbour porpoise, a species of similar size and acoustic repertoire as Hector's dolphin, have indicated strong avoidance reactions to pile-driving noise (Carstensen et al., 2006; Tougaard et al., 2009; Brandt et al., 2011). These studies used passive acoustic monitoring devices (T-PODs or C-PODs) to investigate changes in animal distribution. Using several of these devices at increasing distances from the piling provides a way to detect changes in the number of echolocation clicks detected prior to, during and after piling. For example, Tougaard et al. (2009) and Brandt et al. (2011) found a marked decrease in porpoise clicks over a radius of at least 20 km. At close range (2.6 km from the source), this response lasted up to 72 hours (Brandt et al., 2011). Aerial surveys conducted at the same time showed that the animals actually left the area rather than become silent (Dähne et al., 2013). It is clear, however, that piling also affects echolocation rate; there was a sudden decrease in click rate following the onset of piling noise (Brandt et al., 2011).

A different method, using high definition video recordings, revealed that visual detections of Indo-Pacific bottlenose dolphins in a harbour channel decreased significantly during pile-driving activity in wharf construction (Paiva et al., 2015). This study could not determine whether decreased detections were due to decreased dolphin abundance. Other explanations could include masking of communication signals leading to reduced surface socialising, or a change in foraging behaviour due to reduced prey abundance and/or reduced ability to detect prey. Taken together, the studies mentioned above show that there can be a strong avoidance reaction to pile-driving noise. Due to the uncontrolled nature of studying wild animals, however, it is difficult to confirm whether these reactions were purely due to noise; other factors may include prey movement or unknown environmental changes.

The 2010 and 2011 Christchurch earthquakes extensively damaged the city's port in Lyttelton Harbour. Port development work, in anticipation of a growing increase in container cargo, was combined with the repair work. The construction and repair work included extensive pile-driving (see Ch. 1). The primary aim of this study was to investigate the impact of pile-driving noise on Hector's dolphin distribution in Lyttelton Harbour. Following on from quantifying the noise generated by pile-driving and how it propagates within Lyttelton Harbour (Ch. 3), in this chapter I investigate whether and how Hector's dolphin distribution changes during pile-driving activity. In this chapter I also discuss the ranges at which we might expect temporary threshold shift (TTS) in hearing to occur for Hector's dolphins, depending on the duration the animals may spend at that range.

In this study I used T-PODs to quantify dolphin distribution. These are passive acoustic monitoring devices whose filters can be set to match the narrow-band high-frequency echolocation clicks of Hector's dolphin. Because there is no other biological source of these kinds of sounds in NZ waters, the T-POD detections provide confident identification of Hector's dolphin presence. T-PODs have been used extensively to document habitat use by Hector's dolphins (e.g. Rayment et al., 2009a & b; Dawson et al., 2013). Three T-PODs were moored in Lyttelton; one each in the outer, mid, and inner harbour. Via analysis of the T-POD dolphin detections and the pile-driving records, I aim to quantify if/how dolphin presence is affected by pile-driving noise. Specific questions of interest were: does the number of detections per day differ on days with piling compared to those without piling? Does the detection rate change after a pile-driving event? If there is an effect, how long does this last following the pile-driving event? And lastly, to what extent is this influenced by other factors such as time of day, T-POD location and weather conditions?

4.2 METHODS

Field techniques

Pile-driving was used extensively in the reconstruction of one of the main wharves (Cashin Quay 2) in Lyttelton Harbour. Over the study period, piles driven were within an area 77 m long (along the wharf) and 24 m wide (at the location of the 'Pile-driving label' in Fig. 4.1), comprising 90 pile locations, of which 57 were driven during the monitoring period. Three different pile drivers were used with hammer weights of nine, ten and 14 t.

Echolocation detectors (v.5 T-PODs, numbers 755, 775 & 776, Chelonia Ltd) were moored in Lyttelton Harbour from 19 December 2014 to 25 March 2015, at three distances from the piling. The sites were chosen to represent inner, mid and outer harbour sites (Fig. 4.1) while also considering the safety of our equipment for long term deployment in a busy harbour environment. For this reason the inner and mid T-PODs were moored to existing harbour marker structures while the outer T-POD was moored in a bay well clear of shipping traffic, with a buoy at the surface (see Table 4.1 for properties of the sites where the T-PODs were moored).

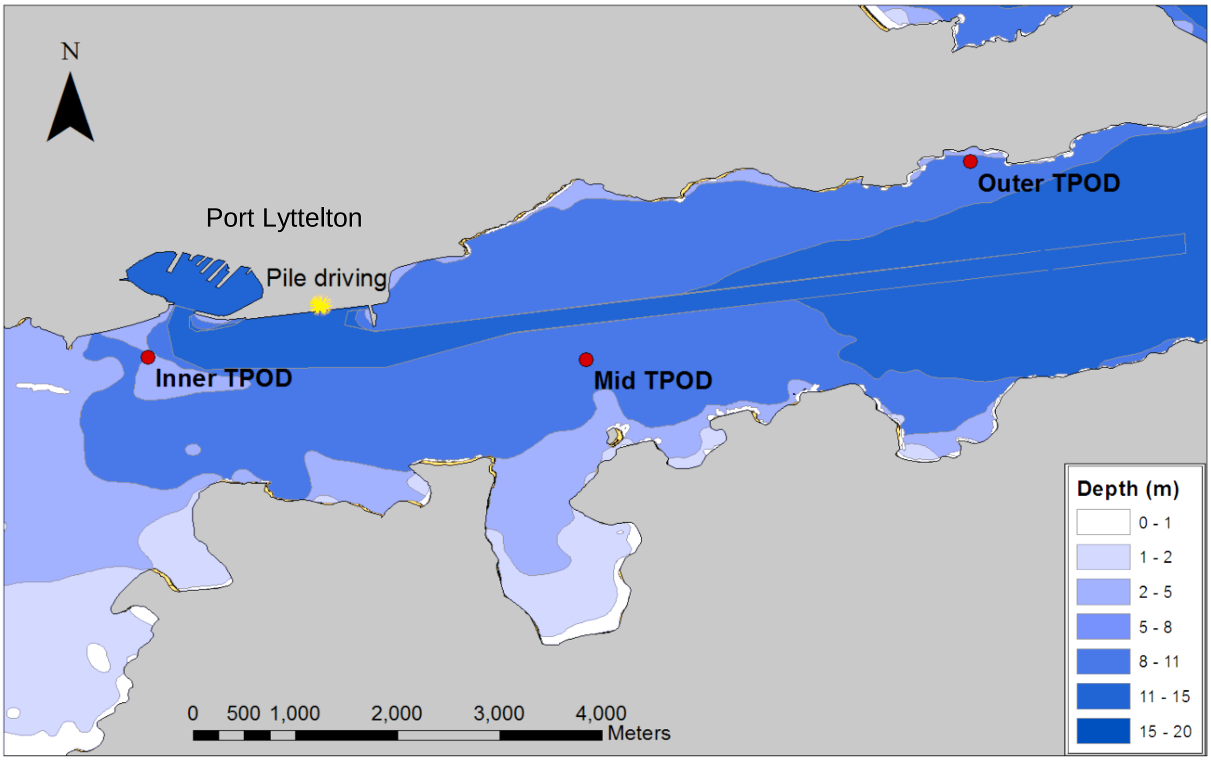

Figure 4.1. T-POD and pile-driving locations in Lyttelton Harbour.

Table 4.1. Site properties for each T-POD location. Substrate information obtained from Chart NZ 6321 (www.linz.govt.nz).

Site	Range to piling (m)	Range to nearest shore (m)	Substrate	Water depth (m)	Height of T-POD above seabed (m)
INNER	1300	330	Mud/Shell	4	2
MID	2000	890	Sand/Mud/Shell	8	2
OUTER	4900	125	Mud	7	2

T-PODs were serviced (data downloaded, batteries replaced, fouling removed) on 7 January (re-deployed on the same day) and 27 February 2015 (re-deployed on 5 March 2015 due to unsuitable weather conditions). The same T-PODs were used at their respective sites for the entire monitoring period, except for the outer site. This T-POD became detached from its mooring sometime between 7 January and 27 February, and was not recovered. The T-POD was replaced with a new device (v.4 No. 484, Chelonia Ltd). The aim of the acoustic monitoring was to detect changes in acoustic activity relative to presence of pile-driving noise. Keeping the T-PODs at the same site meant there was one fewer variable influencing detection rates at each site within the monitoring period. While there may be differences in detection rates among T-PODs, the sensitivities of the T-POD versions used in the current study (v. 4 and 5) are similar and much more standardised than previous versions (Dähne et al., 2006; Verfuß et al., 2008).

In all T-POD deployments, five scans were optimised for the detection of Hector's dolphins (target filter frequency = 130 kHz; reference frequency = 92 kHz; bandwidth = 4; noise adaptation = ++; sensitivity = 10; scan limit = 240), and 1 scan was set at a lower frequency to discriminate between Hector's dolphins and other delphinids (target filter frequency = 50 kHz; reference frequency = 70 kHz; sensitivity = 6). The same settings were used as in Dawson et al. (2013) studying Hector's dolphin habitat use and Rayment et al. (2011) detecting Maui's dolphin clicks. Other studies using T-PODs employed a similar strategy to discriminate between detections of harbour porpoises and bottlenose dolphins (e.g. Philpott et al., 2007, Bailey et al., 2010).

Analyses

Data were processed using the T-POD.exe (v8.24). This software classifies clicks according to the likelihood they are of cetacean origin. The categories are CET HI (high probability), CET LO (lower probability), DOUBTFUL (cetacean and doubtful trains), VERY DOUBTFUL (all trains excluding sonar) and FIXED RATE/BOAT SONAR. It has been shown that CET HI and CET LO (combined as 'Cet All') reliably represent Hector's dolphin detections (Rayment et al., 2009a) so only click trains in these categories were used for further analysis. It must be noted, however, that using only 'Cet All' detections results in a conservative account of habitat use as many genuine Hector's dolphin echolocation trains are classified as DOUBTFUL (Rayment et al., 2009a; see also Thomsen et al., 2005 for a similar result from harbour porpoise).

Click data were exported as detection positive minutes (DPM), the number of minutes in which dolphin clicks were detected over a given period (hour or day). DPM is the recommended metric for studying habitat use and behaviour (Chelonia Ltd 2007) and has been used in other studies assessing impacts of pile-driving (Brandt et al., 2011, 2016, Haelters et al., 2012). The use of this metric also reduces the effect of variation in sensitivity among T-PODs (Dähne et al., 2006).

Pile-driving noise was measured throughout Lyttelton Harbour as described in Ch. 3. The levels measured by the Diamond Harbour DSG (see Fig. 2.1 in Ch. 2) were used in the statistical analysis presented in this chapter. This recorder was moored continuously throughout the monitoring period and recorded at a low sample rate (2500 Hz) to allow storage of the long term data. While this sample rate would not have captured the full spectrum of piling noise (i.e. only up to 1250 Hz), the recordings allow analysis of relative intensity of pile-driving noise at different times in the monitoring period. Additionally, the high frequency part of the noise would already be greatly diminished at this site due to propagation loss.

Other recordings made throughout the harbour (with much higher sampling rates) were used to estimate ranges of TTS onset. These estimates were based on previous studies of TTS in harbour porpoise (Lucke 2009; Kastelein et al., 2013a, 2015) and are presented in the appendix (section 7).

Statistical analyses

Statistical analyses was carried out using the software package R (v 3.2.4, The R Foundation for Statistical Computing, 2016). The effect of pile-driving noise on dolphin detections was investigated using an information theoretic approach (Burnham & Anderson 2002; Anderson 2000) by comparing a suite of competing explanatory models. I used two different types of response variables for the statistical modelling: DPM per day and DPM per hour. DPM per day allows for simpler models as there is no need to account for fine scale temporal patterns in dolphin distribution within each day, but enables investigation of the change in distribution on a day to day basis that is easy to interpret. It does not, however, allow analysis of the fine scale temporal reactions to pile-driving such as the duration of any effects. DPM per hour was, therefore, also modelled. The response variable "waiting time" – the time between subsequent click trains - was also investigated, following Dähne et al., (2013) and Tougaard et al., (2009). The resulting models, however, had very poor fit, with very low R^2 values (< 0.04), and hence were not pursued further.

Histograms of DPM per day and DPM per hour showed that these variables were not normally distributed (Fig. 4.2). Poisson and negative binomial distributions were fitted to each response variable to see which would be best used as the distribution family for fitting the explanatory models (see red and green lines respectively on Fig. 4.2). Visual comparison indicated that the negative binomial distribution provided the closest fit for both response variables. I also used Q-Q plots (comparing the response variable to fitted negative binomial, Poisson, normal, lognormal and gamma distributions) as additional verification. These confirmed the negative binomial distribution as the most appropriate family for modelling the DPM response variables.

For the models of DPM per hour, the explanatory variables consisted of piling related, time related and environmental variables (Table 4.2). The mean sound exposure level (SEL) was used to account for the pile-driving intensity. As it was often not possible to calculate the SEL for every strike within an hour, due to obscuring ambient noise (such as water flow noise or passing boats), a representative sample of ten pile strikes was used to calculate the mean SEL for each hour. To see how long any effects may last following a pile-driving event, the variable time-since-piling was included. The number of minutes of pile-driving in the previous event was included to see if duration of pile-driving influenced DPM per hour. For each hour this was the total piling positive minutes within previous consecutive hours

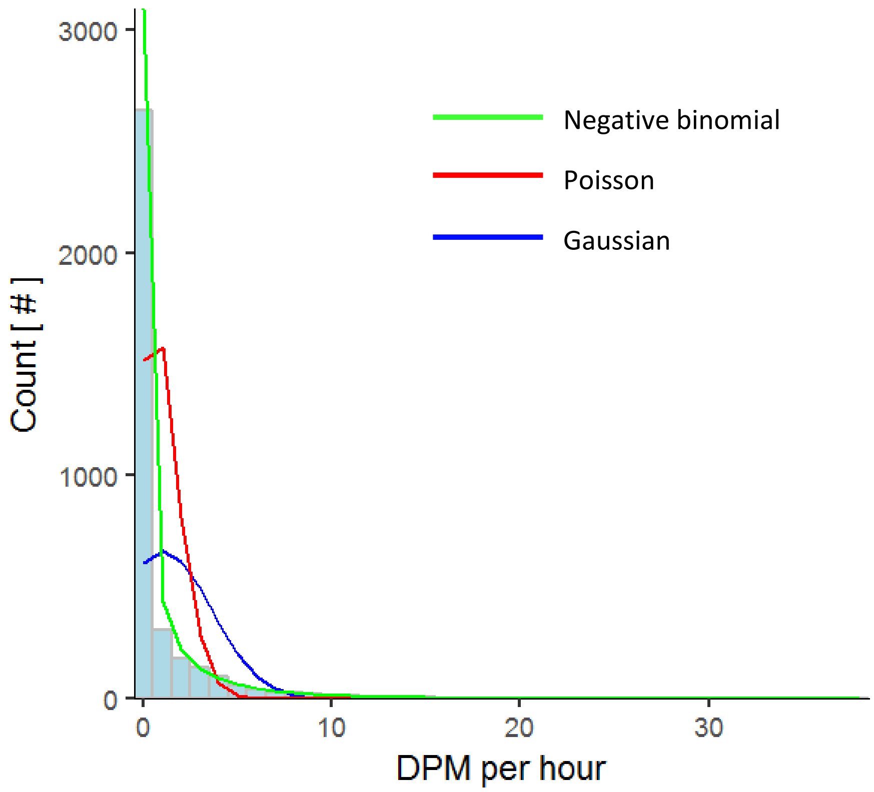

Figure 4.2. Histogram of response variable DPM per hour, comparing the fit of the negative binomial, poisson and Gaussian distributions.

containing pile-driving, up to the current hour. Hourly wind data were provided by Metservice (through Lyttelton Port Company, LPC), and daily wind data were provided by NIWA's national climate database, using weather stations on the wharf. Sound does not propagate as far at high wind speeds due to decreased reflection at the roughly textured water surface and increased attenuation due to increasing aeration of the water. This could lead to a reduction of clicks detected at higher wind speeds. Wind speed and direction have been shown to influence porpoise detections in a previous study of the impact of pile-driving (Brandt et al., 2016). Time of day and time since high tide have also been shown to influence Hector's dolphin distribution in Akaroa harbour, on the south side of Banks Peninsula (Dawson et al., 2013).

Initial data exploration revealed some outliers in the time-since-piling variable due to the Christmas break, which at 17 days was much longer than any other break within piling (max. 90 hours). The dataset was restricted to include data for which time-since-piling did not exceed 150 hours. This limit is more than twice as long as the longest duration of impact observed in harbour porpoise studies (72 hours; Brandt et al., 2011).

The DPM per day dataset had a similar set of explanatory variables (Table 4.3). Piling positive minutes per day was used to account for the amount of piling. Mean SEL per day was calculated by averaging the SELs over the hours that contained piling. The timing and duration of pile-driving were determined using pile-driving records completed by the piling contractor (HEB construction) for LPC, and validated using our long-term acoustic record.

Variance inflation factors (VIFs) were calculated for the explanatory variables to ensure there was no significant correlation among them, using a cut-off value of three (Zuur et al., 2009). None of the variables' VIFs exceeded the cut-off value, therefore collinearity between variables was deemed not significant.

Table 4.2 List of explanatory variables used in the statistical models of DPM per hour

Variable (abbreviation)	**Type**	**Description**
Piling related variables		
Sound Exposure Level (SEL)	Continuous	Mean sound exposure level (dB re 1 µPa^{2}s) of a representative sample of 10 strikes per hour as measured at the Diamond Harbour DSG
Time since piling (TSP)	Continuous	Equals '0' during hours of piling, otherwise equals the minutes since the previous piling event.
Piling duration (Dur)	Continuous	Duration of the previous piling event in minutes.
Time related variables		
Hour of day (Hour)	Continuous, cyclic	Equals '0' for the hour starting at 00:00am, to '23' for the hour starting at 11:00pm
Previous DPM (DPMt1)	Continuous	DPM measured in the preceding hour.
Environmental variables		
Wind speed (Wspd)	Continuous	Averaged over the 10 directly preceding each hour, measured in knots
Wind direction (Wdir)	Continuous, cyclic	Measured in degrees
T-POD position (TPOD)	Factor, 3 levels	Inner (1), mid (2) or outer (3) harbour position
Tide (tide)	Continuous, cyclic	Hours since last high tide

Table 4.3. List of explanatory variables used in the statistical models of DPM per day

Variable (abbreviation)	**Type**	**Description**
Piling related variables		
Sound Exposure Level (SEL)	Continuous	Mean sound exposure level (dB re 1 µPa^{2}s) for each day as measured at the Diamond Harbour DSG
Piling positive minutes (PPM)	Continuous	Total number of minutes that contained pile-driving noise each day
Time related variables		
Previous DPM (DPMt1)	Continuous	DPM measured during previous day.
Environmental variables		
Wind speed (Wspd)	Continuous	Measured in knots at 9 am each day
Wind direction (Wdir)	Continuous, cyclic	Measured in degrees at 9 am each day
T-POD position (TPOD)	Factor, 3 levels	Inner (1), mid (2) or outer (3) harbour position

The effect of the explanatory variables was investigated using Generalised Additive Models (GAMs; Hastie & Tibshirani, 1990) with a negative binomial response, constructed using the package *mgcv* in R. GAMs fit a sum of smooth functions for each covariate, and are particularly useful for modelling the non-linear relationships between cetacean distribution and environmental variables (Forney et al., 2000; Ferguson et al., 2006; Torres et al., 2008). Since the model is additive, the effect of each covariate is considered in addition to the effects of the other covariates (Hastie & Tibshirani, 1990). The choice of basis dimension for smoothing terms is a trade-off between computational efficiency and having enough degrees of freedom to represent the effect of the variable (Wood 2017a). Since computer power was not a limiting factor, the basis dimension was not restricted and left to be chosen during the modelling process for best fit. All smoothed functions were fitted using the default cubic regression spline, except for the circular variables (tide, time of day and wind direction) which were fitted with a cyclic cubic regression spline.

I expected the explanatory variables to have a different effect on the response variable based on T-POD location. Therefore, as well as using a smoothing function for each variable, I also tested a factor interaction term (with the ‘by = TPOD’ argument), which fitted a separate smoothing function for each of the three T-POD locations. Models never contained both the smoothing function of the variable and the factor interaction term as this would be similar to including the same variable twice.

Both response variables had high temporal autocorrelation (tested using the *acf* function in the R package *stats*). One method to account for correlation is to use a correlation structure in a Generalised Additive Mixed Model (GAMM). Using a GAMM (as opposed to a simpler GAM) is currently the only way to use the negative binomial distribution and include a correlation structure (Wood 2017b). However, the methods for model selection of GAMMs, with distributions other than the normal distribution, are not well established (Wood 2017a); for example, it is not possible to use the standard method of comparing model AIC scores. Another approach to account for temporal correlation is to introduce an explanatory variable that has the value of the response at a previous point in time (for instance the DPM of the previous hour or day). This approach was used by Brandt et al. (2016) in a T-POD study investigating the effect of pile-driving noise on harbour porpoise, with DPM per hour as the response variable in their statistical modelling. Therefore, the DPMs in the previous hour, or DPMs on the previous day, were included as explanatory variables in their respective models (Table 4.2 and 4.3).

For each response variable, a suite of GAMs was constructed and their performances compared. I used forward step-wise selection, adding one explanatory variable to the model at a time, each time choosing the variable that gave the lowest AICc score, until adding any other variable no longer decreased the score (see Zuur et al., 2009, Ch. 16). The AICc score (AIC with a correction for finite sample size) is a measure of the trade-off between goodness of fit and complexity of the model, where a lower AICc indicates a more appropriate model (Akaike 1973; Anderson & Burnham 2002). In this case, AICc was used as the sample size, n, of the DPM per day dataset was small compared to the number of parameters, k, i.e. $n/k < 40$ (Burnham & Anderson 2003). The function *dredge* (package *MuMIn*) takes a global model with all explanatory variables and constructs simpler models with all possible combinations of variables. It then ranks the models according to AICc. This function was used to find the top models for the DPM per day response variable and confirmed the same top models as the forward selection process. Due to the large number of explanatory variables, using *dredge* for the DPM per hour response variable was impractical.

The Akaike weight of a model is an estimate of the amount of evidence that it is the best in the set of models and can be interpreted as the approximate likelihood that the model is the best in the set (Anderson et al., 2000). Since there was not one model that had an Akaike weight greater than 0.9 I model averaged all models within ΔAICc of 6 from the top model using the function *model.avg* in the R package *MuMIn*. If a model within this set was a more complicated version of another model (i.e. containing additional terms) and had a higher AICc score than the simpler model, it was excluded from the list of top models (as recommended in Richards et al., 2011). I used the conditional average of the variables (as opposed to the full average) to calculate the estimate for the coefficients of each term (Tables A.1 and A.2). This avoids the problem of a particular variable of interest (in our case the pile-driving related variables) being overshadowed in the full average by variables with stronger effects (Nakagawa & Freckleton 2011). The Akaike weight of each explanatory variable is based on the number of times it occurs in the top models and each model's AICc score. This gives an estimate of the relative importance of each variable (Burnham & Anderson 2002).

An interaction between time-since-piling (TSP) and duration-of-piling (Dur) was included in the modelling of DPM per hour. This was done to investigate if piling events of longer duration increased the length of time after piling that detection rates were affected. A contour plot was used to illustrate the effect of this interaction. This required all the other explanatory variables to be fixed at certain values. *Sound Exposure Level* and *DPMt1* were fixed at their respective mean values, and *Hour*, *tide* and *wind direction* were fixed at values at which DPM per hour at the inner harbour was predicted to be high by the models (i.e. when dolphins are likely present in the inner harbour).

Relationships were considered significant at alpha = 0.05 (i.e. for which the p-value was 0.05 or less).

4.3 RESULTS

The study consisted of 92 days of T-POD monitoring at the inner and mid sites and 41 days at the outer site (Table 4.4), with a combined total of 5256 T-POD hours. During this period pile-driving occurred on 46 days, with an average of 125.5 mins of piling per day (SE = 16.7 mins). This average excludes a 17-day break over Christmas during which no pile-driving occurred. The outer T-POD, while in place, had consistently more detections than the other two (Fig. 4.3).

Table 4.4 T-POD deployment and detections. 'Detection positive days' is the number of days on which at least one dolphin click was detected.

TPOD	Days deployed	Detection Positive Days	Mean DPM per day	Standard Error
Inner	92	82	12.83	1.52
Mid	92	91	29.47	1.97
Outer	41	41	55.27	6.4

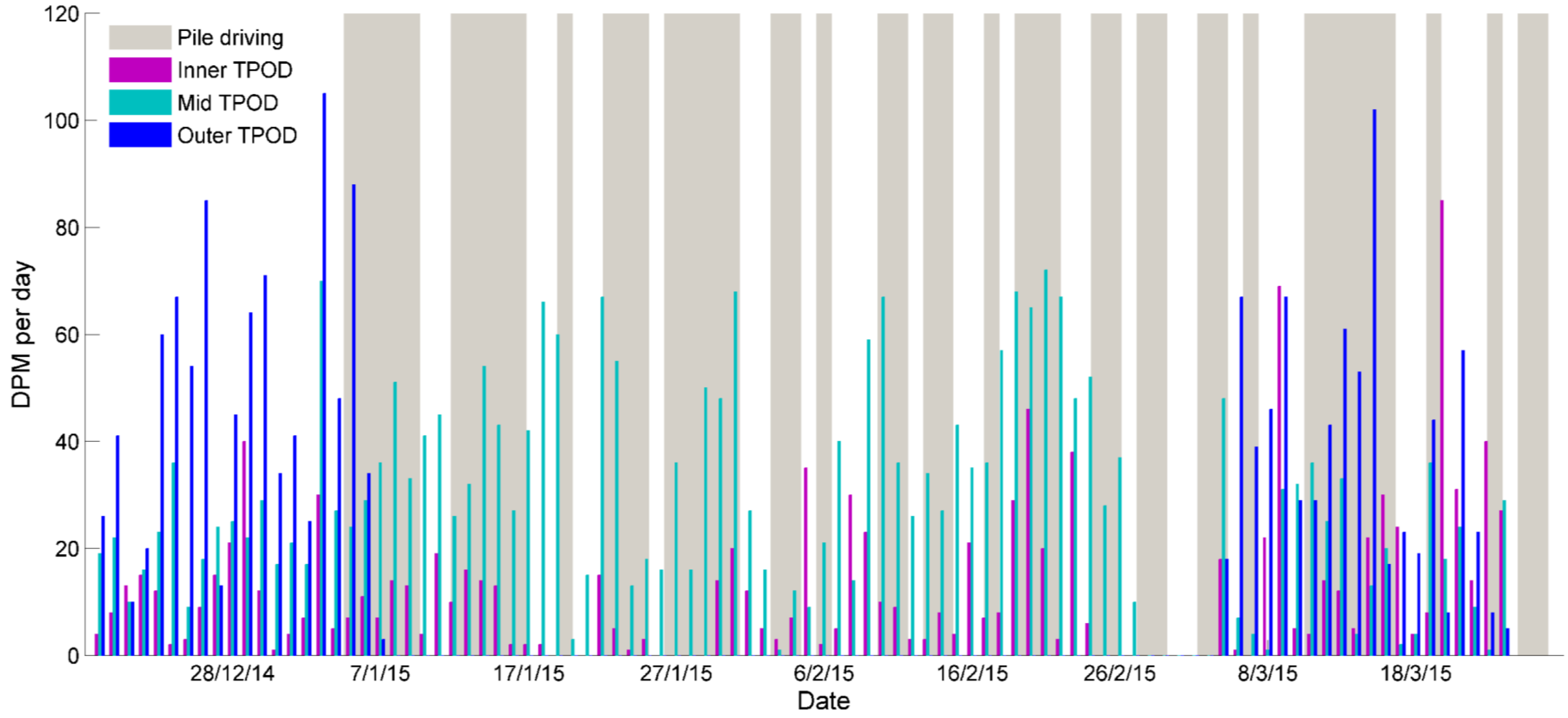

Figure 4.3. DPM totals per day for the three T-PODs in Lyttelton Harbour over the entire monitoring period (19/12/14 – 25/3/15). A day which contained pile-driving activity is marked with a grey background.

Statistical analysis of influences on dolphin detections

DPM per day

The top models, as determined using the AICc score (see Table 4.5), showed that T-POD location, the previous day's DPM, wind speed, wind direction and piling positive minutes (PPM) all explained some of the variation in DPM per day. Model fit for DPM per day was good and satisfied normality (see Fig. A.14). The best fitting model had a deviance explained of 44.2% (Table 4.7).

While not significant, an increase in PPM per day led to a decrease in DPM per day at the inner and outer T-PODs (Figs 4.4a and c, respectively), and an increase in DPM at the mid T-POD (Fig. 4.4b). DPM per day was highest at the outer T-POD and lowest at the inner T-POD (Table A.1). DPM per day decreased significantly with increasing wind speed at the inner and mid T-POD (Fig. 4.5a and b). There was no significant relationship between DPM per day and wind speed at the outer T-POD (Fig. 4.5c). At the inner T-POD, increased detections were seen during westerly winds, and decreased detections during easterly winds (Fig 4.6a). This variable was not significant for the other T-POD locations.

Table 4.5. Results of model selection for GAMs with DPM per day as the response variable. Only models within 6 AICc points of the top model are shown. Rank is based on AICc, 'Wt' is the Akaike weight of the model, '% DE' is the percentage deviance explained by the model and the 'Model' column shows the model structure of the top models, T-POD, ti(DPMt1) and ti(Wspd) were present in all the top models. Terms enclosed by 's()' are smoothed variables, and by 'ti()' are smoothed seperately for each T-POD location.

Rank	**Model**	**df**	**AICc**	**ΔAICc**	**Wt**	**% DE**	**R^2 (adj.)**
1	T-POD + ti(DPMt1) + ti(Wspd) + ti(Wdir) + ti(PPM)	18.9	1746.92	0	0.49	44.2	0.48
2	T-POD + ti(DPMt1) + ti(Wspd) + ti(Wdir)	15.6	1747.25	0.33	0.41	42.2	0.48
3	T-POD + ti(DPMt1) + ti(Wspd)	12	1750.06	3.13	0.1	39.3	0.443

Table 4.6 Akaike weights of each term after model averaging (w_{AICc}), estimated degrees of freedom (edf) and significance (p-value) of each term in the top model. Bold terms are significant at the 5% level.

Term	w_{AICc}	**edf**	**p-value**
TPOD	**1**	**2**	**5.68E-06**
ti(DPMt1):TPOD1	**1**	**2.56**	**0.001**
ti(DPMt1):TPOD2	**1**	**1.00**	**0.008**
ti(DPMt1):TPOD3	1	1.00	0.174
ti(Wspd):TPOD1	**1**	**1.00**	**0.006**
ti(Wspd):TPOD2	**1**	**1.00**	**0.012**
ti(Wspd):TPOD3	1	1.00	0.446
ti(Wdir):TPOD1	**0.9**	**1.78**	**0.006**
ti(Wdir):TPOD2	0.9	0.00	0.387
ti(Wdir):TPOD3	0.9	1.17	0.059
ti(PPM):TPOD1	0.49	1.00	0.062
ti(PPM):TPOD2	0.49	1.00	0.104
ti(PPM):TPOD3	0.49	1.00	0.486

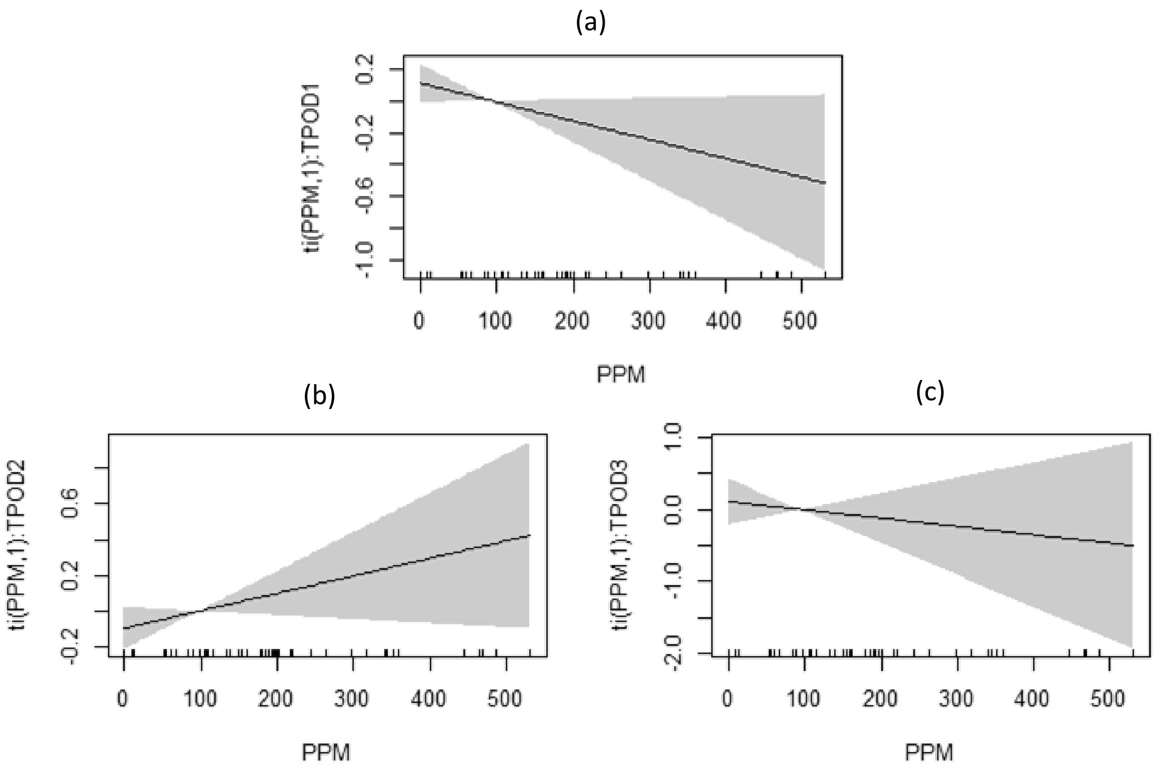

Figure 4.4 The predicted smoothing functions for the variable piling positive minutes per day (PPM, x-axis) and its effect on DPM per day (y-axis) with shaded confidence intervals. Plots a, b and c refer to the inner, mid and outer T-POD locations. Note that the vertical scale varies among plots. The number in brackets following the variable abbreviation on the y-axis gives the estimated degrees of freedom. The ticks along the bottom edge of the plot indicate the values found in the measured data for that variable.

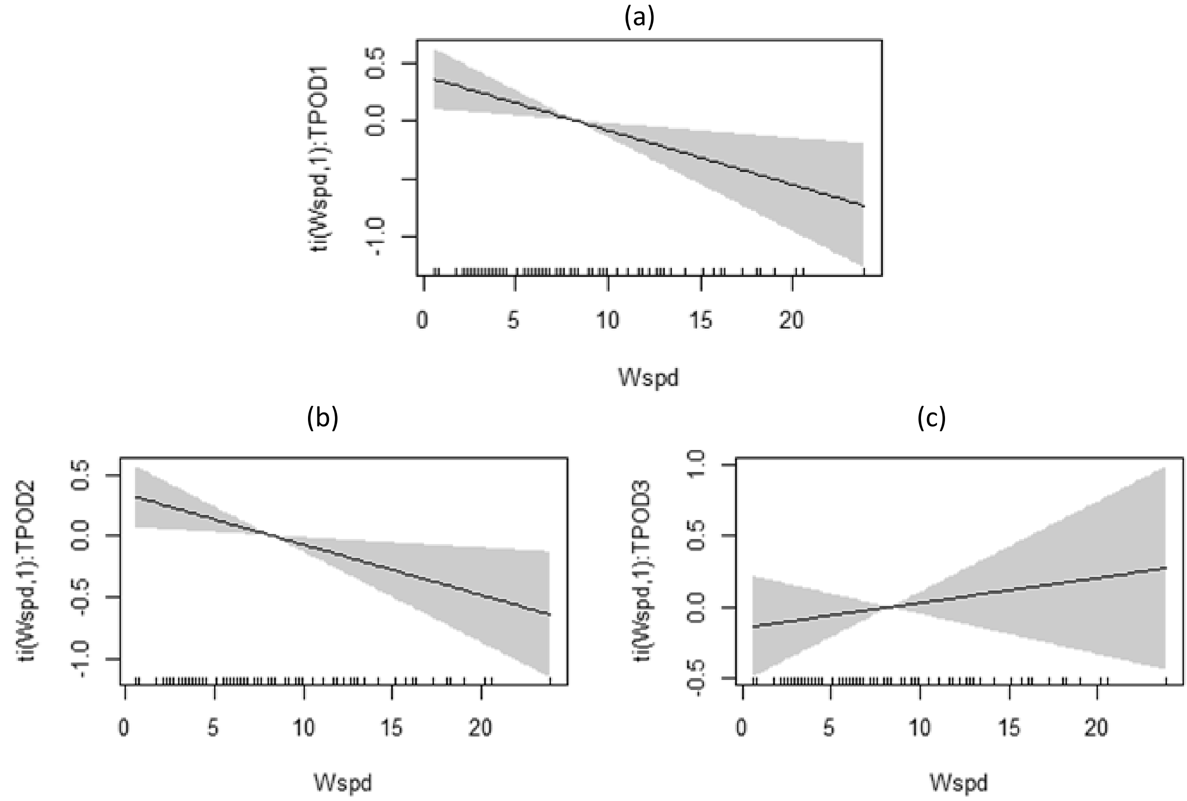

Figure 4.5 The predicted smoothing functions for the variable wind speed (x-axis, in knots) and its effect on DPM per day (y-axis) with shaded confidence intervals. Plots a, b and c refer to the inner, mid and outer T-POD locations. Note that the vertical scale varies among plots. The number in brackets following the variable abbreviation on the y-axis gives the estimated degrees of freedom. The ticks along the bottom edge of the plot indicate the values found in the measured data for that variable.

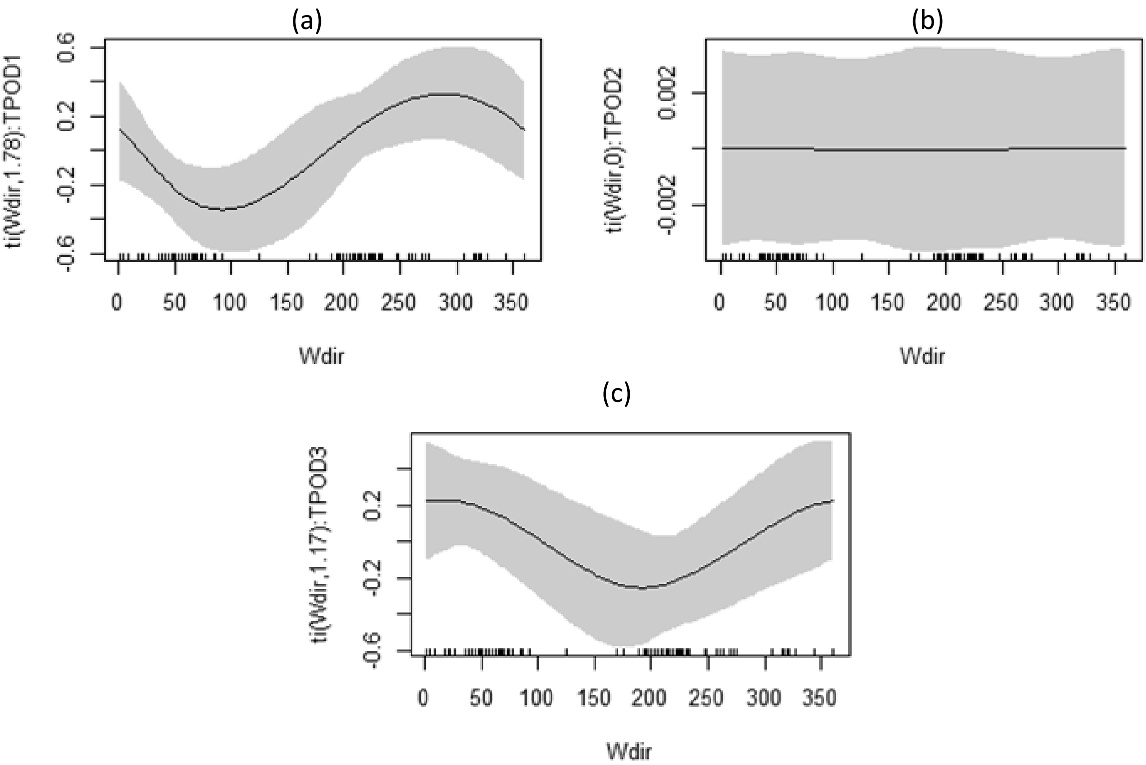

Figure 4.6 The predicted smoothing functions for the variable wind direction (x-axis, in degrees) and its effect on DPM per day (y-axis) with shaded confidence intervals. Plots a, b and c refer to the inner, mid and outer T-POD locations. Note that the vertical scale varies among plots. The number in brackets following the variable abbreviation on the y-axis gives the estimated degrees of freedom. The ticks along the bottom edge of the plot indicate the values found in the measured data for that variable.

DPM per hour

The top models, as determined using AICc scores (see Table 4.7) show that the previous hour's DPM, T-POD location, hour of day, SEL, time-since-piling, tide, wind direction, the interaction between time-since-piling and duration-of-piling, duration-of piling (by itself) and wind speed all explained some of the deviance in DPM per hour. Normality was verified using the Q-Q plot, though the histogram of residuals was skewed to the left and the 'response vs fitted value' graph did not indicate a good model fit (see Fig. A.15). The best model had a percentage deviance explained of 19.3% (Table 4.7).

Time-since-piling was significant at the inner T-POD, with the lowest detection rate seen within 2000 mins (33 hours) after piling (Fig. 4.7a). After this point the rate steadily increased and levelled off around 5000 mins (83 hours). DPM per hour decreased with increasing SEL at all T-POD locations (Fig. 4.8a, b and c), though at the inner T-POD DPM per hour appeared to increase at SELs over 135 dB re 1 µPa^{2}s (Fig. 4.8a). This variable was significant only at the inner T-POD (Table 4.8). An increase in duration of pile-driving led to a decrease in detection rate, up to a duration of about 150 mins (Fig. 4.11b). DPM per hour was highest at the outer T-POD and lowest at the inner T-POD (Table A.2). At the inner T-POD, detection rates were highest around 5-6 am and the lowest around 11-12 pm, with another peak in detections at 5-6 pm (Fig. 4.9a). At the mid T-POD the highest rate was seen around 4-5 pm, and the lowest around 5-6 am (Fig. 4.9b), with no significant effect at the outer T-POD (Fig. 4.9c and Table 4.8). At the inner T-POD, highest detection rates were seen around 100 mins after high tide (Fig. 4.10a), at the mid T-POD rates were highest around low tide (Fig. 4.10b), and at the outer T-POD around high tide (Fig. 4.10c). This variable was significant at the inner and outer T-PODs. Wind direction had the overall effect of increased DPM per hour during northerly winds and decreased during southerly winds (Fig 4.11a). Detection rates tended to decrease with increasing wind speed (Fig. 4.12) though this was not significant (Table 4.8).

Table 4.7. Results of model selection for GAMs with DPM per hour as the response variable. Only models within 6 AICc points of the top model are shown. Rank is based on AICc, 'Wt' is the Akaike weight of the model, '% DE' Is the percentage deviance explained by the model and the 'Model' column shows the model structure of the top models, ti(DPMt1), TPOD, ti(Hour), ti(TSP) , ti(SEL), ti(tide) were present in all the top models. Terms enclosed by 's()' are smoothed variables, and by 'ti()' are smoothed seperately for each T-POD location, except the term 'ti(TSP,Dur)' which is an interaction between the 2 variables.

Rank	**Model**	**df**	**AICc**	**Δ**	**Wt**	**% DE**	**R^2 (adj.)**
1	ti(DPMt1) + TPOD + ti(Hour) + ti(TSP) + ti(SEL) + ti(tide) + ti(TSP,Dur) + ti(Wdir) + s(Dur)	46.4	10491.1	0	0.46	19.3	0.152
2	ti(DPMt1) + TPOD + ti(Hour) + ti(TSP) + ti(SEL) + ti(tide) + ti(TSP,Dur) + ti(Wdir)	43.05	10492.2	1.1	0.27	19.1	0.152
3	ti(DPMt1) + TPOD + ti(Hour) + ti(TSP) + ti(SEL) + ti(tide) + ti(TSP,Dur) + ti(Dur)	41.66	10494.6	3.5	0.08	19.1	0.148
4	ti(DPMt1) + TPOD + ti(Hour) + ti(TSP) + ti(SEL) + ti(tide) + ti(TSP,Dur) + ti(Wspd)	43.99	10494.8	3.7	0.07	18.9	0.148
5	ti(DPMt1) + TPOD + ti(Hour) + ti(TSP) + ti(SEL) + ti(tide) + ti(TSP,Dur)	40.8	10495.6	4.5	0.05	18.8	0.148
6	ti(DPMt1) + TPOD + ti(Hour) + ti(TSP) + ti(SEL) + ti(tide) + ti(Wdir) + s(Dur)	42.75	10496.1	5.0	0.04	18.9	0.158
7	ti(DPMt1) + TPOD + ti(Hour) + ti(TSP) + ti(SEL) + ti(tide) + ti(Wdir)	39.54	10496.4	5.3	0.03	18.7	0.157

Table 4.8 Akaike weights of each term after model averaging (w_{AICc}). Estimated degrees of freedom (edf) and significance (p-value) of each term in the top model (except for s(Wspd), values are from 4th best model) , bold terms are significant at the 5% level

Term	w_{AICc}	edf	p-value
TPOD	**1**	**2**	**< 2e-16**
ti(DPMt1):TPOD1	**1**	**3.01**	**< 2e-16**
ti(DPMt1):TPOD2	**1**	**2.31**	**9.74e-08**
ti(DPMt1):TPOD3	**1**	**2.26**	**1.54e-04**
ti(TSP):TPOD1	**1**	**3.57**	**2.58e-05**
ti(TSP):TPOD2	1	1.00	0.132
ti(TSP):TPOD3	1	1.75	0.355
ti(Hour):TPOD1	**1**	**2.82**	**8.18e-05**
ti(Hour):TPOD2	**1**	**1.98**	**0.001**
ti(Hour):TPOD3	1	0.00	0.643
ti(SEL):TPOD1	**1**	**2.48**	**0.034**
ti(SEL):TPOD2	1	1.00	0.129
ti(SEL):TPOD3	1	1.46	0.098
ti(tide):TPOD1	**1**	**1.66**	**0.019**
ti(tide):TPOD2	1	0.96	0.157
ti(tide):TPOD3	**1**	**1.86**	**0.005**
ti(TSP,Dur)	**0.93**	**3.04**	**0.045**
s(Wdir)	**0.8**	**1.72**	**0.013**
s(Dur)	0.57	2.96	0.185
s(Wspd)	0.08	1.00	0.057

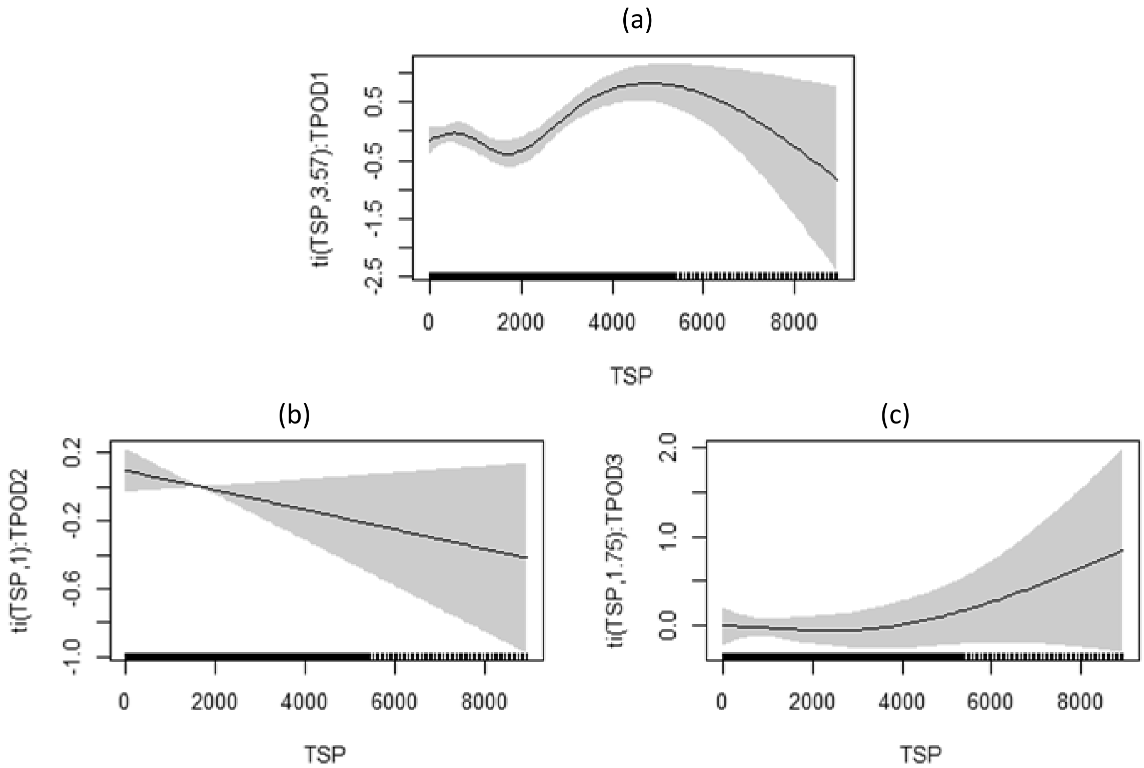

Figure 4.7 The predicted smoothing functions for the variable time since piling (TSP; x-axis, in mins) and its effect on DPM per hour (y-axis) with shaded confidence intervals. Plots a, b and c refer to the inner, mid and outer T-POD locations. Note that the vertical scale varies among plots. The number in brackets following the variable abbreviation on the y-axis gives the estimated degrees of freedom. The ticks along the bottom edge of the plot indicate the values found in the measured data for that variable.

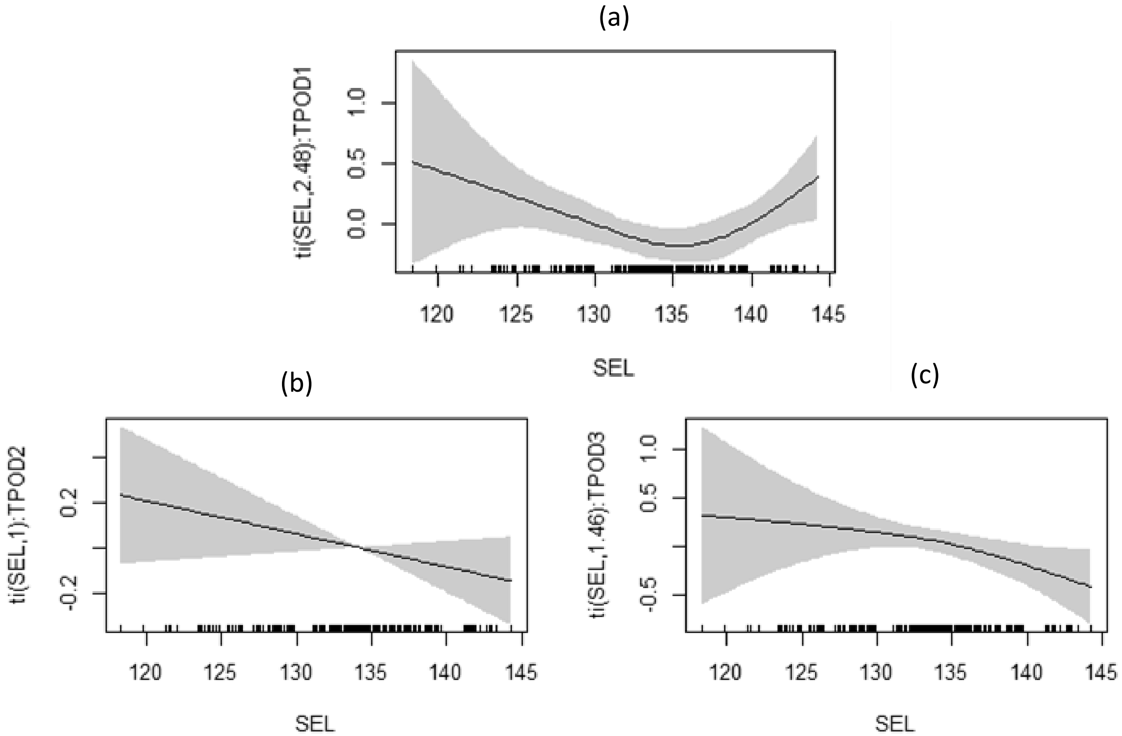

Figure 4.8 The predicted smoothing functions for the variable sound exposure level (SEL; x-axis, in dB) and its effect on DPM per hour (y-axis) with shaded confidence intervals. Plots a, b and c refer to the inner, mid and outer T-POD locations. Note that the vertical scale varies among plots. The number in brackets following the variable abbreviation on the y-axis gives the estimated degrees of freedom. The ticks along the bottom edge of the plot indicate the values found in the measured data for that variable.

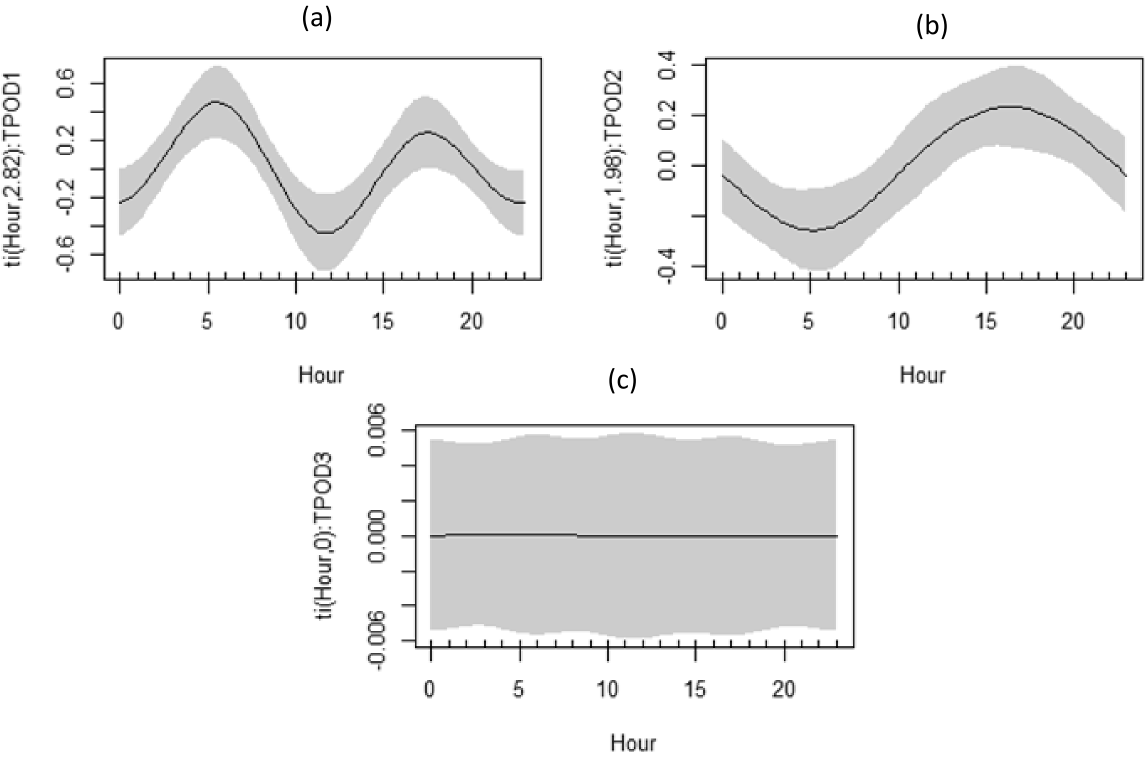

Figure 4.9 The predicted smoothing functions for the variable time of day (Hour; x-axis) and its effect on DPM per hour (y-axis) with shaded confidence intervals. Plots a, b and c refer to the inner, mid and outer T-POD locations. Note that the vertical scale varies among plots. The number in brackets following the variable abbreviation on the y-axis gives the estimated degrees of freedom. The ticks along the bottom edge of the plot indicate the values found in the measured data for that variable.

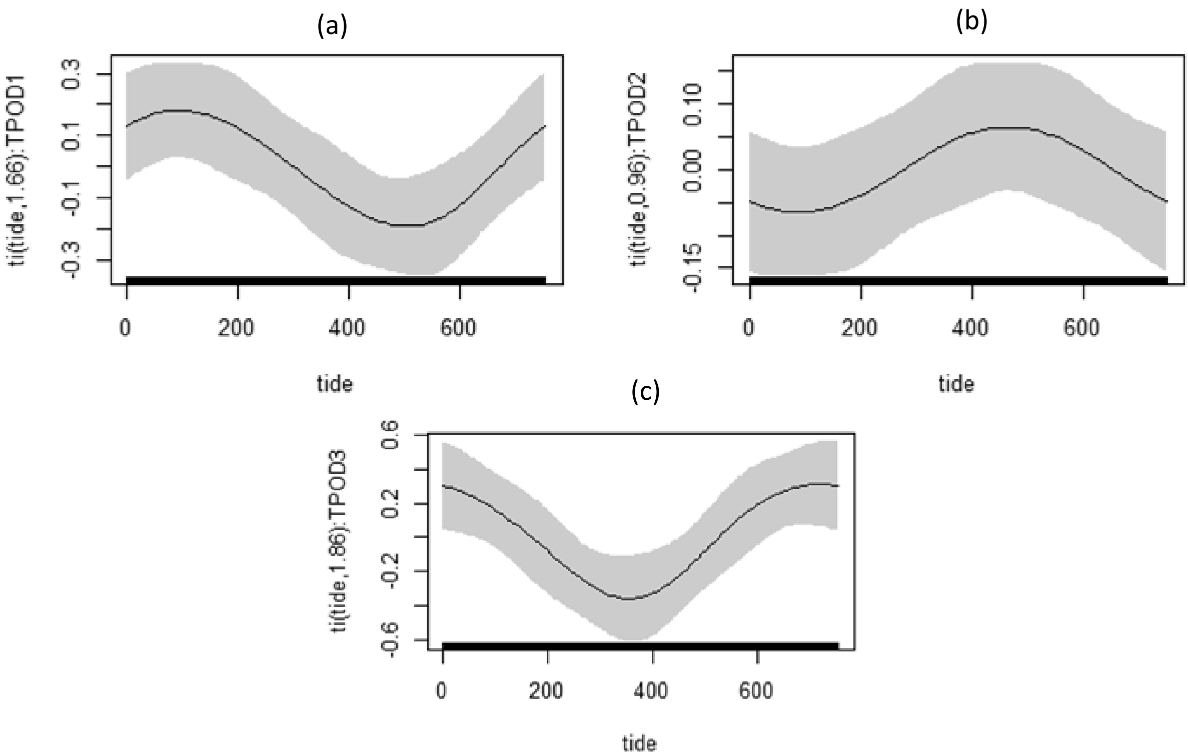

Figure 4.10 The predicted smoothing functions for the variable time since high tide (x-axis, in mins) and its effect on DPM per hour (y-axis) with shaded confidence intervals. Plots a, b and c refer to the inner, mid and outer T-POD locations. Note that the vertical scale varies among plots. The number in brackets following the variable abbreviation on the y-axis gives the estimated degrees of freedom. The ticks along the bottom edge of the plot indicate the values found in the measured data for that variable.

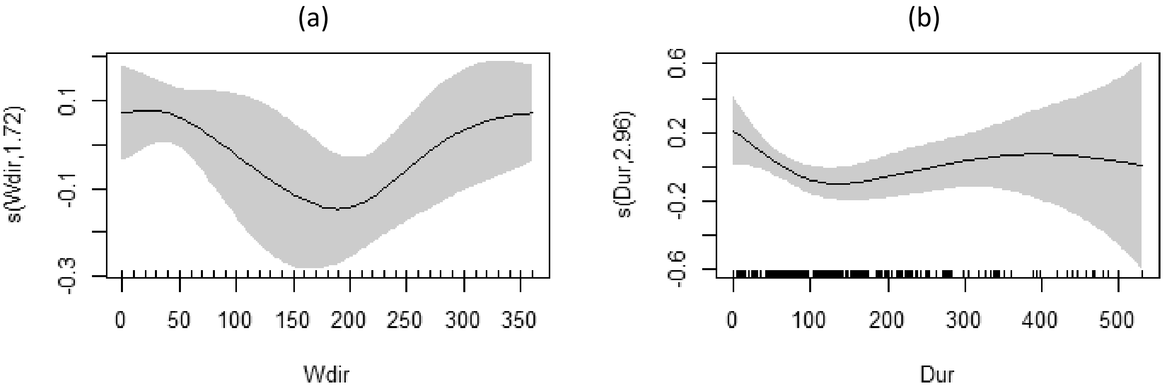

Figure 4.11 The predicted smoothing functions for the variable Wind direction (Wdir; x-axis, in degrees from North) (a) and Duration of previous pile-driving event (Dur; x-axis, in mins) (b) and their effect on DPM per hour (y-axis) with shaded confidence intervals. Note that the vertical scale varies among plots. The number in brackets following the variable abbreviation on the y-axis gives the estimated degrees of freedom. The ticks along the bottom edge of the plot indicate the values found in the measured data for that variable.

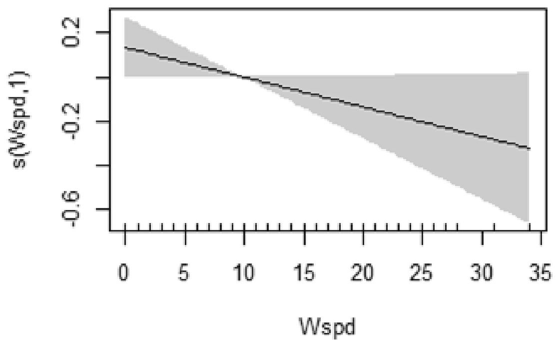

Figure 4.12 The predicted smoothing functions for the variable wind speed (Wspd; x-axis, in knots) and its effect on DPM per hour (y-axis) with shaded confidence intervals. The number in brackets following the variable abbreviation on the y-axis gives the estimated degrees of freedom. The ticks along the bottom edge of the plot indicate the values found in the measured data for that variable.

The interaction between time-since-piling (TSP) and duration-of-piling (Dur), at the inner T-POD (Fig. 4.13), mainly shows decreasing detection rates within the first 2000 mins (33 hours) of piling and detection rates returning to the level of the previous hour (set at 1.1 DPMs) after 3000 – 3500 mins (50-58 hours). There are more subtle effects with duration. For short duration events (< 100 mins) the lowest DPM per hour was seen directly after piling. For longer duration events, however, while DPM per hour directly after the piling event (c. 0.6 mins) was lower than that of the previous hour (1.1 mins), the lowest DPM was seen around 2000 mins (33 hours) after piling, as shown by the 0.4 contour (Fig. 4.13). After 5000 mins since piling, DPM per hour decreased with time.

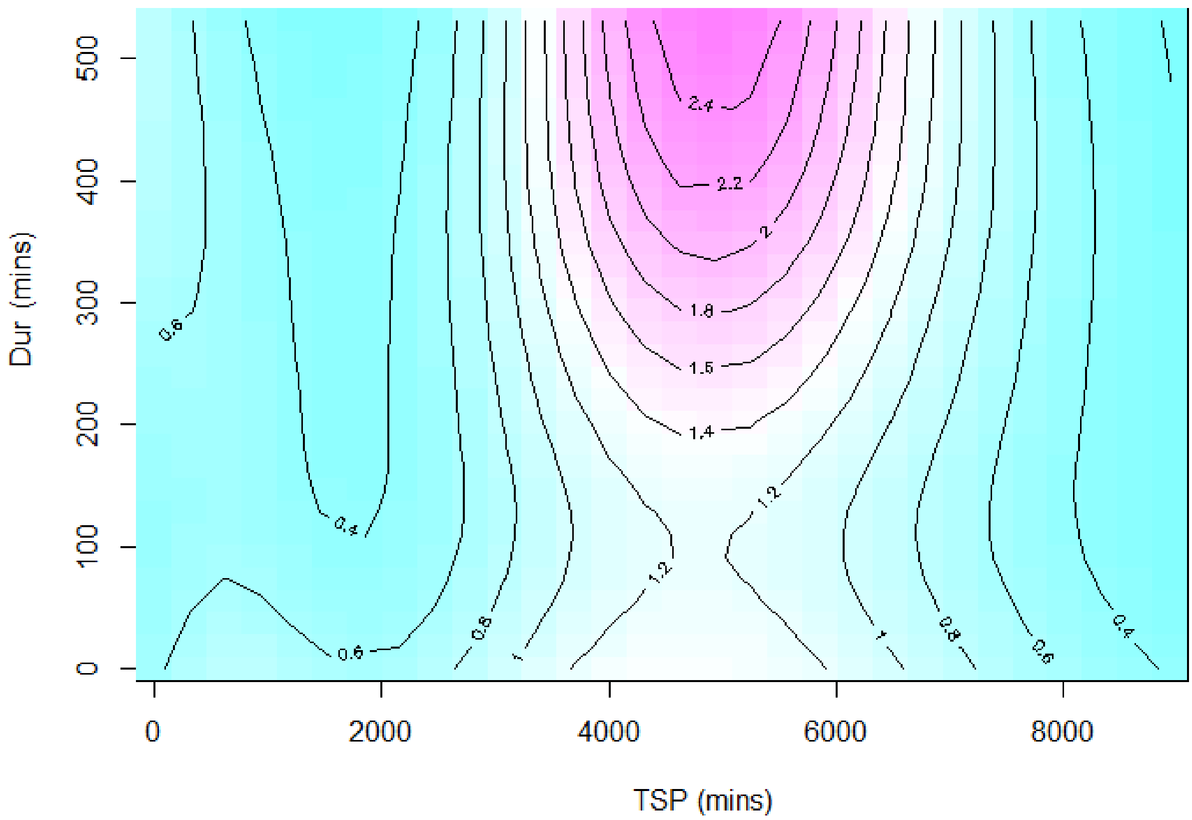

Figure 4.13 Interaction between time-since-piling (TSP) and Duration-of-piling (Dur) calculated in the top model, with contours showing the predicted DPM per hour at the inner TPOD when the other variables are fixed as follows: "Hour"=16 (4 pm), "Wdir"=50 degrees from North, "tide"=100 mins after high tide, "SEL"=134 dB, "DPMt1"=1.1 mins.

4.4 DISCUSSION

T-PODs were used to monitor dolphin distribution in Lyttelton Harbour at three different sites during wharf reconstruction. Dolphin detection rates were highest at the outer T-POD and lowest at the inner T-POD (Fig. 4.3, Tables 4.4, A.1 and A.2). This pattern was also observed during photo ID surveys in Lyttelton Harbour (see Fig. 1.5). A similar relative distribution was found in a study of Hector's dolphin habitat use in Akaroa Harbour (Dawson et al., 2013). While variation in sensitivity among T-PODs has been a problem for previous versions (v.3 and earlier) the sensitivities of the versions used in the current study are much more standardised (Dähne et al., 2006; Verfuß et al., 2008). In addition, the use of DPM (per hour and per day) smooths out the finer scale differences in train detection due to the variation in sensitivities, giving much more similar detection rates (Dähne et al., 2006).

Pile-driving and the effect on dolphin detections

Two measures of detection rates (DPM per day and DPM per hour) were used as response variables in a statistical analysis using GAMs. Both analyses revealed top models containing at least one piling-related variable, indicating that the presence of pile-driving influences the detection rates in Lyttelton Harbour. Time-since-piling, SEL and the interaction of time-since-piling and duration were significant for the DPM per hour response variable.

The models for the DPM per day data had a relatively high percentage deviance explained and R^2 (see table 4.5). The results indicate that detections (DPM) per day at the inner harbour decrease with increasing presence of piling (PPM) (Fig. 4.4a). This effect was also observed in Brandt et al. (2016) assessing the impact of pile-driving on harbour porpoise detections per day. Actual abundance has been estimated from T-POD detections when passive monitoring was combined with visual monitoring. The estimate of abundance is based on animal density being correlated to the number of acoustic detections (Marques et al., 2009; Sveegaard et al., 2011; Khyn et al., 2012). It would be reasonable to conclude that the decrease in detections implies a decrease in abundance. This has been shown in a previous study on the impact of pile-driving on harbour porpoise using aerial surveys combined with acoustic monitoring (Dähne et al., 2013).

Interestingly, at the mid T-POD, detections per day increased with increasing PPM (Fig. 4.4b). This suggests that the dolphins displaced from the inner harbour moved towards the mid harbour area, increasing the chance they were detected by the mid T-POD. This effect was also observed in a study of impact of pile-driving from offshore wind farm construction on harbour porpoise (Dähne et al., 2013), though other studies did not observe a gradient in effect across monitoring stations (Carstensen et al., 2006), even up to 20 km from the piling site (Tougaard et al., 2009)

DPM per hour at the inner harbour T-POD decreased significantly with increasing SEL (Fig. 4.8a) indicating that it is not only the presence of pile-driving but also the intensity that leads to avoidance reactions. This is likely the reason why studies assessing the impact of windfarm construction on harbour porpoise see avoidance reactions at much larger distances (around 20 km; Tougaard et al., 2009; Brandt et al., 2011; Dähne et al., 2013). Pile-driving for windfarms requires much larger piles (around 4 m diameter, compared to 0.6-0.7 m in Lyttelton) and heavier pile drivers, leading to a much higher sound source level (Fricke & Rolfes 2015). Also, the harder substrate found in these offshore locations (sand/gravel, compared to the fluid mud layer in Lyttelton) allows the sound to propagate further (due to increased reflection from the bottom surface), thereby increasing the range at which the sound can be heard.

Duration of impact

Analysis of DPM per hour suggests that the decreasing trend in detection rate following a pile-driving event may last around 33 hours, with the number of detections restoring to the level of the hour prior to exposure after 83 hours (see Figs 4.7a and 4.13). This gradual increase in detections after 33 hours may reflect the gradual return of dolphins to the inner harbour following a pile-driving event. The levelling-off of the trend of detection rate with time-since-piling (as in Brandt et al., 2011) indicates that the previous piling event no longer has an effect on detection rate. This is observed in the current study at 83 hours, although it is then followed by a gradual decline in DPM (see Figs 4.7a and 4.13). The dataset for DPM per hour, however, did not contain many data points for which time-since-piling exceeded 90 hours as this only occurred during the Christmas break period. Therefore, this decrease is not well supported. The maximum duration of effect on detections (83 hours) is comparable to, though slightly longer than the longest duration of effect estimated for the impact of pile-driving on harbour porpoise (72 hours; Brandt et al., 2011), indicating that the two species are similar in their sensitivity to pile-driving noise. It is interesting that the lowest detection rate did not occur immediately after pile-driving, but rather 33 hours later. This does not seem intuitive and is not observed in other studies (e.g. Tougaard et al., 2009; Brandt et al., 2011). More data would be required to investigate if this is a consistent reaction, or an artefact of this study.

DPM per hour decreased with duration of pile-driving up to a duration of 150 mins (Fig. 4.11b), although the relationship was not significant (Table 4.8). There was a significant interaction between time-since-piling and duration of the previous piling event (Table 4.8). For long duration piling events, the decrease in DPM per hour persisted for a longer time after piling had finished (Fig. 4.13). Brandt et al., (2016) also did not observe a clear pattern in the effect of duration on detections, although, in their case the variable was significant. On a daily scale, however, a longer duration of pile-driving per day does lead to lower DPM per day at the inner T-POD (Fig. 4.4a).

Influence of other factors

T-POD location was the most significant influence on detection rate (Tables A.1 and A.2). Also important was time of day, with decreased hourly detections at the inner T-POD between 7 am and 4 pm, with the lowest around midday. This could be due to the disturbance of higher vessel traffic near the wharf and construction activity during working hours, or diel movements of prey (as observed with harbour porpoise; Todd et al., 2009). Diurnal variation in Hector's dolphin habitat use was observed within Porpoise Bay (Bejder & Dawson 2001) and Akaroa Harbour (Dawson et al., 2013), however, there was no evidence of a lower density at the inner harbour during the day as seen in the current study.

Environmental conditions were significant for both datasets. Detection rate tended to be highest around high tide at the inner and outer T-POD (Figs 4.10a and c), and at low tide for the mid T-POD (Fig 4.10b), although, tide was not significant at the latter location (Table 4.8). While tide had a significant effect on Hector's dolphin distribution in Akaroa, the effect showed a different pattern than the present study with more detections seen at mid-tide in the outer harbour (Dawson et al., 2013). A possible driver for the tidal variation in distribution is the movement of prey species. For example, yellow-eyed mullet, identified as a prey species from Hector's dolphin stomach contents (Miller et al., 2012), was most often caught at night time low tides (Manukau Harbour; Morrison et al., 2002). Detection rates of bottlenose dolphins on the coast of Scotland (Mendes et al., 2002) and harbour porpoise in the Bay of Fundy (Johnston et al., 2005) were highest during the incoming tide.

More detections were made at lower wind speeds (Figs 4.5a and b, 4.12). This was possibly due to the click sounds being more attenuated due to the increased amounts of air bubbles in the water and less reflection at the water surface. Increased ambient noise is expected to reduce the number of detections once noise levels are high enough to mask click sounds (Khyn et al., 2008). The opposite trend was observed in Brandt et al., (2016) and was determined to be due to the increased propagation of piling noise at lower wind speeds leading to lower detections. In addition, more noise clicks were recorded at higher wind speeds due to the increased amount of ambient noise giving false-positive detections (Brandt et al., 2016).

At the inner T-POD, wind direction was significant for both DPM per day (Table 4.6), and DPM per hour (Table 4.8), with the highest detection rate seen during westerly winds (Fig. 4.6a) and northerly winds (Fig 4.11a) respectively. A possible explanation for this is that the wind gauge in Lyttelton is sheltered from these wind directions (due to the orientation of the harbour), which may lead to a correlation between these directions and lower wind speed (at which higher detection rates were seen). VIF scores of explanatory variables, however, did not indicate significant collinearity. Easterly winds are funnelled down the harbour which would likely lead to more wind-chop, particularly at the inner T-POD location. This would then lead to decreased detections during easterly winds, as seen in DPM per day at the inner T-POD (Fig. 4.6a).

Zones of potential impact

Pile-driving noise clearly has some influence on Hector's dolphin distribution. Another possible but important impact from the noise is the increased risk of hearing damage, particular at close range to the piling. In addition to monitoring dolphin distribution, zones of potential impact in Lyttelton Harbour were identified based on hearing studies of harbour porpoise (see appendix section 7). A single strike could induce TTS in dolphins within 26 m of the pile-driving while for an hour of exposure to continuous pile-driving noise this range is 376 m (Fig. A.17). The risk of hearing damage increases with duration of exposure and while the pile-driving SEL decreases with range, the area in which TTS could occur would increase with the amount of time a dolphin spends within close range of the wharf (see Fig. A.17). While Hector's dolphins have been seen directly in front of the wharf, it is unknown how long they would normally spend in this area, particularly during pile-driving events. It is likely, however, that, based on the modelling results, events of increased duration lead to increased avoidance in the inner harbour (Figs 4.4a and 4.11b). We observed dolphins near the SoundTrap recorder location, about 370 m from the piling activity (see Fig. A.17), and have many recordings of their clicks (up to 10 consecutive dolphin positive minutes on the SoundTrap), during pile-driving events. Thus, while we cannot determine the likelihood of TTS occurring in Hector's dolphins it is clear there is some risk given measured noise levels in the inner harbour. It must be noted that higher thresholds for TTS onset in dolphins have been suggested (e.g. an SEL of 195 dB re 1 μPa^2s for mid-frequency tones, Finneran et al., 2005). In the present study the lower thresholds were used to give conservative estimates of impact. It is also not unreasonable to imagine Hector's dolphin hearing to be more sensitive than that of harbour porpoise given that source levels of Hector's dolphin clicks are much lower (Kyhn et al., 2009).

The pile-driving noise will likely be audible to dolphins in most of the inner harbour (see Fig. A.19). The range at which Hector's dolphins detect targets was estimated to be 20 m by Kyhn et al. (2009). If this estimate is accurate, pile-driving sounds are unlikely to mask echolocation clicks as the click sound level exceeds the pile-driving source level (in the 1/6 octave-band centred at 125 kHz) even at close range to the piling. It is not known what range Hector's dolphins usually communicate over. Their clicks are possibly audible above ambient noise up to a range of 1000 m (see Fig. A.18). If these provide cues for other dolphins, the introduction of pile-driving would marginally reduce the range at which these cues could be detected. The low potential for masking is mainly due to the clicks being centred at a very high frequency (c. 125 kHz) at which pile-driving strikes have little energy. Environmental cues at much lower frequencies, however, are likely to be masked.

Sticking Point is a 210 m long boulder bank about 500 m from the piling activity, which juts out into the channel. *In situ* noise measurements show that it acts to shield much of the middle and all of the outer harbour from the direct path of pile-driving noise (see Fig. 3.19, Ch. 3). Its shielding effect is highly likely to be important in reducing the zone of disturbance to Hector's dolphin.

Limitations

Several constraints bear on this study. Due to the urgency of construction, there was no pre-construction monitoring period. Ideally there would have been time prior to construction to monitor at the same three T-POD sites. Without this period, I relied on long gaps in the piling programme to establish a baseline. Nevertheless, detection rates during this time may be different to the true baseline levels. Long breaks, other than the Christmas break, in piling activity were rare, and there were usually other noisy construction activities underway (such as vibro-hammering and excavation).

Lyttelton Harbour has frequent commercial and recreational vessel traffic, and hence there are strong constraints on where instruments can be moored. Loss of moored T-PODs due to attachment failure, storms or human interference is common, and difficult to avoid (e.g. Rayment et al. 2011). To minimise interference, our research group has often attached T-PODs to existing structures, such as racing buoys or navigational marks, where they do not attract attention. This often means, however, that T-PODs cannot be moored in ideal locations.

Loss of the outermost T-POD resulted in a much smaller dataset at this location, and this may explain why variables were often not significant at this location, compared to the mid and inner T-POD. However, pile-driving effects on detection of dolphins were generally significant only at the inner T-POD so any effect at the outer T-POD would likely have been small. Additionally any difference in sensitivity between the two instruments used at this site was not accounted for; however, due to the use of more standardised versions of T-PODs this was unlikely to significantly influence the results.

Model checking indicated that the fit for the DPM per hour dataset was not very good and the assumption of normality of residuals was not satisfied (see Fig. A.15). This limits its power to predict the true effects of variables on detection rates and restricts the ability to predict finer scale impacts (such as the duration of impact). The model for DPM per hour had a lower percentage deviance explained and R^2 value compared to the model for DPM per day. This indicates that there were some finer scale movements in the DPM per hour dataset, which were not accounted for in the model, that were not as influential on detection rate per day.

In hindsight it is clear the inner T-POD was not within the expected zone of ‘behavioural change’ based on harbour porpoise studies (see Fig. A.17). We could not have known this without prior knowledge of the pile-driving source levels and propagation characteristics in Lyttelton Harbour, both of which were lower than expected. However, piling related variables did partly explain the variation in detection rates (and therefore likely distribution). This may indicate that the threshold for behavioural change for Hector’s dolphins is lower than that for harbour porpoise, at least in terms of avoidance and/or acoustic activity. In any future research on the pile-driving noise it would be beneficial to place an additional T-POD closer to the source, well within the ‘behavioural change’ zone in order to increase the likelihood of detecting change. The extent of this zone can only be known after measuring the noise at various locations around the harbour.

General conclusions

Pile-driving noise was found to decrease dolphin detection rate at the inner T-POD, with an increase in detections per day seen at the mid T-POD. The most parsimonious explanation is that this is driven by dolphins moving from the inner harbour to the mid harbour when pile-driving is underway. Though environmental variables generally were more important in predicting detection rates, the presence of pile-driving reduced the density of dolphins near the inner T-POD, with decreasing detection rates seen within 33 hours of piling, restoring to pre-piling levels after 50-83 hours. The intensity of piling also affected detection rate, with fewer detections in the inner harbour on days with more piling activity, and fewer detections per hour after longer and louder piling events.

The pile-driving noise measured in Lyttelton Harbour has a range of potential impacts on Hector's dolphin hearing depending on the length of time they spend near the wharf and what range they are from the pile-driving. While these zones do not cover very large areas, it is not known how long Hector's dolphins would tolerate the noise at levels which could induce TTS if there was a sufficient reward for doing so. Masking of environmental sounds is highly likely in the inner harbour. The spatial extent of these impacts is heavily reduced due to the shielding effect of the breakwater at Sticking Point.

Pile-driving has been shown to influence the distribution of Hector's dolphin in Lyttelton Harbour and has been shown to introduce a risk of TTS. Investigating the implications of these impacts at a population level would be a useful focus of future research.

Chapter 5

General discussion

This study investigated the soundscape of Lyttelton Harbour during a period of wharf reconstruction, and how pile-driving noise affected local Hector's dolphins. Ambient noise levels were highly variable and approximately mid-range compared to other noisy underwater environments (e.g. Samuel et al., 2005; Hatch et al., 2008; Bittencourt et al., 2014). Levels of pile-driving noise in Lyttelton were generally lower compared with other studies, due to smaller diameter piles and smaller pile drivers. The shallowness and form of the harbour restricted noise propagation, however, levels could cause temporary hearing damage to Hector's dolphins if they remained at close ranges (see appendix section 7). Hector's dolphins showed a clear avoidance reaction to pile-driving activity within the inner harbour. A decrease in the rate of dolphin echolocation detections was evident on days with piling compared to days without piling. The decreasing trend in detections following pile-driving events generally lasted at least 33 hours, with detection rates recovering to pre-piling levels after 50-83 hours. A simultaneous increase in detections at the mid-harbour T-POD suggests that the animals disturbed by the noise in the inner harbour were displaced toward the mid harbour.

5.1 Implications of Noise Characterisation

Ambient and pile-driving noise in Lyttelton Harbour were recorded at several locations and characterised. General Linear Modelling revealed that the stage within a piling sequence, hammer lift height and pile driver type were significant influences on received noise levels. This information could be used to choose a pile-driving setup which decreases the amount of noise radiated into the water. A smaller pile driver, using lower drop heights would produce lower noise levels, but would require more strikes to complete an entire piling sequence. While lower noise levels would reduce the risk of hearing damage and likely decrease the area over which avoidance reactions would be expected, the increase in duration of pile-driving activity may displace dolphins from the inner harbour for a longer time. More information is needed on whether the noise reduction is worth the increase in pile-driving duration in terms of impact on the animals. Additionally, the pile-driving setup used will clearly be restricted by what is practical for the work that needs to be done.

The map giving contours of noise loss could be used for other sources of anthropogenic sound near the wharf, so long as the source level is known, to estimate what sound levels would be received in different parts of the harbour. In particular, future studies of dolphin habitat use in Lyttelton Harbour may identify specific areas that are important (for example for foraging), for which the received noise level could be estimated. The accuracy of estimated levels will depend on how similar the frequency spectrum of the source is to pile-driving noise used to develop the model. The map would be helpful in estimating the propagation of noise associated with the (currently underway) expansion of the Lyttelton port. Combined with the results of the modelling of dolphin detections, if source levels and noise type are comparable, it would be reasonable to expect avoidance reactions in the inner harbour. Given that SEL was a significant influence on dolphin detections, with decreasing detections seen for increasing SEL, the area in which avoidance reactions may occur should be larger for operations with higher noise source levels.

New Zealand currently has no underwater noise restrictions except for the voluntary code of conduct for seismic surveys (DOC 2008). Measured noise levels for pile-driving in Lyttelton are below limits established in most other countries (Erbe 2013) except those proposed by the Marine Strategy Framework directive in Europe. These suggest restriction of impulsive sounds with an SEL greater than 183 dB re 1 μPa^2s @ 1 m (Tasker et al., 2010). While the average SEL @ 1 m for the pile-driving in Lyttelton was around 182 dB (based on the propagation model), we have measured pile-driving sequences which would have corresponded to a much higher level, up to 194 dB re 1 μPa^2s. Unfortunately, there are many difficulties in determining a safe level of exposure:

- Species with different hearing sensitivities are likely to respond differently to various types of noise sources (e.g. Finneran et al., 2002)
- Threshold levels determined for captive animals in controlled settings are likely to be different for wild animals
- Due to lack of knowledge on what kinds of changes could be biologically significant, short term impacts may not be representative of long term effects and vice versa. There are no published studies on long-term impact of noise exposure on marine mammals.

5.2 Overall implications for the Hector's dolphin population

Hector's dolphins are threatened mainly by commercial and amateur fishing (Gormley et al., 2012). Construction activities had already been identified as another threat (MPI 2007). My study has shown that pile-driving activity affected dolphin distribution in Lyttelton Harbour. While the inner T-POD generally had the lowest detection rates, this does not necessarily imply it is the least important area for the dolphins (compared to the other T-POD sites). Hector's dolphins have often been seen feeding in this area, even feeding around ships in the process of docking. The propeller wash from the ship and tugs stirs up the bottom sediment and may make benthic fish such as flounder more available to the dolphins (Brough, 2015 pers. comm.). If feeding opportunities provide sufficient reward, very high levels of pile-driving noise could be tolerated despite the risk of hearing damage. In this case, the use of 'soft starts' to a piling sequence, which (while required by the pile driver manufacturer) was one of the actions taken by LPC during the port development to "minimise the effect on marine mammals" (LPC 2014), would not be effective.

The level of pile-driving noise (SEL) was inversely related to the rate of T-POD dolphin detections. This was not due to masking of dolphin echolocation sounds (see appendix section 7), and indicates that not only the presence of pile-driving but also its intensity leads to avoidance reactions. This suggests that the use of bubble curtains to reduce the amount of noise radiated into the harbour would likely reduce the impact on the dolphins. Furthermore, a reduction in noise radiated would reduce the area of impact zones, thereby, reducing the risk of inducing TTS in nearby animals. It must be noted, however, that while bubble curtains can reduce the noise level it is not with great consistency (see Brandt et al., 2016). Additionally, bubble curtains will not reduce the noise that is radiated into the sediment and then radiated into the water as it propagates through the sediment (Scholte waves; Tsouvalas & Metrikine 2016). It would be better to reduce the noise at the source if possible. This may be possible by using screw-pile technology, in which the piles are augered into the substrate, rather than pounded with a piling hammer. This technology has been proven for piles of the diameter used in Lyttelton (Saleem, 2011).

It took up to 83 hours (3.5 days) for detection rates to recover to average levels following a single pile-driving sequence. Breaks between piling exceeded that length of time on four separate occasions in the monitoring period. The longest period without any such breaks was 24 days. It is possible that some individuals were displaced from the inner harbour for this entire period due to the continuous disturbance of pile-driving

It is currently impossible to predict what the impact found in this study will mean at a population level. No studies have investigated these effects on cetaceans in the long-term. A framework for predicting the population effects of a disturbance has been proposed as an interim solution to the lack of long-term data (King et al., 2015), however, data on dolphin abundance in Lyttelton would be required before this would be useful. If dolphins are displaced beyond the marine mammal sanctuary, into areas unprotected from gillnetting, it may act to increase bycatch (Forney et al., 2017). Results from the current study suggest, however, that long-distance displacement is unlikely.

Given these results it is important to minimise the risk of impact on Hector's dolphins from pile-driving and other construction work. Currently, LPC's strategy to minimise effects on marine mammals is to use a 'soft start' at the start of a piling sequence to warn animals and give them a chance to move away, and to stop pile-driving if marine mammals are spotted (by "trained marine mammal observers"), within 300 m of the pile-driving (LPC 2014). These methods were clearly not effective for at least some animals, as we have a visual observation within this distance and many acoustic detections on a nearby SoundTrap recorder. As mentioned above, while the use of a bubble curtain around the pile being driven is a simple and cheap method to reduce the noise radiated into the water column, it is not guaranteed to always do so. A potentially more reliable method to reduce impact would be to schedule pile-driving activities during winter as Hector's dolphins are less likely to be found in the inner reaches of harbours at this time (Dawson et al 2013). The noise level threshold for behavioural change of Hector's dolphins (as determined by the change in distribution following pile-driving) will lie somewhere between the noise levels at the inner and mid T-POD, which were 127 and 113 dB re 1 μPa^2s respectively.

5.3 Study Limitations

While this thesis presents robustly measured noise levels for ambient and pile-driving noise, comparison to other studies is difficult due to differences in methods, and metrics. Additionally, the varying nature of ambient noise in a harbour complicates comparison of absolute levels. Providing that methods remain the same, however, the measurements made here will be useful for comparison in any future study in Lyttelton.

Pile-driving had started prior to the beginning of this study. This meant that while we have T-POD data between pile-driving events and during a 17 day Christmas break period, they do not constitute true control data. This is especially so if the pile-driving has a long-term effect on the dolphins. The longest duration of displacement due to pile-driving noise for harbour porpoise was 72 hours (Brandt et al. 2011). Our data contains many instances which would allow for a recovery time of this length. The modelling of the effect of time-since-piling on DPM per hour suggest it takes up to 83 hours for detection rates to return to pre-piling levels. Although there is a gradual decrease in detections seen with increasing time-since-piling after this point, it is unlikely this reflects a true effect as the data were very limited for these lengths of time-since piling.

The T-POD data show that Hector's dolphin detections are influenced by piling noise. While it is very likely that this reflects a change in distribution (Kyhn et al. 2012, Dahne et al. 2013), it is possible that it reflected a change in acoustic behaviour instead (for example see Brandt et al. 2011). Additionally, I have no evidence conclusively linking the changes observed to noise *per se,* nor do other studies assessing the impact of pile-driving on cetaceans (e.g. Tougaard et al., 2009; Brandt et al., 2011; Paiva et al., 2015). It is possible that the impact is indirect, for example, via impacts on dolphin prey.

Ranges from piling at which TTS is likely to occur were determined using results from harbour porpoise studies and the propagation model of pile-driving noise measured in the current study. At a range of 26 m the animal could experience TTS from exposure to a single strike and at a range of 376 m after an hour of exposure (Fig. A.17). While dolphins have been seen within this range, whether they would remain long enough to have their hearing impaired is unknown. Our closest T-POD, at a range of 1300 m from the piling, cannot provide any information on this. The risk of TTS may be very low if the disturbance is enough to keep the dolphins away. However, we have visual and acoustic observations confirming that some Hector's dolphins were present near the wharf during pile-driving events.

Vibro-hammers were used to vibrate the piles into place before pile-driving. Our recordings of these machines show that their noise levels can exceed pile-driving noise (see appendix section 3 for more detail). Moreover, this noise is continuous - it is essentially pile-driving at a very high repetition rate. At close range it is very intrusive to human observers and much louder than any other sound in the environment. In contrast to their records of impact pile-driving, the contractors kept no detailed records of vibro-hammer use. Hence, statistical analysis of their impact on DPM was not practical. Due to the highly invasive nature of this noise, however, it is likely that it had some impact on the distribution of Hector's dolphins, particularly in the inner harbour.

As no studies have been conducted on the hearing sensitivity of Hector's dolphins, we had to assume it would be most similar to that of the harbour porpoise. This assumption is reasonable due to the similarities in communication and echolocation frequencies and body size. While our closest T-POD was not within the "loudness zone" in which we would expect behavioural change in harbour porpoise, clear influences of pile-driving on Hector's dolphin detection rate were observed. It is possible that the results from this study indicate a slightly higher sensitivity to pile-driving in Hector's dolphins. This difference may be due to a difference in hearing sensitivity – if Hector's dolphin have a higher sensitivity this may lead to avoidance reactions beyond the range expected for harbour porpoise. This highlights that it is important to study species-specific responses to anthropogenic disturbance.

5.4 Future research recommendations

1. Noise measurements

Monitoring of noise levels in Lyttelton Harbour is important to ensure it remains tenable as a habitat for sensitive marine species. The method used in the current study is suitable for characterising short term noise events such as pile-driving and other construction noise.

To improve the method for future studies I would recommend:

- As well as measuring at various locations around the harbour, covering a variety of environmental conditions and bathymetry, measuring noise levels at a range of depths at each location would be useful. This would give a three-dimensional picture of the soundscape and could reveal any horizontal layering in received levels. Strong layering is unlikely, however, given how well-mixed the water column was in Lyttelton (see appendix section 4 for CTD profiles). Additionally, it could indicate areas that are affected by shadowing at different depths due to the varying bathymetry, particularly in the channel.

- For ambient noise measurements, include long-term acoustic monitoring at the highest sample rate possible. Sample rate should be at least twice the highest frequency audible to the species of interest, or if this is unknown, twice the highest frequency present in the species' own sounds. A high frequency recorder set up on a duty cycle is useful for this as it samples underwater noise over time within a reasonable memory capacity. Sampling over all hours of the day and over a period of at least a month would give a useful general idea of noise levels. Sound data combined with fine scale data on weather and ship movements would provide a detailed picture of the ambient noise environment.

- If possible include information on bottom layer properties such as thickness, density and acoustic properties (such as sound speed and absorption coefficient) of the material of each layer. This allows for comprehensive (but complex) propagation modelling.

2. Monitoring dolphin distribution using T-PODs

Our T-POD dataset was collected during the construction period. Ideally, monitoring would span a period before and after the construction period. This would allow for a true baseline of detections to be determined from the 'before' data, and would allow detection of any long term effects (at least of greater duration than the longest breaks in construction activity). This would require knowledge of a planned construction project well in advance.

A possible impact on Hector's dolphins is temporary hearing damage. Due to the importance of hearing for the dolphin's survival, temporary hearing loss could lead to significant negative impact on the dolphin's survival success. Therefore, it is important to quantify the risk of this occurring when introducing loud anthropogenic sounds into their habitat. Potential methods for assessing this include using a T-POD at close range to the sound source and/or theodolite monitoring of the area. A limitation of using the T-POD may be that a change in detections may not reflect a change in dolphin density if the noise leads to a change in acoustic behaviour. Additionally, close proximity to the source may increase the risk of damage to the instrument if it is a high traffic area, and would require a hydrophone suited to recording high signal levels without clipping. Visual detections, for instance using a theodolite, would be a useful adjunct to an acoustic study, and could be used to address whether it is distribution or vocalisation rate that changes, or both.

3. Determining the long-term impact of pile-driving

There are two approaches to estimating the long term impact of pile-driving activities on Hector's dolphins. Given enough information about the current state of the population, an interim framework can be used to predict the impact (Harwood et al., 2014; King et al., 2015). The other approach is to conduct a long-term study investigating any changes in the population in response to pile-driving.

The framework for predicting population-level effects uses a model which requires user input of parameters about the population and how the disturbance (e.g. pile-driving) affects individuals. These parameters include: population size, proportion of females and demographic stochasticity, the size of the sub-population which is vulnerable to the noise, the number of days with or without piling and the number of individuals disturbed or that experienced a permanent threshold shift (PTS) in hearing. Currently what is known are the number of days with and without piling for the Lyttelton port repair, and the population characteristics of Hector's dolphins at Banks Peninsula (Slooten 1991; Slooten & Lad, 1991; Slooten et al., 1992; Slooten et al., 2000; Webster et al., 2009). More work is needed to find out the size of the sub-population vulnerable to the noise and the number of animals that were disturbed or experienced PTS. PTS is very unlikely to occur as a result of the pile-driving noise measured in this study, however, the number of animals disturbed could be estimated using the techniques in Marques et al. (2009) and Khyn et al. (2012) to estimate animal density from the number of acoustic detections. This framework was used to predict the long term impact of pile-driving on harbour porpoise, based on T-POD monitoring from 2009 to 2013 during which seven offshore windfarms were constructed (Brandt et al., 2016). The results did not indicate potential population-level effects due to pile-driving, despite clear short term effects. Their input parameters were mostly based on expert judgement and this limited the predictive power of the model.

While the predictive framework is useful, it has many limitations (Brandt et al., 2016) and is merely intended as an interim solution to the lack of long term data (Harwood et al., 2014). If the impacts of pile-driving included reduced fertility, a long-term study would have to monitor the population for at least the length of a generation following the pile-driving operation. Given the age at which females bear their first calf, this would involve at least six to nine years of monitoring. Ideally there would be sufficient monitoring prior to the disturbance to determine baseline levels for the population to compare to long-term data. Clearly this requirement is onerous and usually impractical. Lyttelton, being a busy harbour environment, with many anthropogenic influences such as shipping, dredging and small vessel traffic, presents many confounding influences on the Hector's dolphin population. This is all the more so since these activities are expected to increase. Additionally, it is important to determine the reasons why marine mammals show avoidance reactions to pile-driving. While it seems reasonable to assume it is due to the disturbance of the noise, other explanations such as prey movement (Mueller-Blenkle et al., 2010) or the reduction in echolocation are also possible. The latter is not very likely in Lyttelton, given that detections per day increased at the mid T-POD after piling, suggesting the dolphins moved from the inner to the mid harbour. This could be confirmed by aerial survey (e.g. Dähne et al., 2013) or theodolite monitoring with simultaneous acoustic monitoring during pile-driving activity. Distribution of fish could be monitored acoustically using a vessel equipped with an appropriate echo sounder (Slotte et al., 2004).

This study characterised the Lyttelton Harbour soundscape during port re-construction and used non-invasive methods to study the influence of pile-driving on an endangered species. Pile-driving was shown to affect the distribution of Hector's dolphins in the inner harbour. The noise at close range provided a potential risk of hearing damage. The results provide important information to support management decisions about anthropogenic noise and Hector's dolphins.

References

Aguilar Soto, N., Johnson, M., Madsen, P.T., Tyack, P.L., Bocconcelli, A., & Fabrizio Borsani, J. (2006). Does intense ship noise disrupt foraging in deep-diving Cuvier's beaked whales (*Ziphius cavirostris*)?. *Marine Mammal Science*, 22:690-699.

Ainslie, M.A., & McColm, J.G. (1998). A simplified formula for viscous and chemical absorption in sea water. *The Journal of the Acoustical Society of America*, 103:1671-1672.

Akaike, H. (1973) Information theory and an extension of the maximum likelihood principle. In: '*2nd International Symposium on Information Theory*' (F. Csáki, ed.), pp 267-281. Akadémiai Kiadó, Budapest.

Anderson, D.R., Burnham, K.P., & Thompson, W.L. (2000). Null hypothesis testing: problems, prevalence, and an alternative. *The journal of wildlife management*, 912-923.

Andrew, R.K., Howe, B.M., Mercer, J.A., & Dzieciuch, M.A. (2002). Ocean ambient sound: comparing the 1960s with the 1990s for a receiver off the California coast. *Acoustics Research Letters Online*, 3:65-70.

Arveson, P.T., & Vendittis, D.J. (2000). Radiated noise characteristics of a modern cargo ship. *The Journal of the Acoustical Society of America*, 107:118-129.

Au, W.W.L., Lemonds D.W., Vlachos S., Nachtigall P.E., Roitblat H.L. (2002). Atlantic bottlenose dolphin (*Tursiops truncatus*) hearing threshold for brief broadband signals. *Journal of Comparative Psychology*, 116:151-157.

Au, W.W.L. (1993). *The Sonar of Dolphins*. Springer. 34pp.

Au, W. W., Kastelein, R. A., Rippe, T., & Schooneman, N. M. (1999). Transmission beam pattern and echolocation signals of a harbor porpoise (*Phocoena phocoena*). *The Journal of the Acoustical Society of America*, 106:3699-3705.

Bailey, H., Senior, B., Simmons, D., Rusin, J., Picken, G., Thompson, P.M. (2010). Assessing underwater noise levels during pile-driving at an offshore wind-farm and its potential effects on marine mammals. *Marine Pollution Bulletin* 60:888-897.

Baker, C.S., Chilvers, B.L., Constantine, R., DuFresne, S., Mattlin, R., Van Helden, A., Hitchmough, R. (2010). Conservation status of New Zealand marine mammals (suborders *Cetacea* and *Pinnipedia*), 2009. *New Zealand Journal of Marine and Freshwater Research*, 44:101–115.

Barne, J. H., Robson, C. F., Kaznowska, S. S., Doody, J. P. & Davidson, N. C. *eds* 1996. *Coasts and seas of the United Kingdom. Region 3 North-east Scotland: Cape Wrath to St Cyrus.* Peterborough, Joint Nature Conservation Committee. (Coastal Directories Series.)

Bejder, L. & Dawson, S. (2001). Abundance, residency, and habitat utilisation of Hector's dolphins (Cephalorhynchus hectori) in Porpoise Bay, New Zealand. NZ J Mar Freshw Res 35: 277−287

Bittencourt, L., Carvalho, R.R., Lailson-Brito, J., & Azevedo, A.F. (2014). Underwater noise pollution in a coastal tropical environment. *Marine pollution bulletin*, 83:331-336.

Blackwell, S.B. (2005). Underwater measurements of pile driving sounds during the Port Mackenzie dock modifications, 13-16 August 2004. *Report from Greeneridge Sciences*, <alaskafisheries.noaa.gov>

Brandt, M.J., Diederichs, A., Betke, K., Nehls, G. (2011). Responses of harbour porpoises to pile driving at the Horns Rev II offshore wind farm in the Danish north sea. *Marine Ecology Progress Series* 421:205-216.

Brandt, M.J., Dragon, A.C., Diederichs, A., Schubert, A., Kosarev, V., Nehls, G., Wahl, V., Michalik, A., Braasch, A., Hinz, C., Ketzer, C. (2016). Effects of offshore pile driving on harbour porpoise abundance in the German Bight. <http://bioconsult-sh.de/site/assets/files/1573/1573.pdf> *Retrieved on 27th January 2017*

Brough, T., Dawson, S., Slooten, E. (2014). Marine Mammals and the Port Lyttelton Development. An environmental Impact Assessment. Dunedin, New Zealand: University of Otago

Burnham, K.P., & Anderson, D.R. (2002) *Model Selection and Multimodel Inference: A Practical Information-Theoretic Approach*. Springer-Verlag, New York.

Burnham, K.P., & Anderson, D.R. (2003). *Model selection and multimodel inference: a practical information-theoretic approach*. Springer Science & Business Media.

Canterbury Earthquake Recovery Authority. (2011). Canterbury Earthquake Recovery Act 2011. New Zealand Legislation. <http://www.legislation.govt.nz/act/public/2011/0012/latest/DLM3653522.html>

Carstensen, J., Henriksen, O.D., & Teilmann, J. (2006). Impacts of offshore wind farm construction on harbour porpoises: acoustic monitoring of echolocation activity using porpoise detectors (T-PODs). *Marine Ecology Progress Series*, 321:295-308.

Castellote, M., Clark, C.W., & Lammers, M.O. (2012). Acoustic and behavioural changes by fin whales (*Balaenoptera physalus*) in response to shipping and airgun noise. *Biological Conservation*, 147:115-122.

Chelonia Ltd (2007). T-POD Reference Guide. <http://www.chelonia.co.uk/T-POD_downloads.htm> *Retrieved on 20th of January 2017*

Chen, C.T., & Millero, F.J. (1977). Speed of sound in seawater at high pressures. The Journal of the Acoustical Society of America, 62(5), 1129-1135.

Cobo, P., Kormann, J., & Ranz Guerra, C. (2007). Underwater noise impact of offshore wind farms during construction and operation phases. 14th International congress on sound and vibration, Cairns Australia

Curtis, R. J. (1985). Sedimentation in a rock-walled inlet, Lyttelton Harbour, New Zealand.

Dähne, M., Verfuß, U.K., Diederichs, A., Meding, A., Benke, H. (2006) T-POD test tank calibration and field calibration. In: Leeney, R.H., Tregenza, N.J.C. Proc. Workshop Static Acoustic Monitoring of Cetaceans, 20th Annual Meeting of the European Cetacean Society, Gdynia, Poland 2 April 2006. European Cetacean Society. www.seaturtle.org/mtrg/personnel/SAM_report_ECS_2006.pdf

Dähne, M., Gilles, A., Lucke, K., Peschko, V., Adler, S., Krügel, K., Sundermeyer, J. & Siebert, U. (2013). Effects of pile-driving on harbour porpoises (Phocoena phocoena) at the first offshore wind farm in Germany. *Environmental Research Letters*, 8:025002.

David, J.A. (2006). Likely sensitivity of bottlenose dolphins to pile-driving noise. Water and Environment Journal, 20:48-54.

Dawson, S.M. & Thorpe, C.W. (1990). A quantitative analysis of the acoustic repertoire of Hector's dolphin. *Ethology* 86:131-145

Dawson, S.M. (1991a). Incidental catch of Hector's dolphins in inshore gillnets. Marine Mammal Science 7:283-295

Dawson, S. M. (1991b). Clicks and communication: the behavioural and social contexts of Hector's dolphin vocalizations. *Ethology*, *88*(4), 265-276.

Dawson, S.M. (2009). Cephalorhynchus dolphins. *In: "Encyclopedia of Marine Mammals" (Perrin, W.F., Würsig, B. & Thewissen, J.G.M, Eds.). Academic Press. San Diego. 2nd Edition. pp.* 191–196.

Dawson, S.M., Fletcher, D., Slooten, E. (2013) Habitat use and conservation of an endangered dolphin. *Endangered Species Research* 21: 45–54.

De Jong, C.A.F. & Ainslie, M.A. (2008). Underwater radiated noise due to the piling for the Q7 Offshore Wind Park. *Journal of the Acoustical Society of America*, 123:2987.

De Jong, C.A.F., Ainslie, M.A., & Blacquière, G. (2011). Standard for measurement and monitoring of underwater noise, Part II: procedures for measuring underwater noise in connection with offshore wind farm licensing. *Report no. TNO-DV*, C251.

Department of Conservation (2008). Marine Mammals Protection (Banks Peninsula Sanctuary) Amendment Notice 2008. Issued under the authority of the Acts and Regulations Publication Act 1989. Gazette 25 September 2008.

Duncan, A.J., McCauley, R.D., Parnum, I., & Salgado-Kent, C. (2010). Measurement and modelling of underwater noise from pile driving. In *Proceedings of 20th International Congress on Acoustics* (pp. 23-7).

Dyndo, M., Wiśniewska, D. M., Rojano-Doñate, L., & Madsen, P. T. (2015). Harbour porpoises react to low levels of high frequency vessel noise. *Scientific reports*, 5:11083.

Erbe, C. (2009). Underwater noise from pile driving in Moreton Bay, Qld. *Acoustics Australia*, 37:87.

Erbe, C. (2013). International Regulation of Underwater Noise. *Acoustics Australia*, 41.

Erbe, C., Williams, R., Sandilands, D., & Ashe, E. (2014). Identifying modeled ship noise hotspots for marine mammals of Canada's Pacific Region. *PloS one*, *9*(3), e89820.

Estes, J.A., Tinker, M.T., Williams, T.M., and Doak, D.E. (1998). Killer whale predation on sea otters linking oceanic and nearshore ecosystems. *Science* 282:473-476.

Everest, F.A., Young, R.W., & Johnson, M.W. (1948). Acoustical characteristics of noise produced by snapping shrimp. *The Journal of the Acoustical Society of America*, 20:137-142.

Ferguson, M.C., Barlow, J., Reilly, S.B., & Gerrodette, T. (2005). Predicting Cuvier's (Ziphius cavirostris) and Mesoplodon beaked whale population density from habitat characteristics in the eastern tropical Pacific Ocean. *Journal of Cetacean Research and Management*, 7:287.

Fernández, A., Edwards, J.F., Rodriguez, F., De Los Monteros, A.E., Herraez, P., Castro, P., Jaber, J.R., Martin, V. and Arbelo, M. (2005). “Gas and fat embolic syndrome” involving a mass stranding of beaked whales (family Ziphiidae) exposed to anthropogenic sonar signals. *Veterinary Pathology*, 42:446-457.

Filadelfo, R., Mintz, J., Michlovich, E., D'Amico, A., Tyack, P.L., & Ketten, D.R. (2009). Correlating military sonar use with beaked whale mass strandings: what do the historical data show?. *Aquatic mammals*, 35:435.

Finneran, J.J., Schlundt, C.E., Dear, R., Carder, D.A., & Ridgway, S.H. (2002). Temporary shift in masked hearing thresholds in odontocetes after exposure to single underwater impulses from a seismic watergun. *The Journal of the Acoustical Society of America*, 111:2929-2940.

Finneran, J.J., Carder, D.A., Schlundt, C.E., & Ridgway, S.H. (2005). Temporary threshold shift in bottlenose dolphins *(Tursiops truncatus)* exposed to mid-frequency tones). *The Journal of the Acoustical Society of America*, 118:2696-2705.

Forney, K.A., Southall, B.L., Slooten, E., Dawson, S.M., Read, A.J., Baird, R.W., & Brownell, R.L., Jr. (2017). Nowhere to go: noise impact assessments for marine mammal populations with high site fidelity. *Endangered Species Research*, 32:391–413.

Forrest, T.G., Miller, G.L., & Zagar, J.R. (1993). Sound propagation in shallow water: implications for acoustic communication by aquatic animals. *Bioacoustics*, 4:259-270.

Fricke, M.B., & Rolfes, R. (2015). Towards a complete physically based forecast model for underwater noise related to impact pile driving. *The Journal of the Acoustical Society of America*, 137: 1564-1575.

Gaggero, T., Rizzuto, E., Karasalo, I., Ostberg, M., Folegot, T., Six, L., van der Schaar, M. & Andre, M. (2015). Validation of a simulation tool for ship traffic noise. InOCEANS 2015-Genova (pp. 1-7). IEEE.

Goold, J.C. (1996) Acoustic assessment of populations of common dolphin (Delphinus delphis) in conjunction with seismic surveying. *Journal of the Marine Biological Association of the UK*, 76:811–820

Goossens, H., & Zwolsman, J. J. (1996). An evaluation of the behaviour of pollutants during dredging activities. *Terra et Aqua*, 20-28.

Gormley, A.M., Dawson, S.M., Slooten, E., Bräger, S. (2005). Capture recapture estimates of Hector's dolphin abundance at Banks Peninsula, New Zealand. *Marine Mammal Science* 21:204-216.

Gormley, A.M., Slooten, E., Dawson, S., Barker, R.J., Rayment, W., du Fresne, S., Bräger, S. (2012) First evidence that marine protected areas can work for marine mammals. *Journal of Applied Ecology* 49:474-480.

Gray, H., & Van Waerebeek, K. (2011). Postural instability and akinesia in a pantropical spotted dolphin, *Stenella attenuata*, in proximity to operating airguns of a geophysical seismic vessel. *Journal for Nature Conservation*, 19:363-367.

Haelters, J., Van Roy, W., Vigin, L., & Degraer, S. (2012). The effect of pile driving on harbour porpoises in Belgian waters. *Offshore wind farms in the Belgian part of the North Sea. Heading for an understanding of environmental impacts. Royal Belgian Institute of Natural Sciences, Brussels*, 127-143.

Harwood, J. (2001) Marine mammals and their environment in the twenty-first century. *Journal of Mammalogy* 82:630-640.

Harwood, J., King, S., Schick, R., Donovan, C. & Booth, C. (2014). A Protocol for Implementing the Intern Population Consequences of Disturbance (PCOD) Approach: Quantifying and assessing the Effects of UK Offshore Renewable Energy Developments on Marine Mammal Populations. REPORT NUMBER SMRUL-TCE-2013-014. Scottish Marine and Freshwater Science 5/2, 1–90.

Hastie, T.J. & Tibshirani, R.J. (1990) *Generalized additive models*. Chapman & Hall, Boca Raton, FL

Hatch, L.T., Clark, C.W., Van Parijs, S.M., Frankel, A.S., & Ponirakis, D.W. (2012). Quantifying loss of acoustic communication space for right whales in and around a US National Marine Sanctuary. *Conservation Biology*, 26:983-994.

Haelters, J., Van Roy, W., Vigin, L., & Degraer, S. (2012). The effect of pile driving on harbour porpoises in Belgian waters. *Offshore wind farms in the Belgian part of the*

North Sea. Heading for an understanding of environmental impacts. Royal Belgian Institute of Natural Sciences, Brussels, 127-143.

Hildebrand, J.A. (2009). Anthropogenic and natural sources of ambient noise in the ocean. *Marine Ecology Progress Series*, 395:5-20.

Jansen, H.W., & de Jong, C.A.F. (2015). Experimental assessment of underwater radiated sound of different ship types. In OCEANS 2015-Genova(pp. 1-8). IEEE.

Jensen et al. (1994) Computational Ocean Acoustics, AIP Press, New York

Jensen, F. B., Kuperman, W. A., Porter, M. B., & Schmidt, H. (2011).*Computational ocean acoustics*. Springer Science & Business Media.

Jefferson, T.A., Hung, S.K., & Würsig, B. (2009). Protecting small cetaceans from coastal development: Impact assessment and mitigation experience in Hong Kong. *Marine Policy*, 33:305-311.

Johnson, C.S. (1968). Masked Tonal Thresholds in the bottle-nosed porpoise, *J. Acoust. Soc. Am.* 44:965-967.

Johnston, D.W., Westgate, A.J., & Read, A.J. (2005). Effects of fine-scale oceanographic features on the distribution and movements of harbour porpoises Phocoena phocoena in the Bay of Fundy. *Marine Ecology Progress Series*, 295:279-293.

Kastelein, R.A., Bunskoek, P., Hagedoorn, M., Au, W.W., & de Haan, D. (2002). Audiogram of a harbor porpoise (*Phocoena phocoena*) measured with narrow-band frequency-modulated signals. *The Journal of the Acoustical Society of America*, 112:334-344.

Kastelein, R.A., Janssen, M., Verboom, W.C., & de Haan, D. (2005). Receiving beam patterns in the horizontal plane of a harbor porpoise (*Phocoena phocoena*). *The Journal of the Acoustical Society of America*, 118:1172-1179.

Kastelein, R.A., Hoek, L., De Jong, C.A.F., and Wensveen, P.J. (2010). The effect of signal duration on the underwater detection thresholds of a harbor porpoise (*Phocoena phocoena*) for single frequency-modulated tonal signals between 0.25 and 160 kHz. *J. Acoust. Soc. Am*. 128:3211–3222.

Kastelein, R.A., Gransier, R., Hoek, L., Olthuis, J., (2012). Temporary threshold shifts and recovery in a harbor porpoise (*Phocoena phocoena*) after octave-band noise at 4 kHz. J. *Acoust. Soc. Am*. 132:3525–3537. http://dx.doi.org/10.1121/1.4757641.

Kastelein, R.A., Hoek, L., Gransier, R., & de Jong, C.A. (2013a). Hearing thresholds of a harbor porpoise (*Phocoena phocoena*) for playbacks of multiple pile driving strike sounds. *The Journal of the Acoustical Society of America*, 134:2302-2306.

Kastelein, R.A., van Heerden, D., Gransier, R., & Hoek, L. (2013b). Behavioral responses of a harbor porpoise (Phocoena phocoena) to playbacks of broadband pile driving sounds. *Marine environmental research*, 92:206-214.

Kastelein, R.A., Gransier, R., & Hoek, L. (2013c). Comparative temporary threshold shifts in a harbor porpoise and harbor seal, and severe shift in a seal. *The Journal of the Acoustical Society of America*, 134:13-16.

Kastelein, R.A., Hoek, L., Gransier, R., Rambags, M., & Claeys, N. (2014). Effect of level, duration, and inter-pulse interval of 1–2 kHz sonar signal exposures on harbor porpoise hearing. *The Journal of the Acoustical Society of America*, 136:412-422.

Kastelein, R.A., Gransier, R., Marijt, M.A., & Hoek, L. (2015). Hearing frequency thresholds of harbor porpoises (*Phocoena phocoena*) temporarily affected by played back offshore pile driving sounds. *The Journal of the Acoustical Society of America*, 137:556-564.

King, S.L., Schick, R.S., Donovan, C., Booth, C.G., Burgman, M., Thomas, L., & Harwood, J. (2015). An interim framework for assessing the population consequences of disturbance. *Methods in Ecology and Evolution*, 6:1150-1158.

Knudsen, V.O., Alford, R.S., & Emling, J.W. (1948). Underwater ambient noise. *J. Mar. Res.*, 7:410-429.

Kyhn, L. A., Tougaard, J., Teilmann, J., Wahlberg, M., Jørgensen, P. B., & Bech, N. I. (2008). Harbour porpoise (*Phocoena phocoena*) static acoustic monitoring: laboratory detection thresholds of T-PODs are reflected in field sensitivity. *Journal of the Marine Biological Association of the UK*, 88:1085-1091.

Kyhn, L.A., Tougaard, J., Jensen, F.H., Wahlberg, M., Stone, G.S., Yoshinaga, A., Beedholm, K. and Madsen, P.T. (2009). Feeding at a high pitch: Source parameters of narrow band, high-frequency clicks from echolocating off-shore hourglass dolphins and coastal Hector's dolphins. *Journal of the Acoustical Society of America*, 125:1783–1791.

Kyhn, L.A., Tougaard, J., Thomas, L., Duve, L.R., Stenback, J., Amundin, M., Desportes, G. & Teilmann, J. (2012). From echolocation clicks to animal density—Acoustic sampling of harbor porpoises with static dataloggers. *The Journal of the Acoustical Society of America*, 131:550-560.

Lepper, P.A., Robinson, S.P., Ablitt, J., & Dible, S.A. (2009). Temporal and spectral characteristics of a marine piling operation in shallow water. Proc. NAG/DAGA Int. Conference on Acoustics, Rotterdam, March 2009.

Lippert, T., & von Estorff, O. (2014). The significance of parameter uncertainties for the prediction of offshore pile driving noise. *The Journal of the Acoustical Society of America*, 136:2463-2471.

Lucke, K., Lepper, P.A., Blanchet, M.A., & Siebert, U. (2008). Testing the acoustic tolerance of harbour porpoise hearing for impulsive sounds. *Bioacoustics*, 17:329-331.

Lucke, K., Siebert, U., Lepper, P.A. and Blanchet, M. (2009). Temporary shift in masked hearing thresholds in a harbor porpoise (*Phocoena phocoena*) after exposure to seismic airgun stimuli, *J. Acoust. Soc. Am.* 125:4060–4070.http://dx.doi.org/10.1121/1.3117443

Lucke, K., Lepper, P.A., Blanchet, M.A., & Siebert, U. (2011). The use of an air bubble curtain to reduce the received sound levels for harbor porpoises (Phocoena phocoena). *The Journal of the Acoustical Society of America*, 130:3406-3412.

Madsen, P. T. (2005). Marine mammals and noise: Problems with root mean square sound pressure levels for transients. *The Journal of the Acoustical Society of America*, 117:3952-3957.

Madsen, P.T., Wahlberg, M., Tougaard, J., Lucke, K., Tyack, P.L. (2006) Wind turbine underwater noise and marine mammals: Implications of current knowledge and data needs. *Marine Ecology Progress Series* 309:279-295.

Malme, C.I., & Beranek, B. (1995). Sound propagation. In *WJ Richardson, CR Greene, Jr., CI Malme, & DH Thomson, Marine mammals and noise,* 59-86.

MarineTraffic (2016) Port of Fremantle. <http://www.marinetraffic.com/en/ais/details/ports/768> *Retrieved on 15th December 2016.*

Marsh, H.W., & Schulkin, M. (1962). Shallow-Water Transmission. *The Journal of the Acoustical Society of America,* 34:863-864.

Marques, T.A., Thomas, L., Ward, J., DiMarzio, N., & Tyack, P.L. (2009). Estimating cetacean population density using fixed passive acoustic sensors: An example with Blainville's beaked whales. *The Journal of the Acoustical Society of America*, 125:1982-1994.

McDonald, M.A., Hildebrand, J.A., Wiggins, S.M., & Ross, D. (2008). A 50 Year comparison of ambient ocean noise near San Clemente Island: A bathymetrically complex coastal region off Southern California. *The journal of the Acoustical Society of America*, 124:1985-1992.

McKenna, M.F., Ross, D., Wiggins, S.M., & Hildebrand, J.A. (2012). Underwater radiated noise from modern commercial ships. *The Journal of the Acoustical Society of America*, 131:92-103.

McQuinn, I.H., Lesage, V., Carrier, D., Larrivée, G., Samson, Y., Chartrand, S., Michaud, R. & Theriault, J. (2011). A threatened beluga (*Delphinapterus leucas*) population in the traffic lane: Vessel-generated noise characteristics of the Saguenay-St. Lawrence Marine Park, Canada. *The Journal of the Acoustical Society of America*, 130:3661-3673.

Mendes, S., Turrell, W., Lütkebohle, T., & Thompson, P. (2002). Influence of the tidal cycle and a tidal intrusion front on the spatio-temporal distribution of coastal bottlenose dolphins. *Marine Ecology Progress Series*, 239:221-229.

Menze, S., Rettig, S., Opzeeland, I.C., Kindermann, L., & Boebel, O. (2013). Ambient noise monitoring in the Southern Ocean applying EU good environmental status descriptors.

Merchant, N.D., Blondel, P., Dakin, D.T., & Dorocicz, J. (2012). Averaging underwater noise levels for environmental assessment of shipping. *The Journal of the Acoustical Society of America*, 132:343-349.

Merchant, N.D., Fristrup, K.M., Johnson, M.P., Tyack, P.L., Witt, M.J., Blondel, P., & Parks, S. E. (2015). Measuring acoustic habitats. *Methods in Ecology and Evolution*, 6:257-265.

Miller, L.A., Wahlberg M. (2013). Echolocation by the harbor porpoise: life in coastal waters. *Frontiers in physiology* 4

Miller, E., Lalas, C., Dawson, S., Ratz, H., Slooten, E. (2012) Hector's dolphin diet: the species, sizes and relative importance of prey eaten by *Cephalorhynchus hectori*, investigated using stomach content analysis. Mar Mamm Sci, doi: 10.1111/j.1748-7692.2012.00594.x

Ministry of Primary Industries (MPI) (2007). Hector's and Maui's Dolphin Threat Management Plan. New Zealand Government. <doc.govt.nz>

Mooney, T.A., Nachtigall, P.E., Breese, M., Vlachos, S., & Au, W.W. (2009). Predicting temporary threshold shifts in a bottlenose dolphin (Tursiops truncatus): The effects of noise level and duration. *The Journal of the Acoustical Society of America*, 125:1816-1826.

Morrison, M.A., Francis, M.P., Hartill, B. W., & Parkinson, D.M. (2002). Diurnal and tidal variation in the abundance of the fish fauna of a temperate tidal mudflat. *Estuarine, Coastal and Shelf Science*, 54: 793-807.

Mueller-Blenkle, C., McGregor, P.K., Gill, A.B., Andersson, M.H., Metcalfe, J., Bendall, V., Sigray, P., Wood, D.T. & Thomsen, F. (2010) Effects of Pile-driving Noise on the Behaviour of Marine Fish. COWRIE Ref: Fish 06-08, Technical Report 31st March 2010

Müller, A., & Zerbs, C. (2011). *Offshore wind farms. Measurement instruction for waterborne sound measurements*. 88:607. Tech. Rep.

Munger, L.M., Wiggins, S.M., & Hildebrand, J.A. (2011). North Pacific right whale up-call source levels and propagation distance on the southeastern Bering Sea shelf. *The Journal of the Acoustical Society of America*, *129*(6), 4047-4054.

Nachtigall, P.E., Supin, A.Y., Pawloski, J., & Au, W.W. (2004). Temporary threshold shifts after noise exposure in the bottlenose dolphin (Tursiops truncatus) measured using evoked auditory potentials. *Marine Mammal Science*, 20:673-687.

Nakagawa, S., & Freckleton, R.P. (2011). Model averaging, missing data and multiple imputation: a case study for behavioural ecology. *Behavioral Ecology and Sociobiology*, 65:103-116.

Nedwell, J., Langworthy, J., & Howell, D. (2003). Assessment of sub-sea acoustic noise and vibration from offshore wind turbines and its impact on marine wildlife; initial measurements of underwater noise during construction of offshore windfarms, and comparison with background noise. *Subacoustech Report* ref: 544R0423, published by COWRIE.

Nedwell, J.R., Workman, R., Parvin, S.J., (2005). The assessment of likely levels of piling noise at Greater Gabbard and its comparison with background noise, including piling noise measurements made at Kentish Flats. Subacoustech Report, 633R0115, Southampton.

Nedwell, J.R., Parvin, S.J., Edwards, B., Workman, R., Brooker, A.G., Kynoch, J.E. (2007) Measurement and interpretation of underwater noise during construction and operation of offshore windfarms in UK waters. Report for COWRIE, Newbury, UK. <tethys.pnnl.gov>

Norro, A., Haelters, J., Rumes, B., Degraer, S. (2010) Underwater noise produced by the piling activities during the construction of the Belwin offshore wind farm. Pp. 37-51. In Degraer, S., Brabant, R., Rumes, B. eds. *Offshore wind farms in the Belgian part of the North Sea*. Royal Belgian Institute of Natural Sciences Management. Unit of the North Sea Mathematical Models, Marine Ecosystem Management Section.

Norton, G.V., & Novarini, J.C. (1996). The effect of sea-surface roughness on shallow water waveguide propagation: A coherent approach. *The Journal of the Acoustical Society of America*, 99:2013-2021.

Nowacek, D.P. (2015). Seismic surveys and marine wildlife: Impacts, the lack thereof, and thoughts on managing both. *The Journal of the Acoustical Society of America*, 138:1848-1848.

Nowacek, D.P., Clark, C.W., Mann, D., Miller, P.J., Rosenbaum, H.C., Golden, J. S., Jasny, M., Kraska, J., & Southall, B. L. (2015). Marine seismic surveys and ocean noise: time for coordinated and prudent planning. *Frontiers in Ecology and the Environment*, 13:378-386.

Padovese, L.R. (2015). Underwater sound pressure levels in the Port of Santos: Representative sample of forty-five days. In *2015 IEEE/OES Acoustics in Underwater Geosciences Symposium (RIO Acoustics)* (pp. 1-4). IEEE.

Paiva, E.G., Kent, C.P.S., Gagnon, M.M., McCauley, R., & Finn, H. (2015). Reduced Detection of Indo-Pacific Bottlenose Dolphins (*Tursiops aduncus*) in an Inner Harbour Channel During Pile Driving Activities. *Aquatic Mammals*, 41:455-468.

Philpott, E., Englund, A., Ingram, S., & Rogan, E. (2007). Using T-PODs to investigate the echolocation of coastal bottlenose dolphins. *Journal of the Marine Biological Association of the United Kingdom*, 87:11-17.

Piggott, C.L. (1964). Ambient sea noise at low frequencies in shallow water of the Scotian Shelf. *The Journal of the Acoustical Society of America*, 36:2152-2163.

Pine, M. K., Jeffs, A. G., & Radford, C. A. (2014). The cumulative effect on sound levels from multiple underwater anthropogenic sound sources in shallow coastal waters. *Journal of applied ecology*, 51:23-30.

Port Lyttelton Company (PLC) (2014). The Port Lyttelton Plan. <www.portlytteltonplan.co.nz>

Porter, M., & Collins, M. (2005). Underwater acoustic propagation modelling software – AcTUP V2.2L. Centre for Marine Science and Technology. <http://cmst.curtin.edu.au/products/underwater/>

R Development Core Team (2016) *R: a language and environment for statistical computing*. Version 3.2.4. R Foundation for Statistical Computing, Vienna, Austria. Available at: http://www.r-project.org/.

Radford, C., Jeffs, A., Tindle, C., & Montgomery, J. C. (2008). Resonating sea urchin skeletons create coastal choruses. *Marine Ecology Progress Series*, 362:37-43.

Rako, N., Fortuna, C.M., Holcer, D., Mackelworth, P., Nimak-Wood, M., Pleslić, G., Sebastianutto, L., Vilibić, I., Wiemann, A. & Picciulin, M. (2013). Leisure boating noise as a trigger for the displacement of the bottlenose dolphins of the Cres–Lošinj archipelago (northern Adriatic Sea, Croatia). *Marine pollution bulletin*, 68:77-84.

Rayment, W.J., Dawson, S., & Slooten, E. (2009a). Trialling an automated passive acoustic detector (T-POD) with Hector's dolphins (Cephalorhynchus hectori). *Journal of the Marine Biological Association of the United Kingdom*, 89:1015–1022. http://doi.org/10.1017/S0025315409003129

Rayment, W.J., Dawson, S., & Slooten, E. (2009b). Use of T-PODs for acoustic monitoring of Cephalorhynchus dolphins: a case study with Hector’s dolphins in a marine protected area. *Endangered Species Research*, 10:333–339.

Rayment W., Dawson S., Slooten E. (2010) Seasonal changes in distribution of Hector's dolphin at Banks Peninsula, New Zealand: Implications for protected area design. *Aquatic Conservation: Marine and Freshwater Ecosystems* 20:106-116.

Rayment, W., Dawson, S., Scali, S., & Slooten, L. (2011). Listening for a needle in a haystack: passive acoustic detection of dolphins at very low densities. *Endangered Species Research*, 14:149-156.

Reeves, R.R., Dawson, S.M., Jefferson, T.A., Karczmarski, L., Laidre, K., O’Corry-Crowe, G., Rojas-Bracho, L., Secchi, E.R., Slooten, E., Smith B.D., Wang J.Y., Zhou K. (2013) *Cephalorhynchus hectori*. The IUCN Red List of Threatened Species. Version 2015.3: <www.iucnredlist.org> *Accessed on 4 November 2015.*

Reinhall, P.G. & Dahl, P.H. (2011) Underwater Mach wave radiation from impact pile driving: theory and observation. *Journal of the Acoustical Society of America* 130:1209–1216.

Richards, S.A., Whittingham, M.J., & Stephens, P.A. (2011). Model selection and model averaging in behavioural ecology: the utility of the IT-AIC framework. *Behavioral Ecology and Sociobiology*, 65:77-89.

Richardson, W.J., Green, C.R., Malme, C.I., Thomson, D.H. (1995) *Marine Mammals and Noise*. Academic Press- Elsvier, USA.

Richardson, W., & Würsig, B. (1997) Influences of man-made noise and other human actions on cetacean behaviour. *Marine and Freshwater Behaviour and Physiology*, 29:1-4

Robinson, S.P., Lepper, P., & Ablitt, J. (2007). The measurement of the underwater radiated noise from marine piling including characterisation of a" soft start" period. In *Oceans 2007-Europe* (pp. 1-6). IEEE.

Robinson, S.P., Lepper, P.A., & Hazelwood, R.A. (2014). Good practice guide for underwater noise measurement. *NPL Good Practice Guide*, Guide No. 133, ISSN: 1368-6550

Rodkin, R.B. & Reyff, J. A. (2008) Underwater sound from marine pile driving. *Bioacoustics* 17:138-140

Rolland, R.M., Parks, S.E., Hunt, K.E., Castellote, M., Corkeron, P.J., Nowacek, D.P., Wasser, S.K. and Kraus, S.D. (2012). Evidence that ship noise increases stress in right whales. *Proceedings of the Royal Society of London B: Biological Sciences*, 279:2363-2368.

Romano, T.A., Keogh, M.J., Kelly, C., Feng, P., Berk, L., Schlundt, C.E., Carder, D.A. & Finneran, J.J. (2004). Anthropogenic sound and marine mammal health: measures of the nervous and immune systems before and after intense sound exposure. *Canadian Journal of Fisheries and Aquatic Sciences*, 61:1124-1134.

Ross, D. (2013). *Mechanics of underwater noise*. Elsevier.

Saleem, Z. (2011). Alternatives and modifications of Monopile foundation or its installation technique for noise mitigation. *Report by Delft University of Technology for Stichting De Noordzee (the North Sea Foundation).*

Salgado-Kent, C., McCauley, R., Parnum, I., & Gavrilov, A. (2012). Underwater noise sources in Fremantle inner harbour: dolphins, pile driving and traffic. In *Proceedings of the Acoustical Society of Australia*. Acoustical Society of Australia.

Samuel, Y., Morreale, S.J., Clark, C.W., Greene, C.H., & Richmond, M.E. (2005). Underwater, low-frequency noise in a coastal sea turtle habitat. *The Journal of the Acoustical Society of America*, 117:1465-1472.

Schlundt, C.E., Finneran, J.J., Carder, D.A., & Ridgway, S.H. (2000). Temporary shift in masked hearing thresholds of bottlenose dolphins, Tursiops truncatus, and white whales, Delphinapterus leucas, after exposure to intense tones. *The Journal of the Acoustical Society of America*, 107:3496-3508.

Schlundt, C.E., Dear, R.L., Carder, D.A., & Finneran, J.J. (2006). Growth and recovery of temporary threshold shifts in a dolphin exposed to midfrequency tones with durations up to 128 s. *The Journal of the Acoustical Society of America*, 120:3227-3227.

Shumway, G. (1960). Sound speed and absorption studies of marine sediments by a resonance method. *Geophysics*, 25:451-467.

Slooten, E., & Lad, F. (1991). Population biology and conservation of Hector's dolphin. *Canadian Journal of Zoology*, 69:1701-1707.

Slooten, E. (1991). Age, growth and reproduction in Hector's dolphins. *Can. J. Zool.* 69:1689–1700.

Slooten, E., Dawson, S.M., Lad, F. (1992) Survival rates of photographically identified Hector's dolphins from 1984 to 1988. *Marine Mammal Science* 4:327-343.

Slooten, E., Fletcher, D., Taylor, B.L. (2000) Accounting for uncertainty in risk assessment: Case study of Hector's dolphin mortality due to gillnet entanglement. *Conservation Biology* 14:1264-1270

Slooten, E., Dawson, S.M. (2009) Assessing the effectiveness of conservation management decisions: Likely effects of new protection measures for Hector's dolphin (Cephalorhynchus hectori). *Aquatic Conservation: Marine and Freshwater Ecosystems* 20:334-347

Slooten, E. (2013) Effectiveness of area-based management in reducing bycatch of the New Zealand dolphin. *Endangered Species Research* 20:121-130

Slotte, A., Kansen, K., Dalen, J., Ona, E. (2004). Acoustic mapping of pelagic fish distribution and abundance in relation to a seismic shooting area off the Norwegian west coast. Fisheries Research 67, 143–50.

Southall, B.L., Bowles, A.E., Ellison, W.T., Finneran, J.J., Gentry, R.L., Green, C.R., Kastak, D., Ketten, D.R., Miller, J.H., Nachtingall, P.E., Richardson, W.J., Thomas, J.T., Tyack, P.L. (2007) Marine mammal noise-exposure criteria: Initial scientific recommendations. *Bioacoustics* 17:273-275

Sveegaard, S., Teilmann, J., Berggren, P., Mouritsen, K.N., Gillespie, D., and Tougaard, J. (2011). Acoustic surveys confirm the high-density areas of harbour porpoises found by satellite tracking. – ICES Journal of Marine Science, 68: 929–936.

Tanabe S., Mori T., Tatsukawa R., Miyazaki N. (1983) Global pollution of marine mammals by PCBs, DDTs and HCHs (BHCs). *Chemosphere* 12:1269-1275

Tasker, M.L., Amundin, M., Andre, M., Hawkins, A., Lang, W., Merck, T., Scholik-Schlomer, A., Teilmann, J., Thomsen, F., Werner, S. and Zakharia, M. (2010). Marine Strategy Framework Directive Task Group 11 Report Underwater noise and other forms of energy. *Report No. EUR, 24341*.

Teilmann, J. Miller, L.A., Kirketerp, T., Kastelein, R.A., Madsen, P.T., Nielsen, B.K., & Au, W.W. (2002). Characteristics of echolocation signals used by a harbour porpoise (*Phocoena phocoena*) in a target detection experiment. *Aquatic Mammals*, 28:275-284

Thompson, P.M., Lusseau, D., Barton, T., Simmons, D., Rusin, J., & Bailey, H. (2010). Assessing the responses of coastal cetaceans to the construction of offshore wind turbines. *Marine pollution bulletin*, 60:1200-1208.

Thompson, P.M., Hastie, G.D., Nedwell, J., Barham, R., and others (2013) Framework for assessing impacts of pile-driving noise from offshore wind farm construction on a harbour seal population. *Environmental Impact Assessment Review* 43:73-85

Thomsen, F., van Elk, N., Brock, V., & Piper, W. (2005). On the performance of automated porpoise-click-detectors in experiments with captive harbor porpoises (*Phocoena phocoena*). *The Journal of the Acoustical Society of America*, 118:37-40.

Todd, V.L., Pearse, W.D., Tregenza, N.C., Lepper, P.A., & Todd, I.B. (2009). Diel echolocation activity of harbour porpoises (*Phocoena phocoena*) around North Sea offshore gas installations. *ICES Journal of Marine Science: Journal du Conseil*.

Torres, L., Read, A., & Halpin, P. (2008) Fine scale habitat modelling of a top marine predator: do prey data improve predictive capacity? *Ecological Applications*, 18:1702–1717.

Tougaard, J., Carstensen, J., Teilmann, J., Bech, N.I., Skov, H., & Henriksen, O.D. (2005). Effects of the Nysted Offshore wind farm on harbour porpoises. *Annual Status Report for the T-POD Monitoring Program*.

Tougaard, J., Carstensen, J., Teilmann, J., Skov, H., & Rasmussen, P. (2009). Pile driving zone of responsiveness extends beyond 20 km for harbor porpoises (*Phocoena phocoena (L.)*). *The Journal of the Acoustical Society of America*, 126:11-14.

Tougaard, J., Wright, A. J., & Madsen, P. T. (2015). Cetacean noise criteria revisited in the light of proposed exposure limits for harbour porpoises. *Marine pollution bulletin*, 90:196-208.

Tsouvalas, A., & Metrikine, A.V. (2014). A three-dimensional vibroacoustic model for the prediction of underwater noise from offshore pile driving. *Journal of Sound and Vibration*, 333:2283-2311.

Tyack, P.L., Zimmer, W.M., Moretti, D., Southall, B.L., Claridge, D.E., Durban, J.W., Clark, C.W., D'Amico, A., DiMarzio, N., Jarvis, S. and McCarthy, E., (2011). Beaked whales respond to simulated and actual navy sonar. *PloS One*, 6:e17009.

Tynan, C.T., & DeMaster, D.P. (1997) Observations and predictions of arctic climatic change: Potential effects on marine mammals. *Arctic* 50:308-322.

Urick, R. J., (1983) ‘Principles of underwater sound’, 3rd ed, Peninsula publishing, California

Verfuß, U. K., Dähne, M., Diederichs, A., & Benke, H. (2008). Applications and analytical methods for T-POD deployment in environmental impact studies for wind farms:

comparability and development of standard methods. *Offshore wind farms and marine mammals: impacts & methodologies for assessing impacts*, 27.

Villadsgaard, A., Wahlberg, M., & Tougaard, J. (2007). Echolocation signals of wild harbour porpoises, *Phocoena phocoena*. *Journal of Experimental Biology*, 210:56-64.

Webster, T.A., Dawson, S.M., & Slooten, E. (2009). Evidence of sex segregation in Hector's dolphin (*Cephalorhynchus hectori*). *Aquatic Mammals*, 35:212.

Weilgart, L.S. (2007). The impacts of anthropogenic ocean noise on cetaceans and implications for management. *Canadian Journal of Zoology*, 85:1091-1116.

Weir, C.R. (2008). Overt Responses of Humpback Whales (*Megaptera novaeangliae*), Sperm Whales (*Physeter macrocephalus*), and Atlantic Spotted Dolphins (*Stenella frontalis*) to Seismic Exploration off Angola. *Aquatic Mammals*, 34:71-83.

Wenz, G.M. (1962) Acoustic ambient noise in the ocean: spectra and sources, *Journal of the Acoustical Society of America*, 34:1936-1956.

Wood, S. (2017a). Frequently Asked Questions for package mgcv. R documentation. <https://stat.ethz.ch/R-manual/R-devel/library/mgcv/html/mgcv-FAQ.html> *Retrieved on 14th March 2017*

Wood, S. (2017b). mgcv: Mixed GAM Computation Vehicle with GCV/AIC/REML Smoothness Estimation . R package version 1.8-17.

Würsig, B., Greene, C.R., Jefferson, T.A. (2000) Development of an air bubble curtain to reduce underwater noise of percussive piling. *Marine Environmental Research*, *49*(1), 79-93.

Würsig, B., & Greene, C.R. (2002). Underwater sounds near a fuel receiving facility in western Hong Kong: relevance to dolphins. *Marine Environmental Research*, 54:129-145.

Yang, L., Xu, X., Huang, Z., & Tu, X. (2015). Recording and Analyzing Underwater Noise During Pile Driving for Bridge Construction. *Acoustics Australia*, 43:159-167.

Yoder, N. (2009). Peakfinder (https://www.mathworks.com/matlabcentral/fileexchange/25500-peakfinder-x0--sel--thresh--extrema--includeendpoints--interpolate-), Mathworks File Exchange. Retrieved June 2015.

Zampolli, M., Nijhof, M.J., de Jong, C.A., Ainslie, M.A., Jansen, E.H., & Quesson, B.A. (2013). Validation of finite element computations for the quantitative prediction of underwater noise from impact pile driving. *The Journal of the Acoustical Society of America*, 133:72-81.

Zuur, A.F., Ieno, E.N., Walker, N.J., Saveliev, A.A., & Smith, G.M. (2009). *Mixed effects models and Extensions in Ecology with R*. Springer.

Appendix

1. LOW FREQUENCY CUT-OFF IN SHALLOW WATER

Shallow water sound propagation has a low frequency cut-off dependent on depth (Jensen et al. 2011):

$$f_c = \frac{c_w}{4D\sqrt{1 - \left(\frac{c_w}{c_b}\right)^2}}$$

where c_w is the sound speed in the water column, c_b is the sound speed in the bottom layer and D is the water depth. This formula holds only when the water column and bottom layer are homogeneous. Lyttelton Harbour depths range from 0 m at the coastlines to 15 m in the outer harbour. The area of likely disturbance to dolphins has a range of depths from 14 m, near the wharf and channel, to 5 m, on the southern coast of the harbour opposite the wharf. Figure A.1 shows the cut-off frequency with depth for the various bottom layers in Lyttelton Harbour. The sedimentation of this harbour is not well known but a study by Curtis (1985) indicates a north/south division in the bottom layer with mud to the north and sandy mud (10-50% sand) to the south, with some muddy sand (sand 50-90%) near diamond harbour. It is unclear how mud is defined in that study but here we assume it is somewhere between silty sand and silty clay. Thus f_c could range from 55 Hz in 14 m of water with a fine sand bottom layer, to around 2 kHz in 5 m of water with a silty clay bottom (see Fig. A.1).

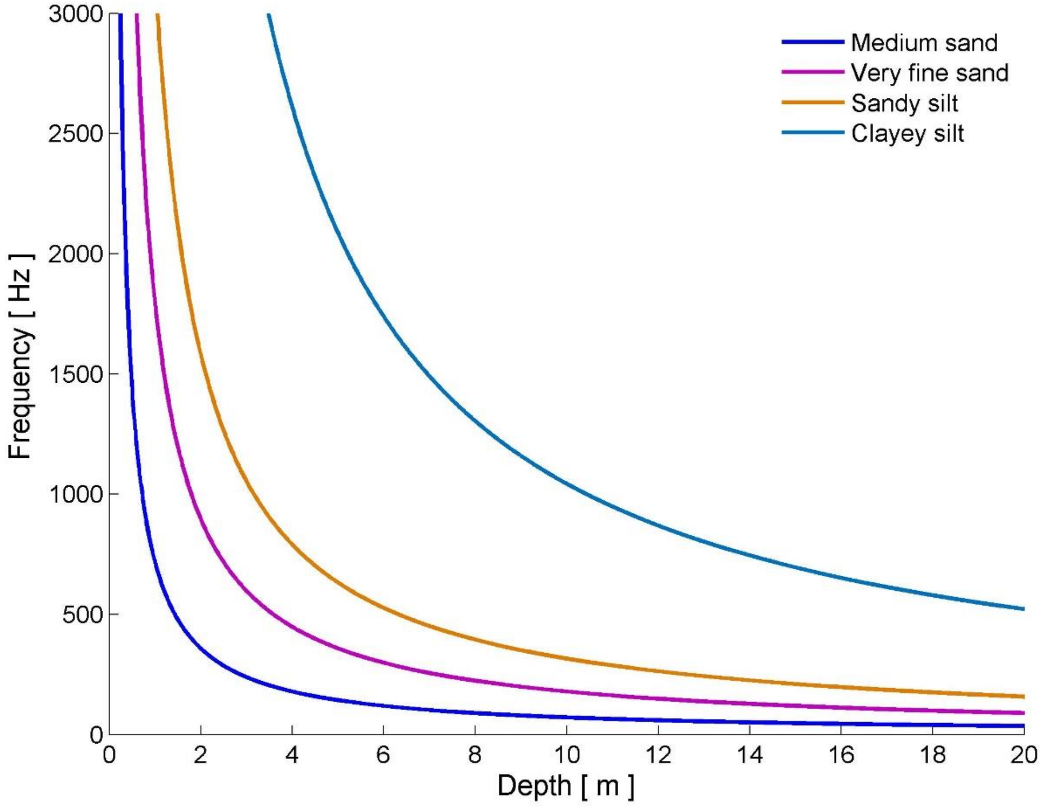

Figure A.1 Lower cut-off frequency in shallow water for 4 different types of bottom layers: Medium sand (c_b 1785 ms^{-1}), very fine sand (c_b 1550 ms^{-1}), sandy silt (c_b 1526 ms^{-1}) and clayey silt (c_b 1516 ms^{-1},) values from Shumway 1960, with c_w 1515 ms^{-1}, the average value for Lyttelton.

2. AMBIENT NOISE SOURCES

In this section I describe a small selection of anthropogenic noise sources that we consider part of the ambient noise in Lyttelton Harbour. The following vessels were regularly seen in Lyttelton harbour and therefore, their sounds were often present on our recordings of ambient and pile-driving noise. Hector's dolphins are exposed to their sounds, from these or similar types of vessels, on a daily basis.

- Diamond Harbour ferry, *Black Diamond*: This ferry crosses the harbour between Lyttelton and Diamond Harbours at least once an hour during the day. The ferry is 12 m long, built in 2001 with a total engine power of 2 x 165 kW (diesel) (P. Milligan pers. comm., November 2016). Recordings of this vessel were made using the SoundTrap which was moored about 320 m from the ferry's route just outside the channel. At the closest point of approach (CPA) the broadband SPL (with a maximum of 130 dB) is at least 20 dB higher than the preceding ambient noise level (Fig. A.2). This elevated noise level persists at the recording location for around 3 minutes. The power spectral density (Fig. A.3) of this pass shows the broadband nature of the noise and the change in frequency as it approaches and retreats the CPA. The sound contains most energy between 100 Hz and 10 kHz. We used the best fitting propagation model for Lyttelton Harbour as described in section 3.3 to provide an estimate of the boat's source level:

$$SL_{DHF} = 130 + 12.6*\log_{10}(320) + 0.0095*320$$

$$= 165 \text{ dB re } 1\ \mu\text{Pa (Broadband SPL)}$$

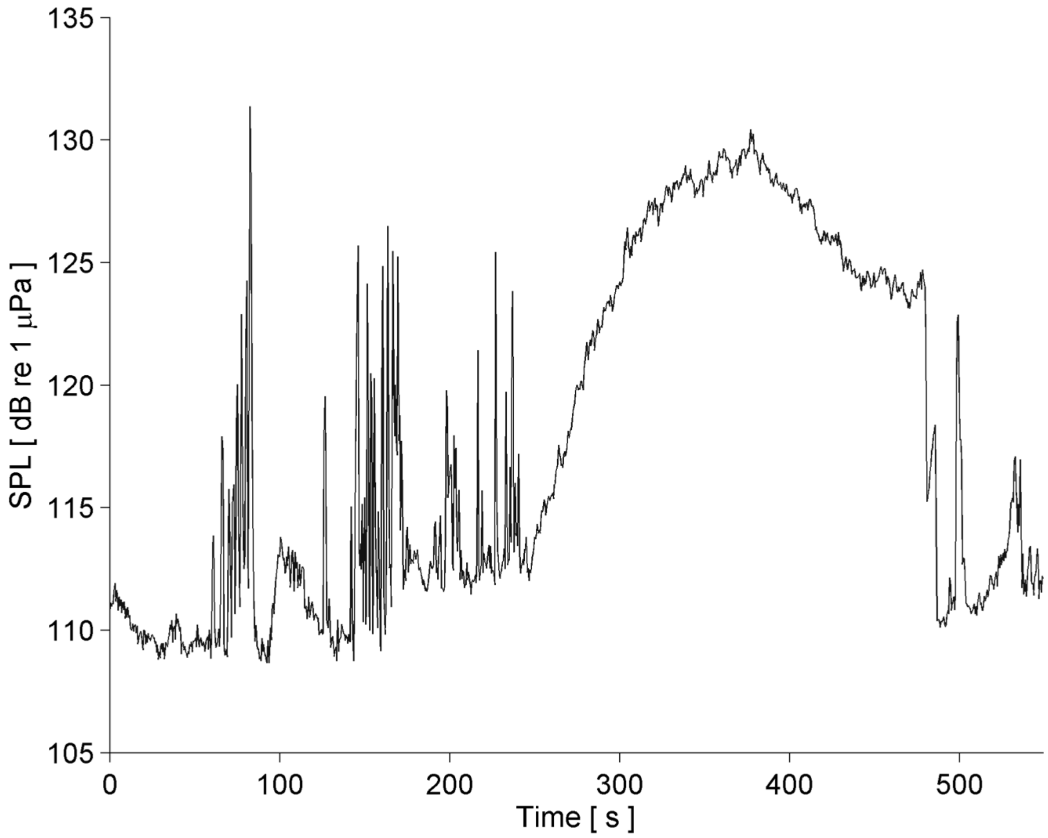

Figure A.2 Broadband SPL of DHF passing ST recorder, CPA ~320 m. Frequency range 30 Hz – 144 kHz.

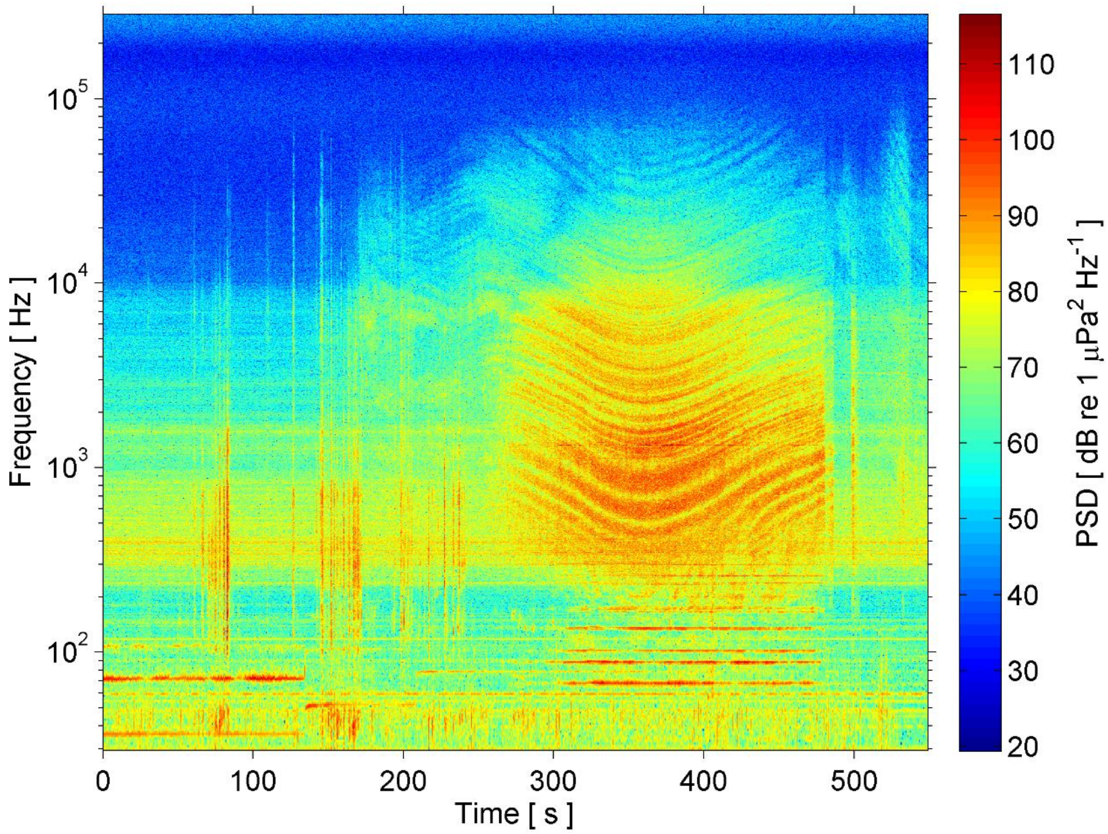

Figure A.3 Power spectral density of DHF passing ST recorder, CPA ~320 m. Frequency range 30 Hz – 144 kHz.

- The '*Fiordlander 1*': This boat was used as the ferry boat while the normal vessel was out of service. It is a 15.9 m long steel boat built in 1963, with a total engine power of 2 x 203kW (Milligan pers. comm 2016). Recordings were made from the research vessel using the boat-based platform. The change in broadband SPL as *Fiordlander 1* passes with a CPA of 113 m is shown in figure A.4 with corresponding PSD in figure A.5. An estimate of the boat's source level is:

$$SL_{Fiordlander1} = 135 + 12.6*\log_{10}(113) + 0.0095*113$$

$$= 162 \text{ dB re } 1\ \mu\text{Pa (Broadband SPL)}$$

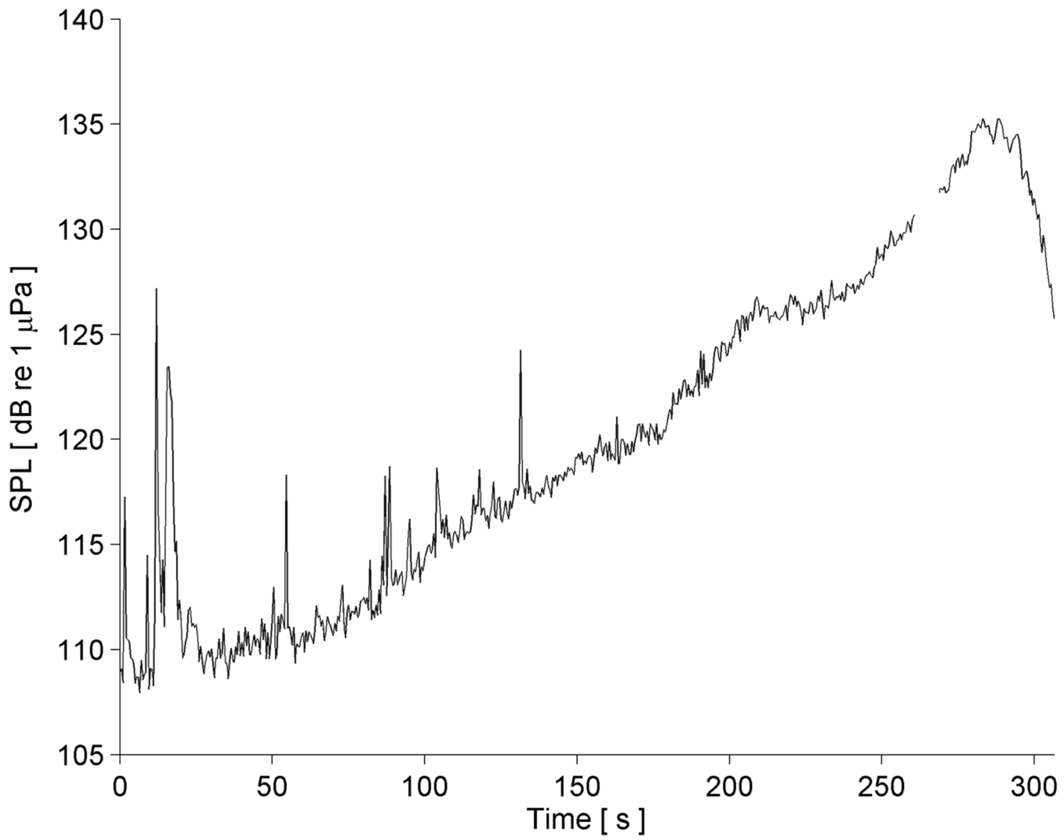

Figure A.4 Broadband SPL of 'Fiordlander' passing research vessel, CPA 113 m. Frequency range 30 Hz – 96 kHz. There is a gap of 7 s around time 265 s due to missing data.

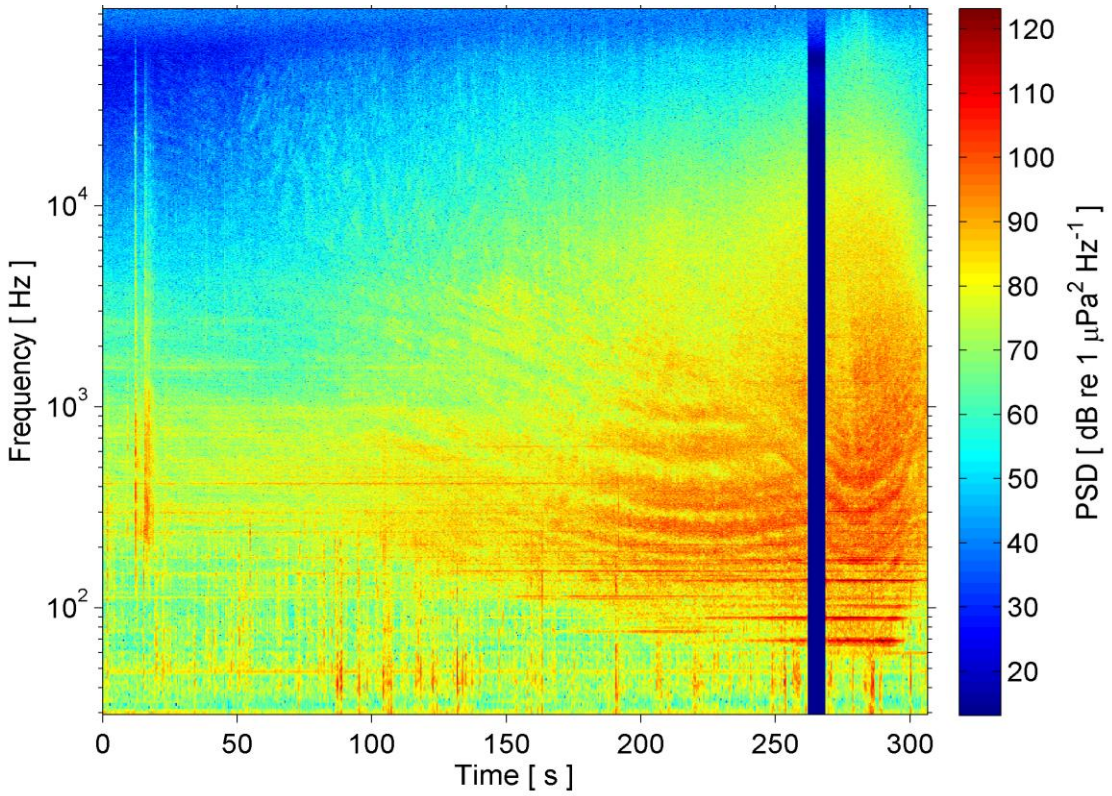

Figure A.5 Power spectral density of 'Fiordlander 1' passing research vessel, CPA 113 m. Frequency range 30 Hz - 96 kHz. Vertical blue stripe indicates missing data.

- The *Austro Carina*: This is a 26 m fishing vessel with a gross tonnage of 141 t, built in 1977 (Marine Traffic, 2015), powered by a 400 hp (~300 kW) diesel engine with a 3-bladed propeller with a cruising speed of 9 knots. The only informative recording of fishing vessels in Lyttelton Harbour is of this boat and is shown in figures A.6 and A.7. However, this also contained pile-driving noise. Fortunately, it is easy to distinguish the two noise sources and provides a way to visualise the differences between them. There is a clear difference in peak levels. While the pile-driving source was at a much larger range of ~390 m from the RV, compared to a CPA of 33 m for the boat, the piling is much louder. The frequency range that contains most energy is very similar for both sources, however the lower extreme for pile-driving is around 50 Hz whereas for the boat this is around 100 Hz (Fig. A.7).

An estimate of the boat's source level is:

$$SL_{\text{Austro Carina}} = 145 + 12.6*\log_{10}(33) + 0.0095*33$$

$$= 164 \text{ dB re } 1\ \mu\text{Pa (Broadband SPL)}$$

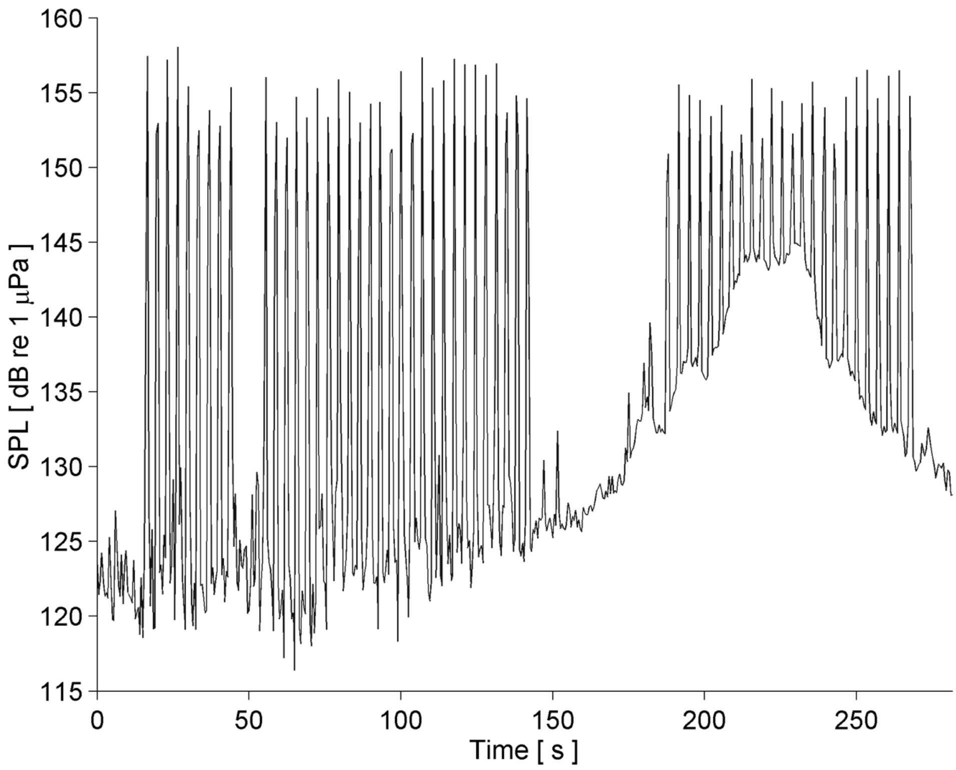

Figure A.6 Broadband SPL of Austro Carina passing research vessel, CPA 33 m, during piling. Frequency range 30 Hz - 96 kHz

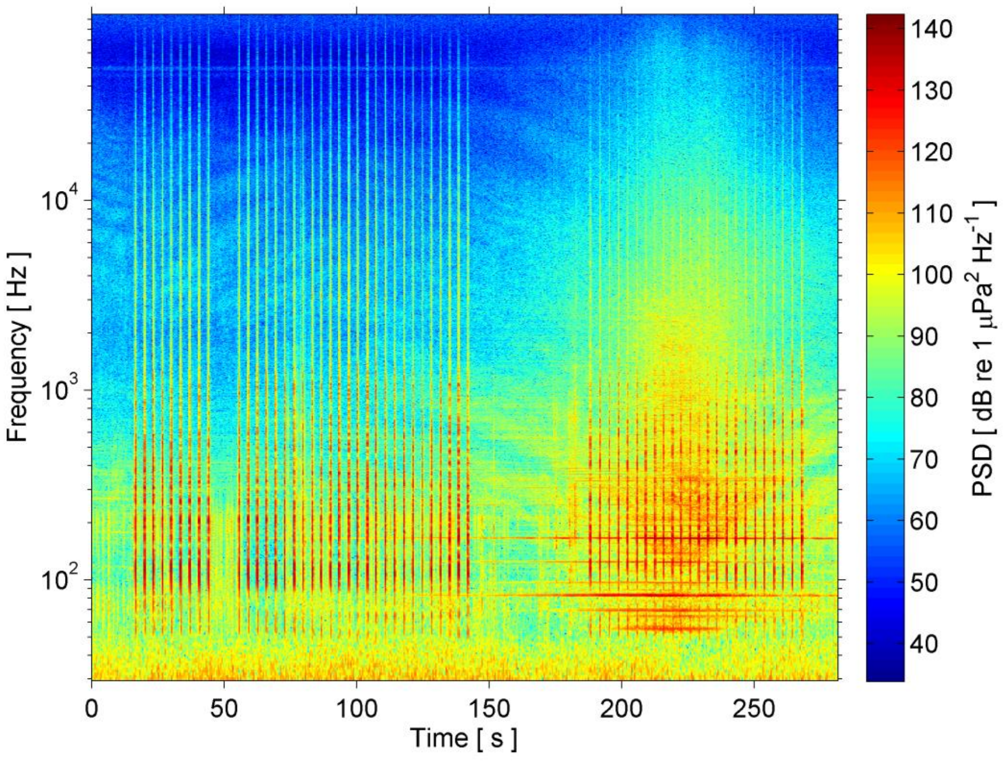

Figure A.7 PSD of Austro Carina passing research vessel, CPA 33 m, during piling. Frequency range 30 Hz - 96 kHz.

3. VIBRO-HAMMER NOISE

Before the start of a pile-driving sequence, the pile is positioned using a vibro-hammer, which vibrates the pile into the first ~20 m of sediment. This is also a very loud process and radiates high levels of broad band noise into the harbour environment (Figs. A.8 and A.9).

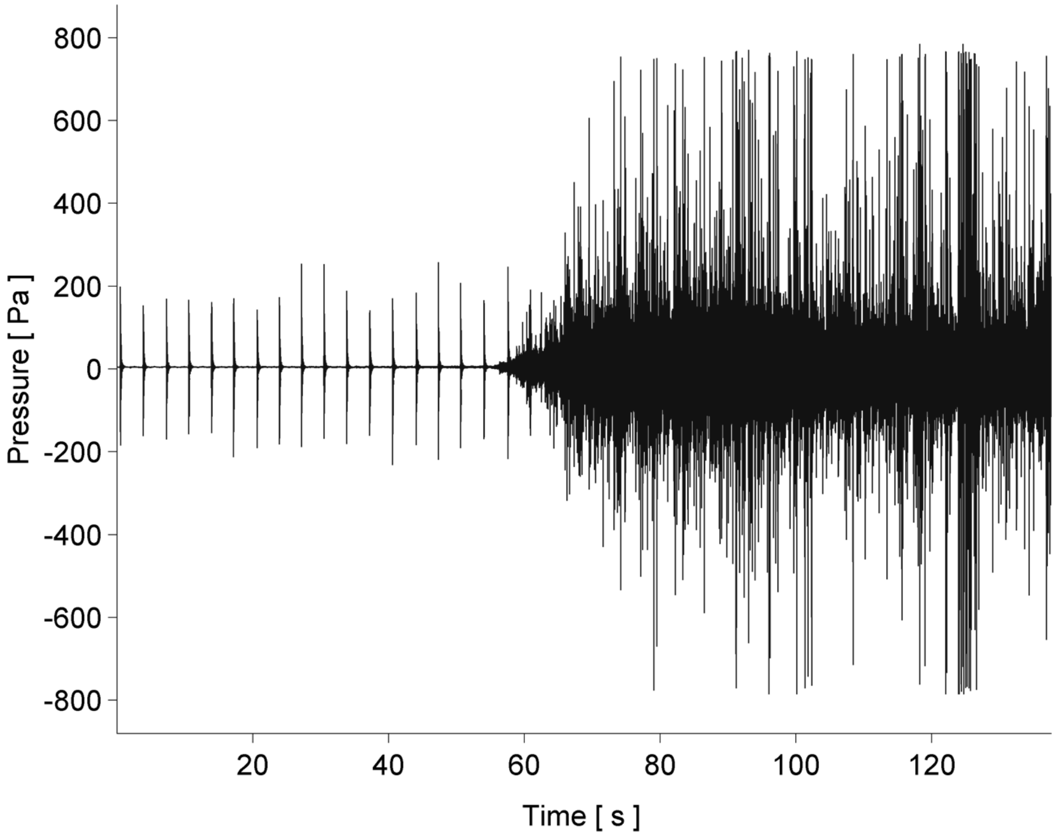

Figure A.8. Pressure wave form of pile-driving (entire record) and vibro noise (starting at ~55 s mark till end), recorded at a range of 370 m with a frequency range 30 Hz – 144 kHz. Note: recording of vibro noise was clipped so maximum levels shown may be underestimates.

Vibro noise was usually much louder than pile-driving noise at close range – the SPL_{pp} of the vibro noise in figure A.9 was 184 dB re 1 µPa, while pile-driving noise at this range was generally 10 dB lower than this. Both noise sources are broadband though the vibro noise tends to have less energy in the low frequency range, but with a similar peak frequency of about 300 Hz (see Fig. A.10). From the limited number of recordings we had of vibro noise it appeared the vibro events were only a few minutes in duration but could occur several times within an hour.

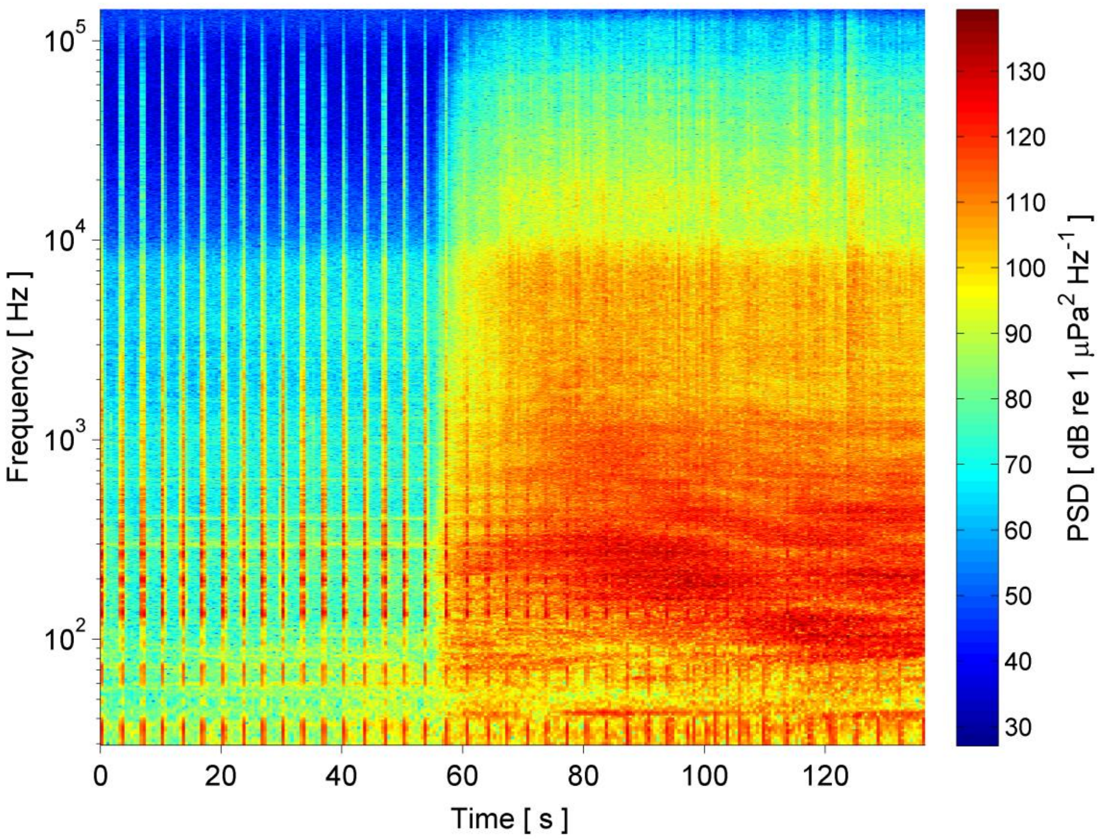

Figure A.9 Power spectral density of pile-driving (entire record) and vibro noise (starting at ~55 s mark till end), recorded at a range of 370 m with a frequency range 30 Hz – 144 kHz. Note: recording of vibro noise was clipped so maximum levels shown may be underestimates.

4. CTD PROFILES

A CTD measures Conductivity and Temperature with Depth in the water column. CTD drops were made at every recording location to investigate properties of the water column throughout the harbour and to enable the calculation of sound speed in the water. Measurements at four of these locations are presented here (Figs A.11 – A.14) showing the water column is mostly uniform in temperature and salinity up to a depth of about 7 m (see figs A.13 and A.14). Note that the temperature range on figure A.13 and the salinity range on figures A.13 and A.14 are broader than on the other graphs. The sound speed values at each depth are given along the right side of the graph (in blue). Note that these are not evenly spaced values on an axis but rather the calculated sound speeds based on the salinity and temperature at each depth. The sound speed was calculated in the data processing software SBE data processing (Seabird Electronics Inc.), using the calculation as described in Chen & Millero (1977).

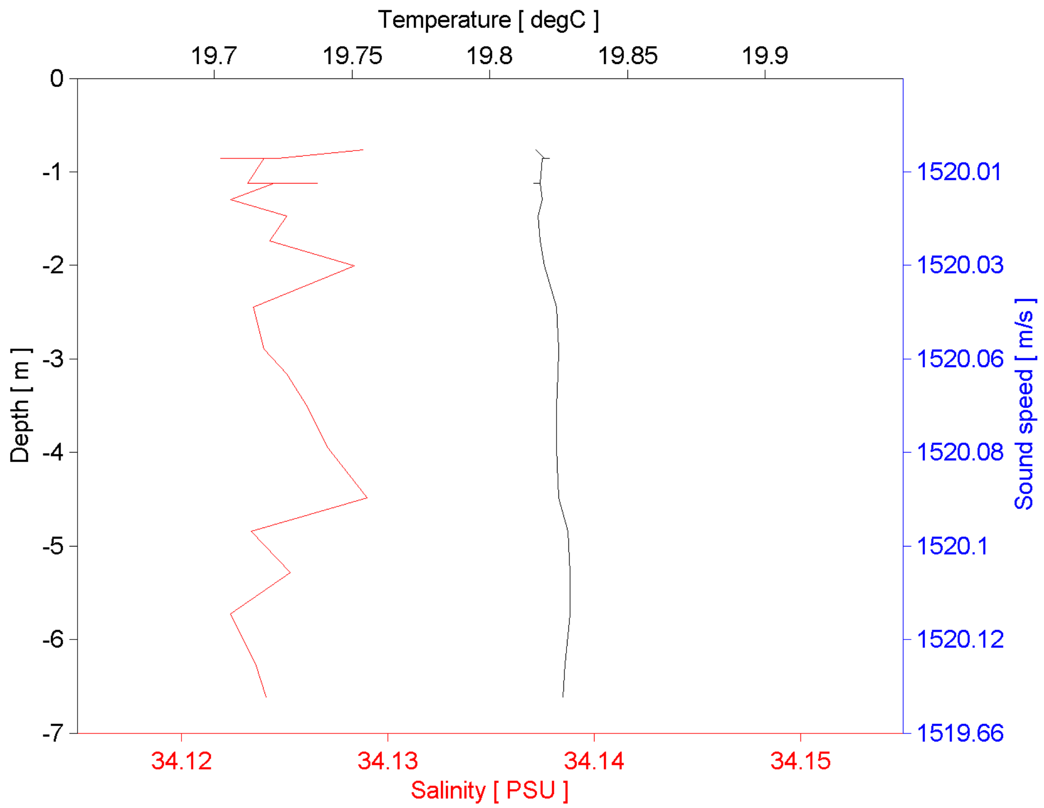

Figure A.10 CTD profile at channel DSG location, on 6/1/15

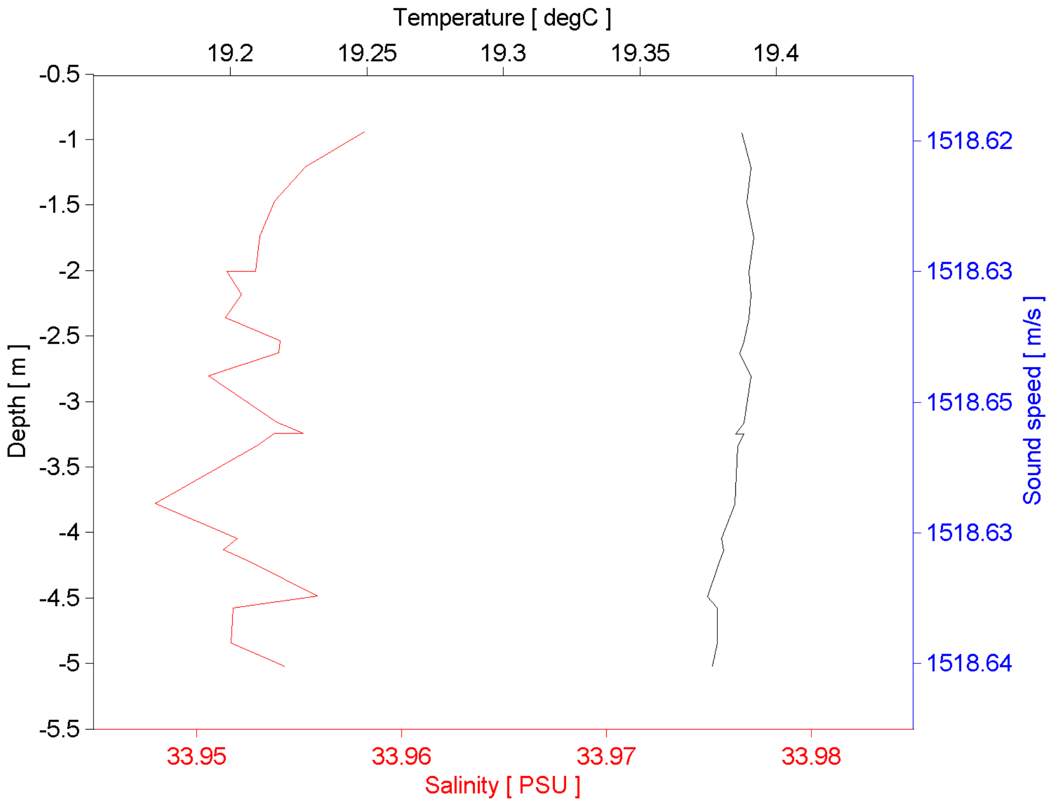

Figure A.11 CTD profile at Ripapa Bay, on 6/1/15

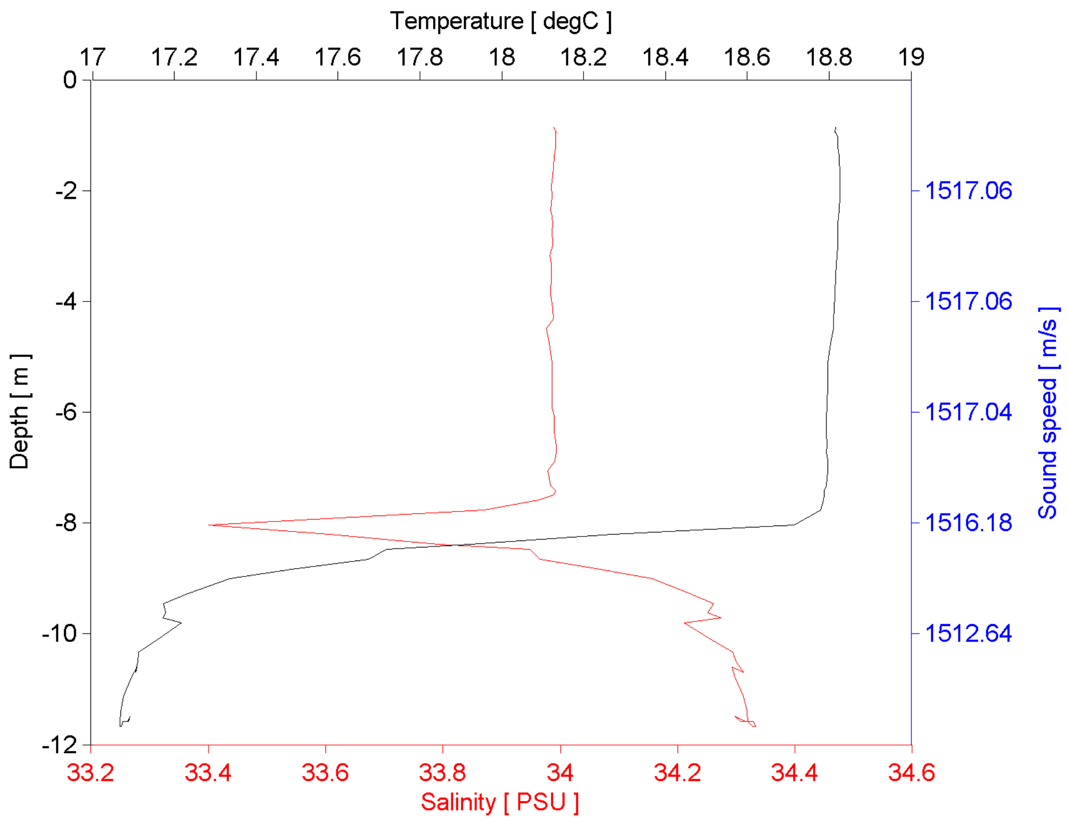

Figure A.12 CTD profile at harbour entrance, on 12/1/15

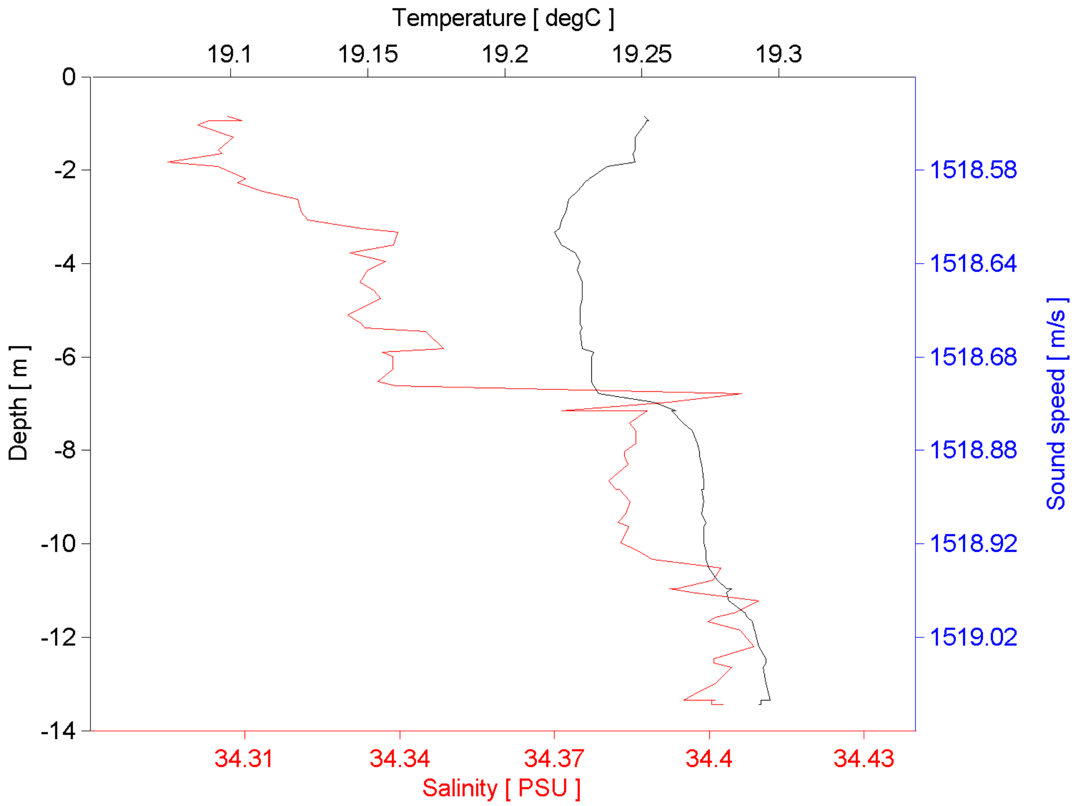

Figure A.13 CTD profile in front of wharf, on 27/1/15

5. MODEL CHECKING

Model checking was done using the R function *gam.check* from the *mgcv* package. The Q-Q plot (top left plot) and histogram of residuals (bottom left plot) are used to check that the residuals are normally distributed. The top right plot is used to asses homogeneity and the bottom right plot to asses model fit. Ideally the residuals are normally distributed and line up with the red line in the Q-Q plot, the residuals vs linear predictor should be randomly distributed (with no patterns) and the response vs fitted values should be evenly distributed around a straight diagonal line.

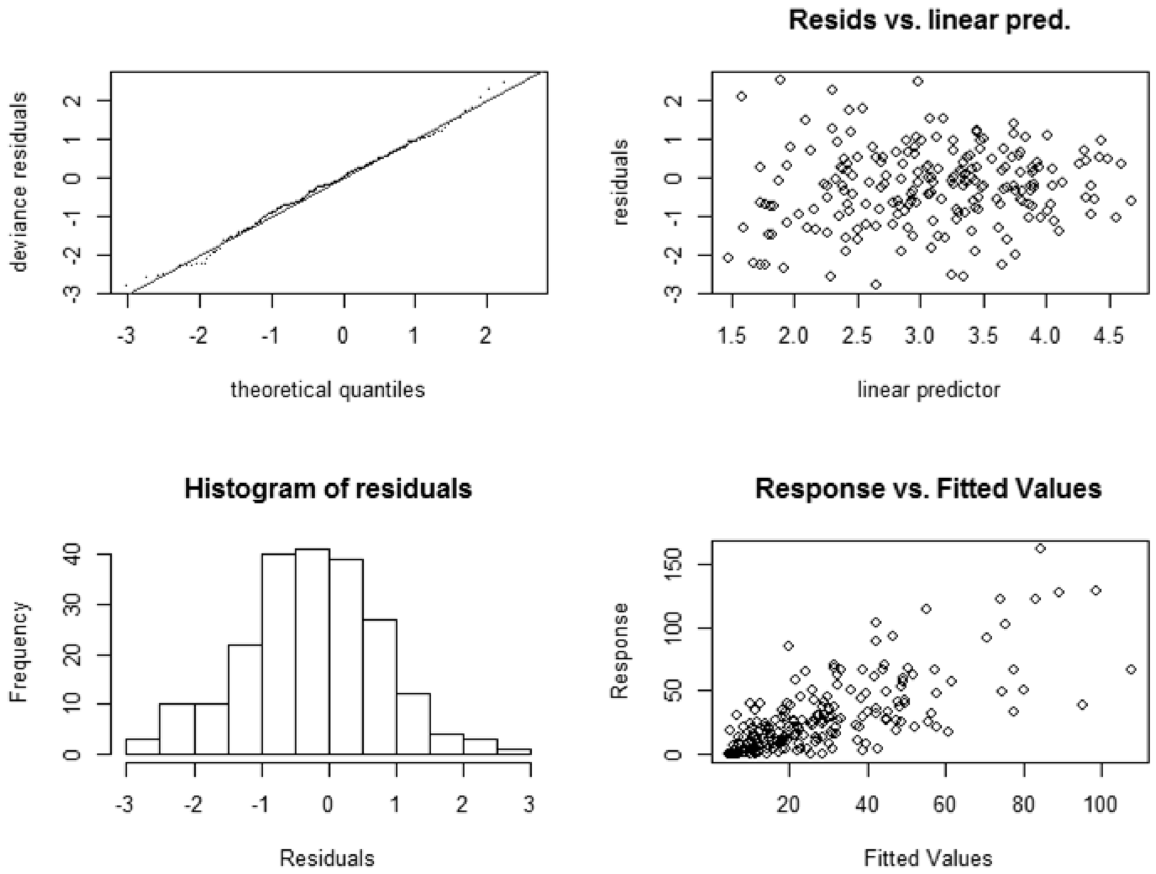

Figure A.14 Diagnostic plots for the best model of DPM per day

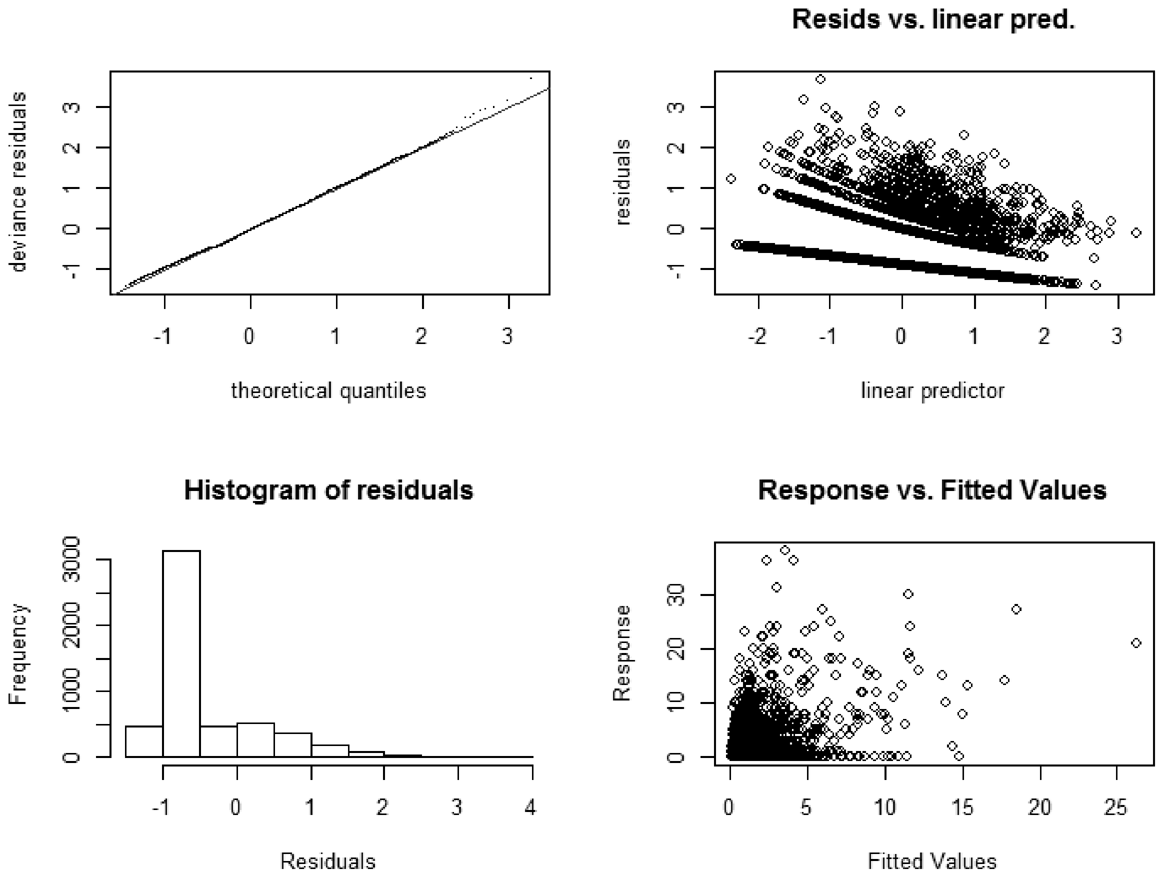

Figure A.15 Diagnostic plots for the best model of DPM per hour

6. MODEL COEFFICIENT TABLES

The smooth functions fitted to each variable using GAMs are complex functions that cannot be expressed in terms of a single number like in linear models. During the fitting process a basis dimension was chosen (by the algorithm) to adequately represent the effect of each explanatory variable on the response. The more "wiggly" the effect, the more dimensions are required. The coefficients for each dimensions fitted for all parameters are given for the models of DPM per day (Table A.1) and DPM per hour (Table A.2).

Table A.1 Conditional average of parameter estimates after model averaging the model set for DPM per day in table 4.5. Terms with p-values ≤ 0.05 are in bold. 'Estimate' gives the coefficient for each basis dimension fitted (the number following the '.' after each term).

Term	Estimate	SE (adj.)	P-value
Intercept	**2.702**	**0.146**	**< 2e-16**
TPOD2	**0.593**	**0.170**	**4.50e-04**

TPOD3	**1.107**	**0.225**	**9.00e-07**
ti(DPMt1):TPOD1.1	**0.548**	**0.184**	**0.003**
ti(DPMt1):TPOD1.2	0.270	0.232	0.245
ti(DPMt1):TPOD1.3	0.295	0.392	0.452
ti(DPMt1):TPOD1.4	3.941	5.614	0.483
ti(DPMt1):TPOD2.1	**0.081**	**0.030**	**0.007**
ti(DPMt1):TPOD2.2	**0.182**	**0.068**	**0.007**
ti(DPMt1):TPOD2.3	**0.505**	**0.189**	**0.007**
ti(DPMt1):TPOD2.4	**1.684**	**0.629**	**0.007**
ti(DPMt1):TPOD3.1	0.032	0.022	0.145
ti(DPMt1):TPOD3.2	0.071	0.049	0.144
ti(DPMt1):TPOD3.3	0.198	0.136	0.144
ti(DPMt1):TPOD3.4	0.660	0.452	0.144
ti(Wspd):TPOD1.1	**-0.012**	**0.005**	**0.011**
ti(Wspd):TPOD1.2	**-0.088**	**0.033**	**0.009**
ti(Wspd):TPOD1.3	**-0.384**	**0.146**	**0.009**
ti(Wspd):TPOD1.4	**-0.736**	**0.280**	**0.009**
ti(Wspd):TPOD2.1	**-0.011**	**0.004**	**0.014**
ti(Wspd):TPOD2.2	**-0.080**	**0.032**	**0.012**
ti(Wspd):TPOD2.3	**-0.348**	**0.139**	**0.012**
ti(Wspd):TPOD2.4	**-0.668**	**0.267**	**0.012**
ti(Wspd):TPOD3.1	0.005	0.006	0.395
ti(Wspd):TPOD3.2	0.039	0.044	0.384
ti(Wspd):TPOD3.3	0.168	0.193	0.384
ti(Wspd):TPOD3.4	0.323	0.371	0.384
ti(Wdir):TPOD1.1	**-0.288**	**0.125**	**0.021**
ti(Wdir):TPOD1.2	0.019	0.145	0.893
ti(Wdir):TPOD1.3	0.151	0.145	0.298
ti(Wdir):TPOD2.1	-1.02e-05	0.002	0.996
ti(Wdir):TPOD2.2	-4.54e-05	0.002	0.984
ti(Wdir):TPOD2.3	-3.65e-05	0.003	0.990
ti(Wdir):TPOD3.1	0.060	0.143	0.674
ti(Wdir):TPOD3.2	-0.289	0.177	0.103
ti(Wdir):TPOD3.3	-0.288	0.177	0.104
ti(PPM):TPOD1.1	-0.029	0.016	0.065
ti(PPM):TPOD1.2	-0.112	0.060	0.064
ti(PPM):TPOD1.3	-0.223	0.121	0.064
ti(PPM):TPOD1.4	-0.521	0.282	0.064
ti(PPM):TPOD2.1	0.024	0.015	0.107
ti(PPM):TPOD2.2	0.091	0.056	0.106
ti(PPM):TPOD2.3	0.182	0.113	0.106
ti(PPM):TPOD2.4	0.426	0.264	0.106
ti(PPM):TPOD3.1	-0.028	0.041	0.489
ti(PPM):TPOD3.2	-0.108	0.156	0.488
ti(PPM):TPOD3.3	-0.216	0.312	0.489
ti(PPM):TPOD3.4	-0.505	0.730	0.489

Table A.2 Conditional average of parameter estimates after model averaging the model set for DPM per hour in table 4.7. Terms with p-values ≤ 0.05 are in bold. 'Estimate' gives the coefficient for each basis dimension fitted (the number following the '.' after each term).

Term	Estimate	Adjusted SE	Pr(>|z|)
(Intercept)	**-8.31e-01**	**6.56e-02**	**< 2e-16**
TPOD2	**9.72e-01**	**8.26e-02**	**< 2e-16**
TPOD3	**1.26**	**1.19e-01**	**< 2e-16**
ti(DPMt1):TPOD1.1	**2.15**	**2.23e-01**	**< 2e-16**
ti(DPMt1):TPOD1.2	**2.00**	**5.18e-01**	**0.00011**
ti(DPMt1):TPOD1.3	**2.42**	**8.13e-01**	**0.00289**
ti(DPMt1):TPOD1.4	2.78	4.06	0.4937
ti(DPMt1):TPOD2.1	**8.46e-01**	**1.42e-01**	**< 2e-16**
ti(DPMt1):TPOD2.2	**6.93e-01**	**3.10e-01**	**0.02534**
ti(DPMt1):TPOD2.3	4.07e-01	7.01e-01	0.56183
ti(DPMt1):TPOD2.4	-6.21e-01	4.04	0.87795
ti(DPMt1):TPOD3.1	**8.26e-01**	**1.96e-01**	**2.40e-05**
ti(DPMt1):TPOD3.2	**1.13**	**3.40e-01**	**0.000915**
ti(DPMt1):TPOD3.3	**1.23**	**5.23e-01**	**0.018758**
ti(DPMt1):TPOD3.4	1.56	1.32	0.237336
ti(TSP):TPOD1.1	2.22e-02	1.28e-01	0.86226
ti(TSP):TPOD1.2	**-3.68e-01**	**1.17e-01**	**0.001685**
ti(TSP):TPOD1.3	**3.76e-01**	**1.27e-01**	**0.003066**
ti(TSP):TPOD1.4	-7.44e-01	7.84e-01	0.34232
ti(TSP):TPOD2.1	1.51e-02	1.16e-02	0.190605
ti(TSP):TPOD2.2	-5.75e-03	4.78e-03	0.228216
ti(TSP):TPOD2.3	-1.07e-01	8.12e-02	0.188624
ti(TSP):TPOD2.4	-3.66e-01	2.79e-01	0.189816
ti(TSP):TPOD3.1	-1.80e-02	4.40e-02	0.683021
ti(TSP):TPOD3.2	-4.98e-02	7.90e-02	0.528072
ti(TSP):TPOD3.3	-5.67e-02	1.52e-01	0.708176
ti(TSP):TPOD3.4	9.26e-01	5.77e-01	0.108546
ti(Hour):TPOD1.1	**5.34e-01**	**1.42e-01**	**0.000163**
ti(Hour):TPOD1.2	**-3.68e-01**	**1.46e-01**	**0.011787**
ti(Hour):TPOD1.3	**3.24e-01**	**1.48e-01**	**0.028941**
ti(Hour):TPOD2.1	**-2.42e-01**	**9.33e-02**	**0.009351**
ti(Hour):TPOD2.2	8.59e-02	9.62e-02	0.372128
ti(Hour):TPOD2.3	**2.44e-01**	**9.23e-02**	**0.008246**
ti(Hour):TPOD3.1	8.95e-05	4.23e-03	0.983134
ti(Hour):TPOD3.2	-5.26e-05	5.15e-03	0.991838
ti(Hour):TPOD3.3	-6.53e-05	4.23e-03	0.987674
ti(SEL):TPOD1.1	-4.51e-01	3.50e-01	0.197639
ti(SEL):TPOD1.2	-6.19e-02	7.95e-02	0.436172
ti(SEL):TPOD1.3	-4.58e-01	2.42e-01	0.058317
ti(SEL):TPOD1.4	2.49e-01	2.05e-01	0.223434
ti(SEL):TPOD2.1	-1.43e-01	8.32e-02	0.086541
ti(SEL):TPOD2.2	5.81e-02	3.37e-02	0.085304
ti(SEL):TPOD2.3	-1.81e-01	1.05e-01	0.085567

ti(SEL):TPOD2.4	-2.21e-01	1.28e-01	0.085227
ti(SEL):TPOD3.1	-4.86e-02	3.81e-01	0.898504
ti(SEL):TPOD3.2	1.35e-01	7.32e-02	0.065702
ti(SEL):TPOD3.3	-1.56e-01	3.24e-01	0.630043
ti(SEL):TPOD3.4	**-5.10e-01**	**2.45e-01**	**0.037372**
ti(tide):TPOD1.1	8.77e-02	9.25e-02	0.342909
ti(tide):TPOD1.2	-1.34e-01	1.05e-01	0.199976
ti(tide):TPOD1.3	**-2.02e-01**	**9.45e-02**	**0.032444**
ti(tide):TPOD2.1	-2.90e-02	5.64e-02	0.607688
ti(tide):TPOD2.2	6.11e-02	6.71e-02	0.362409
ti(tide):TPOD2.3	6.15e-02	5.73e-02	0.282533
ti(tide):TPOD3.1	-1.49e-01	1.39e-01	0.28311
ti(tide):TPOD3.2	**-4.45e-01**	**1.56e-01**	**0.004368**
ti(tide):TPOD3.3	2.66e-03	1.40e-01	0.984821
ti(TSP,Dur).1	**-1.38e-02**	**6.36e-03**	**0.03006**
ti(TSP,Dur).2	**-1.94e-02**	**8.78e-03**	**0.027523**
ti(TSP,Dur).3	**-1.63e-01**	**7.04e-02**	**0.020607**
ti(TSP,Dur).4	**-4.17e-01**	**1.80e-01**	**0.020435**
ti(TSP,Dur).5	**-1.91e-02**	**8.07e-03**	**0.018172**
ti(TSP,Dur).6	**-2.67e-02**	**1.12e-02**	**0.01696**
ti(TSP,Dur).7	**-2.25e-01**	**9.20e-02**	**0.014325**
ti(TSP,Dur).8	**-5.77e-01**	**2.36e-01**	**0.014453**
ti(TSP,Dur).9	-2.16e-03	9.71e-03	0.823935
ti(TSP,Dur).10	-3.02e-03	1.35e-02	0.823082
ti(TSP,Dur).11	-2.56e-02	1.12e-01	0.819547
ti(TSP,Dur).12	-6.56e-02	2.88e-01	0.819717
ti(TSP,Dur).13	-8.67e-03	5.82e-02	0.881583
ti(TSP,Dur).14	-1.22e-02	8.15e-02	0.88155
ti(TSP,Dur).15	-1.03e-01	6.88e-01	0.881476
ti(TSP,Dur).16	-2.63e-01	1.77	0.881484
s(Wdir).1	2.01e-02	4.00e-02	0.616112
s(Wdir).2	-1.10e-02	6.49e-02	0.865062
s(Wdir).3	-6.04e-02	8.01e-02	0.451137
s(Wdir).4	-1.28e-01	7.97e-02	0.10821
s(Wdir).5	**-1.67e-01**	**6.92e-02**	**0.015923**
s(Wdir).6	-9.43e-02	5.97e-02	0.11395
s(Wdir).7	7.37e-04	6.66e-02	0.991161
s(Wdir).8	4.36e-02	6.19e-02	0.481332
s(Dur).1	2.16e-01	1.20e-01	0.071067
s(Dur).2	-1.05e-01	3.49e-01	0.763441
s(Dur).3	-2.65e-02	6.15e-02	0.66691
s(Dur).4	-1.19e-02	2.14e-01	0.95568
s(Dur).5	-3.04e-03	5.19e-02	0.953291
s(Dur).6	-2.71e-02	1.81e-01	0.880946
s(Dur).7	1.59e-03	3.60e-02	0.964813
s(Dur).8	-3.83e-02	6.42e-01	0.95243
s(Dur).9	-2.30e-01	2.00e-01	0.249538
s(Wspd).1	1.59e-04	4.20e-03	0.969801

s(Wspd).2	6.90e-05	6.29e-03	0.991245
s(Wspd).3	-1.31e-05	2.22e-03	0.995281
s(Wspd).4	-2.03e-05	3.72e-03	0.995644
s(Wspd).5	-1.60e-05	2.20e-03	0.994182
s(Wspd).6	2.33e-05	3.50e-03	0.994686
s(Wspd).7	-1.68e-05	2.19e-03	0.993879
s(Wspd).8	1.27e-06	1.56e-02	0.999935
s(Wspd).9	-7.30e-02	3.85e-02	0.057974

7. ESTIMATED ZONES OF IMPACT

Recordings throughout the harbour were used to estimate ranges of TTS onset. These estimates were based on previous studies of TTS in harbour porpoise. There are a number of studies that have measured TTS in harbour porpoise in response to various sound stimuli (e.g., Kastelein et al., 2012; 2013c; 2014) but only a few specifically looked at impulsive sounds (Lucke 2009; Kastelein et al., 2015).

As described in section 1.3, sound can influence dolphins in a range of ways, from hearing the noise, to behavioural change, to injury. The criteria for onset of injury is a temporary threshold shift (TTS) in hearing. Prediction of TTS onset in harbour porpoise has been shown to depend on a combination of duration and peak sound pressure levels of the noise, though not in line with an equal energy model (Mooney et al., 2009). Hence different ranges of impact are suggested based on different types of noise exposure.

Single impulse

A 6 dB TTS was induced in a trained harbour porpoise after exposure to a single airgun pulse with an SEL of 164 dB re 1 µPa^{2}s (Lucke et al., 2009). I used the propagation model fitted to the pile-driving noise measurements (Fig. A.16) to provide an overall representation of the pile-driving noise level with range in Lyttelton Harbour (see section 3.4 for more detail). This model (using a source level of 182 dB re 1 µPa^{2}s) implies an SEL of 164 dB would occur in Lyttelton at a range of about 26 m from the pile-driving. However, this range is well within the near field of the pile-driving noise (see section 3.3.1) so it is likely an overestimate.

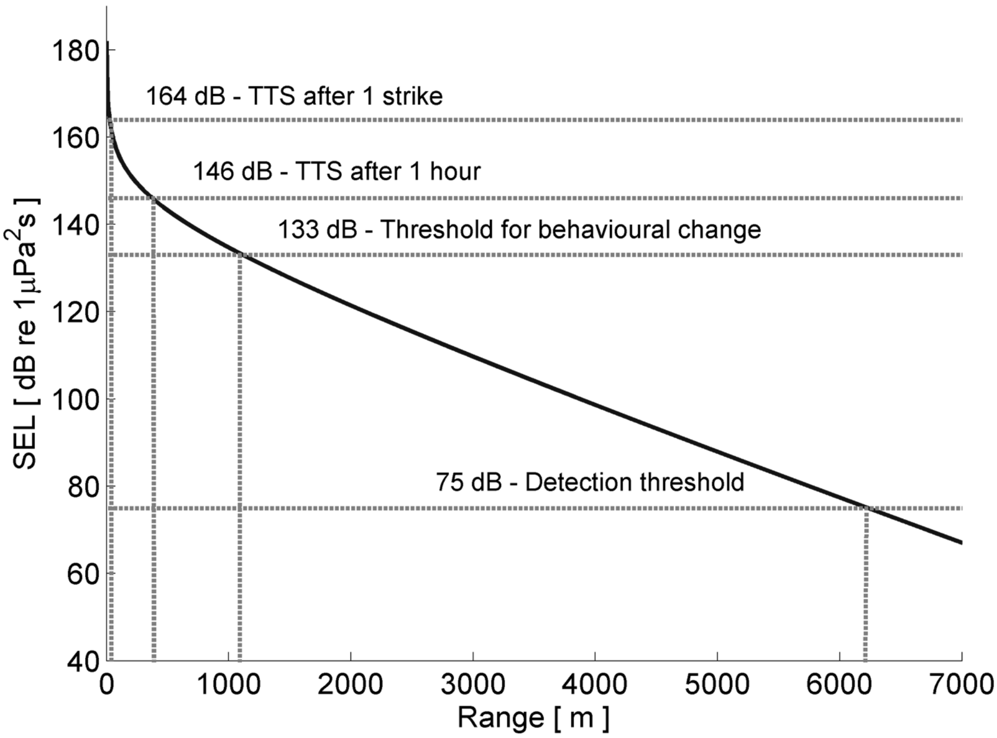

Figure A.16 Propagation model representing overall loss of piling noise with range as measured in Lyttelton Harbour, with horizontal lines at SELs known to cause TTS in harbour porpoise after a single exposure (26 m), 1 hour of exposure (376 m), threshold of behavioural change (1120 m) and pile-driving noise detection threshold (6280 m).

Cumulative exposure of one hour

A 2.3 dB TTS was induced in a trained harbour porpoise after exposure to one hour of played-back pile-driving noise (2760 strikes with an inter-pulse-interval of 1.3s) (Kastelein et al., 2015). The strikes had an SEL of 146 dB re 1 µPa^{2}s. Using the propagation model this level would occur at a range of about 376 m from the pile-driving (see Fig. A.16). Using the map of loss contours (Fig. 3.17) this would occur at the loss contour of 36 dB and cover an area of approximately 0.38 km^2 (see red area in Fig. A.17). It must be noted that the original recording of the pile-driving used in the playback was made with a sampling frequency of 62 kHz therefore contained no frequencies above 31 kHz. Harbour porpoise hearing, however, reaches maximum sensitivity around 130 kHz – frequencies that are certainly present in pile-driving strikes recorded at close range. This could lead to an underestimation of impact for actual (as opposed to recorded then played back) pile-driving noise.

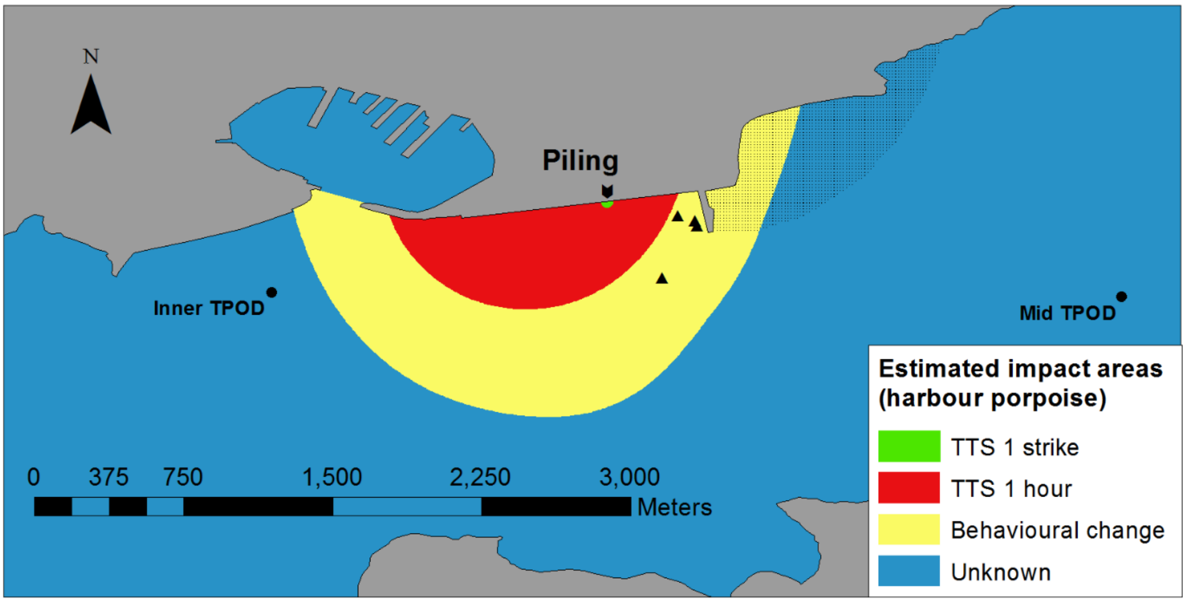

Figure A.17 Approximate zones (based on harbour porpoise studies) in which TTS could occur: Dolphins in green area could experience TTS after exposure to 1 strike and in red area after 1 hour. Behavioural change may be expected in the yellow area. Black triangles are locations where dolphins were visually observed from the RV during pile-driving. 'Dotted' region indicates where impact area boundary is likely inaccurate due to shadowing effect of breakwater on the spreading of noise.

While an inter-strike-interval around 1.3 s was observed in the present study, larger intervals up to 4.5 s were also observed, particularly for the higher hammer lift-height settings (producing generally louder pile-driving noise). Cumulative sound exposure level depends only on the individual strike's SEL and the number of exposures, hence a larger inter-strike-interval would require a longer period of exposure before inducing the same TTS.

Masking

A likely negative impact on Hector's dolphins will be the masking of environmental sound cues. It is not known at what maximum range Hector's dolphins may attempt to communicate, however these distances are not expected to be beyond a few hundred metres due to the high absorption and, therefore, rapid attenuation of high frequency sound in seawater. The pile-driving noise can be heard on recordings made over a large area within the harbour; it is reasonable to assume a high probability of these sounds being heard by Hector's dolphins almost anywhere within Lyttelton Harbour. However, the amount of masking for an intermittent sound like pile-driving will be less than that for a continuous sound. Since pile-driving noise has most of its energy in the low to mid frequency range, the potential for masking of the high frequency clicks produced by Hector's dolphins is reduced. The potential for masking depends on the dolphin's range from the pile-driving (Fig. A.18). For a dolphin (at the origin of the graph in Fig. A.18) at a distance of 1200 m or more from the pile-driving (blue line in Fig. A.18), its clicks will be masked by the ambient noise before the pile-driving noise. At a distance of 800 m from the pile-driving, the click will be masked at a range of 735 m from the dolphin – the point where the pile-driving noise generated at 800 m (purple line) exceeds the level of the echolocation click (black line). For pile-driving at 500 m (red line) from the echo-locating dolphin, the click would only be masked if the receiving animal was

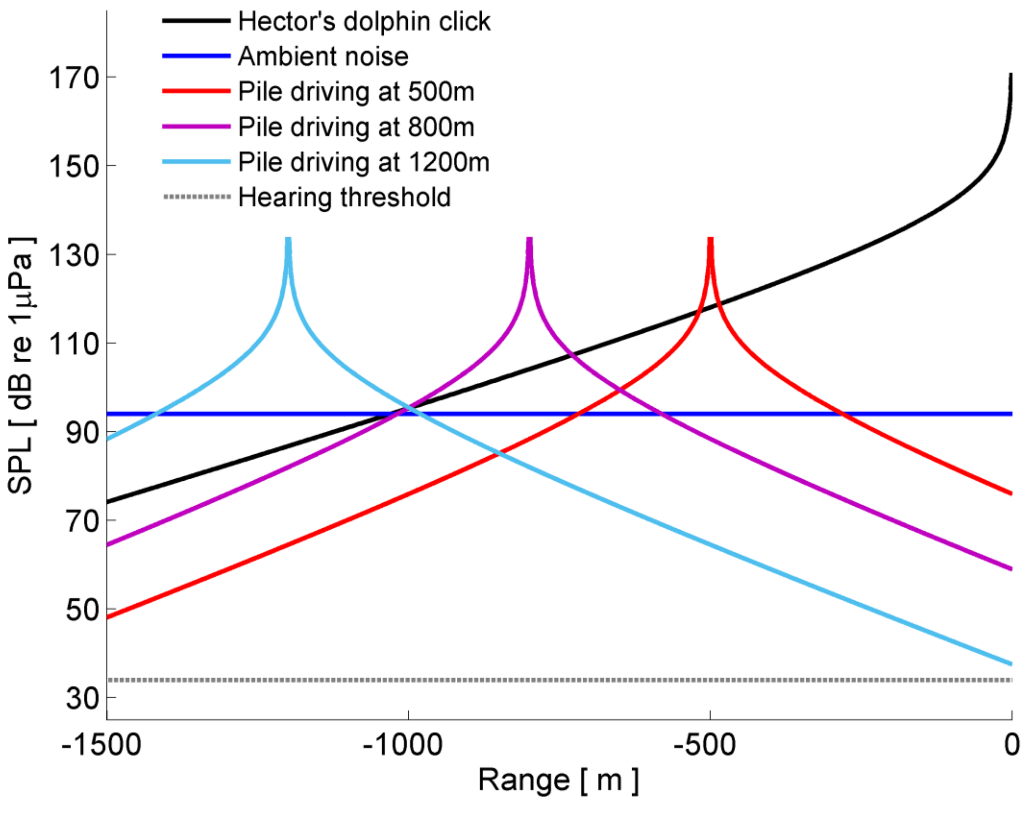

Figure A.18 Pile-driving noise (1/6 octave-band level at centre frequency 125 kHz) with range, at varying distances (see legend) from a dolphin at the origin. Blue line gives estimate of ambient noise 1/6 octave-band at centre frequency 125 kHz.

within about 15 m of the pile-driving (in which case it would have bigger problems). Note that the pile-driving noise in the figure represents the level in the 1/6 octave-bands with centre frequency 125 kHz. This 1/6 octave bandwidth has been used to approximate the masking bandwidth (range of frequencies which can mask a pure tone signal) for bottlenose dolphins (Johnson 1968; David 2006). The source level for this band (134 dB re 1 µPa @ 1 m) was estimated from the power spectral density of a recording made at 100 m from the pile-driving. This is far enough away to be in the far field, but presents a very conservative estimate of source level.

The source SPL_{0p} for the dolphin click was based on the peak-to-peak source level from Kyhn et al., (2009) by subtracting 6 dB (representing the halving in pressure from peak-to-peak to zero-to-peak) to give 171 dB re 1 µPa @ 1 m. It must be noted that the levels in Fig. A.17 are estimates. The decreasing sound level with range was calculated using the propagation model fitted in section 3.4 with the absorption coefficient increased to 0.0481 dB/m – the calculated coefficient for a sound with a frequency of 125 kHz (Ainslie and McColm 1998) in average Lyttelton conditions (Temperature = 17 ^{0}C, depth = 7 m, Salinity = 34 PSU)). However, the fitted absorption coefficient for broadband piling noise was higher than expected (as this may represent the additional absorption due to the bottom layer properties of Lyttelton), therefore the calculated coefficient of 0.0481 dBm^{-1} may still be too low, leading to an overestimation of range in which it can be heard above ambient noise.

Pile-driving noise has much more masking potential for environmental cues (e.g., from prey and predators) as these are at a much lower frequency than echolocation clicks and pile-driving has much more energy in these frequency ranges. It does appear, however, that masking of echolocation signals is not likely to be a serious problem.

Behavioural change

A trained harbour porpoise exposed to a playback of pile-driving noise in a pool began to change its behaviour once the single strike SEL reached 133 dB re 1 $\mu Pa^2 s$ (Kastelein et al., 2013b). This threshold was estimated to be similar to what was observed in studies of wild harbour porpoise (Tougaard et al., 2009; Brandt et al., 2011; Bailey et al., 2010; Dahne et al., 2013). For the pile-driving in Lyttelton Harbour, this threshold would occur at a range of about 1120 m and at the loss contour of 49 dB (see Figs. A.16 and A.17)

Hearing Threshold

The unmasked hearing threshold of pile-driving noise in a trained harbour porpoise was measured in a quiet pool (Kastelein et al., 2013a). The maximum threshold level for detection was at an SEL of 75 dB re 1 µPa^{2}s. This would occur at the loss contour of 107 dB, therefore well beyond the loss of 83 dB required for the pile-driving noise to be at the level of the average ambient noise (see section 3.4). For the quietest ambient noise conditions in Lyttelton the pile-driving noise would then be detected in an area up to 35 km^2 (see Fig. A.19). Using the propagation model, an SEL of 75 dB (excluding ambient noise) would occur at a range of about 6280 m (see Fig. A.16). However, for most of the time the ambient noise level is much higher, with an average broadband SPL of 118 dB re 1 µPa (see section 2.4). Hence, the range estimate will be an overestimate, as the masking of the ambient noise will increase the detection threshold for the pile-driving noise.

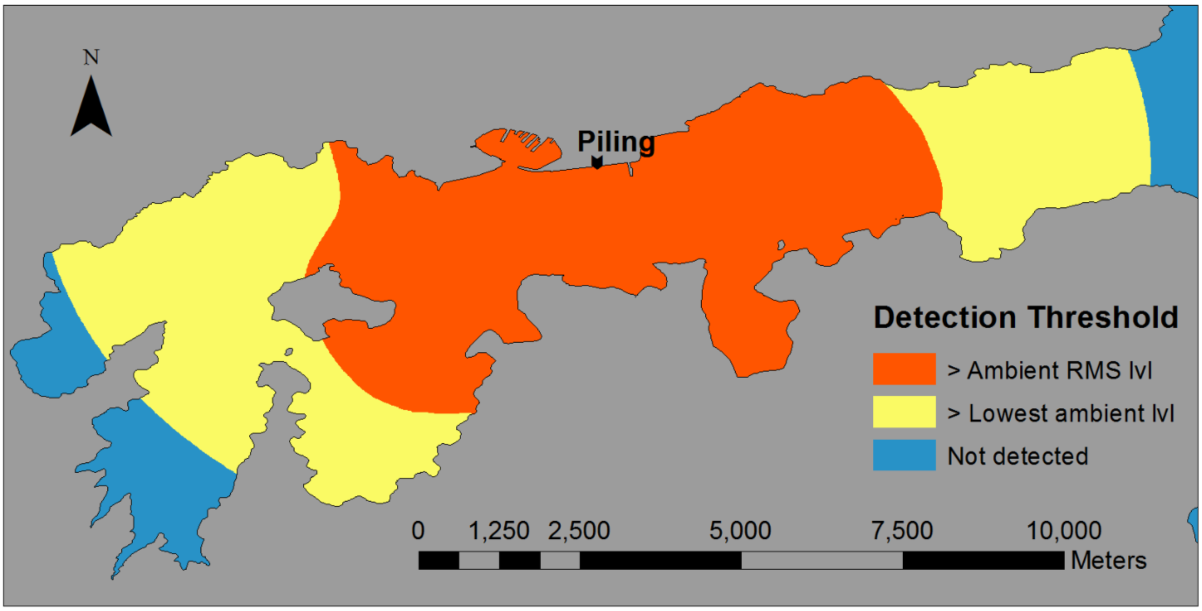

Figure A.19 Approximate zones in which pile-driving sound will be detected by Hector's dolphins. Orange area is where pile-driving noise normally exceeds ambient noise, yellow area is where Hector's dolphins would expect to hear pile-driving noise above the quietest ambient noise levels.

Frequency weighting

Different species have different frequency ranges of best hearing. These are broadly grouped into three categories (for marine mammals): low, mid and high frequency specialists. A frequency filter for each group can be used to weight the frequencies in a sound: in the range of best hearing the frequencies are weighted higher than the frequencies outside this range. This process is known as M-weighting and has been used in some studies of pile-driving noise impacts on harbour porpoise (e.g., Bailey et al., 2010). M-weighting is believed to give a better estimate of the noise level as experienced by the animal. Harbour porpoise and Hector's dolphin both belong to the 'high frequency' group. The weighting function, M_F, is given by (Southall et al., 2007):

$$M_F = 20log_{10}\left[\frac{R(f)}{\max(R(f))}\right]$$

where $$R(f) = \frac{f^2 f_{high}^2}{\left(f^2+f_{high}^2\right)\left(f^2+f_{low}^2\right)}$$

Here, f_{high} and f_{low} correspond to the upper and lower range of best hearing. For 'high-frequency cetaceans' (*sensu* Southall et al., 2007) these correspond to 180 kHz and 200 Hz respectively. M-weighting the pile-driving noise recorded in Lyttelton tends to give a lower overall SEL by up to 4 dB (see Fig. A.20). This effect decreases with range as the frequency range of the pile-driving noise becomes less broad. Energy in the lower frequency range is likely reduced due to poor propagation in shallow water (Jensen et al., 2011) while energy in the high frequency range is reduced due to high absorption with range (Malme 1995).

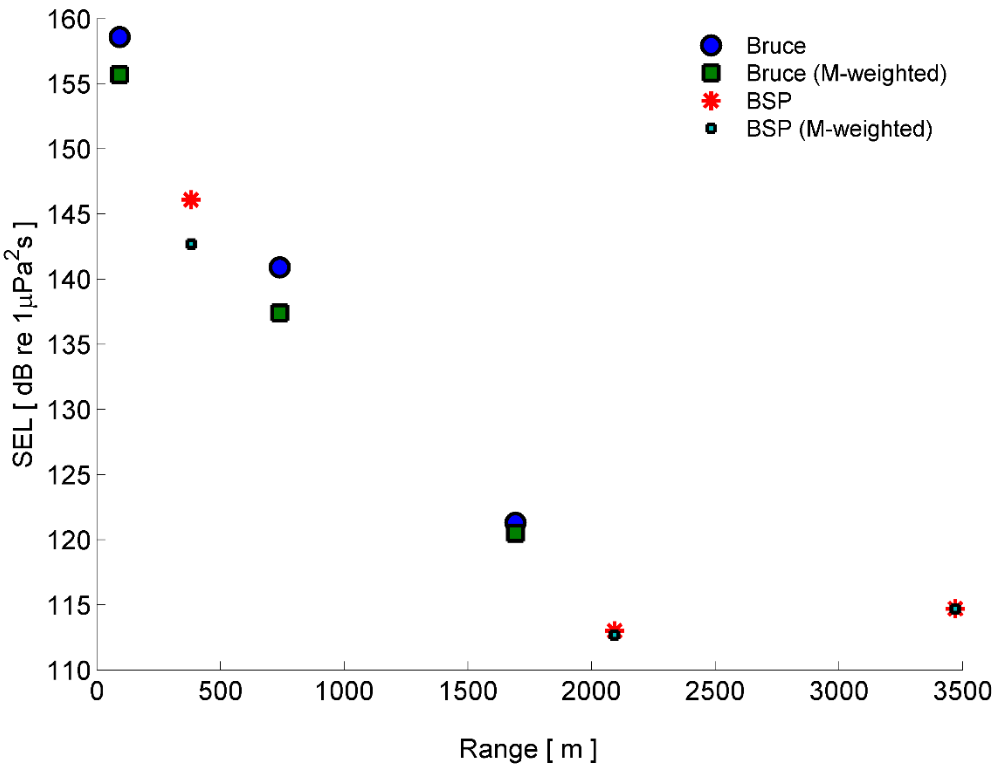

Figure A.20 SEL and M-weighted SEL with range of the two loudest pile drivers in Lyttelton.